Imperial College of Science, Technology and Medicine
Faculty of Natural Sciences
Department of Life Sciences
Grantham Institute for Climate Change

Crop production and global food security in relation to climate variation: an empirical analysis

Xavier Michel Pierre Gilbert

Submitted in part fulfilment of the requirements for the degree of
Doctor of Philosophy in Computing of the University of London and
the Diploma of Imperial College, April 2021

Abstract

The challenge of meeting increasing global food demand is amplified by climate change. Crop yield is vulnerable to extreme conditions, including heatwaves, droughts and downpours, leading to widespread concern about negative effects of climate change on food security. This thesis describes a novel empirical analysis of total production, yields and harvested area data for three major crops (wheat, maize and soybean), using a unique, global, gridded agricultural time-series data set. Trend analysis is applied to changes in production, yield and harvested area of these three crops. Machine learning is used to quantify their responses to climate. A new methodology is introduced to identify "shocks".

Results show a more complex dynamics of agricultural production than is suggested by current literature. Large changes in regional production, driven by harvested area rather than yield, have been driven by policy shifts. A large "killing degree-day" sum depresses yields for some regions and crops, but enhances them in others. Heat deficits can be as deleterious as heatwaves. Shocks can be negative or positive. Production variability has increased, but major negative shocks have been few, and have not become more frequent. Production shocks have been caused as often by changes in harvested area as in yield.

These findings do not support a universal negative effect of climate change on crop production. Moreover, stable global food supplies will not be assured by maximizing yields. It is equally important that farmers in different countries and environments grow a variety of crops. Climate-related risk is currently concentrated in the most productive baskets, exposing the global food supply to avoidably high risk. Increasing frequencies of climate extremes in the main producing areas only make such shocks more likely. Various measures that are not directly related to climate would help to make global food supplies more resilient.

Declaration of Originality

This thesis is an account of research undertaken at Imperial College London, Faculty of Natural Sciences, London, United Kingdom, in collaboration with the Grantham Institute for Climate Change and the University of Minnesota, Minneapolis, United States of America.

Except where acknowledged in the customary manner, the material presented in this thesis is, to the best of my knowledge, original and has not been submitted in whole or part for a degree in any university.

Copyright Declaration

Acknowledgements

I would like to express my sincere gratitude to:

My supervisor Professor Iain Colin Prentice for accepting to be the supervisor of this thesis. I am profoundly thankful for his mentorship, comprehension, kindness, dedication, guidance, input and support throughout the period of this research. I am thankful for his meticulous revisions, patience and encouragements throughout the thesis process and the writing period. I am humbled by his input, his stunning knowledge and scientific devotion, and the permanent push to challenge knowledge and results.

Dr James Gerber and Dr Paul West (Co-Directors & Lead Scientists of the Institute On The Environment, IonE, University of Minnesota, Minneapolis, USA), and Jonathan Foley (Former Director of IonE) for offering me the incredible opportunity to collaborate with the University of Minnesota and giving me access to an exceptional source of knowledge and data that this thesis is based on. I will never be thankful enough for their help, guidance and friendliness.

James Gerber, who became a friend to me, and his family for their generosity and kindness. They opened their home, hosted me during my visits and always made sure I never lacked anything and felt comfortable. I will never forget.

Peder Engstrom, Global Landscape Initiative Alumni, GIS expert, for his numerous help when I was a GIS rookie. Peder also made me feel part of a family when I was far away from mine during the beautiful but harsh Minnesotan winter.

Graham MacDonald (Assistant Professor in the Department of Geography, McGill University, Montreal, Canada), for his numerous inputs and encouragements. I enjoyed the many discussions and the good moments spent after work. Graham, like the people I have met and mentioned above, has this incredible ability to make someone feel proud of what they are doing and never judge.

Kate, Kevin, and all my friends at the University of Minnesota. They made me feel part of something bigger.

The Grantham Institute, Imperial College London, London, United Kingdom, members of staff for their kindness. They welcomed me and helped me through a slightly chaotic start when I arrived in the United Kingdom on a snowy day.

Dr Kleoniki Gounaris (Director of Postgraduate Studies) and James Ferguson (Postgraduate Administrator), Faculty of Natural Sciences, Department of Life Sciences, Imperial College London. When life came on the way, they did not hesitate to support me and made the finalization of this thesis possible.

My parents and sisters for their enthusiasm, support, love, values, humour.

I have not enough words to express my gratefulness.

Coco Hayes for her love, presence and understanding throughout ups and downs of the thesis.

Contents

List of Tables

List of Figures

Chapter 1

Introduction

1.1 A demographic explosion

The agricultural sector faces the challenge of increasing production in order to feed a world population that is projected to rise to 9 billion by the middle of the 21st century (Godfray et al. 2010, Rosenzweig et al. 2013). Based on the observed relationship between per capita gross domestic product (GDP) and demand for calories (including human consumption, feed crops, fish production and losses during food production), Tilman et al. (2011) projected a doubling in the global demand for crops from 2005 to 2050. Thus, population growth alone will substantially increase the challenge of ensuring food security. This challenge is amplified by the vagaries of national policies, and by the need for agricultural systems worldwide to adapt to a changing climate.

1.1.1 Coping with food deficits

Food security, and the perceived risk of Malthusian famine, are not new concerns. However, throughout history, famines have been caused not only by population growth but also – more often – by wars, embargoes, crop failures (following unexpected weather events, or pests and diseases), and inefficient or unsuitable agricultural practices. From 1960 to 1990, the Green Revolution alleviated global food deficits by dramatically improving crop yields. Improvements were achieved by agronomic measures that targeted four cereal crops in particular: wheat, maize, barley and rice. In 2004 those four crops accounted for 55% of the total global cropland. The combined use of fertilizers, pesticides and irrigation greatly contributed to reducing yield gaps (differences between actual and potential yield). A doubling

of agricultural food production between 1965 and 1999 was attained with the help of an increase in phosphorus and nitrogen fertilization, as well as an increase in the amount of irrigated cropland (see Figure 1.1, extracted from Tilman et al. (2002)). Plant breeding and genetic improvements were also major contributors to the success of the Green Revolution. Characteristics of higher-yielding cultivars developed then include short stature (associated with increased harvest index, the ratio of grain to plant biomass), tolerance to cold, heat or drought (allowing expansion of planting areas), and short growth-duration cultivars (lowering exposure to summer stress during grain filling, and allowing harvesting twice within a year) (Vergara et al. 1966). The introduction of resistance to targeted pests and diseases also contributed greatly to stabilizing yields worldwide (Davies 2003).

1.1.2 Future prospects

Variability in crop yields worldwide is explained mainly by three drivers: climate, fertilizer use and irrigation (Mueller et al. 2012, Ray et al. 2013, West et al. 2014). However, as agricultural systems and society face new trade-offs, measures applied during the Green Revolution to increase yields are unlikely to be as effective as they were in solving the challenge of meeting the still-increasing demand for food. Farming systems now face the challenge of evolving toward "sustainable intensification" (Tscharntke et al. 2012, West et al. 2014, Bellmann 2019). The costs of intensive farming systems are progressively increasing the costs of production (Tilman 1999), as food production systems are becoming more intensive in terms of capital as well as resources. Thus, there is a widely recognized need to re-examine the future of food production.

1.1.3 Future prospects: fertilisation

A significant increase in production (45% to 70% for most crops) is theoretically attainable by closing yield gaps (Mueller et al. 2012, West et al. 2014), but the practicality of doing so depends on many factors including infrastructure and finance. Yield ceilings may already have been attained on an increasing proportion of agricultural land (Mueller et al. 2012), suggesting that further increases in fertilizer application will not be effective (Tilman et al. 2001). Overuse of fertilizer moreover comes with heavy environmental costs, including water table pollution, which are best avoided.

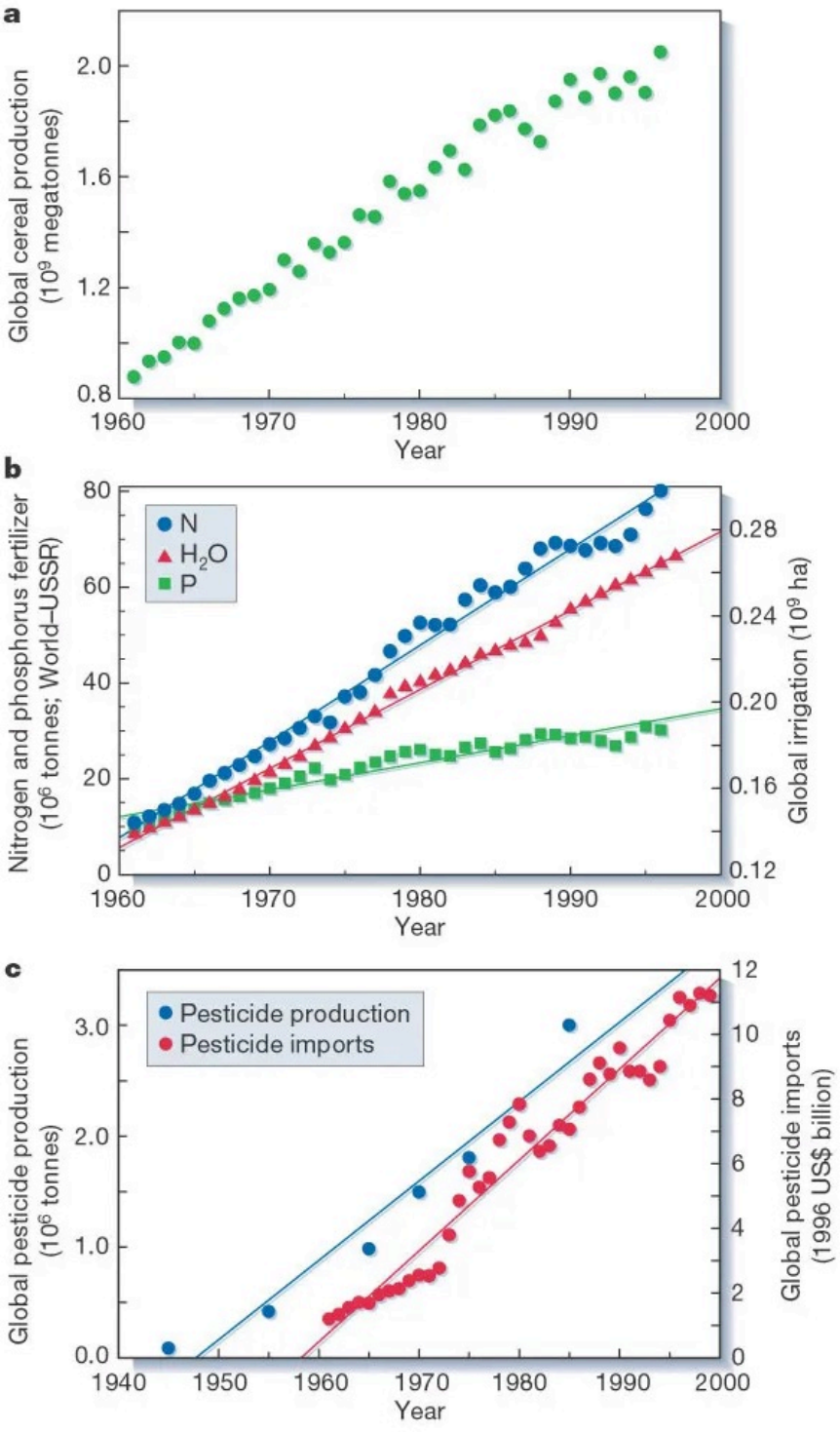

Figure 1.1: (a) Total global cereal production; (b), total global use of nitrogen and phosphorus fertilizer (except former USSR not included) and area of global irrigated land; and (c), total global pesticide production and global pesticide imports (summed across all countries). Extracted from Tilman et al. (2002)

1.1.4 Future prospects: irrigation and competition for water

According to the Food and Agriculture Organisation (FAO) of the United Nations, about 20% of the world's cultivated area contributes 40% of the food supply. On average, irrigated crop yields are 2.3 times higher than yields of rainfed crops Dowgert & Fresno (2010). Irrigated agriculture contributes greatly to the world food supply. But available water for irrigation is in competition with water resources required for other purposes. Foley et al. (2011) showed the dramatic environmental consequences of the inefficient use of irrigation water (measured in litres of irrigation water per calorie produced) in India, for example. In the long run, depletion of aquifers will lead to shrinking harvests, although currently, at the global scale, it is estimated that millions of people depend on and are fed by the practice (Brown 2012).

1.1.5 Future prospects: land availability

According to the FAO, croplands and grazing lands cover 38% of the terrestrial surface, with 1.53 and 3.38 billion hectares respectively. These uses of land comprise the areas most suitable for farming. The remaining areas are mostly of poor quality, subject to adverse climate conditions, or covered by mountains, deserts, tundra or nature reserves (Foley et al. 2011).

1.1.6 Future prospects: evolution of diets

Income growth is correlated with changes in dietary preferences and patterns of consumption. The former in particular has accelerated the demand for meat, and led to structural shifts in agricultural systems towards specialized, high-input and resource-intensive production. FAOSTAT's figures (2017) show an increase in meat and poultry production by nearly tenfold since 2000. Cassidy et al. (2013) estimated that “36% of the calories produced by crops are being used for animal feed and only 12% of those feed calories ultimately contribute to the human diet”. The drawback of these production systems is the hastening transition to a poorer calorie conversion rate (relative to that of direct consumption of cereal crops), diverting food production and leading to an inefficient food production system overall. Cassidy et al. (2013) estimated the conversion factors at around 2-4 kg of grain per kg of meat for non-ruminants, and 7 kg of grain per kg of beef. Changes in dietary preferences could have commensurate benefits to both the natural environment and global food security. According

to Cassidy et al. (2013), growing food for direct human consumption could increase the quantity of available calories by as much as 70%, and feed an additional 4 billion people.

1.1.7 Future prospects: the resilience of agricultural markets

Food security assessment at the global scale requires consideration not only of whether production will meet demand, but also of the capability of an industry or a country to buy staple crops or commodities on the global market. As a case study: in 2009, the Black Sea region accounted for about one quarter of wheat exports. But the 2010 summer heat wave and drought caused a major crop failure and grain shortage (down by 40%). This calamity prompted an export ban up to mid-2011, and a governmental decision was made to reallocate some 3 million tonnes of grain to cope with cattle feed scarcity (Brown 2012). The same author estimated that as a consequence of this summer, total world grain stocks dropped by 9.7% within 72 days. The fallout included a 60% hike in wheat prices on commodity markets. Major market players were able to cope with this price increase; but low and middle-income countries were not, and were forced to diversify their imports.

In many parts of the world, producers have the infrastructure and resources to moderate the impact of climate and weather variability on agricultural systems, from provisioning to distribution. However, regions such as Sub-Saharan Africa, marked by a high frequency of drought events and 89% of cereal production depending on rainfall, are much less resilient to climate variability (Cooper 2004, Challinor et al. 2007, Yang & Huntingford 2018, Kupika et al. 2018).

1.2 The challenges of climate change

Anthropogenic increases of greenhouse gas concentrations are driving the Earth system into a new state (Sanford et al. 2014), of which one consequence is an increase in the vulnerability of food production systems – as extreme events including floods, heatwaves and droughts are major causes of crop failure (Schellnhuber et al. 2012). The rising concentration of CO_2 in the atmosphere, and its role in warming the Earth, are established facts as reported by the Intergovernmental Panel on Climate Change (IPCC) Fifth Assessment Report (AR5) (Stocker et al. 2013). AR5 pointed to directional changes in the state of the climate system, the most prominent being a warming of oceans and land and an increase of global mean temperatures (up by 0.85°C during 1888-2012). The linkages between the rise in atmospheric

CO_2 and the increase in monthly global mean surface temperatures are illustrated in Figure 1.2 (IPCC 2018).

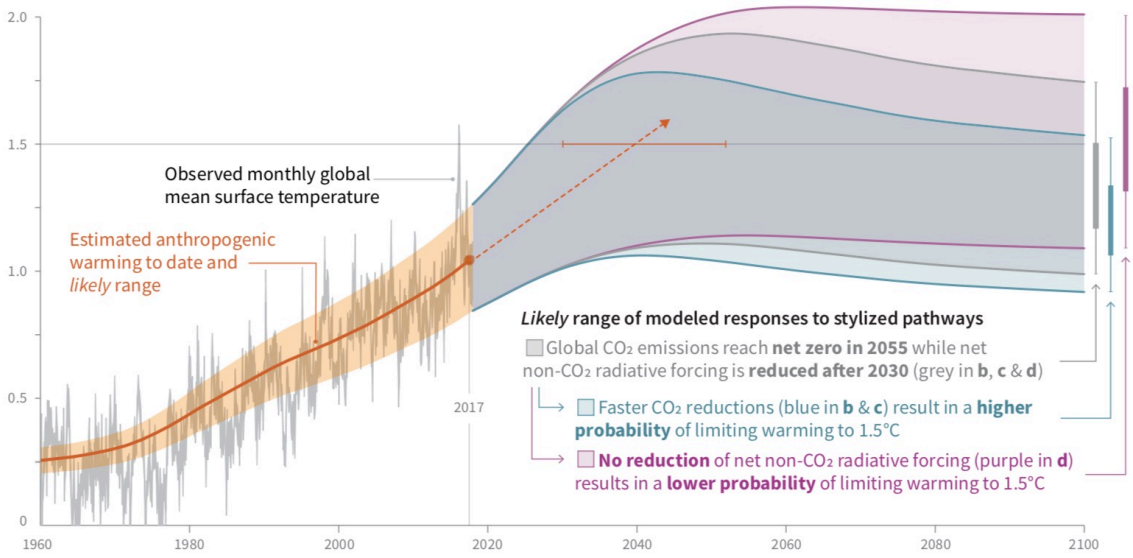

Figure 1.2: Observed monthly global mean surface temperature (GMST, grey line up to 2017, from the HadCRUT4, GISTEMP, CowtanWay, and NOAA datasets) change and estimated anthropogenic global warming (solid orange line up to 2017, with orange shading indicating assessed likely range). Orange dashed arrow and horizontal orange error bar show respectively the central estimate and likely range of the time at which 1.5°C is reached if the current rate of warming continues. The grey plume on the right of the panel shows the likely range of warming responses, computed with a simple climate model, to a stylized pathway (hypothetical future) in which net CO_2 emissions decline in a straight line from 2020 to reach net zero in 2055 and net non-CO_2 radiative forcing increases to 2030 and then declines. Extracted from IPCC (2018).

There is naturally concern about how the changing climate is likely to affect food production, and what steps might be taken to mitigate its effects. However, the current state of knowledge in this field is incomplete and beset by major uncertainties, both in climate change itself – even under the same climate mitigation scenario, different models yield divergent predictions of changes in regional climates, especially precipitation regimes – and in the impacts on agriculture of changes in atmospheric CO_2 and climate. A recent special report (IPCC 2018) reasserted the link between anthropogenic emissions an global warming. It included a section on agricultural impacts, which broadly pointed to the advantages of stronger action to mitigate climate change. But it did not present a clear picture of how agriculture might adapt to the climate changes that are already "in the pipeline", expected to take place even under the strongest emissions-reduction scenarios.

Projections of future climate-change impacts start by modelling climate change itself. In a common design, a global general circulation model (GCM) with relatively coarse spatial resolution (currently

about 2°) is used to simulate the response of the climate to large-scale forcings, particularly changes in greenhouse gas concentrations. A higher-resolution regional climate model (RCM) is then used to refine the GCM projections in order to account for complex topographical features and land cover heterogeneity (Giorgi & Mearns 1999). Unlike GCMs, RCMs can resolve fine-scale spatial features of the distribution of precipitation. RCMs are particularly useful in regions of complex orography (Wilby et al. 2002, Frei et al. 2006). The GCM provides initial conditions, and time-dependent meteorological conditions around the boundary of the embedded RCM.

One problem with this design is that the coupling goes only one way (from GCM to RCM) with no feedback. Another is that the RCM inherits any systematic errors present in the GCM. The ability of RCMs to capture observed extremes in precipitation is generally poor (Durman et al. 2001, Rauscher et al. 2010). Durman et al. (2001), in their comparative study of extremes of daily precipitation in Europe, demonstrated that biases in the simulation of mean precipitation on large scales persist from the GCM into the embedded RCM.

Empirical downscaling methods provide an alternative strategy to downscale the global projections made by GCMs (Cavazos 1999, Busuioc et al. 1999, 2001, Busuioc & von Storch 2003, Von Storch & Navarra 2013). Statistical downscaling relies on fitted statistical relationships between local climate variables (predictands) and large-scale climatic variables (predictors) (Laflamme et al. 2016). The underlying assumption is that "the large-scale climatic state and local to regional physiography (e.g. topography, land-sea distribution, LUCC) condition the regional scale climate" (Wilby et al. 2004). Briefly, statistical downscaling models can be divided into three main categories (Maraun et al. 2010, Bhuvandas et al. 2014) as follows. Perfect prognosis (PP) means that the relationship between predictands and predictors is established based on observations alone. Model output statistics (MOS) means that gridded observations and RCM outputs are used simultaneously to establish the statistical relationship for downscaling. Stochastic weather generators are hybrid models that produce statistical distributions of outcomes based on PP or MOS. All these approaches suffer from the problem that statistical relationships between smaller- and larger-scale weather phenomena – implicitly assumed constant (Samadi et al. 2011) – may not hold under climate change (Wilks 1992, Jenkins & Lowe 2003).

Exclusive reliance on GCM projections to assess future climate-change impacts is thus fraught with risks. Analysis of historical climate and crop data might be, at least, an important complement to studies based on climate modelling. Historical climate data also have limitations. The number and

coverage of weather stations contributing to the NOAA Global Historical Climate Network (GHCN) of the US Natonal Oceanic and Atmospheric Administration (NOAA) increased after the early 20th century to reach a maximum in the 1960s. There are still numerous regions with sparse or short records (e.g. Africa, South America). Also, weather stations are being gradually abandoned (e.g. in India, Australia) especially in rural, high-latitude and high-altitude locations (D'Aleo & Watts 2010). Nonetheless, historical climate data provide a foundation for empirical analysis of the impacts of climate variations and trends on ecosystems and plants that is entirely independent of climate models.

The next major source of uncertainty is crop models. A crop model should ideally be sufficiently complex to capture the response of the crop to the environment (including extremes) while minimizing the number of parameters that cannot be estimated from data (Katz 2002). Today's complex "process-based" crop models depart greatly from this ideal. Developed originally for regional, crop-specific applications (e.g. Sinclair & Seligman (2000), Katz (2002), Challinor et al. (2004)), these models are far too complex, and require too detailed input information, to be reliable or robust in global applications. This situation has direct parallels in the modelling of natural ecosystems (Prentice et al. 2015). Examples of crop models that are widely used today include SUCROS (Goudriaan & Van Laar 1994, Bouman et al. 1996), the IBSNAT models (Uehara & Tsuji 1993), the Agricultural Production System Simulator APSIM (McCown et al. 1996), Sirius (Jamieson et al. 1998) and DAISY (Abrahamsen & Hansen 2000). Such models can have 700 or more parameters, including functions of soil composition, cultivar, and management. The default values of parameters used in global applications of these models have often been derived from a single calibration, and therefore rarely yield an accurate fit when applied to different sets of conditions (Bechini et al. 2006). It should be no surprise that current complex crop models yield highly inconsistent global predictions, even of current crop yields, and *a fortiori* of crop yields in a changing climate.

1.2.1 Trends, variability and extremes in global temperature

Meteorological data reveal a warming trend during the past 150 years (Jones et al. 1999). One manifestation of this warming is the increase in the occurrence of heatwaves (Rahmstorf & Coumou 2011, Huntingford et al. 2013), which is to be expected simply due to a shift of the probability distribution towards warmer temperatures. Any change in the variability of temperature has been considered small in comparison (IPCC 2007). Several studies however suggest that a simple shift in the mean of the statistical distribution of temperatures fails to explain recent record-breaking

events in Europe and Russia (Easterling et al. 2000, Rahmstorf & Coumou 2011, Hansen et al. 2012, Huntingford et al. 2013). Individual weather stations, especially in Europe and North America (which are densely monitored), show evidence of a recent increase in temperature variability (Huntingford et al. 2013). Globally averaged temperatures show less evidence of this trend, and climate models even suggest a possible decline in interannual temperature variability linked to reduced sea-ice thickness (Huntingford et al. 2013). Nevertheless, changes in variability have occurred in some regions. The largest changes in standard deviation, across seasons and hemispheres, have occured in the Northern Hemisphere spring and summer, and the Southern Hemisphere summer and autumn (Hansen et al. 2012, Huntingford et al. 2013).

According to Hansen et al. (2012) there has been a shift in the probability distribution of temperature anomalies over the past three decades in favour of a higher frequency of low- to very low-probability (three-sigma) heat events during the summer season. For Gaussian probability distributions of anomalies, the likelihood of exceeding a three-sigma event is only 0.13%. This result conforms with the CMIP5 projections reported in AR5. Schellnhuber et al. (2012) presented even more alarming results, reporting that the occurrence of five-sigma events will also increase.

Extreme events are not only projected to become more frequent, but are also to influence a larger proportion of the land area (Hansen et al. 2012), as a consequence of global warming. Rahmstorf & Coumou (2011) showed that the Russian heat wave of 2010 would not have taken place without climate warming, at a confidence level of 80%. Their key finding was that "the number of record-breaking events increases approximately in proportion to the ratio of warming trend to short-term standard deviation; short-term variability thus decreases the number of heat extremes, whereas a climatic warming increases it" (Rahmstorf & Coumou 2011). The most recent IPCC reports (Stocker et al. 2013, IPCC 2018, Hoegh-Guldberg et al. 2018) support Rahmstorf & Coumou (2011), stating that the frequency of heat waves is likely to have increased in Europe (Greece, 2003), Asia (Russia, 2010) and Australia (2009). In Europe, the five hottest summers during the past 500 years, all occurred after 2002, with 2003 and 2010 being such exceptional outliers (Schellnhuber et al. 2012) that they were called "mega-heatwaves" (Barriopedro et al. 2011).

1.2.2 Trends, variability and extremes in the hydrological cycle

Human-induced global warming has been shown to influence on the hydrological cycle (Trenberth 1999, Allen & Ingram 2002, Huntington 2006, Seager et al. 2010, Kummu et al. 2014). The direct consequences for agriculture are mediated by changes in precipitation regimes (frequency and intensity) and soil moisture content, the impacts of which include reduction of final yields and even crop failure owing to prolonged periods of drought, and crop damage due to excessively heavy rainfall. According to AR5, warming of the lower atmosphere is enhancing evaporation while there has been an upward trend in the moisture content of the atmosphere since 1973, as the water-holding capacity of air increases by about 7% per degree of warming. The resulting increase in the amount of precipitable water held in the atmosphere leads to stronger rainfall – hence increasing risks of flooding – and snowfall events (Trenberth 1999, Trenberth et al. 2003). Kunkel et al. (1999) provided evidence that, in the USA, one- to seven- day extreme precipitation events showed an increase in frequency by 3% per decade during 1931-1996.

Trenberth et al. (2003) argued that in regions with high rainfall amounts, increases in heavy rainfall rate should follow or even exceed the increase in the water-holding capacity of the atmosphere, since rainfall is primarily fed by low-level moisture convergence. This argument contrasts with findings by Li et al. (2013), who showed that the response of precipitation to changes in temperatures is constrained by water availability and that observed and simulated changes in precipitation are actually smaller than the changes in the saturation vapour pressure; the local surface evapotranspiration rates from the total land area cannot increase at the rate called for by the the increasing water-holding capacity of the atmosphere. One interpretation is that evaporation is limited by surface energy balance (notably the total net radiation that can be used for evaporation) and that the increase is more likely in the range of 2-4% rather than 7% per degree (Sun et al. 2012, Li et al. 2013). In monsoon areas, however, precipitation appears to be increasing at the full rate of 7% per degree, and to be often heavier than before.

Increasing precipitation in some regions is expected to lead to reductions in others. Where circulation is vigorous, the air is continuously saturated with water vapour. The energy advected to regions of convergence is then unavailable in another regions. Subtropical latitudes (especially mediterranean-type climates) are both observed and projected to be drying. Li et al. (2013) showed drying in the Mediterranean, southwestern USA and southern African regions; these changes are consistent with

projected changes in the Hadley Circulation. The phenomenon of wet regions becoming wetter while dry regions become drier has been called "the rich get richer" (Seager et al. 2010, Trenberth 2011, Trenberth et al. 2014). The generality of this phenomenon has been challenged (e.g. Porter et al. (2019)), but the heterogeneity of changes in rainfall – with drying in some areas and wetting in others – is an undisputed feature of both model projections and the recent observational record. The mean time interval between successive heavy rainfall events is also expected to increase by $\sim$5% K^{-1} (Hennessy et al. 1997, Trenberth et al. 2003), implying an increase in both the intensity of rainfall events and the duration of droughts. Sun et al. (2012) found no significant trend in the temporal evolution of global mean precipitation, and a reduction of variance over land areas owing to a redistribution of precipitation. However, at regional scale, this redistribution potentially has major consequences for agriculture.

Caution is needed when drawing conclusions about regional drought trends under climate change. Some projections point to a significant global increase of drought – for example, a projected doubling of very dry areas from 1970s to 2000s (Dai et al. 2004, Dai 2013) and an increase in the area at risk of drought to 44% in 2100, from the current 15% (Schellnhuber et al. 2012). But other assessments, e.g. Sheffield et al. (2012), have shown no change in global drought over the past 60 years. According to Trenberth et al. (2003), part of the disagreement stems from the use and the formulation of Palmer Drought Stress Index (PDSI), which is based on the Thornthwaite equation for potential evapotranspiration, which in turn depends (incorrectly) on temperature alone. The problems of the PDSI have been discussed extensively (Hobbins et al. 2008, Donohue et al. 2010, Van der Schrier et al. 2011, Dai 2013, Trenberth et al. 2014). Other problems lie in (a) the datasets used to determine evapotranspiration and (b) whether due account is taken of natural variability – especially the El Niño/Southern Oscillation, which is a major cause of drought in tropical regions.

Trenberth et al. (2014) concluded that the anthropogenic contribution to the location and timing of drought is not yet discernible. In the context of a warming climate, however, agricultural drought episodes are projected to show a higher intensity and impact due to warming. Warming is expected to drive the available water capacity of the soil to come nearer to the permanent wilting point due to increased evaporation of soil water. Approaching dryness, the cooling effect resulting from the change of state of water declines and surfaces start to heat, compounding the damage to plants. The combination of increasing evapotranspiration, less frequent rainfall, increased temperature and drying thereby increases the intensity, duration and adverse effects of drought (Trenberth et al. 2003).

Climate change may therefore expand the domain affected by drought, in subtropical dry regions in particular.

Agriculture can also suffer due to extremes of precipitation. Heavy rainfall can physically damage crops, enhance soil erosion, and trigger floods. Excess soil moisture is also a major factor leading to crop losses because of the anoxic conditions that it creates (Crawford 2003), increasing risks of pest and disease, and chemical changes in flooded soils – their reduced state leads to the depletion of NO_3^- and accumulation of Fe^{2+}, Mn^{2+}, NH_4^+ and S^{2-} (Ponnamperuma 1972, 1984) – and because it can hinder access to fields by machinery, hence delaying planting and harvesting operations. During the 1993 Mississippi floods, about 70% of total crop losses occurred in upland areas because the soil saturation followed the sustained heavy rains (Rosenzweig et al. 2002).

1.2.3 Implications of climate change for the agricultural sector

Agriculture (including crop and livestock production) is a major contributor to increases in atmospheric greenhouse gas concentrations, accounting for up to 30% of anthropogenic emissions (Tubiello et al. 2013, Smith et al. 2014, Bauer et al. 2016). Thus, cropping systems are partially responsible for climate changes that affect them. AR5 made projections, with levels of confidence ranging from low to high, about the expected impact of global changes in the climate system on agricultural production. The following impacts, both positive and negative, were indicated as expected effects of global warming: increased potential for the production of some crops, especially in mid- to high latitudes, with temperature increases between 1 and 3°C; decreased potential for food production in regions experiencing temperature increases > 3°C; and decreased potential for food production at lower latitudes (especially seasonally dry regions) for temperature increases > 2°C. This last category is a particular concern because many low- and middle-income countries are implicated.

These projections represent a "big picture" at best. Regional crop responses are likely to be more complex. The IPCC projections were based on the assessment of a large but fragmented set of publications. The spread in the results from the different authors is rooted in the diversity of modelling frameworks, and implies high uncertainty in the IPCC's projections. Consecutive IPCC reports, moreover, have been inconsistent. In the case of maize, for example, the IPCC Fourth Assessment Report (AR4) suggested a increase in production under moderate warming, while AR5 suggested a loss under the same conditions. Porter et al. (2019) highlighted the sources of such inconsistencies

between IPCC reports, and the consequences for food security of our lack of firm knowledge about climate-change impacts.

1.2.4 Temperature effect on crop yields

Studies of the effects of higher temperatures on crop productivity indicate that since the 1980s global maize and wheat production may have been significantly reduced relative to a counterfactual scenario without climate change (Schellnhuber et al. 2012). The negative effects on agricultural production might also have been underestimated owing to the nonlinear response of yield to temperatures. Peng et al. (2004) estimated a decline in the production of grain in the Philippines by up to 10% per degree of warming during the growing season. Many other studies have found an increasing risk of crop yield reduction associated with warming and drying, with estimated losses ranging between 10 and 50% (e.g. Jones & Thornton (2009), Schlenker & Roberts (2009), Schlenker & Lobell (2010), Tigchelaar et al. (2018)). Reduced rates of yield improvement in cereals have also been reported (Peltonen-Sainio et al. 2009) and in some cases, the rate of yield improvement has stagnated, as observed in the case of oilseed rape yields since the mid 1980s by Berry & Spink (2006). However, Semenov (2007) argued that a warmer climate should benefit crops whose phenological stages are determined by temperature sums. According to his simulations and projections, crops whose reproductive phase is especially sensitive to super-optimal temperatures (such as wheat) will mature earlier in a warmer climate, leading to an earlier onset of anthesis and avoidance of high-temperature extremes.

The large spread of estimates of the impact of temperature on future crop yields is partly a consequence of methodological differences. Numerous approaches have been used in impact studies, ranging from simply equating average future impacts to yield losses observed in historical droughts (Boko et al. 2007, Parry et al. 2007), to process-based modelling (Rosenzweig et al. 1994, Rosenzweig & Parry 1994, Fischer et al. 2001, Jones & Thornton 2003), statistical time-series analysis (Lobell & Burke 2008, Lobell et al. 2008), and cross-sectional analyses (Kurukulasuriya et al. 2006). Some of these methodologies however are flawed. For example, predicting future crop failures based on present interannual variability (Lobell, Schlenker & Costa-Roberts 2011) is problematic, because it assumes that farmers will not adapt to changes in climate. On time scales of five years or longer it is possible – indeed it is economically necessary – for farmers to adapt to changes that they experience. The spatial pattern of crop yields levels implicitly includes adaptation, and should thus provide more relevant information on the impacts of climate change.

1.2.5 Precipitation effects on crop yield

Water availability is a fundamental control of crop yield, but the lack of consensus about current trends and future trajectories of the hydrological cycle makes it hard to assess its potential role. The uncertainty in assessment of recent and future drought trends is compounded by the interaction of phenological timing with drought risks. For example, short-growth cultivars may be particularly drought-sensitive because they have little time to recover from a stress event. On the other hand, short-growth cultivars are less likely to be hit by summer droughts. This example shows how the choice of crop varieties is an important aspect of adaptation, and illustrates the dangers inherent in risk assessments that do not take adaptation into account.

1.2.6 Rising CO_2 and crop yields

There is considerable interest in modelling CO_2 effects on plant physiology, growth and primary production (Ziska 2008) because of the known positive effect of CO_2 increase on photosynthesis in C_3 plants, and water-use efficiency in both C_3 and C_4 plants. Plant physiological principles suggest that the negative effects of both increasing temperature and decreasing soil moisture should be mitigated, at least in part, by the effects of enhanced CO_2 (Brooks & Farquhar 1985, Long et al. 2006). The most reliable experimental information on CO_2 effects on crop growth comes from Free-Air Carbon dioxide Enrichment (FACE) experiments. A robust finding of FACE experiments on crops is the decrease of stomatal conductance and water use by plants at high CO_2 (Ainsworth & Rogers 2007, Ainsworth & Long 2021). In C_3 plants, total dry matter production (above and below ground) and yield have consistently shown positive responses to CO_2 (Ainsworth & Long 2005, Ainsworth 2008, De Graaff et al. 2006, Van Groenigen et al. 2013, Ainsworth & Long 2021). C_4 plants have shown little or no enhancement of dry matter production in FACE studies (Ainsworth & Long 2021), but C_4 plants (like C_3 plants) show reduced stomatal conductance at high CO_2, which should reduce the effects of water stress under drought conditions (Leakey et al. 2009). There is currently no consensus about how important the effects of rising CO_2 have been in increasing the yields of crops. It is likely that these physiological effects have contributed, even if only to a limited extent, to rising crop yields over time. There are however no firm grounds to assume major yield increases due to the expected rise in CO_2 in the future, given all the other aspects of environmental change that inevitably accompany it.

1.3 Aims and objectives of the thesis

The task of doubling the world's agricultural production during the next three to five decades is expected to exert significant pressure on the global agricultural system. Assessing the climate change-induced risks for the food sector is extremely challenging. It requires abilities, arguably well beyond the state-of-the-art, to forecast climate change accurately at sufficient spatial resolution; to simulate crop yields across different environments and crops; and to translate the resulting simulations into economic indicators, in order to assess food security implications and impacts on human welfare.

More broadly, there is a major difficulty in translating research outputs, especially when fraught with multiple uncertainties, into actionable information for the benefit of end-users. Farmers, wholesalers, retailers, investors and policy makers alike have limited perception of the full range of possible climate change impacts, either at a specific location or over larger regions. Scenarios needed by end-users fall into two categories: projection of likely long-term trends (about three to five decades) and prediction of variability on shorter time scales. Long-term trend projections are relevant for planning future infrastructures and production facilities, while short-term variability is relevant for agricultural management and market investment. In this context, it seems unwise for research on food security and the dynamics of food production to rely exclusively on complex, coupled models of climate change, crop productivity and commodity prices (McCown et al. 1996, Jones et al. 1998, Jones & Thornton 2003, Levin 2006, Dimaranan & McDougall 2006, Koester 2008, Maraun et al. 2010, Rosenzweig et al. 2014, Nelson & Shively 2014), as implemented for example in the Agricultural Model Intercomparison and Improvement Project, AGMIP[1] – and appropriate to conduct complementary research based on analysis of actual, observed long-term trends and short-term variability in crop production.

The research described in this thesis represents such a complementary approach to the assessment of the controls of agricultural production, focusing on the three crops (maize, soybean and wheat) that are the most traded on international commodity markets. The approach adopted is firmly rooted in observations – of both climate and crop yields, harvested area and production – and relies on a unique global gridded agricultural time-series data set provided by the University of Minnesota, which allows a degree of detail in the assessment that has not previously been possible due to the coarse resolution of existing (mainly national) data sets for much of the world. Analyses are conducted in a simple conceptual framework, seeking to identify the main drivers of crop production over time in the main

[1] https://agmip.org/

producing areas for each crop. The approach is statistical rather than process-based, and is therefore not able to distinguish, for example, how different biophysical controls (such as solar radiation or CO_2) influence crop growth and reproductive allocation, or to make forecasts. It is however focused on the observed dynamics of crop production, and allows the separation of yield variations (with a strong climatic imprint) from changes in planted or harvested area, which are strongly influenced by socio-economic and historical factors. Its overarching objectives are (a) to obtain a new, empirically grounded perspective on how the global food system works today and has worked over the past few decades; and (b) to gain new insights into the interplay of climate and other factors in determining the production of staple crops.

Chapter 2 uses statistical techniques to analyse trends in yield, harvested area and total production in the main production areas (baskets) for each crop. Chapter 3 uses machine learning to analyse how different agroclimatic variables have influenced crop yields in each basket. Chapter 4 introduces a novel methodology for the detection of shocks, and applies it to assess the characteristics of yield, harvested-area and production shocks. Chapter 5 discusses the results and considers their implications for our understanding of food security and the factors that contribute, positively or negatively, to risks in the global food supply chain.

Chapter 2

Agricultural trends and global food security

Abstract

The challenge of feeding the world's growing population has highlighted the need to better understand the nature, and causes, of trends and variations in the production of major agricultural crops. This analysis of recent trends decomposes production into its components: yield, and planted (or harvested) area. Changes in production, yield and area during the period 1961 to 2012 are analysed for the three staple crops (maize, soybean and wheat) that are most traded on international markets. The dynamics of yield and planted area are analysed within regions or "baskets", defined by a clustering algorithm, which are not necessarily linked to geopolitical boundaries. The sensitivity of each crop, in each region, to heat stress is quantified using widely used agroclimatic indices. Key findings include that (a) both trends and more rapid variation in the production of each crop can be driven by planted area as well as yield; and (b) that the sensitivities of each crop to warming vary greatly from region to region. It is suggested that the extreme spatial concentration of major producing areas for major crops poses an inherent risk to global food security that is amplified by climate change.

2.1 Introduction

The Sustainable Development Goal to "end hunger, achieve food security ... and promote sustainable agriculture", will not be achieved solely by attempting to maximize crop yields. There are good reasons to consider also the *stability* of production, especially in the face of global climate change, to which some of today's major producing regions are particularly sensitive; and to investigate not only how much food is produced, but also where it is produced, and on how much land.

The task of doubling the world's agricultural production to meet the projected demand over the next 30–40 years faces not only physical and biological, but also environmental and sustainability constraints (Godfray et al. 2010, Tilman et al. 2011). Can we grow our way to global food security, while reducing our impact on land and water resources?

Figure 2.1 depicts the striking predominance of agriculture on planet Earth, and highlights the fact that arable land is scarce. This figure also makes a compelling case about the potential threat to the Amazon rain forest, which could be considered – in a narrow perspective – to represent one of the few opportunities to expand the area of arable land.

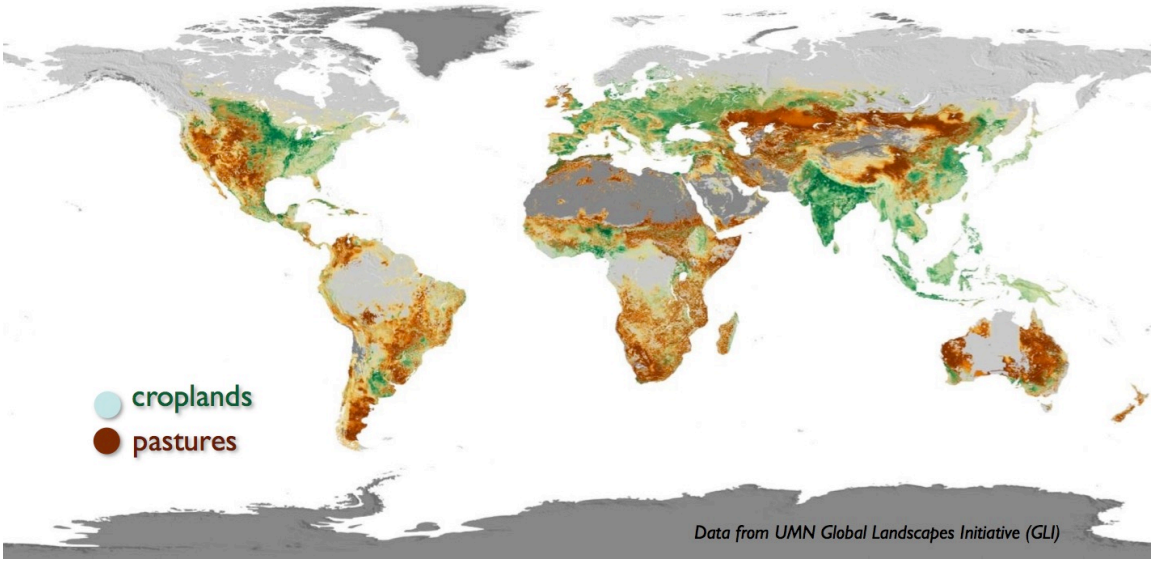

Figure 2.1: Global agricultural land use: croplands and pastures distributions. Data provided by the University of Minnesota, Institute on the Evironment, adapted from Foley et al. (2005), Monfreda et al. (2008, 2009), mapping courtesy of J.S. Gerber and P. Engstrom.

According to the Food and Agriculture Organization (FAO) of the United Nations, croplands and grazing lands cover 1.53 and 3.38 billion hectares respectively. These uses of land account for 38% of

the land surface. Most of the remaining area is covered by mountains, deserts, tundra or ecological reserves, or experiences climate conditions unsuitable for agriculture (Foley et al. 2011, West et al. 2014). The residual lands available to agriculture are mostly of poor quality (in terms or structure, composition or climate) and, if converted, probably would not support the same crop output and yield levels as existing farmlands (Young 1999).

A significant increase in production (45% to 70% for most crops) could be attained by closing yield gaps (Mueller et al. 2012): in other words, allowing crops to achieve their potential yields through improved management, including adequate fertilizer inputs and (where possible) irrigation. However, across much of the developing world, the trend is for production to be increased instead by increasing the planted acreage. In the wet tropics, primary forest is still being burnt down and the land used for cattle production (following the increasing demand for meat and dairy consumption) for a year and then converted to soybean, which is mainly shipped to China as animal feed. In recent decades farmland in (especially) Amazonia and Indonesia has increased by 2-3%, mainly driven by deforestation (Mueller et al. 2014, West et al. 2014). Meanwhile, however, urbanization is encroaching on farmland; at a rate of 16 million ha per year (Holmgren 2006) in the USA, China and India. Considering deforestation combined with urbanization, the net global change of agricultural area has been small.

Even if yields are increasing globally, they are not keeping up with projected demands (Ray et al. 2013). With a rising demand for crop production on the one hand and physical, environmental and sustainability constraints on the other, business-as-usual has become unsustainable. The global food system can no longer anticipate, nor has the required resilience, to reliably meet demand. The strategies available to increase the resilience of the global food system are: (1) closing yield gaps (West et al. 2014); (2) changes in diets (Cassidy et al. 2013); and (3) re-engineering the system to mitigate risk (Foley et al. 2011, West et al. 2014).

Closing yield gaps is a potentially powerful approach (Cassman et al. 2003, Tilman et al. 2011, Mueller et al. 2012, West et al. 2014, Phalan et al. 2014, Pradhan et al. 2015, Zhang et al. 2016). It is estimated that the USA, western Europe and parts of India, China and Brazil have reached at least 75% of potential yields. Nearly three-quarters of under-achieving regions in terms of crop yields could reach a similar level to western Europe solely by increasing nutrient inputs, while about a sixth could do so by increased use of irrigation (Mueller et al. 2012). In the case of wheat, the gap between potential and actual production increased 2.75–fold during the five decades after 1961 (Mueller et al. 2012): potential production has increased at an average rate of $\sim$14 metric tons (mt) per year while actual

production increased at less than half this rate. If potential yields continue to climb at a higher rate than actual yields, closing yield gaps constitutes an increasingly important opportunity to make the global food system more resilient to production shocks, and better able to meet the increasing demand.

Closing yield gaps is also a sustainable approach, as production is thereby increased on available land while pressure on natural ecosystems is not increased (Cassman et al. 2003, Tilman et al. 2011). However, there is a geographic imbalance in the use of fertilizer: even though increased nutrient inputs could significantly improve yields in some regions, large surpluses are applied in some regions. West et al. (2014) estimated that about half of the excess of nitrogen (i.e. nitrogen fertilizer that is applied, but not needed) is concentrated in only a quarter of the worlds cropland area. Similar figures apply to phosphorus. Major production areas including the USA, China and India account for around 65% of the excess application of nitrogen and phosphorus. In these regions, the amount of nitrogen and phosphorus applied could be reduced by nearly 30% with no reduction in yields (West et al. 2014). Other authors, including Mueller et al. (2014), have highlighted the efficiency gain from more precisely tailored application of nitrogen fertilizer.

Shifting farmed lands toward sustainable intensification is only one piece of the puzzle, however. First, food waste reduction provides additional leverage to grow our way towards global food security and meet future demands. Gustavsson et al. (2011) estimated the food production being wasted along the supply chain, from the field to the plate, to range from 30 to 50% globally. Second, Cassidy et al. (2013) and West et al. (2014) assessed the gains achievable through a reallocation of crop outputs. According to their findings, up to ∼70% more calories would be available to humans if the share of the production allocated to animal feed and non-food uses (e.g. biofuels) were instead available for direct consumption. Cassidy et al. (2013) also showed how relatively small changes in consumption, and wastage of animal products in particular, could have a substantial effect on available calories. Similar findings were presented by MacDonald et al. (2015), who estimated that over 20% of global production is traded for animal feed and non-food uses – and that redirection of this production to direct consumption could feed as many as 2.5 billion people.

Above, I have outlined strategies that could address the challenge of more sustainably meeting the increasing global demand for food. However, there have been few attempts to account for the contribution of systemic risk on the global production of crops, especially in the context of a changing climate.

Discussion of the challenge of adequately meeting the growing demand for food, even sustainably, has tended to emphasize long-term trends in production (Godfray et al. 2010, Paillard et al. 2011) and yield (Grassini et al. 2013, Ray et al. 2013, West et al. 2014). Omitted from this discourse are (a) interannual variability and its heterogeneity across regions, (b) the potential trade-off between absolute production output and stability of the food supply, (c) the fact that production is not solely determined by the yield of a crop but also by the harvested area of the crop. Here, I propose a decomposition of global crop outputs and their variability into "leverages" that quantify the relative contribution of observed yield and harvested area to the variation in the production. To circumvent the limitations of the classic approach whereby crop-growing regions are defined by geopolitical borders (Ben-Ari & Makowski 2014), I introduce the concept of the "basket", which is a relatively homogeneous geographic and climatic region, rather than a geopolitical one. Baskets are likely to better capture regional interannual variability, since climatic influences are linked to regions rather than nations.

2.2 Material and methods

2.2.1 Datasets

Crop data

I analysed global gridded datasets of maize, soybean and wheat that comprise data on annual yield, harvested area and production, with a grid resolution of 5 arc minutes. These unique datasets, obtained from the University of Minnesota, synthesize about 2.7 million census observations spanning the period 1961 to 2012. They are the outcome of more than a decade of data collection and aggregation performed by the Institute On The Environment (IonE) and the Global Landscape Initiative (GLI) at the University of Minnesota. The data collection process included the collection and cross-validation of data from major sources including the United States Department of Agriculture (USDA) and the Food and Agriculture Organization (FAO) Corporate Statistical Database; but also the digitization of census data, obtained from buying or borrowing hundreds of census books all over the world, through national libraries and government agencies.

A few inevitable limitations on the quality of the data should be noted. Data quality can vary across regions of the world for multiple reasons related to quality control and frequency of data collection. In many developing countries, including India, yield measurements are conducted during

crop-cutting experiments that have been tightly linked to the agricultural insurance sector since its emergence, providing an incentive for accuracy. Because of the complexity of the process of data collection, however, data may suffer from mistakes made by field operators (errors in measurements, typographical errors, and mistakes in digitizing hand-written documents). Further mistakes might be made as the data are transferred to census books or national databases. There can also be unknown temporal trends in data quality. These issues have been partially addressed through the work done at the University of Minnesota in cross-validating the data between sources. It is important also to note that the data for developing countries has proved to be extensive, and often available at much higher spatial resolution than the publicly available data from the FAO. Finally this dataset is, to the best of my knowledge, the most comprehensive globally gridded dataset for agriculture available to research, hence its use to underpin a number of key papers on the agricultural system published from 2010 onwards (Portmann et al. 2010, Foley et al. 2011, Ray et al. 2012, 2015, Mueller et al. 2012, 2014, Ray et al. 2013, Cassidy et al. 2013, West et al. 2014, Tigchelaar et al. 2018).

This chapter focuses on maize, soybean and wheat. These staples are the three most important globally traded crops, by both volume and economic value. Having multiple uses, including biofuel and animal fodder, means that variability in their production can impact multiple supply chains. Rice was not included in part because, according to the GLI, the available time series data for rice are significantly less reliable than those for maize, soybean and wheat.

Climate data

Climate data were obtained from the WATCH–WFDEI (WFD) climate dataset (Harding et al. 2011, Weedon et al. 2014). This dataset covers the global land area on a 0.5°x 0.5°grid, with three-hourly temporal resolution. It is based on the ERA-Interim reanalysis with bias correction (towards global observed values) applied to temperature and precipitation (Sheffield et al. 2006, Boucher & Best 2010, Harding et al. 2011). It has been widely used in global analyses, including agriculture and climate impacts research (Portmann et al. 2010, Foley et al. 2011, Mueller et al. 2012, Ray et al. 2012, 2013, Rosenzweig et al. 2013, 2014, Schneider et al. 2014, Ray et al. 2015). It is also one of the reference datasets and the basis of much research carried out in the framework of the Agricultural Model Intercomparison and Improvement Project (AgMIP) (Rosenzweig et al. 2013). From the WATCH–WFDEI data set I extracted the maximum daily temperature that I use to derive the agroclimatic variables defined in the following section.

2.2.2 Agroclimatic variables

Temperature and precipitation anomalies can cause deviations from the expected yield of a crop (Lobell & Burke 2008, Lobell, Bänziger, Magorokosho & Vivek 2011, Lobell, Schlenker & Costa-Roberts 2011), and these variables have been used in analyses of climate impacts on crop growth and yield. However, these basic meteorological variables do not represent well the processes by which crops are affected by the climate. For this reason, more "plant-centred" indices have been adopted widely for statistical analyses of yield-climate relationships. These indices including the cumulative sum of favourable temperatures (above a threshold) that drive the developmental phases of a crop, known as growing degree days (GDD) (Chang 2011), and the cumulative sum of degrees above a higher threshold that can harm crop development, known as killing degree days (KDD) (Tigchelaar et al. 2018). Such "agroclimatic variables" have been shown to be useful indicators of how crops respond to climate anomalies (Butler & Huybers 2013, 2015, Chavez et al. 2015).

High temperatures can negatively affect yield in various way including hampering crop growth and reducing grain filling (Sánchez et al. 2014). Several studies have found the effects of superoptimal temperatures on crop yields to be more important than anomalies in precipitation (Lobell, Bänziger, Magorokosho & Vivek 2011, Butler & Huybers 2013, 2015, Tigchelaar et al. 2018). It should be noted also that effects of droughts are likely to manifest through high air (and leaf) temperatures due to stomatal closure and reduced transpiration, leading to an increase in the partitioning of net radiation to sensible rather than latent heat (Jones 2013). In this chapter, accordingly, I focus on a small set of proxies for heat stress. (Later, in Chapter 3, I investigate stresses related to temperature and precipitation by means of a larger set of agroclimatic variables.) To quantify the yield response to superoptimal temperatures in this chapter, I have used the sum of killing degree days (ΣKDD, the annual sum of degrees above 32°C) and the number of hot days (nHotDays, the annual number of days with temperatures above 32°C). On day d, I define KDD as

$$KDD_d = \begin{cases} T_{max,d} - T_{kdd} & \text{if } T_{max,d} > T_{kdd} \\ 0 & \text{if } T_{max,d} \leq T_{kdd} \end{cases} \tag{2.1}$$

Where $T_{max,d}$ is the maximum daily temperature and T_{kdd} is the temperature thresholds for killing degree days. I selected a threshold of 32°C based on values used in the literature (Hesketh et al. 1973, Porter & Gawith 1999, Egli et al. 2005, Schlenker & Roberts 2006, Setiyono et al. 2007, Cai et al.

2009, Abendroth et al. 2011, Butler & Huybers 2013, 2015, Gourdji et al. 2013, Asseng et al. 2015, Teixeira et al. 2013, Sánchez et al. 2014, Chavez et al. 2015), which range from 30° to 36°C. ΣKDD is then obtained by summing daily values (KDD_d) over the year.

2.2.3 Regionalization

I consider eleven, seven and ten regions (called "baskets" throughout this thesis) for maize, soybean and wheat respectively (SI, Section 2.6, Figure 2.11 and Table 2.2). The baskets were determined according to the following procedure.

1. For each grid cell I computed the cumulative sum of the production and harvested area for the period 1961 to 2012. I used the cumulative sum in order to build spatial distributions that are not skewed by the effect of averaging over time, and yet take into account that for a given grid cell, the production and harvested area might have increased during the period studied. I also computed the global total cumulative sum of production and harvested area for each crop during the same period.

2. I defined "bounding boxes" as the following continental/subcontinental regions: North America, South America, Europe, Eastern Europe, Africa, Asia, India, Australia. This step was necessary for the subsequent classifiation steps to work, in order to allow for very different general levels of production and harvested area in different continents (for example, maize production in Africa as compared to North America and China). The coordinates of the bounding boxes where computed using the function `ST_Envelope` in the open-source Geographic Information System (GIS) software `PostGIS`. As an example, for North America, the bounding box was computed on the geometry of North America, obtain from Natural Earth[1], a database of open-source GIS geometries.

3. For each bounding box separately, I ran a spatial clustering procedure on the following variables: longitude, latitude, cumulative production and cumulative harvested area, using the p–max regionalization algorithm (Duque et al. 2012) as implemented by the method `region` in the Python spatial analysis library `PySAL`. A key motivation behind the selection of this algorithm is that no predefined number of regions is required; instead, the algorithm requires the user to define the constraints of the optimization on target variables so that a minimum threshold is

[1] https://www.naturalearthdata.com/

met for these target variables within a region. For the basket selection, I imposed the constraint that every region should contain grid cells where (a) the proportion of harvested area is at least 5% of the total grid cell area and greater than the 25th percentile of the spatial distribution of harvested area for the region, and (b) the cumulative production is above the 25th percentile of the distribution of cumulative production. The percentile values were chosen by trial and error, with two additional optimization constraints: (a) for each bounding box, no more than four regions should be identified; and (b) a region can be considered as a basket if all the grid cells it contains together represent at least 1% of the global cumulative production for the period 1961 to 2012.

4. Finally, for each region identified, I computed the bounding box of the region and computed a contour as the smallest (in area) continuous polygon that includes all grid cells of the region, using the methods `threshold` and `findContours` in the Python `OpenCV` image detection library.

In the final results of this regionalization, the maize baskets accounted for 67% of the average world production (for the whole period 1961 to 2021) and 56% of world average planted area. The corresponding figures for wheat are 60% and 50%, and for soybean, 75% and 68%, respectively. A map (Figure 2.11) representing the location of the baskets for each crop as well as their names (Table 2.2) as used in this thesis can be found in Supplementary Information (section 2.6). More statistics on the baskets' proportion of global production and harvested area are given in Tables 2.3 and 2.4 (SI).

2.2.4 Interannual variability

Residuals

To characterize and compare baskets for their variability in production, harvested area and yield, I investigated the distribution of the time-series residuals. I defined residuals in production r_{it} at year t in basket i as

$$r_{it} = P_{it} - \mu_{it} \tag{2.2}$$

where P_{it} is the observed production in metric tons per hectare (mt/ha) and μ_{it} is the expected production (mt/ha) at year t in basket i for a given crop. To estimate values of μ_{it} I used a linear,

quadratic or cubic regression models fitted by ordinary least squares (OLS) using the function `lm` in the R programming language. The models were fitted to the time-series of each basket, and the model with the lowest Akaike Information Criterion (AIC) was selected to detrend the time series. The residuals were checked for the presence or absence of autocorrelation using ACF plots (R functions `acf` and `lm`). The interannual variability V_i of each basket was estimated from the variance as

$$V_i = \frac{1}{T} \sum_{t=1}^{T} (r_{it} - \overline{r_i})^2 \tag{2.3}$$

where $\overline{r_i}$ is the average of anomalies for the period 1961–2012, and is equal to zero by definition. Hence, the variance of the residuals in each basket i is

$$V_i = \frac{1}{T} \sum_{t=1}^{T} r_{it}^2 \tag{2.4}$$

Finally I computed the standard deviation of the residuals for each basket i as:

$$S_i = \sqrt{\frac{1}{T} \sum_{t=1}^{T} r_{it}^2} \tag{2.5}$$

Variance and standard deviation have been widely used to quantify and compare the instability of production and yield in different regions (Osborne & Wheeler 2013, Ben-Ari & Makowski 2014). Other metrics used for this purpose include non-parametric statistics such as the interquatile range (IQR), and the coefficient of variation (CV) (Tsay 2014); CV however is not suitable here as the analysis focuses on residuals, whose mean is zero. The robustness of the analysis to the chosen metrics is further analysed in Supplementary Information (Section 2.6, Table 2.5), where it is shown that the rankings of baskets are consistent for alternative metrics.

Statistical comparison of variance and standard deviation

The Fligner-Killeen test is one of several designed to assess the homogeneity of variances between groups. The motivation for using the Fligner-Killeen test over alternatives it that it is the most robust when the data deviate from a normal distribution (Beyene & Bekele 2016). For each crop and each agricultural variables, I tested the homogeneity of variance between each pair of baskets using the R

function `fligner.test` in the package `stats`.

2.2.5 Simpson diversity index

The Simpson diversity index is most commonly used to quantify species diversity. I use it here in a different way to characterize the evolution of the spatial distribution of hectares under a given crop among the different baskets. High values of the Simpson index mean a concentration of the production in a few regions; low values indicate a more even distribution among regions. The Simpson diversity index S at time t is expressed as

$$S_t = \sum_{i=1}^{N} \omega_{it}^2 \tag{2.6}$$

where ω_{it} is the ratio of the area in the ith region at year t to the total baskets area, with N the number of baskets for the crop being considered.

$$\omega_{it} = \frac{S_{it}}{\sum_{i=1}^{N} S_{it}} \tag{2.7}$$

2.2.6 Leverages

The observed agricultural production is the product of observed yield and harvested area. To quantify the relative contribution of observed yield and harvested area to the variation in the production, I define a metric called "leverage", denoted L. L is the ratio of the change in harvested area to the change in yield. Thus, with P_t the production at year t, Y_t the yield at year t and A_t the acreage at time t, we have ΔP, the change in production between t and $t+1$ as

$$\Delta P = (Y * A)' = Y_t \Delta A + A_t \Delta Y + \Delta A \Delta Y \tag{2.8}$$

where ΔY and ΔA are the changes in yield and acreage, respectively, between t and $t+1$. Therefore

$$\Delta P = A_{t+1} \Delta Y + Y_t \Delta A \tag{2.9}$$

with $A_{t+1}\Delta Y$ the contribution of the increment in yield (noted dY for convenience) and $Y_t\Delta A$ the contribution of the increment in area (dA) to the production.

I define the leverage as $L = dA/dY$. When $\mid L \mid > 1$ the area has a greater contribution to the incremental change in production, and when $\mid L \mid < 1$ the yield has a higher contribution to the incremental change in production.

2.2.7 Principal Component Analysis (PCA)

In data sets including many variables, the covariance matrix can be too large to be analysed directly because the number of pairwise comparisons increases with the square of the number of variables – quickly making interpretation impossible. Principal Components Analysis (PCA) is the standard method used to reduce the dimensionality of such a dataset. The method finds linear combinations of variables that account for the maximum proportion of the variance in all variables. The first principal component accounts for the largest proportion of total variance; the second, uncorrelated to the first, accounts for the largest proportion of the remaining variance; and so on. Here, PCA was applied in order to characterize groups of individuals (the baskets) by variables (leverages). Graphical plots of the positions of individuals in the space defined by the first two (or first few) principal components provide a convenient summary in which, to an approximation, more similar individuals are shown closer together and less similar individuals further apart.

To make progress in understanding the type of leverages as well as how crops and baskets contrast in leverages, I performed a PCA using the R function `prcomp` from the package `stats`. For each crop, I computed a PCA on the count of each type of leverage (Section 2.3.3) in each basket. When performing a PCA, a few methodological decisions must be made: whether to center the data on the means for each variable (this is normally recommended), whether to normalize the data to unit variance (this is necessary when variables are in different units), and the number of components retained for analysis. Here, the data were mean-centred, and because all variables in the dataset are in the same units, normalization was not carried out. There is no general rule as to how to choose the number of principal components to consider, and no statistical test is applicable, so this decision is usually made pragmatically (Jolliffe 2002, Peres-Neto et al. 2005). However a scree plot (a plot of the eigenvalues – proportional to the amount of variance explained – for successive components, in descending order) can be a useful guide. Based on such a plot, the number of components to use "is determined at

the point, beyond which the remaining eigenvalues are all relatively small and of comparable size" (Peres-Neto et al. 2005). The number of principal components chosen for each PCA (Section 2.3.3, Figure 2.7) according to this method was five for maize and wheat, and four for soybean.

To help interpret the principal components, I focused on those variables that were most strongly and significantly correlated with each component, computed using the R function `dimdesc` in the package `FactoMineR`. I also used the metric called `cos2` (square cosine, square coordinates) to quantify the importance of each component for a given variable (Abdi & Williams 2010). This metric was computed using the R functions `get_pca_var` and `get_pca_ind` in the package `factoextra`.

2.3 Trends and variability in crop outputs

This section investigates the trends in crop output, as well as the factors that influence the variability of crop production.

2.3.1 Trends in production: an analysis

Figure 2.2 visualizes the time evolution of production in each basket for the three crops considered. Trends were computed using locally weighted linear regressions (LOESS) for maize and soybean, and General Additive Models (GAM) for wheat. Each model was fitted by ordinary least squares (OLS) using the R functions `loess` and `gam` for each time series of production for each crop and for each basket. The objective was not to select the best-fitting model for each one of the baskets, but rather the best fitting model across baskets for each crop, based on the AIC, by summing the AIC of models across baskets. LOESS and GAM are both relatively flexible models and in this application they yielded closely similar results, except that GAM is more sensitive to local extrema (as shown e.g. by wheat in Figure 2.2). (For trends in harvested area and yield, as well as global trends, see SI, Figures 2.12, 2.13, and 2.14.)

Figure 2.2 plots the series with common x (time) and y (production) axes. It shrinks the time axis, and sets the y axis to the maximum production for each crop across all baskets. Hence, this visualization emphasizes contrasts in production among regions. The baskets are sorted by their average production during 1961–2012. Overall, the three crops present an upward trend in production. Maize trends are approximately linear and show a correlation between the level of production and the slope of the

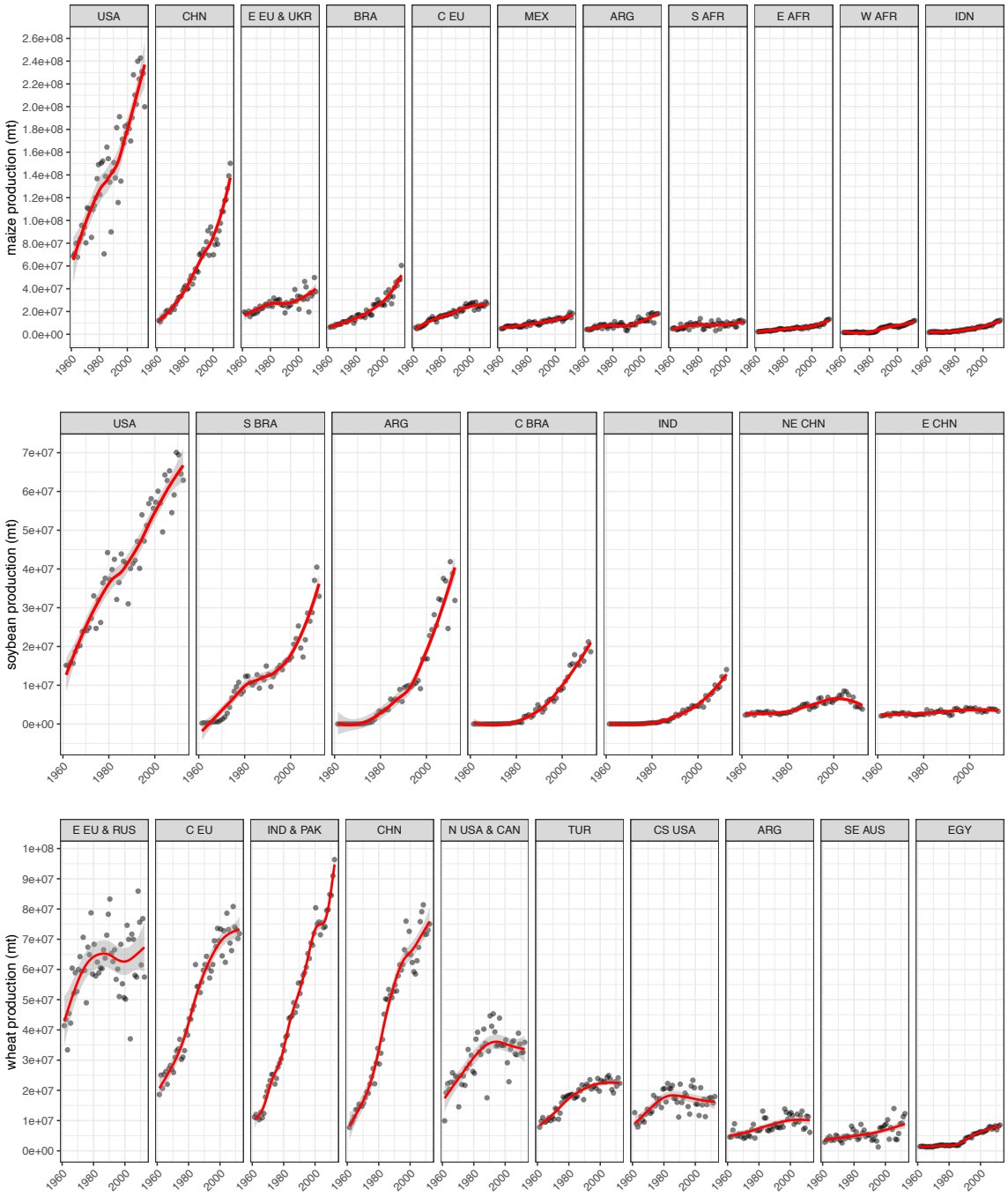

Figure 2.2: Levels and trends in production of maize, soybean and wheat (top to bottom) from 1961 to 2012 in the main producing areas (baskets).

trend. Soybean time series show acceleration over time (the USA is an exception, with a more linear trend); production drastically increased from the 1980s onwards, especially in Argentina, Brazil, and India. As for maize, soybean shows a correlation between the level of production and the slope of the trend. Trends in wheat production are more complex. In contrast with the other two crops, despite the overall increase in production, seven out of the ten baskets show reversal or flattening from the 1980s (CS USA, Eastern Europe & Russia) or the 1990s (Northern USA & Canada, Turkey) onwards. Reversal or flattening are mostly observed in baskets with lower production.

Maize and soybean both show greater variability in the baskets with higher production. The USA (globally the largest production area for maize and soybean, and fourth for wheat) has the highest variability across the entire period. The Eastern Europe & Ukraine basket for maize is distinctive in showing a substantial increase in variability from the 1990s. These observations suggest that the variability (as indicated visually, by the distributions of the data around the trends) in global maize and soybean output is mainly contained in one single basket, which is also the biggest producer. Wheat contrasts with maize and soybean, as all baskets show high variability in production over time. Eastern Europe & Russia shows by far the highest variability, while most of the variability in total global production is contained in North America and Europe.

The apparent correlation between slope and level of production (at the start and towards the present) points to a specialization of producing areas and concentration of production. This can be interpreted as follows. When a region is engaged into a specific crop, agricultural systems and practices – and the agricultural economy – develop around that crop. Figure 2.2 depicts several examples. For example, while initially insignificant, crop production in Central Brazil peaked from the 1980s accompanying deforestation and expansion of agriculture into the Amazon rainforest. Soybean in India was originally encouraged to counter malnutrition and protein deficiency; a research effort that began in the 1960s, along with the processing capacity of oil mills being under-used, created a fertile framework for the development of a soybean market. Soybean quickly became a suitable crop to meet a shortage of edible oil and proteins and its production rose thereafter.

An unplanned side-effect of such contingent historical factors, however, seems to be a high degree of concentration of current production – and along with it, a high degree of variability – of each crop in a rather small number of baskets.

2.3.2 Decomposing global crop outputs and variability

Production, yield and area variability contrasts between regions, and between crops

Figure 2.3 presents the distribution of production, area and yield anomalies for maize, soybean and wheat. The Fligner-Killeen test for homogeneity of variance between baskets, and the correlation between the mean production (or harvested area, or yield) per basket and the interannual variability in production (or harvested area, or yield), are summarized in Tables 2.5, 2.6 and 2.7 in the Supplementary Information of this chapter (Section 2.6).

Maize: The USA shows the largest amplitude in production anomalies and is roughly 2.5 times larger in production than the second and third baskets (China and Eastern EU & Ukraine). There is a strong asymmetry in the USA, with a long tail towards the minimum and higher density in the maximum. This pattern is found in both area and yield – suggesting that production anomalies are driven by covariation in yield and area, with many positive anomalies offset by more sporadic (low likelihood), extreme (high impact) losses. The USA contains most of the variability in production. In other baskets the distribution of production, area and yield are more symmetric. The largest producers show a high variability in all three variables; the smallest producers show comparatively more variability in area than in yield. About half of the baskets show a large variability in yield, with the most sensitive regions being USA, Eastern Europe & Ukraine, Argentina, South Africa and Central Europe.

Soybean shows the lowest variability in the distribution of anomalies in production and yield: about three to four times lower than the variability of maize yields and between 50 to 80% of the variability observed in wheat yields. Yield distributions are more similar among baskets than the other two crops. Most of the variability is concentrated in the top three producers. The variability of soybean production in the USA seems more influenced by the planted area than by the yield. Argentina's soybean production is more influenced by variability in yield; southern Brazil shows great variability in both planted area and yield.

Wheat production shows the second largest variability in production after maize. The largest producers show asymmetry in production toward negative values. India and Pakistan, despite being a major producing region, is distinguished by low variability in production; this is due to both a low variability in planted area but also, notably, the most stable yields among all the baskets. Eastern Europe & Russia show the highest variability of all baskets, with high variability in planted area and

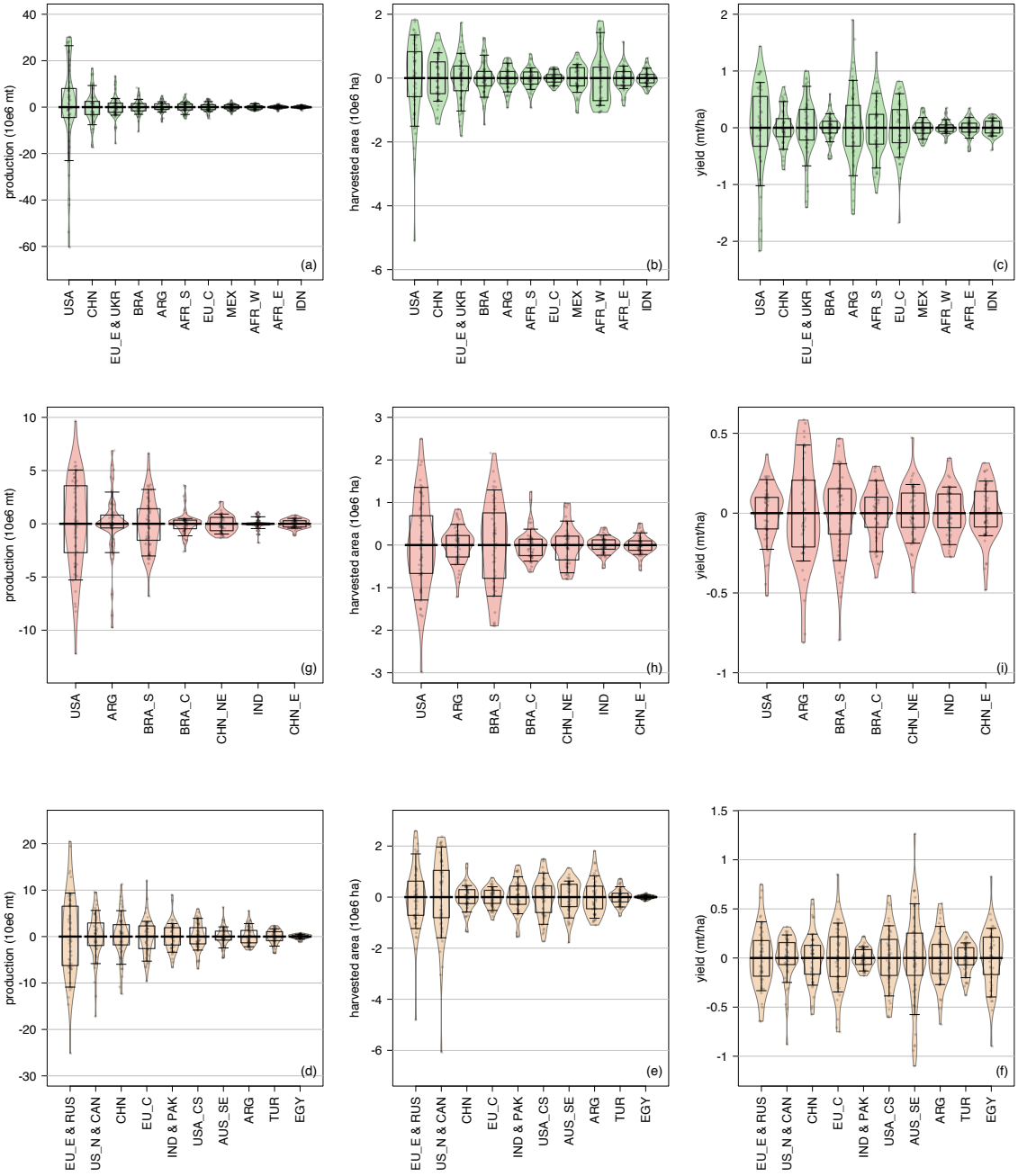

Figure 2.3: (a)–(f) Box plots of production (mt/ha), area (ha) and yield (mt/ha) residuals for maize (green), soybean (red) and wheat (orange). Residuals are calculated each year for the period 1961–2012 for each basket (section 2.2.4, equation 2.2). Box plots limits represent the 25th, 50th and 75th percentiles. The arms extend to the 10th and 90th percentiles. The beans represent the smoothed density distribution of the data and extend to the maximum and minimum values. Baskets are ordered by decreasing standard deviation in production.

compounded by high variability in yield. Australia displays the highest variability in yield. Egypt, the smallest producer, has a roughly constant planted area but the second largest variability in yield. The highest interannual variability in wheat yields is concentrated in dry regions with hot summers.

Concentration of production in the topmost baskets

Figure 2.4 depicts the temporal evolution of the Simpson index. Figure 2.5 depicts the evolution of the spatial distribution of planted areas for each crop and each basket during the study period, as percentages of the world's total planted area for each crop.

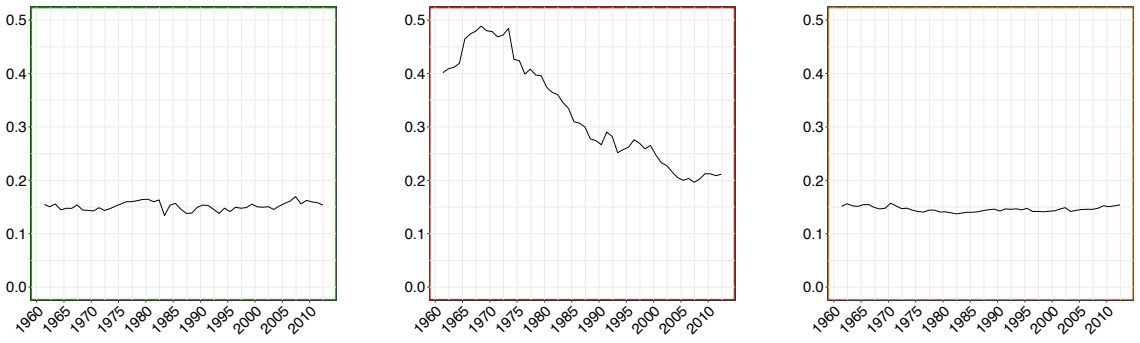

(a) Maize (b) Soybean (c) Wheat

Figure 2.4: (a)–(c) Simpson diversity index for maize ((a), green), soybean ((b), red) and wheat ((c), orange) across all baskets for the period 1961–2012.

Maize shows relative stability in the lowest-producing baskets. The major expansion of maize in the USA (up by 65%) was buffered by the changes in other baskets. Maize area distributions are marked by the reallocation of production to China, which displays the steepest increase, gaining roughly 5% of the world planted areas between 1961 and 2012 (China more than doubled its total cultivated area) as well as increases in production in Brazil and Africa. In the same period, Eastern Europe and Ukraine show the biggest loss in percentage of world production, as area expansion ceased. The concentration of maize in the USA is notable, as the USA also shows the highest variability in maize yield.

Soybean: The higher Simpson index value for soybean (Figure 2.4b) shows that its production is the most spatially concentrated of the three crops. Moreover, the evolution of the index over time bears a striking resemblance to the time series of the proportion of soybean worldwide that is grown in the USA. This high concentration of soybean in the USA necessarily implies a high risk to the global supply if the US soybean crop were to fail. The index is marked by four structural changes: (a) a

short increase in concentration until the late 1960s driven by the concentration of production in the USA; (b) a stagnating trend until the mid 1970s due to unchanging planted area in the USA, together with a decrease in China and Egypt, balanced by an increase in South America; (c) a downward trend until the mid 2000s, driven by the increase in planted area in South America, while the rate of area expansion in the USA declined or even stagnated from 1980 to 1995, accompanied by an increase in planted area in India, Argentina and Central Brazil; and (d) a stabilizing trend from the mid 2000s onward. Argentina shows the largest increase in planted area.

Despite the concentration of soybean production, however, there was an overall de-concentration towards 2012. In 1961, the top three baskets accounted for over 66% of the world acreage and 74% of the global production of soybean. These numbers declined to 48% (acreage) and 54% (production) in 2012 (SI, Tables 2.3 and 2.4).

Wheat shows a redistribution of planted area over time. The planted area of wheat in India and Pakistan increased 2.5–fold, while Eastern Europe and Russia showed decreases of about 30%. The northern USA and Canada show a singular pattern, with a sharp increase (up by 50%) in acreage between the 1970s and 1995; the acreage then returned to 1970s levels from the 2000s onward. There was a major reduction of planted area in Eastern Europe and Russia. The concentration of wheat in the topmost baskets is an issue, given its high yield variability (Figure 2.3).

India's most notable feature in this analysis is to have increased its planted areas of soybean and wheat so rapidly, to become the single major producer in Asia. China on the other hand stands out by a massive expansion in just one of the crops, i.e. maize.

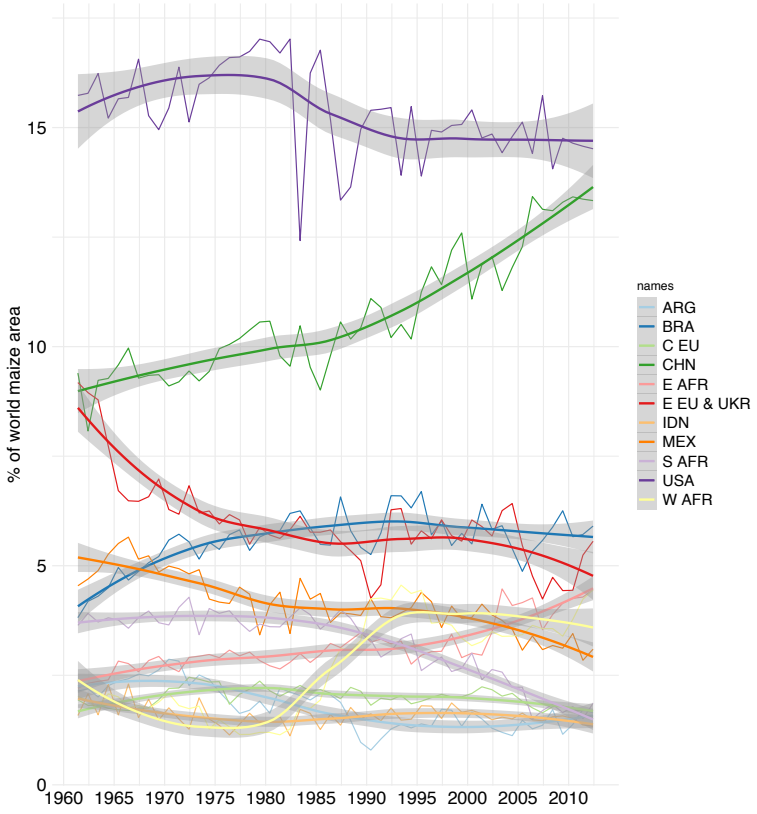

(a) Maize

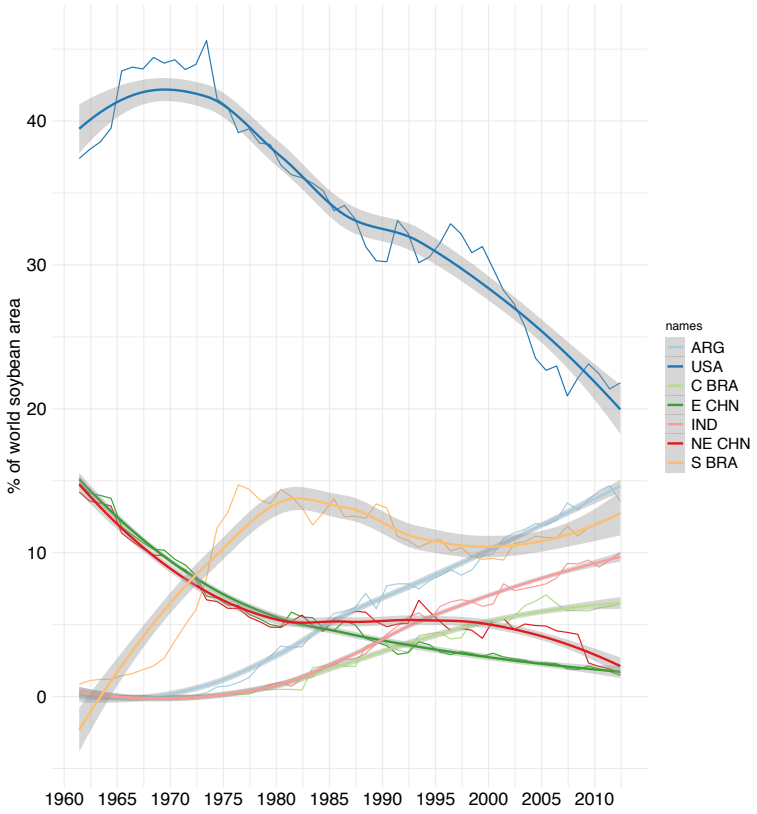

(b) Soybean

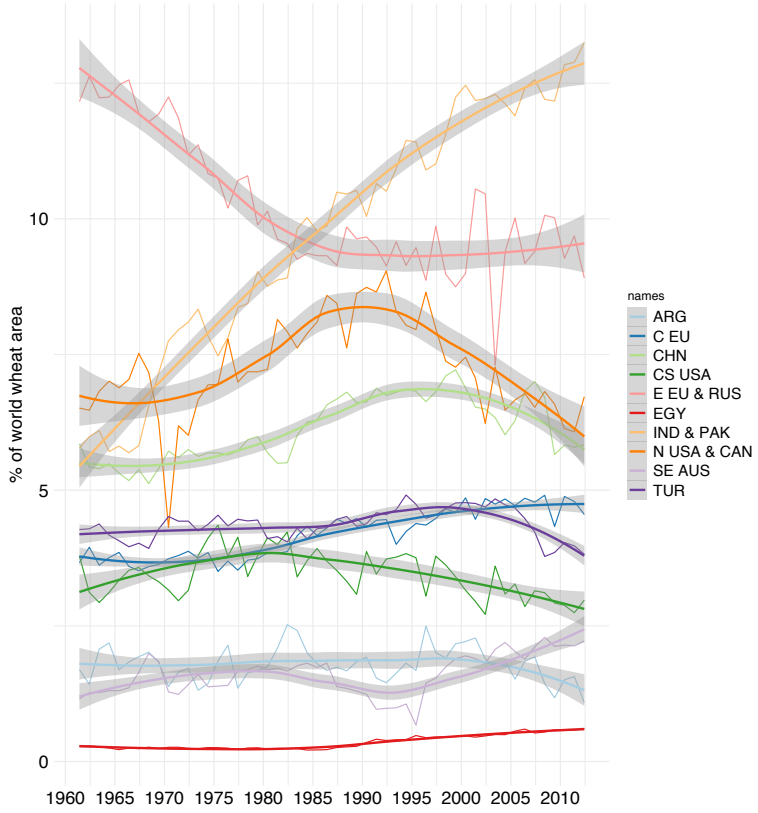

(c) Wheat

Figure 2.5: Spatio-temporal evolution of the distributions of cultivated areas in % of the total global cultivated area among baskets between 1961 and 2012 for maize, soybean and wheat.

2.3.3 Factor dominance in the variability of crop production

Crop production is the product of yield and planted area. The latter is driven by economic factors including incentives, trades and prices. The acreage is known early in a crop season. Yield variations however are strongly influenced by climate – about a third of yield variation is due to climate variability, according to Ray et al. (2015) – as well as by technologies, genotypes, agricultural practices and soil properties. Because of the structural nature of acreage, its interannual rate of change is expected to be lower than that of changes in yield, which are more uncertain in spite of the global upward trends in yield between 1961 and 2012. Shocks in production are thus less likely to stem from shocks in planted area (e.g. maize in the USA basket in 1983). For the same reason, acreage has been used as an important proxy for estimating crop production at the beginning of the season, whereas yield is not known until the harvest.

In this section I decompose the changes in production in changes in yield and changes in area and enquire as to the leverage of these two variables on the change of production. The goal is to make progress in the global analysis of systemic risks in global food security, by profiling baskets according to the dominance of changes in yield, harvested area or both.

Trends, contributions and leverage: Figure 2.6 depicts the evolution of production, yield and acreage. The trend (blue dotted line) was calculated using the method described in section 2.2.4. The bottom two bar plots, both colour-coded, represent the *contribution* and *leverage* of each factor. The contribution is a stacked bar plot with dA in brown and dY in yellow.

Eight classes of leverage on production are distinguished by a colour code. Increases in production are represented in green, pale green, light brown and pale yellow; reductions in red, orange, brown and yellow. The eight cases are defined as follows:

- *Green*: increasing production due to area and yield increases, with area dominant.
- *Pale green*: increasing production due to area and yield increases, with yield dominant.
- *Red*: declining production due to area and yield decreases, with area dominant.
- *Orange*: declining production due to area and yield decreases, with yield dominant.
- *Light brown*: increasing production, with increasing area outweighing declining yield.

- *Brown*: declining production, with declining yield outweighing increasing area.
- *Pale yellow*: increasing production, with increasing yield outweighing declining area.
- *Yellow*: declining production, with declining yield outweighing increasing area.

Heatmaps: Figure 2.7 shows heatmaps of the frequency of type of leverages for the three crops considered. The leverages are coded as `(1)(2)L`, with `(1)` being the sign of dA and dY (where for example `(++)` means both are positive), `(2)` being the sign of the change in production, and `L` being the dominant driver (`A` for area, `Y` for yield).

PCA (Figures 2.7b, 2.7d and 2.7f): for **maize**, Table 2.8 indicates that the first principal component contrasts the dominance of harvested-area leverage (right side) versus yield leverage (left side). The second component, although it explains a much smaller proportion of the variance, shows a strong negative correlation with baskets that experience production losses due to a simultaneous reduction of harvested area and yield. For **soybean**, the contributions and correlations are less clear. The first principal component broadly divides the baskets between those showing production gains due to a simultaneous increase in yield and harvested area (left side), and those showing production gains due an increase in yield that compensates for a reduction in harvested area (right side). The second principal component is mostly explained by a positive covariance in yield and harvested area leading to a positive gain in production (Table 2.8). The first principal component for **wheat** contrasts baskets where production gains are due to a strong leverage of yield (left side) versus those showing a stronger leverage of harvested area (right side). The second principal component contrasts baskets with production losses due to both yield and harvested area with other baskets.

At the global level, harvested area is the leading proxy for production

Aggregating at the global level and considering all crops together, production shows a greater positive correlation with acreage (0.77, $p < 0.01$) than with yield (0.65, $p < 0.01$). This correlation appears in Figures 2.2, 2.12 and 2.13. There is a striking resemblance between the ordering of baskets as a function of the average production, and their ordering as a function of average harvested area. In terms of **acreage**, there was a large predominance of wheat in 1961, representing 90 Mha, followed by maize (57 Mha) and soybean (16 Mha). Planted areas of wheat increased until the 1980s and have been on a slight downward slope since then, reaching 106 Mha in 2012. Meanwhile maize and soybean

showed a steady increase (soybean the fastest), reaching 100 Mha and 70 Mha respectively in 2012. In terms of **yield**: maize is the highest yielding crop, while all three crops showed increase in yield, with maize showing the steepest slope. In terms of **production**: wheat and maize showed similar levels of production until 1995, when maize production took off while wheat production declined.

Variations in yield versus area: regional contrasts

A general inference from Figures 2.6 and 2.7 is the heterogeneity of patterns across crops and baskets. This section does not profile each basket, but rather describes the general features of the topmost baskets. I let the Figures speak for themselves as regards the finer details. I use the term positive covariance to refer to the situation when yield and acreage variation have the same sign, and negative when they have opposite signs.

Maize gains in production display a strong pattern and are mostly influenced by a positive covariance of yield and acreage, with yield dominant, especially in the largest baskets (USA and China). In Indonesia, by contrast, gains and losses are mostly driven by changes in acreage (Figures 2.6e, 2.7a and 2.7b). The Indonesian basket is not of major importance for the production of maize; but this trait reveals the importance of considering the leverage in a systemic risk analysis, as planting decisions here apparently outweigh weather-related risks. This trait is also observed in Mexico, where variability in production is due to a greater leverage of acreage relative to yield.

With regards to losses, the USA and East Africa show a very high potential climate sensitivity as negative increments in production are mostly due to yield failure, even when acreage increases. Overall, maize shows a high yield dominance (for both gains and losses), indicating a potential important sensitivity of the crop to weather impacts or agricultural practices.

Soybean shows a greater heterogeneity across baskets, linked to the changes in soybean production dynamics described in section 2.3.2. Originally concentrated in the USA, soybean production rapidly expanded in Southern America and South East Asia, thus production increased due to increasing acreage. In some baskets including India the change in acreage dominated up to the 2000s, later becoming almost insignificant as the acreage stabilized.

Production losses for soybean were most often due to yield losses (or crop failures) in the topmost baskets (USA, Brazil, Argentina). Soybean production in China is small but characterized by large variability in both yield and acreage.

For **wheat**, year-on-year changes in production were influenced by a positive covariance of yield and acreage, with yield dominant. Egypt provides an exception, characterized by a dominance of acreage and a low influence of yield. Production changes in Turkey and Australia show a high sensitivity to interannual yield variations and were particularly affected by crop failures. Argentina shows no strong pattern.

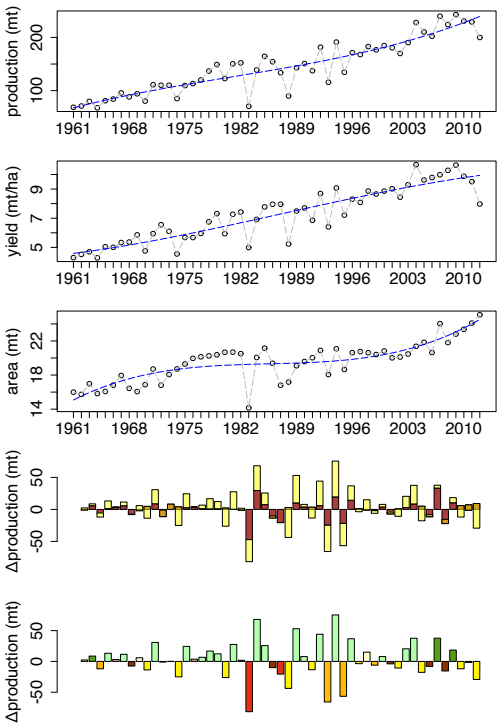

(a) Maize USA

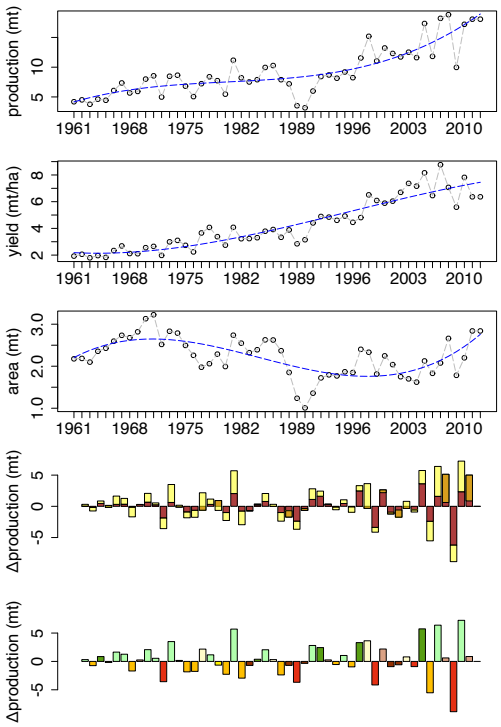

(b) Maize Argentina

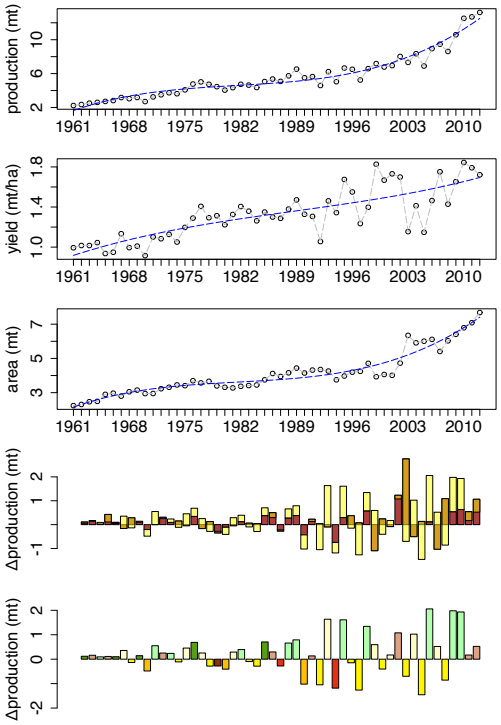

(c) Maize East Africa

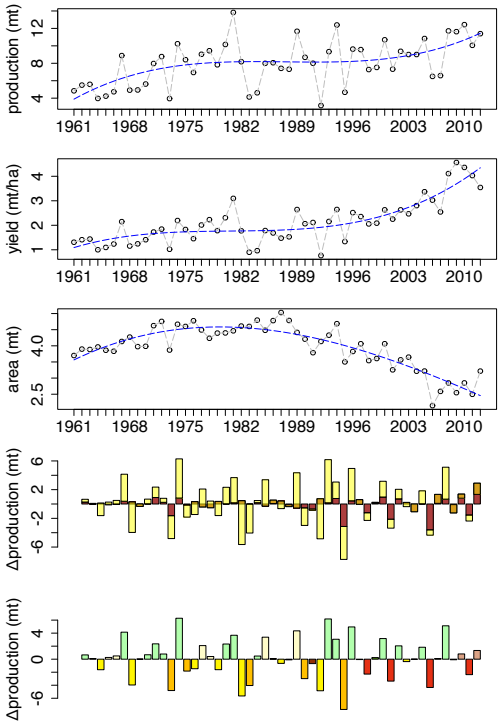

(d) Maize South Africa

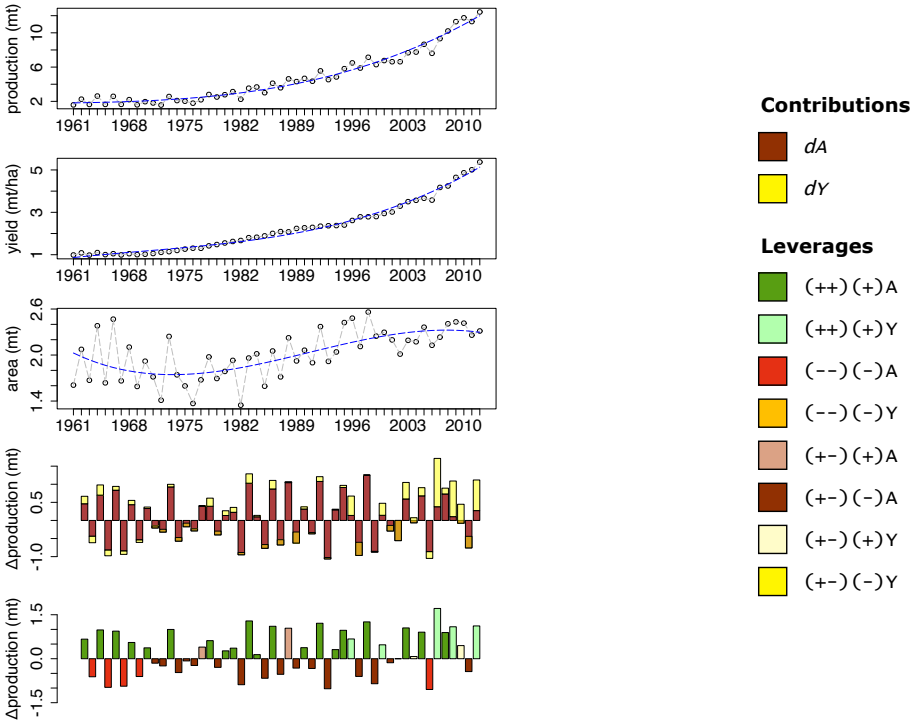

(e) Maize Indonesia

(f) Legend

Figure 2.6: Maize production (mt), yield (mt/ha), area (ha), yield and area contributions to the production and leverages (top to bottom of each panel), in the USA, Argentina, East Africa, South Africa and Indonesia (from top left to bottom right).

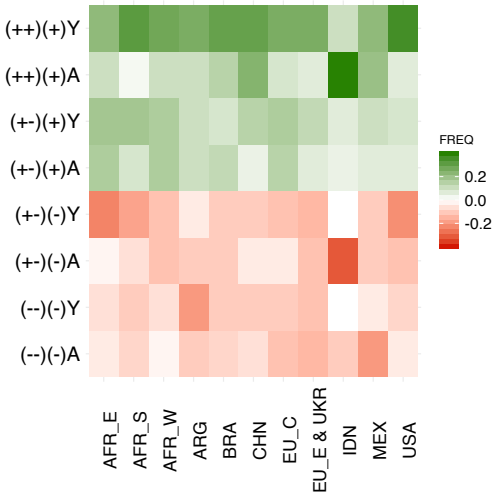

(a) Maize heatmap

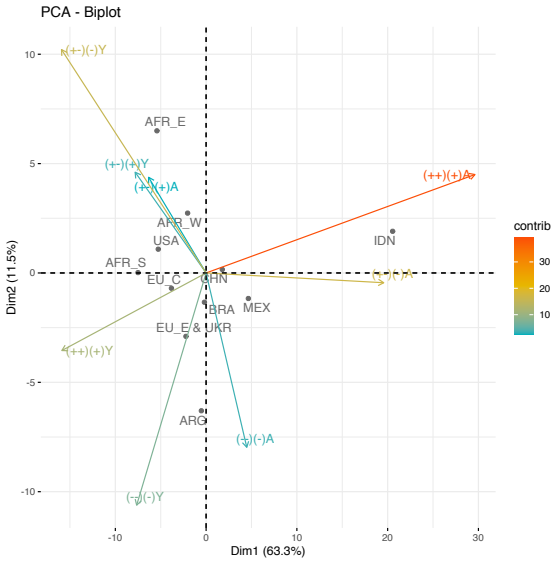

(b) Maize PCA

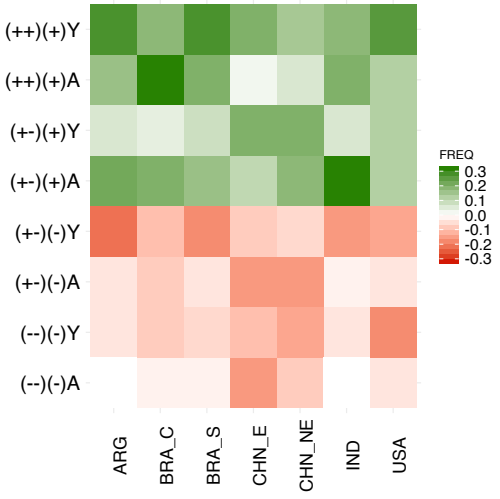

(c) Soybean heatmap

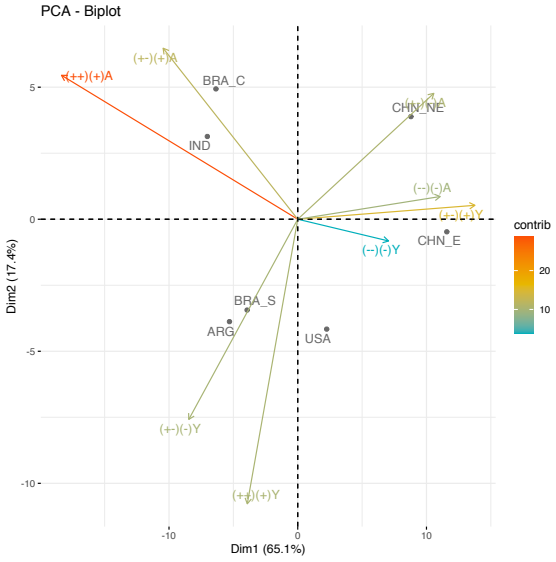

(d) Soybean PCA

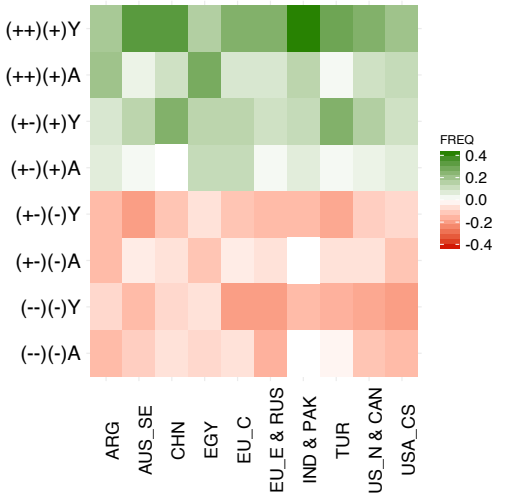

(e) Wheat heatmap

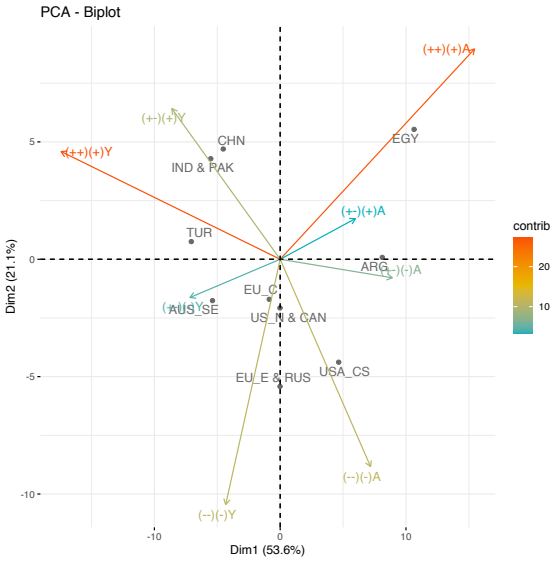

(f) Wheat PCA

Figure 2.7: Heatmaps and Principal Component Analysis (PCA) of the leverages of yield and area in baskets, from top to bottom: maize (a)–(b), soybean (c)–(d) and wheat (e)–(f). Variables (leverages) are colour coded according to their contribution (in percentage) to the first principal component (Dim1), (see Section 2.6, Table 2.10).

2.4 Climate sensitivity of crop production

Potential impacts of climate change on yield have been assessed by running "process-based" crop models with input from climate models. However, there are still large differences among the results of different models (Guereña et al. 2001, Busuioc & von Storch 2003, Webb et al. 2013, Rosenzweig et al. 2014). An alternative approach, adopted here, is based on the empirical analysis of yield data in relation to agroclimatic variables.

Numbers of hot days (nHotDays) and Killing Degree Days (KDD) have both been shown to be good proxies for the effect of heat stress on the yields of grain crops generally (Schlenker & Roberts 2006, 2009, Gourdji et al. 2013, Butler & Huybers 2013, 2015, Chavez et al. 2015). These studies have mostly been focused on national or regional crop production. Extending this approach globally to the case of maize, soybean and wheat baskets (Figures 2.8, 2.9 and 2.10), a high correlation emerges between the number of days when temperature exceeds 32°C, and a reduction in yield. The results however are not identical for every basket, or for every crops. Not every basket shows negative responses – either to the number of hot days, or the cumulative amount of killing degree days.

The most outstanding feature of the spatial response of yield to heat stress is the strong contrast between the USA and everywhere else. In all baskets, yield shows an overall response to heat stress that is either positive or negative, but with spatial variability within the basket. USA maize, USA soybean and USA/Canada wheat are the only baskets showing a homogeneous negative correlation, and these baskets present the highest correlations and the greatest proportion of significance (proportion of pixels in the basket with $p < 0.05$). In the USA, correlations go up to 0.79, with associated yield losses that can be as large as 6 metric tons per hectare for maize – about half of the average yield of a state such as Iowa, a major producer.

Eastern Europe shows the second highest correlation, after the USA, between heat stress and yield loss, with correlation of 0.78 for maize and 0.64 for wheat. Another important characteristic of the Eastern European baskets is a west/east dipole with Romania, Bulgaria, Hungary, Slovakia and the western part of the Ukraine showing negative responses to heat stress, while the rest of the basket (central and eastern Ukraine, Russia) shows a medium to strong positive correlation of yield with nHotDays or ΣKDD for both maize and wheat (up to 0.53 and 0.64 respectively).

In South America the response is relatively homogeneous for maize and soybean. In Brazil, yield is mostly positively affected by nHotDays and ΣKDD, while the response is negative in Argentina.

Wheat in Argentina shows a mixed response.

In Central America, Western Europe, Africa and Asia, the most noticeable trait of the response is the high heterogeneity of its spatial distribution and amplitude, and a heterogenous response across crops where baskets overlap. In these four regions, the correlations vary between -0.7 to +0.7, and the proportion of significance relative to the basket is much lower than in the rest of the world. Furthermore, and in the same regions, the correlations of yield with nHotDays and ΣKDD differ the most, and can be of opposite sign – whereas they are mostly of the same order of magnitude and sign in the other baskets. The India/Pakistan wheat basket illustrates this last point clearly on Figure 2.10: in Uttar Pradesh and Punjab, the yield response to nHotDays is positive, while the response to ΣKDD is negative. The explanation for this counterintuitive behaviour might lie in a positive correlation of long hot periods with high solar radiation, combined with damage at very high temperatures.

Table 2.1 summarizes the year-to-year changes in critical temperatures ($> 32°C$) and yield losses over the different baskets. More than two-thirds of the largest yield losses (i.e. the largest year-on-year reduction in yield: Table 2.1) were associated with a positive anomaly of ΣKDD or nHotDays (64%, 86% and 70% for maize, soybean and wheat respectively) and over 40% were associated with anomalies greater than 1.5 standard deviations (71%, 50%, 43% for maize, soybean and wheat respectively). Two further general points can be drawn from Table 2.1. First, the largest losses match record-breaking heatwave events, as described in Coumou & Rahmstorf (2012). Second, the USA once again appears as a special case. In all baskets, roughly 50—75% of the largest losses occurred post-2000, whereas in the USA, 50–75% of the largest losses occurred pre–2000.

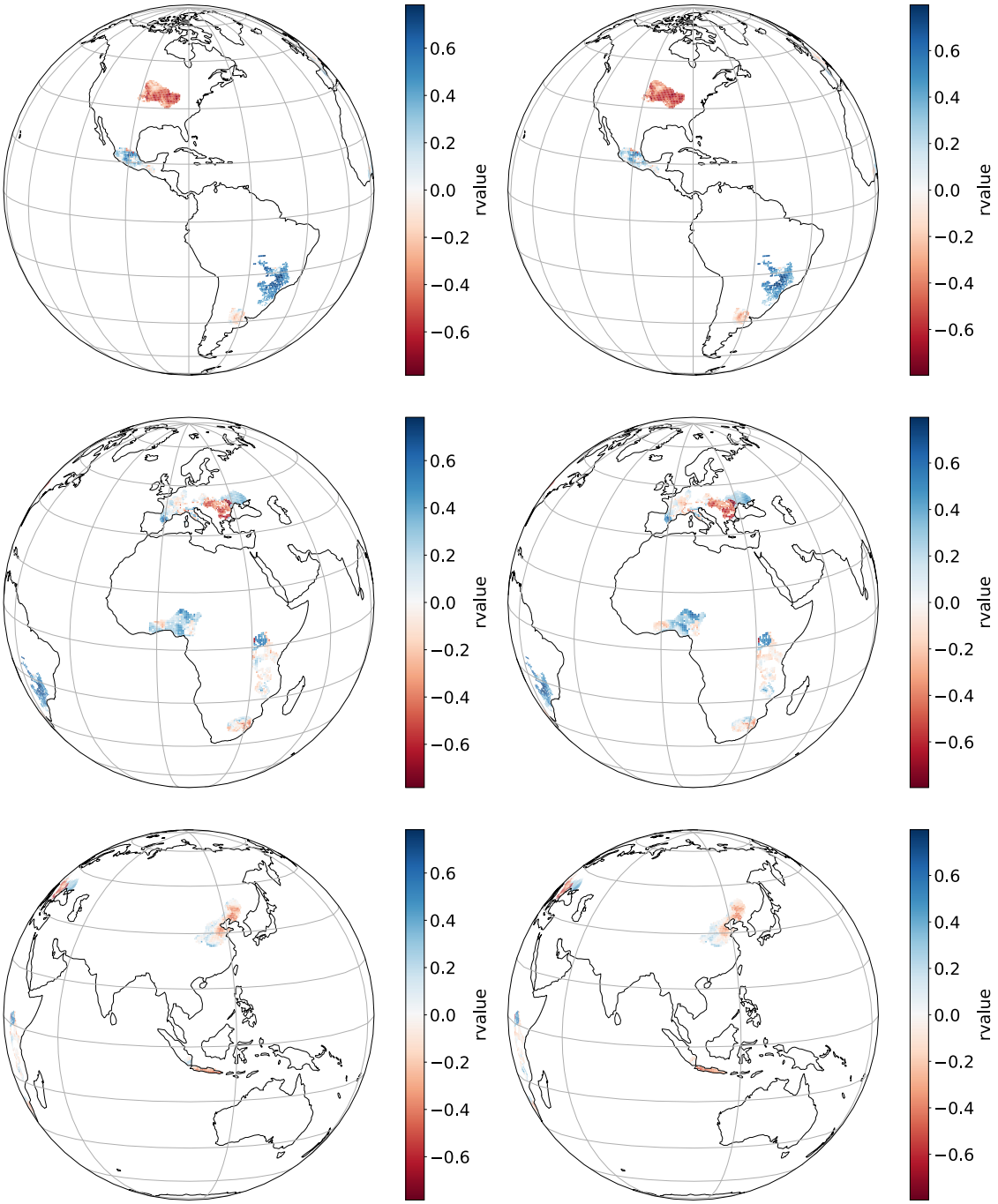

Figure 2.8: **Maize** yield and heat stress. Correlation between number of hot days and maize yield (left panels) and ΣKDD and maize yield (right panels). The coefficient of correlation used is the Pearson correlation coefficient, computed using the `linregress` function from the Python library `scipy.stats`.

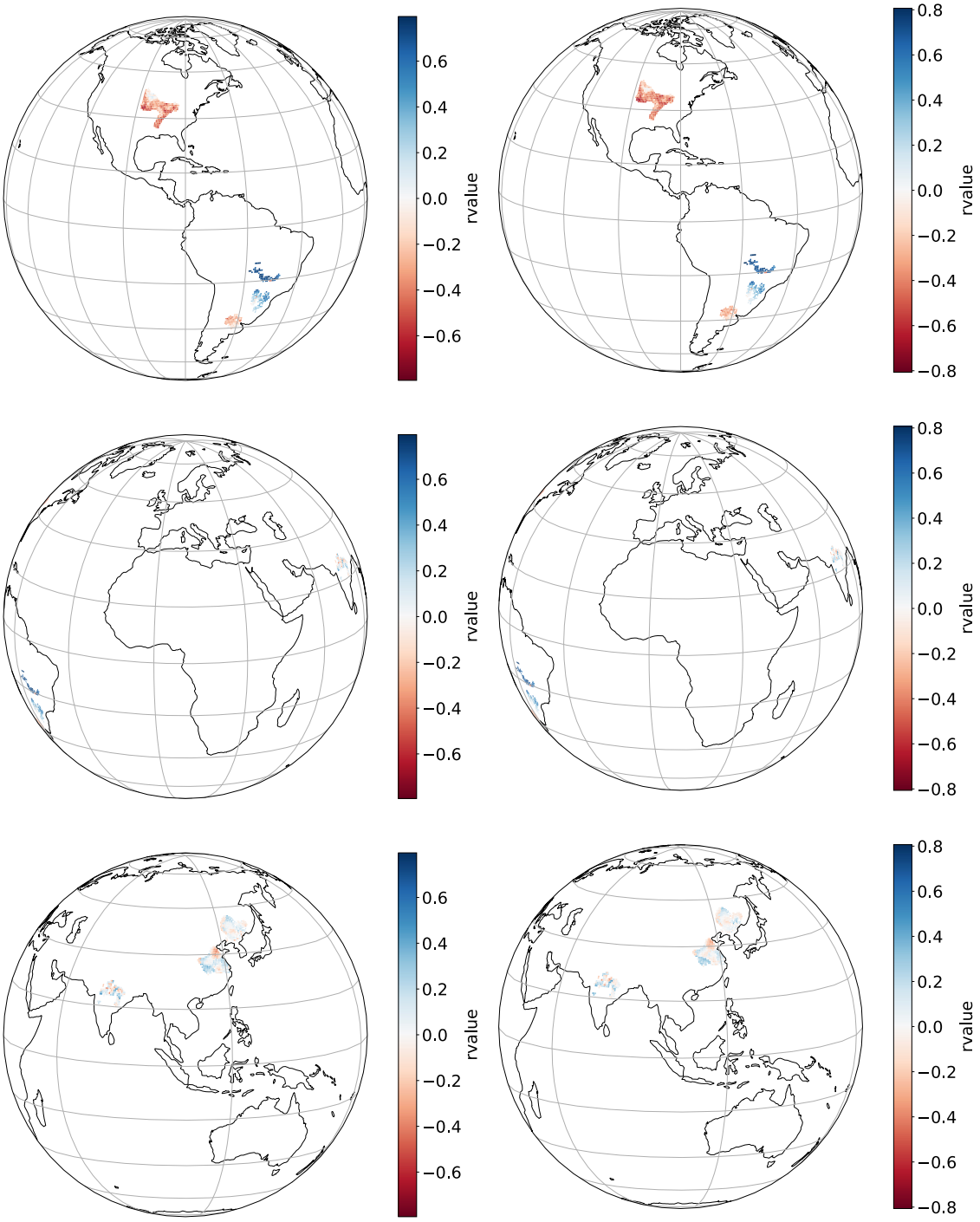

Figure 2.9: **Soybean** yield and heat stress. Correlation between number of hot days and soybean yield (left panels) and ΣKDD and soybean yield (right panels). The coefficient of correlation used is the Pearson correlation coefficient, computed using the `linregress` function from the Python library `scipy.stats`.

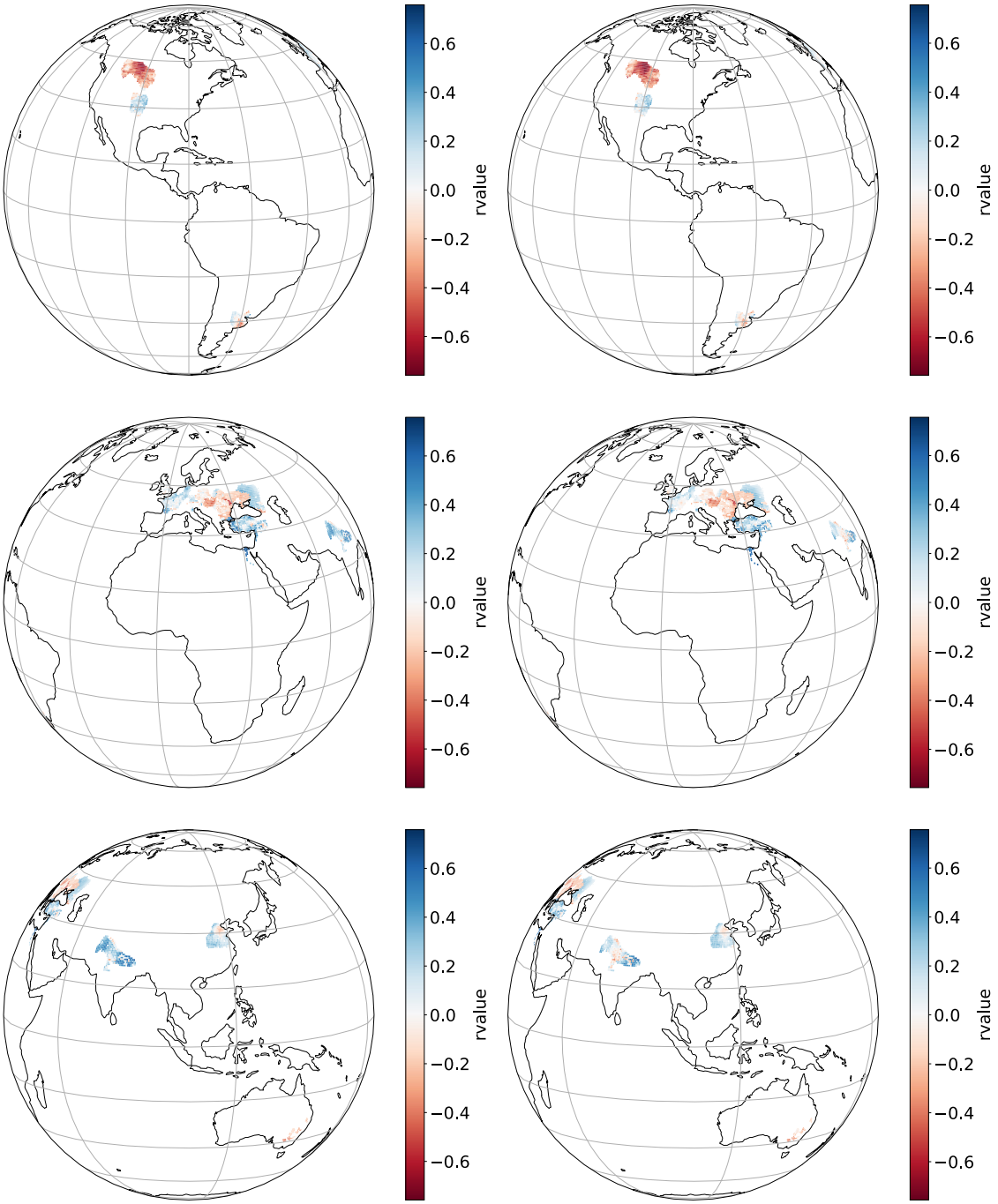

Figure 2.10: **Wheat** yield and heat stress. Correlation between number of hot days and wheat yield (left panels) and ΣKDD and wheat yield (right panels). The coefficient of correlation used is the Pearson correlation coefficient, computed using the `linregress` function from the Python library `scipy.stats`.

Crop	Basket	Largest yield loss	Change yield (%)	Year	% Global production	Change nHotDays (%)	nHotDays anomaly*	Change ΣKDD (%)	ΣKDD anomaly*
MAIZE	ARG	-1.7	-20.89	2006	1.72	16.75	0.6	46.28	0.8
	BRA	-0.58	-11.55	2009	5.35	4.39	0.14	10.1	0.42
	C EU	-2.02	-21.45	2003	3.34	210.78	2.98	330.9	3.09
	CHN	-1.21	-21.72	1997	11.99	145.98	2.41	149.87	1.96
	E AFR	-0.54	-32.05	2003	1.15	3.16	1.2	12.83	1.57
	E EU & UKR	-1.87	-39.93	1992	4.53	110.91	-0.39	145.96	-0.73
	IDN	-0.09	-2.4	2006	1.10	3.98	0.56	-5.2	-0.11
	MEX	-0.38	-10.9	2011	1.7	14.25	1.6	19.44	1.82
	S AFR	-1.35	-63.9	1992	0.6	108	1.68	143.67	1.69
	USA	-2.29	-26.26	1993	24.58	73.55	-0.72	86.96	-0.69
	W AFR	-0.22	-13.44	2000	1.02	3.63	-0.06	0.94	-0.2
SOYBEAN	ARG	-1.18	-39.03	2009	11.21	10.3	1.7	6.24	1.27
	C BRA	-0.51	-15.53	2012	7.87	-6.3	0.5	-3.56	0.8
	E CHN	-0.41	-22.23	2005	1.45	20.66	0.96	45.92	1.8
	IND	-0.28	-23.8	2004	3.11	1.25	0.4	-0.35	0.51
	NE CHN	-0.34	-17.27	2000	3.93	35.25	2.15	39.96	1.68
	S BRA	-0.91	-31.54	2004	9.80	-4.38	-0.23	-24.76	-0.8
	USA	-0.44	-15.11	1995	38	41.85	0.32	102.01	0.32
WHEAT	ARG	-0.96	-29.82	2008	1.06	47.66	1.19	42.64	0.97
	C EU	-0.74	-9.56	2010	11.53	19.61	0.4	23.32	0.44
	CHN	-0.78	-15.54	1998	11.1	-30.39	-0.23	-35.77	-0.7
	CS USA	-0.6	-20.58	2000	2.68	57.27	1.44	78.47	0.94
	E EU & RUS	-0.65	-17.56	2012	8.77	62.16	1.81	71.64	1.6
	EGY	-0.81	-12.67	2010	1.10	12.18	2.68	28.38	3.06
	IND & PAK	-0.13	-4.26	2001	12.87	-3.05	0.33	-7.14	-0.21
	N USA & CAN	-0.37	-15.94	2001	5	53.37	1.12	68.29	0.97
	SE AUS	-2.20	-69.19	2006	0.65	21.22	1.86	20.82	1.72
	TUR	-0.39	-16.54	1999	3.4	-8.69	0.26	-16.79	0.16

* Standardized anomalies

Table 2.1: Year to year change in critical temperatures (> 32°C) and yield losses. The table shows the largest change in yield per crop and basket as a function of change in nHotDays and ΣKDD during the period 1979 to 2012, based on the WATCH Forcing Data ERA Interim climate dataset (Weedon et al. 2014) three-hourly data set.

2.5 Discussion and conclusions

This chapter brings new perspectives to the large-scale analysis of crop production dynamics. The concentration of crops in regions with above-average variability inflates production variability at the global scale (Figure 2.3 and Table 2.5). Most of the global variation in maize production can be attributed to the topmost producers, above all the USA; this concentration carries a substantial risk because of the exceptionally high sensitivity of US maize yield to heat-related stress (Figure 2.8). Soybean has shown the most significant structural changes of the three crops considered. However the redistribution of soybean production, with increased in acreage in South America, did not reduce global production variability – as Brazil and Argentina have shown comparable levels of variability in production, and even greater variability in yield, than the USA. The contrasting responses to heat-related stress of Brazil and Argentina nonetheless may alleviate the risk of crop failures induced by climatic events. For wheat, production interannual variability is generally less contrasted in the top most producers except for the Eastern Europe & Russia basket. The expansion of wheat cultivation in China, with muted yield variability, has contributed to stabilizing production. India and Pakistan, with low variability in both acreage and yield, represent a further potential to decrease systemic risk to the global production of wheat.

Given their importance in the world supply, a drop in yield in one major basket can substantially impact global production. Strong correlations between weather patterns and yield variations have been identified in main producing regions. However I found no significant correlations in food-insecure regions (mostly Africa), (Figures 2.8, 2.9 and 2.10). This does not mean there is no impact, but suggests a more nuanced picture. More generally, the concentration of crop production in baskets represents a risk mainly because of their weight in the world supply, while food-insecure regions represent a risk because less productive areas are associated with higher risks of drought.

In order to maximise agricultural production, allocating cultivated areas to the highest-yielding regions might seem to be a good strategy. In the context of climate change, however, the resulting concentration of production increases the systemic risk for global food security. The results of this chapter highlight the potential benefits of promoting yield and acreage stability over maximizing output. This point is well illustrated by the case of the USA and Eastern European baskets, both of which show high sensitivity to heat-related stress. East and South East Asia present significant potential for "deconcentration" of this risk.

Stock levels are an additional issue. Relative to global consumption, stock levels of major crops have shown a downward trend. In 2012, the ratio of year-end stocks of wheat to global consumption was 3.5 months – down by half from 1961, with a downward trend of nearly one day of stock resilience lost every year between 1961 and 2012 (FAOSTAT (2016)). Declining stocks, relative to consumption, imply decreasing resilience in the global food system even in the absence of climate change.

Given current trends in production versus demand, diets, and concentration of production, there is a need to improve the resilience of global agriculture and address its main vulnerability, which is climate change (Ray et al. 2015, Porter et al. 2019). I have drawn attention to the potential gain in resilience through producing more food on a smaller area, which can be achieved by closing yield gaps. Results presented in this chapter also suggest the possibility of increasing resilience by diversifying the regions where major crops are grown.

A few limitations relating to methodological and theoretical choices made in this chapter should be noted.

The first limitation concerns the choice of the measure of instability. Variance and standard deviation are commonly used metrics to quantify risk in production (Ben-Ari & Makowski 2014, Ben-Ari et al. 2016). In the present application standard deviation is used to quantify deviation from a trend; its meaning is therefore contingent, to some extent, on the method used for detrending. There are many alternative ways to fit a trend (Calderini & Slafer 1998, Iizumi et al. 2013, 2014, Licker et al. 2013, Ben-Ari & Makowski 2014), each with its advantages and disadvantages. On the other hand, some studies have indicated that measures of instability or volatility are relatively insensitive to the choice of detrending method (Ben-Ari & Makowski 2014, Ben-Ari et al. 2016, Cernay et al. 2015). This topic is treated in greater depth in Chapter 4 where I use an ensemble of time-series models to identify and quantify "shocks" in production, yield and area.

The second limitation concerns the choice of a common critical temperature threshold of 32°C (T_{kdd} as defined in section 2.2.2) for all regions and crops. A review of the literature on temperature stress effects on maize, soybean and wheat revealed a wide range of cardinal temperatures (that is, the optimal temperature for crop growth, and the low- and high-temperature thresholds beyond which negative impacts are seen), as well as the critical temperatures for severe damage (Porter & Gawith 1999). Variation in all of these quantities is to be expected among crop varieties, and with agronomic practices (for example, irrigation to support plant growth during periods of superoptimal

temperatures). Even the critical temperature T_{kdd} is not constant in reality. The literature supplies values ranging from 30° to 35°C for maize, 31° to 34°C for soybean, and 31° to 36°C for wheat (Hesketh et al. 1973, Porter & Gawith 1999, Egli et al. 2005, Schlenker & Roberts 2006, Setiyono et al. 2007, Cai et al. 2009, Abendroth et al. 2011, Butler & Huybers 2013, 2015, Gourdji et al. 2013, Asseng et al. 2015, Teixeira et al. 2013, Sánchez et al. 2014, Chavez et al. 2015), thus providing no evidential basis for the use of different values for different crops. Information about the temperature tolerances of some specific cultivars exists, but by no means all, and in any case there is no global data source on which cultivars are grown in which areas. Therefore, the pragmatic decision was made to use a generic value of 32°C for T_{kdd}, being in the mid-range of published values for all three crops. It is possible that some of the apparent variation across regions in crop responses to nHotDays and KDD may be due to variations in T_{kdd} that could not be accounted for in this analysis.

The final limitation noted here concerns the summation of KDD over an annual period. This is a simplification, but it works on the premise that in spite of the heterogeneity in the crop calendar, growing phases are aligned to the seasons. Therefore, roughly speaking, crops will face similar temperatures across the different development phases, and stresses during the same phases. Heat stress, for example, is more likely to occur after the vegetative growth phase and in the reproductive development phase; suboptimal temperatures are most likely to be encountered during the early vegetative growth phase.

In conclusion: I have shown that the concentration of risk in limited regions (baskets) increases the exposure of the global food supply chain to production shocks, and implies an avoidably large sensitivity to climate change. I focused on heat stress as this is the most obvious risk to crop production in currently planted areas subject to a warming climate. In the next chapter I analyse the sensitivity of major crops to a more complete set of agroclimatic variables, including water stress variables.

2.6 Supplementary information

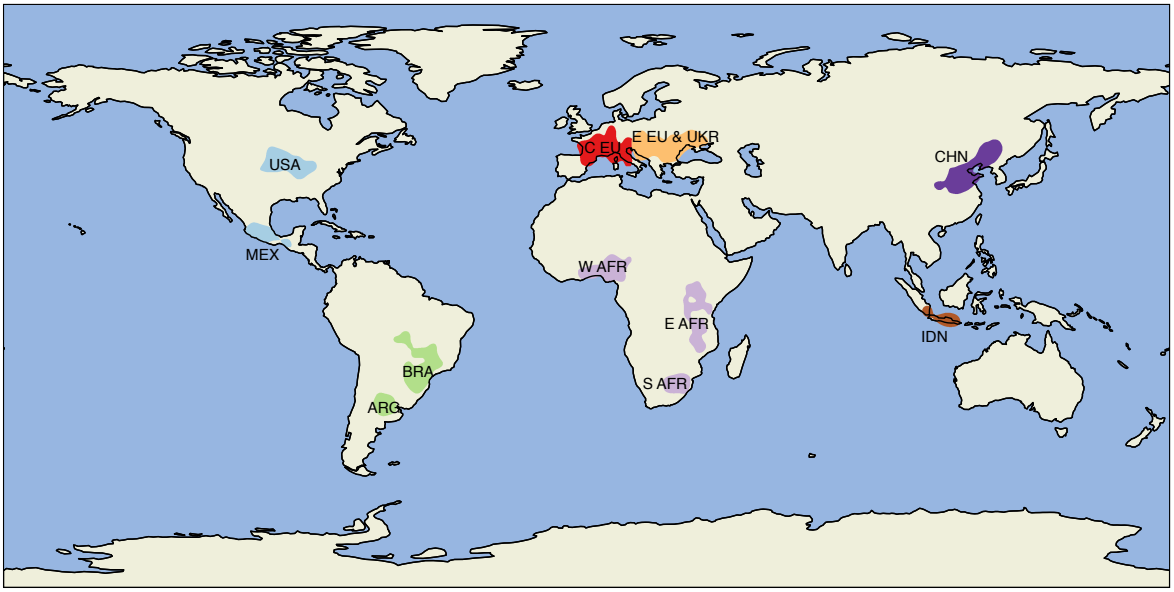

(a) Maize

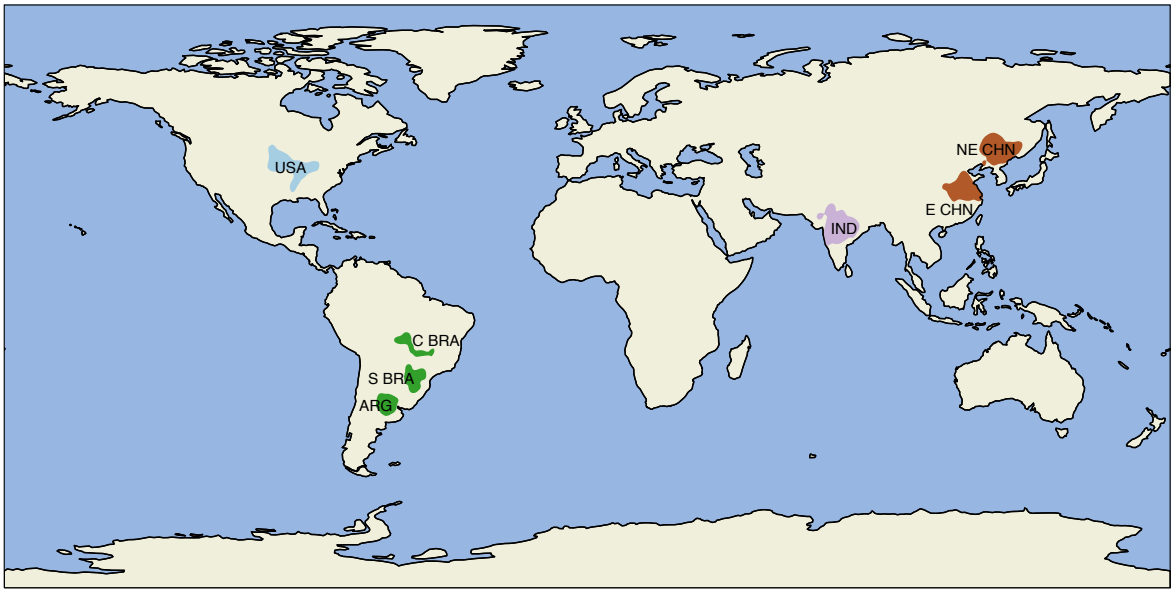

(b) Soybean

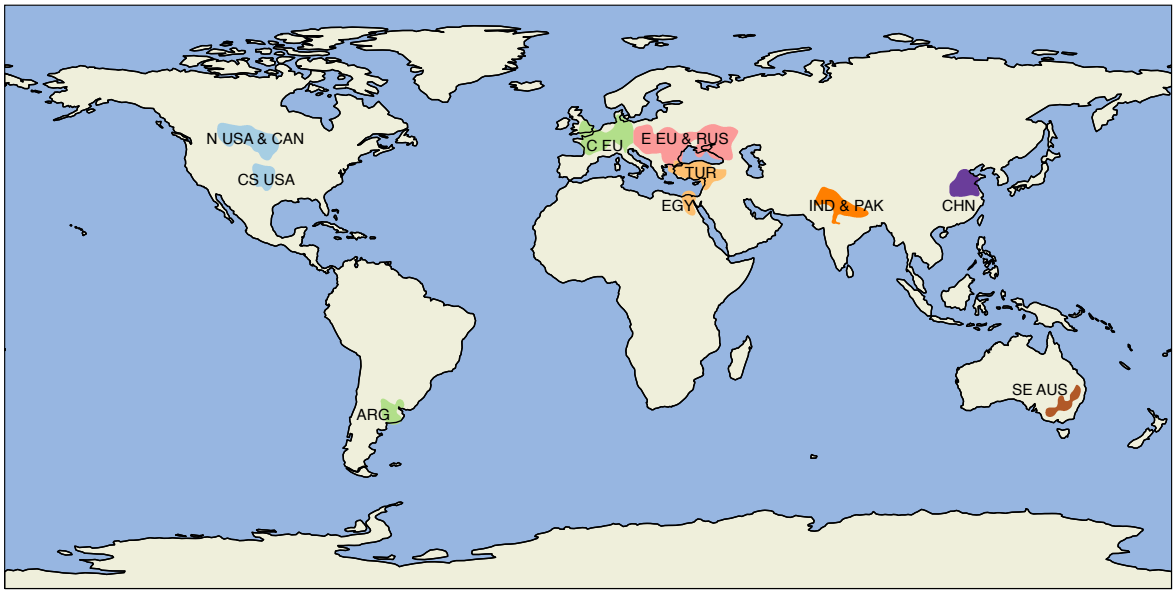

(c) Wheat

Figure 2.11: Maps of baskets for maize (a), soybean (b) and wheat (c). Baskets computed using the same bounding box share the same colour, with the exception of Europe, where a different color scheme is used to better distinguish baskets that are close neighbours or when their contours intersect (but not overlap by definition).

Bounding box	Basket short name	Basket long name
Maize		
North America	USA	United States of America
North America	MEX	Mexico
South America	BRA	Brazil
South America	ARG	Argentina
Europe	C EU	Central Europe
Europe	E EU & UKR	Eastern Europe and Ukraine
Africa	S AFR	South Africa
Africa	E AFR	East Africa
Africa	W AFR	West Africa
Asia	CHN	China
Asia	IDN	Indonesia
Soybean		
North America	USA	United States of America
South America	ARG	Argentina
South America	S BRA	South Brazil
South America	C BRA	Central Brazil
India	IND	India
Asia	NE CHN	North East China
Asia	E CHN	Eastern China
Wheat		
North America	N USA & CAN	Northern United States and Canada
North America	CS USA	Central United States of America
South America	ARG	Argentina
Europe	C EU	Central Europe
Europe	E EU & RUS	Eastern Europe and Russia
Europe	TUR	Turkey
Africa	EGY	Egypt
India	IND & PAK	India and Pakistan
Asia	CHN	China
Australia	SE AUS	South Eastern Australia

Table 2.2: Baskets: bounding boxes (used in the regionalization method), short names (as used in the Tables and Figures) and long names.

	1961				1980			
	production	% world (p)	harvested area	% world (ha)	production	% world (prod)	harvested area	% world (ha)
Maize								
USA	68,732,680	34.7	15,993,917	15.7	122,783,480	32.0	20,671,616	17.0
MEX	4,932,298	2.5	4,618,698	4.5	9,790,839	2.6	5,012,437	4.1
BRA	6,209,778	3.1	3,878,996	3.8	16,329,150	4.3	7,022,780	5.8
ARG	4,188,860	2.1	2,175,777	2.1	5,464,800	1.4	1,992,024	1.6
C EU	5,932,124	3.0	1,970,391	1.9	15,371,356	4.0	2,615,032	2.1
E EU & UKR	19,623,160	9.9	9,332,174	9.2	26,199,822	6.8	6,950,446	5.7
S AFR	4,840,296	2.4	3,699,567	3.6	10,155,099	2.7	4,399,280	3.6
E AFR	2,227,950	1.1	2,241,952	2.2	4,050,333	1.1	3,311,908	2.7
W AFR	1,622,714	0.8	2,057,997	2.0	1,451,432	0.4	1,458,524	1.2
CHN	12,226,714	6.2	9,551,825	9.4	42,624,312	11.1	12,897,462	10.6
IDN	1,587,653	0.8	1,608,094	1.6	2,775,278	0.7	1,786,370	1.5
Total	**132,124,227**	**66.6**	**57,129,387**	**56.0**	**256,995,902**	**67.1**	**68,117,878**	**55.9**
Soybean								
USA	15,142,563	57.4	8,673,554	37.4	37,292,248	46.7	18,398,590	36.9
ARG	629	0.0	635	0.0	3,055,679	3.8	1,749,153	3.5
S BRA	226,616	0.9	197,701	0.9	12,288,408	15.4	7,176,394	14.4
C BRA	2,701	0.0	2,215	0.0	469,716	0.6	253,779	0.5
IND	3,567	0.0	7,968	0.0	371,556	0.5	488,277	1.0
NE CHN	2,295,009	8.7	3,299,559	14.2	3,052,939	3.8	2,396,017	4.8
E CHN	2,080,296	7.9	3,437,628	14.8	2,475,507	3.1	2,427,423	4.9
Total	**19,751,381**	**74.9**	**15,619,260**	**67.3**	**59,006,053**	**73.9**	**32,889,632**	**66.0**
Wheat								
N USA & CAN	9,929,374	4.6	13,019,261	6.5	25,669,294	6.0	16,846,422	7.2
CS USA	12,648,192	5.8	7,570,912	3.8	20,606,464	4.8	9,609,345	4.1
ARG	4,584,334	2.1	3,385,655	1.7	6,716,880	1.6	4,070,895	1.7
C EU	18,628,446	8.6	7,322,058	3.7	43,779,756	10.2	8,965,504	3.8
E EU & RUS	41,433,312	19.1	24,310,806	12.2	68,322,480	15.9	23,636,662	10.1
TUR	7,817,148	3.6	8,545,647	4.3	18,296,098	4.3	9,575,180	4.1
EGY	1,394,218	0.6	563,122	0.3	1,686,000	0.4	539,476	0.2
IND & PAK	11,162,730	5.2	11,542,648	5.8	33,164,544	7.7	20,413,130	8.8
CHN	7,720,854	3.6	11,709,312	5.9	28,735,830	6.7	13,270,969	5.7
SE AUS	2,854,728	1.3	2,314,392	1.2	4,830,161	1.1	3,946,514	1.7
Total	**118,173,337**	**54.5**	**90,283,813**	**45.4**	**251,807,507**	**58.7**	**110,874,096**	**47.4**

Table 2.3: Total production and harvested area per basket, share of the world production (% world (p)) and harvested area (% world (ha)) in 1961 and 1980.

	2000				2012			
	production	% world (p)	harvested area	% world (ha)	production	% world (p)	harvested area	% world (ha)
Maize								
USA	184,547,136	31.5	20,826,802	15.4	199,867,392	23.4	25,069,828	14.5
MEX	12,372,209	2.1	5,166,844	3.8	18,257,368	2.1	5,345,142	3.1
BRA	25,555,082	4.4	7,434,032	5.5	60,459,080	7.1	10,198,078	5.9
ARG	13,229,335	2.3	2,246,866	1.7	18,070,016	2.1	2,839,674	1.6
C EU	26,535,458	4.5	2,820,001	2.1	26,933,288	3.2	2,929,177	1.7
E EU & UKR	22,026,854	3.8	8,172,211	6.0	37,349,408	4.4	9,598,900	5.6
S AFR	10,692,159	1.8	4,064,631	3.0	11,395,958	1.3	3,216,244	1.9
E AFR	6,775,178	1.2	4,061,459	3.0	13,219,824	1.5	7,680,010	4.4
W AFR	5,964,116	1.0	4,294,914	3.2	12,052,988	1.4	7,687,290	4.5
CHN	69,880,536	11.9	14,988,414	11.1	150,197,120	17.6	23,027,188	13.3
IDN	6,763,147	1.2	2,296,472	1.7	12,431,665	1.5	2,313,742	1.3
Total	**384,341,209**	**65.7**	**76,372,646**	**56.5**	**560,234,107**	**65.6**	**99,905,271**	**57.8**
Soybean								
USA	57,218,352	36.0	21,413,816	29.8	62,894,372	26.5	22,521,910	21.8
ARG	16,824,682	10.6	7,129,370	9.9	31,873,436	13.4	14,026,092	13.6
S BRA	17,279,416	10.9	6,904,065	9.6	32,945,250	13.9	13,175,141	12.8
C BRA	9,256,593	5.8	3,643,446	5.1	18,651,622	7.9	6,680,688	6.5
IND	4,540,308	2.9	4,631,990	6.4	14,044,230	5.9	10,327,638	10.0
NE CHN	6,252,514	3.9	3,807,703	5.3	3,831,176	1.6	1,692,071	1.6
E CHN	4,109,841	2.6	2,167,321	3.0	3,272,850	1.4	1,530,999	1.5
Total	**115,481,705**	**72.7**	**49,697,712**	**69.1**	**167,512,936**	**70.6**	**69,954,540**	**67.8**
Wheat								
N USA & CAN	36,688,388	6.3	15,861,433	7.5	35,899,640	5.5	14,277,505	6.7
CS USA	15,513,077	2.7	6,720,025	3.2	17,966,024	2.7	6,317,014	3.0
ARG	12,636,025	2.2	4,708,019	2.2	6,113,679	0.9	2,309,439	1.1
C EU	73,380,872	12.7	10,342,662	4.9	71,847,504	11.0	9,668,591	4.6
E EU & RUS	50,171,016	8.7	19,144,274	9.0	57,489,604	8.8	18,924,924	8.9
TUR	23,294,964	4.0	10,153,936	4.8	22,319,058	3.4	8,108,922	3.8
EGY	6,373,376	1.1	1,002,437	0.5	8,539,992	1.3	1,294,206	0.6
IND & PAK	80,405,000	13.9	26,530,712	12.5	96,344,408	14.7	28,128,674	13.2
CHN	64,893,892	11.2	14,664,354	6.9	75,011,960	11.4	12,397,280	5.8
SE AUS	8,847,394	1.5	4,146,434	1.9	12,312,063	1.9	4,718,662	2.2
Total	**372,204,004**	**64.3**	**113,274,287**	**53.4**	**403,843,932**	**61.6**	**106,145,218**	**49.9**

Table 2.4: Total production and harvested area per basket, share of the world production (% world (p)) and harvested area (% world (ha)) in 2000 and 2012.

	Min	Max	Q25	Q50	Q75	IQR	Range	SD	SE	CI	Skew	Kurtosis
Maize												
USA	-60.45	30.33	-4.46	0.48	8.01	12.47	90.78	19.82	2.75	5.52	-0.94	1.21
CHN	-17.35	16.72	-3.21	0.20	2.49	5.70	34.07	6.83	0.95	1.90	0.03	0.50
EU E & UKR	-15.64	13.33	-2.22	-0.22	1.73	3.95	28.97	4.66	0.65	1.30	-0.02	2.46
BRA	-10.58	8.33	-1.61	-0.18	1.53	3.14	18.91	3.11	0.43	0.87	-0.25	1.88
ARG	-6.38	4.87	-0.99	-0.05	1.41	2.40	11.25	2.13	0.29	0.59	-0.47	1.10
AFR S	-4.98	5.67	-1.23	-0.03	1.31	2.54	10.65	2.11	0.29	0.59	-0.05	0.17
EU C	-4.95	3.64	-1.08	0.09	1.02	2.10	8.59	1.81	0.25	0.50	-0.25	0.15
MEX	-3.11	3.04	-0.70	0.01	0.89	1.59	6.15	1.19	0.17	0.33	-0.07	-0.04
AFR W	-1.74	1.67	-0.81	0.04	0.51	1.32	3.42	0.94	0.13	0.26	0.09	-0.97
AFR E	-1.85	1.43	-0.33	0.00	0.42	0.75	3.28	0.63	0.09	0.17	-0.43	0.69
IDN	-1.53	0.88	-0.30	-0.12	0.42	0.72	2.42	0.51	0.07	0.14	-0.20	-0.01
Soybean												
USA	-12.24	9.66	-2.72	0.18	3.58	6.30	21.90	4.34	0.60	1.21	-0.43	-0.05
ARG	-9.76	6.89	-0.39	-0.02	0.82	1.21	16.64	2.89	0.40	0.80	-0.89	2.92
BRA S	-6.82	6.63	-1.55	-0.02	1.41	2.96	13.46	2.53	0.35	0.70	0.09	0.13
BRA C	-2.62	3.61	-0.46	0.10	0.34	0.80	6.23	1.01	0.14	0.28	0.73	2.86
CHN NE	-1.34	2.08	-0.65	-0.12	0.60	1.25	3.42	0.80	0.11	0.22	0.46	-0.28
IND	-1.79	1.13	-0.11	-0.02	0.06	0.17	2.92	0.50	0.07	0.14	-0.48	2.32
CHN E	-1.11	0.82	-0.30	0.01	0.29	0.59	1.93	0.41	0.06	0.11	-0.32	-0.20
Wheat												
EU E & RUS	-25.17	20.52	-6.24	-0.64	6.54	12.78	45.69	8.88	1.23	2.47	-0.02	0.15
US N & CAN	-17.22	9.62	-1.91	0.30	2.93	4.84	26.83	5.06	0.70	1.41	-0.84	1.64
CHN	-12.38	11.29	-1.79	0.01	2.57	4.36	23.67	4.59	0.64	1.28	-0.25	0.56
EU C	-9.64	12.07	-2.59	0.41	2.29	4.88	21.71	3.92	0.54	1.09	0.16	0.75
IND & PAK	-6.65	8.97	-1.83	-0.02	1.92	3.75	15.62	2.94	0.41	0.82	0.43	0.92
USA CS	-6.95	5.98	-1.57	-0.36	1.92	3.49	12.94	2.81	0.39	0.78	-0.07	-0.28
AUS SE	-4.61	6.34	-0.76	-0.13	1.17	1.93	10.95	2.04	0.28	0.57	0.17	0.95
ARG	-2.89	5.57	-1.34	-0.44	1.32	2.66	8.45	1.91	0.26	0.53	0.69	-0.19
TUR	-3.59	2.35	-0.89	0.10	1.05	1.94	5.94	1.51	0.21	0.42	-0.62	-0.31
EGY	-1.18	0.74	-0.23	0.03	0.33	0.56	1.92	0.45	0.06	0.13	-0.63	-0.11

Table 2.5: Summary statistics of the distributions of the residuals r_{it} in production (Equation 2.2, Figure 2.3).

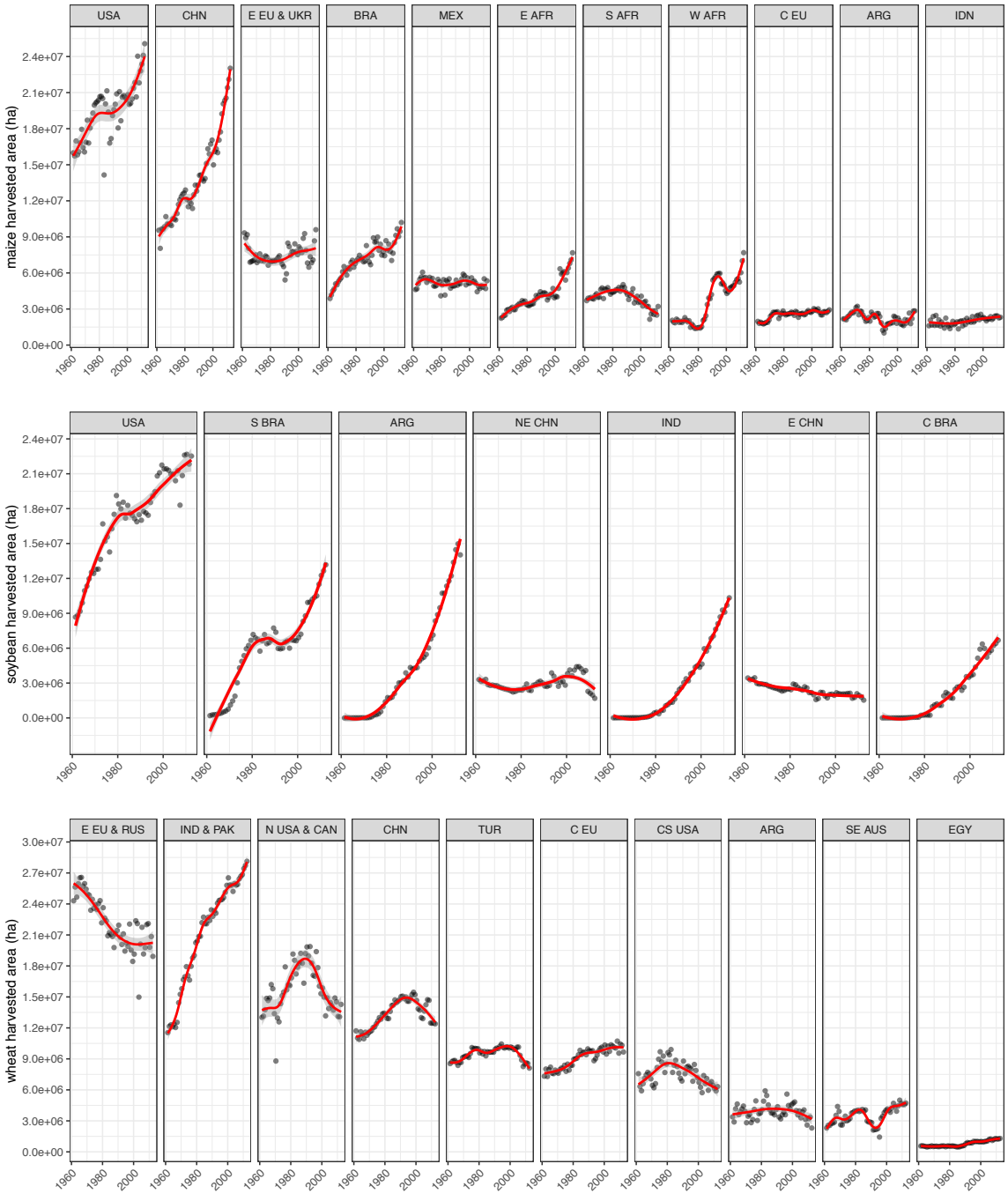

Figure 2.12: Levels and trends in area of maize, soybean and wheat (top to bottom) from 1961 to 2012 in the main producing areas (baskets).

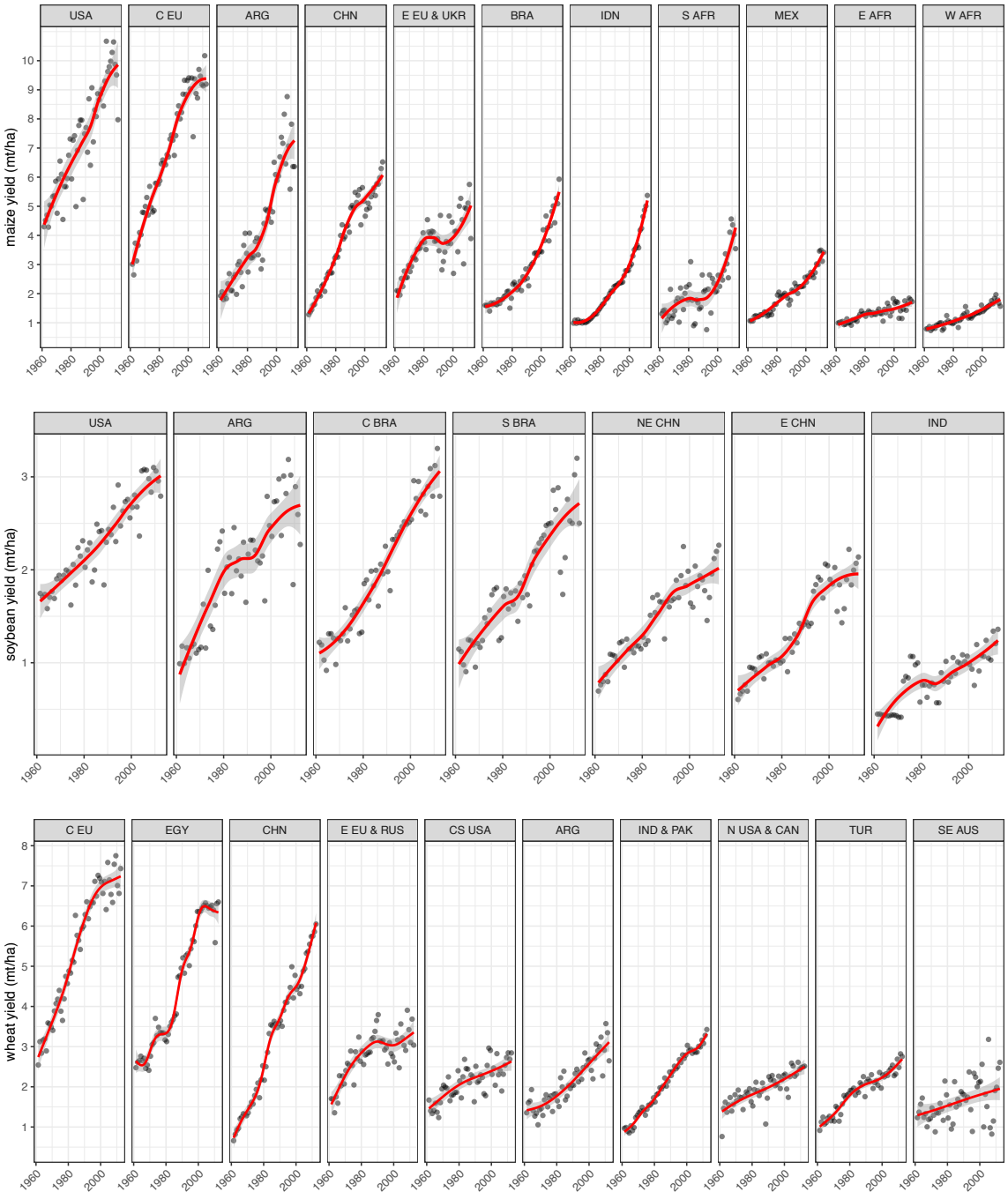

Figure 2.13: Levels and trends in yield of maize, soybean and wheat (top to bottom) from 1961 to 2012 in the main producing areas (baskets).

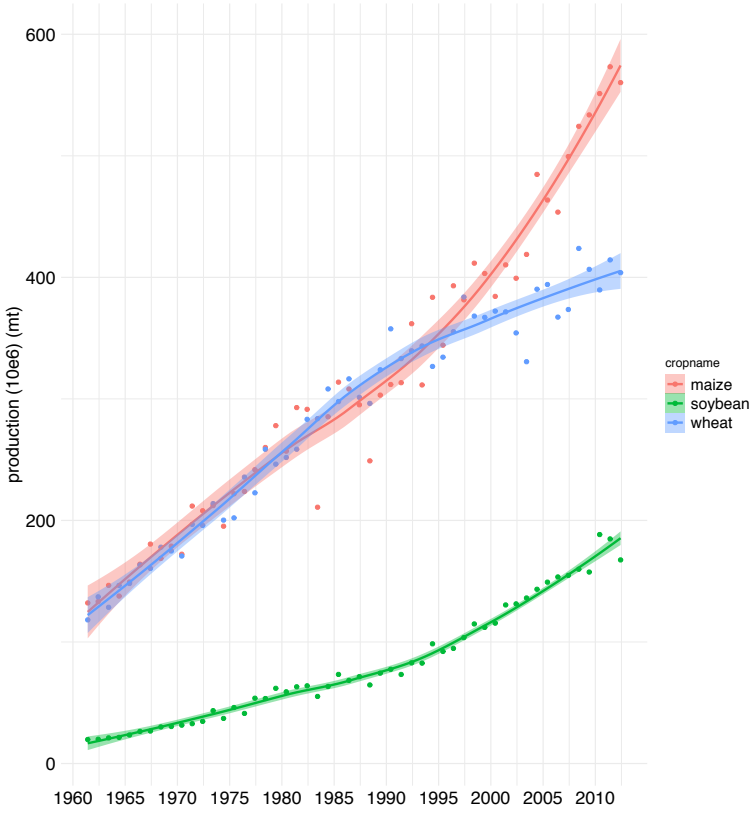

(a) Production (10e6) (mt)

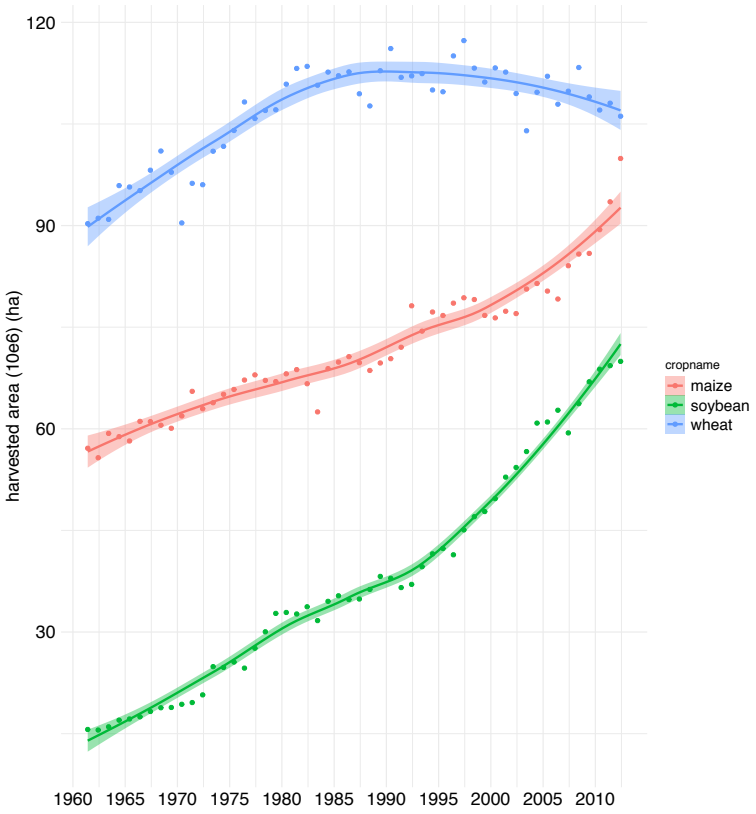

(b) Harvested area (10e6) (ha)

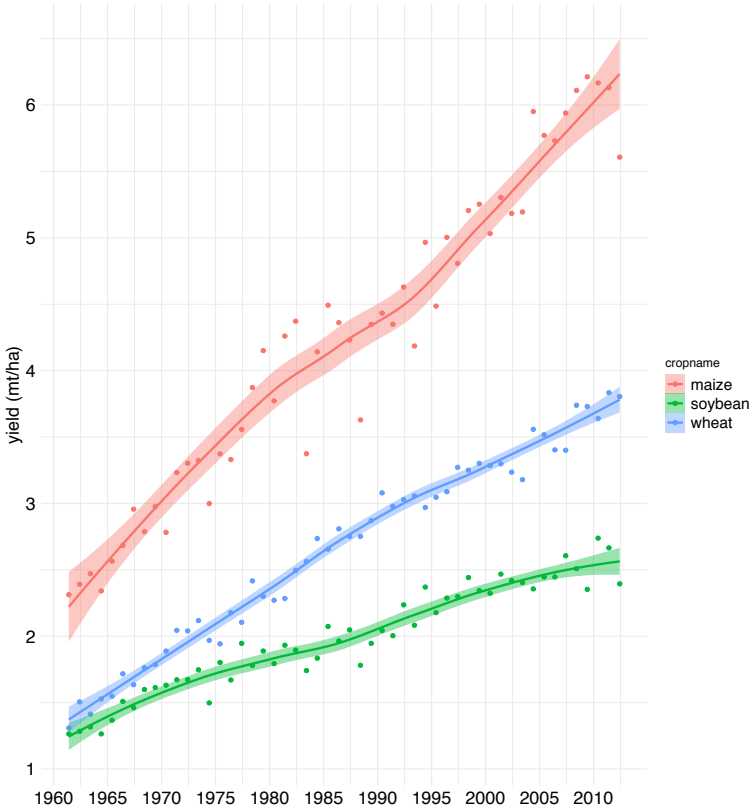

(c) Yield (mt/ha)

Figure 2.14: Temporal evolution of the global (all baskets) production, harvested area and yield between 1961 and 2012 for maize, soybean and wheat.

Table 2.6: Fligner Killeen pairwise tests for homogeneity of group variances for *maize production* (Figure 2.3).

Baskets		**Fligner Killeen**	
Basket (1)	**Basket (2)**	**p–value**	**Is different**
USA	MEX	0.00	TRUE
USA	BRA	0.00	TRUE
USA	ARG	0.00	TRUE
USA	EU C	0.00	TRUE
USA	EU E & UKR	0.00	TRUE
USA	AFR S	0.00	TRUE
USA	AFR E	0.00	TRUE
USA	AFR W	0.00	TRUE
USA	CHN	0.00	TRUE
USA	IDN	0.00	TRUE
MEX	BRA	0.00	TRUE
MEX	ARG	0.07	FALSE
MEX	EU C	0.04	TRUE
MEX	EU E & UKR	0.00	TRUE
MEX	AFR S	0.00	TRUE
MEX	AFR E	0.00	TRUE
MEX	AFR W	0.15	FALSE
MEX	CHN	0.00	TRUE
MEX	IDN	0.00	TRUE
BRA	ARG	0.08	FALSE
BRA	EU C	0.04	TRUE
BRA	EU E & UKR	0.10	FALSE
BRA	AFR S	0.21	FALSE
BRA	AFR E	0.00	TRUE
BRA	AFR W	0.00	TRUE

Table 2.6: Fligner Killeen pairwise tests *(continued)*

Basket (1)	**Basket (2)**	**p–value**	**Is different**
BRA	CHN	0.00	TRUE
BRA	IDN	0.00	TRUE
ARG	EU C	0.76	FALSE
ARG	EU E & UKR	0.00	TRUE
ARG	AFR S	0.60	FALSE
ARG	AFR E	0.00	TRUE
ARG	AFR W	0.00	TRUE
ARG	CHN	0.00	TRUE
ARG	IDN	0.00	TRUE
EU C	EU E & UKR	0.00	TRUE
EU C	AFR S	0.31	FALSE
EU C	AFR E	0.00	TRUE
EU C	AFR W	0.00	TRUE
EU C	CHN	0.00	TRUE
EU C	IDN	0.00	TRUE
EU E & UKR	AFR S	0.01	TRUE
EU E & UKR	AFR E	0.00	TRUE
EU E & UKR	AFR W	0.00	TRUE
EU E & UKR	CHN	0.02	TRUE
EU E & UKR	IDN	0.00	TRUE
AFR S	AFR E	0.00	TRUE
AFR S	AFR W	0.00	TRUE
AFR S	CHN	0.00	TRUE
AFR S	IDN	0.00	TRUE
AFR E	AFR W	0.01	TRUE
AFR E	CHN	0.00	TRUE
AFR E	IDN	0.42	FALSE

Table 2.6: Fligner Killeen pairwise tests *(continued)*

Basket (1)	Basket (2)	p–value	Is different
AFR W	CHN	0.00	TRUE
AFR W	IDN	0.00	TRUE
CHN	IDN	0.00	TRUE

	R^2	R^2-adj	intercept	intercept.pval	y.mean	y.mean.pval
Maize						
production	0.985	0.984	183682.6361	0.504	0.1332	0.000
harvested area	0.709	0.677	210035.0154	0.039	0.0487	0.001
yield	0.583	0.537	0.0667	0.512	0.0879	0.006
Soybean						
production	0.814	0.776	644098.3180	0.135	0.0983	0.005
harvested area	0.645	0.574	240049.8716	0.127	0.0539	0.030
yield	0.190	0.028	0.1083	0.267	0.0534	0.328
Wheat						
production	0.648	0.604	797667.2519	0.365	0.0911	0.005
harvested area	0.349	0.268	291232.0267	0.220	0.0356	0.072
yield	0.031	-0.090	0.2248	0.026	0.0138	0.627

Table 2.7: Summary statistics for the correlation between the mean production (or harvested area, or yield) per basket and the interannual variability in production (or harvested area, or yield).

	Variable	Correlation	p–value
Maize			
Dim1	(++)(+)A	0.950	0.000
	(+-)(-)A	0.844	0.001
	(+-)(+)Y	-0.634	0.036
	(+-)(-)Y	-0.779	0.005
	(++)(+)Y	-0.813	0.002
Dim2	(–)(-)Y	-0.724	0.012
Soybean			
Dim1	(+-)(+)Y	0.986	0.000
	(–)(-)A	0.928	0.003
	(+-)(-)A	0.857	0.014
	(++)(+)A	-0.885	0.008
Dim2	(++)(+)Y	0.928	0.003
Wheat			
Dim1	(++)(+)Y	0.897	0.000
	(+-)(-)Y	0.703	0.023
	(++)(+)A	-0.839	0.002
	(+-)(-)A	-0.852	0.002
Dim2	(–)(-)A	-0.686	0.029
	(–)(-)Y	-0.804	0.005

Table 2.8: PCA, correlations variables - dimensions.

	contribution		cos2	
Individuals	**Dim 1**	**Dim 2**	**Dim 1**	**Dim 2**
Maize				
USA	4.324	1.011	0.365	0.016
MEX	3.367	1.166	0.384	0.024
BRA	0.005	1.530	0.003	0.145
ARG	0.043	33.947	0.005	0.729
EU C	2.270	0.418	0.490	0.016
EU E & UKR	0.767	7.185	0.177	0.302
AFR S	8.756	0.000	0.880	0.000
AFR E	4.566	36.122	0.341	0.490
AFR W	0.647	6.404	0.125	0.225
CHN	0.494	0.021	0.061	0.000
IDN	65.671	3.105	0.980	0.008
Soybean				
USA	1.238	15.840	0.121	0.413
ARG	6.894	13.759	0.536	0.287
BRA S	3.791	10.824	0.490	0.374
BRA C	9.904	22.282	0.452	0.273
IND	12.091	8.986	0.607	0.121
CHN NE	18.938	13.815	0.789	0.154
CHN E	32.858	0.208	0.941	0.002
Wheat				
US N & CAN	0.000	2.966	0.000	0.447
USA CS	5.867	13.258	0.469	0.418
ARG	17.877	0.004	0.814	0.000
EU C	0.206	2.005	0.027	0.105
EU E & RUS	0.000	20.254	0.000	0.868
TUR	13.571	0.390	0.649	0.007
EGY	30.761	21.112	0.776	0.210
IND & PAK	8.281	12.654	0.336	0.202
CHN	5.570	15.214	0.332	0.357
AUS SE	7.867	2.143	0.652	0.070

Table 2.9: PCA, contribution and cos2 (in percentage) of the individuals (*baskets*) to the first and second principal components.

	contribution		cos2	
Variable	**Dim 1**	**Dim 2**	**Dim 1**	**Dim 2**
Maize				
(++)(+)A	45.068	5.722	26.345	0.608
(++)(+)Y	12.978	3.555	7.586	0.378
(+-)(+)A	2.065	5.409	1.207	0.575
(+-)(+)Y	3.139	5.998	1.835	0.638
(+-)(-)A	19.677	0.056	11.503	0.006
(+-)(-)Y	13.036	29.466	7.620	3.132
(–)(-)A	1.031	17.950	0.603	1.908
(–)(-)Y	3.006	31.844	1.757	3.385
Soybean				
(++)(+)A	33.451	11.018	19.497	1.720
(++)(+)Y	1.525	43.069	0.889	6.724
(+-)(+)A	10.861	15.553	6.331	2.428
(+-)(+)Y	18.829	0.103	10.974	0.016
(+-)(-)A	11.102	8.426	6.471	1.315
(+-)(-)Y	7.116	21.306	4.147	3.326
(–)(-)A	12.169	0.274	7.093	0.043
(–)(-)Y	4.946	0.251	2.883	0.039
Wheat				
(++)(+)A	27.974	23.887	10.299	3.464
(++)(+)Y	35.548	6.270	13.087	0.909
(+-)(+)A	4.193	0.892	1.544	0.129
(+-)(+)Y	8.691	12.267	3.200	1.779
(+-)(-)A	9.317	0.185	3.430	0.027
(+-)(-)Y	6.029	0.791	2.220	0.115
(–)(-)A	6.049	23.219	2.227	3.367
(–)(-)Y	2.199	32.489	0.810	4.711

Table 2.10: PCA, contribution and cos2 (in percentage) of the variables (*leverages*) to the first and second principal components.

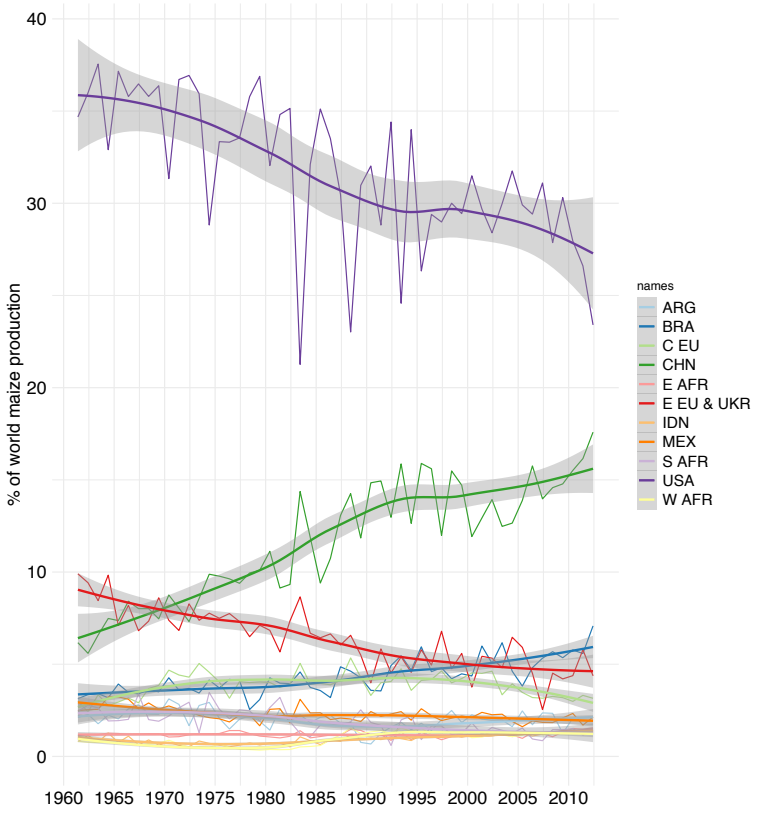

(a) Maize

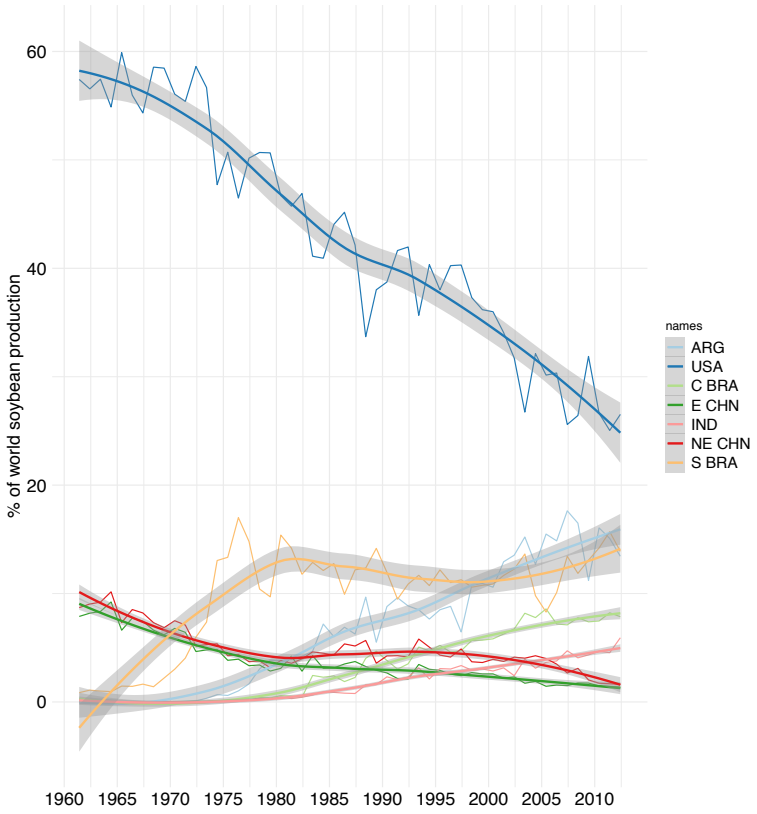

(b) Soybean

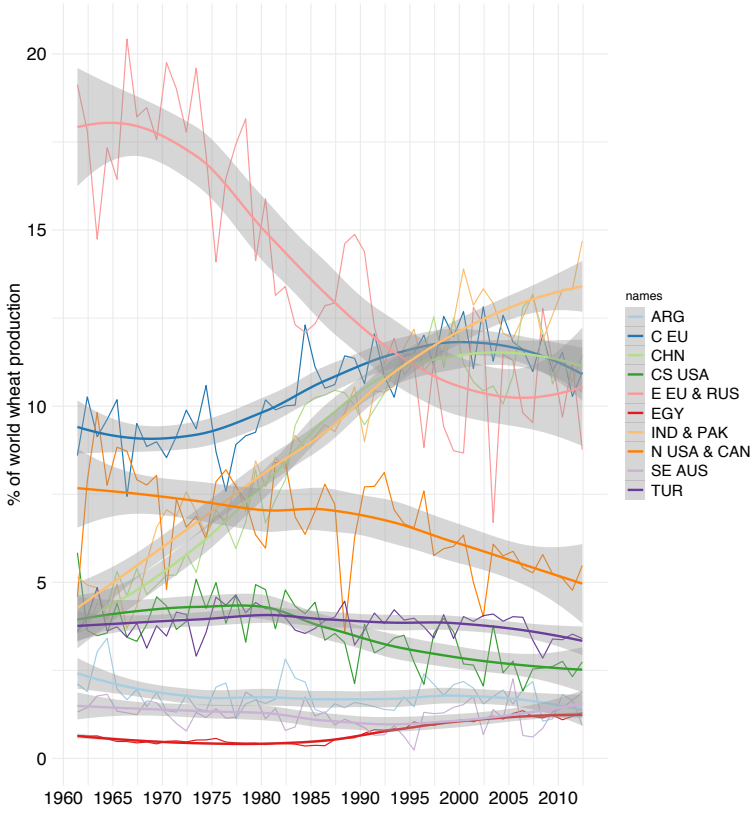

(c) Wheat

Figure 2.15: Spatio-temporal evolution of the distributions of production in % of the total global production among baskets between 1961 and 2012 for maize, soybean and wheat.

Chapter 3

Yield variations and climate

Abstract

It is important to understand better how continuing climate change is likely to influence regional and global agricultural production. The analysis presented in this chapter is based on the evidence for actual climate impacts contained in historical time series. It makes use of "plant-centred" variables (agroclimatic indices) that have been widely used in the analysis of yield-climate relationships. Calculated from standard meteorological measurements, these are used because they relate to specific aspects of the environment that influence plant growth. Values of these indices for the main producing areas (baskets) of maize, soybean and wheat were input to a machine learning model (the Gradient Boost Machine, GBM) in order to quantify how the regional production of these crops has been affected by climate variations and trends. Functional forms of the crop responses to each variable were derived from the fitted GBM models to assess regional changes in yield, the climatic sensitivity of yield, and the risks to agricultural production during the overlapping periods 1979–1999 and 1992–2012. This analysis revealed strong regional contrasts in the responses of each crop to different aspects of climate. Cumulative measures of stress (such as temporal sums of sub- or super-optimal temperatures) emerged as stronger predictors of yield than measures of either the duration or the frequency of stress events. Measures related to temperature dominated over measures related to water availability. At the global scale, the impact of three key variables – the sum of killing degree days, the deficit in growing degree days, and the precipitation sum – on yield was reduced compared to the impacts seen in specific regions, indicating a degree of buffering due to the different climatic patterns, and crop responses, shown by individual regions. Together with global increases in planted area, this buffering

helped to limit production losses. Nonetheless, continuing climate change carries risks, which could be mitigated by adaptation (including varietal selection and agricultural practices) in major producing areas and potentially also by re-distribution of the production areas for different crops.

3.1 Introduction

Contemporary climate change entails global warming (observed and projected increases in mean temperatures, which also imply increasing frequency of high-temperature extremes) and changes in precipitation regimes which, in many regions, include both increases in the incidence of intense precipitation events and increases in the duration and intensity of droughts (Berg et al. 2013, Lobell et al. 2014). The effects of high temperatures, especially, have been a focus of much agroclimatic research, because it is well established that extremely high air temperatures can adversely affect plant development and ultimately crop yield. On the other hand, there appears to be a bias in the recent literature, with a strong emphasis on these adverse high-temperature impacts and much less on other dimensions of climate impacts, including the potential alleviation of low-temperature inhibition of crop growth, and the potential adverse impacts of both heavy rainfall and drought (Schlenker & Roberts 2009, Lobell, Bänziger, Magorokosho & Vivek 2011, Hussain et al. 2018).

"Stationarity" is the hypothesis that the distribution of a variable holds over time and hence that the past is a good predictor of the future. A growing body of literature agrees that "stationarity is dead" (Milly et al. 2008) due to climate change during the past few decades. The most important causes of recent climate change are anthropogenic, with greenhouse gas increases (due to fossil fuel burning above all) being the dominant driver at a large scale, but with additional local influences due to expanding cities and the resulting expansion of the heat-island effect, irrigation, agricultural expansion (especially when accompanied by deforestation) and reforestation. Meanwhile interannual variability continues, and introduces a large element of unpredictability. Climate is characterized by probability distributions of climate variables, and climate change implies that these distributions shift over time. Changes in the frequency and magnitude of extreme weather events are thus an unavoidable consequence of climate change, giving rise to concerns about the vulnerability of agricultural systems, and of society more broadly.

A key point about extreme events, well established in the literature, is that an increase in low-probability events can have greater impacts than the change in the mean (Hansen et al. 2012). The

events themselves also become more extreme, and are often described by superlatives – for example the Horn of Africa in 2011 experienced its "worst" drought in sixty years, Russia in 2010 experienced its "hottest" summer since 1500, and so on. Figure 3.1 illustrates the link between an observed positive mean shift in European summer temperatures and the occurrence of "hottest" events. Coumou & Rahmstorf (2012) nonetheless showed an incomplete picture by (a) emphasizing mid-latitude regions; (b) not focusing on the main areas of production; and (c) highlighting record-breaking events rather than the exceedance of thresholds, which is more relevant for most climate impacts. More generally, despite a voluminous literature, many studies focusing on global climate-change impacts on crops suffer from biases towards high-temperature effects, and towards the USA in particular (Schlenker & Roberts 2006, 2009, Cai et al. 2009, Ummenhofer et al. 2015, Butler & Huybers 2013, 2015, Lobell et al. 2014, Tigchelaar et al. 2018).

This work aims to bridge a gap in the literature by performing a data-driven global analysis on maize, soybean and wheat, and quantifying the influence of several agroclimatic variables, relating to different aspects of climate, on the weather-driven risks of production loss. In a previous chapter (Chapter 2) I noted the remarkable regional heterogeneity of crop responses to the sum of killing degree days. Here I expand that analysis by considering more indices, and screening them for their importance in the determination of crop yields.

3.2 Material and methods

3.2.1 Datasets

The Gradient Boosting Machines (GBM) was used to analyse the controls on crop yield empirically, without pre-defining any specific functional forms for these controls. As input to the GBM models, I have relied on the same datasets described and used in Chapter 2. The crop data come from global gridded datasets of maize, soybean and wheat production, yield and harvested area with a grid resolution of five arc minutes, spanning the period 1961 to 2012, and with a temporal resolution of one year, obtained from the University of Minnesota's Institute on the Environment, Global Landscape Initiative (Chapter 2, Section 2.2.1). The climate data were obtained from the WATCH-WFDEI (WFD) climate dataset (Harding et al. 2011, Weedon et al. 2014) which covers the global land area on a 0.5°grid, with three-hourly temporal resolution spanning the period from 1979 to 2012. From this

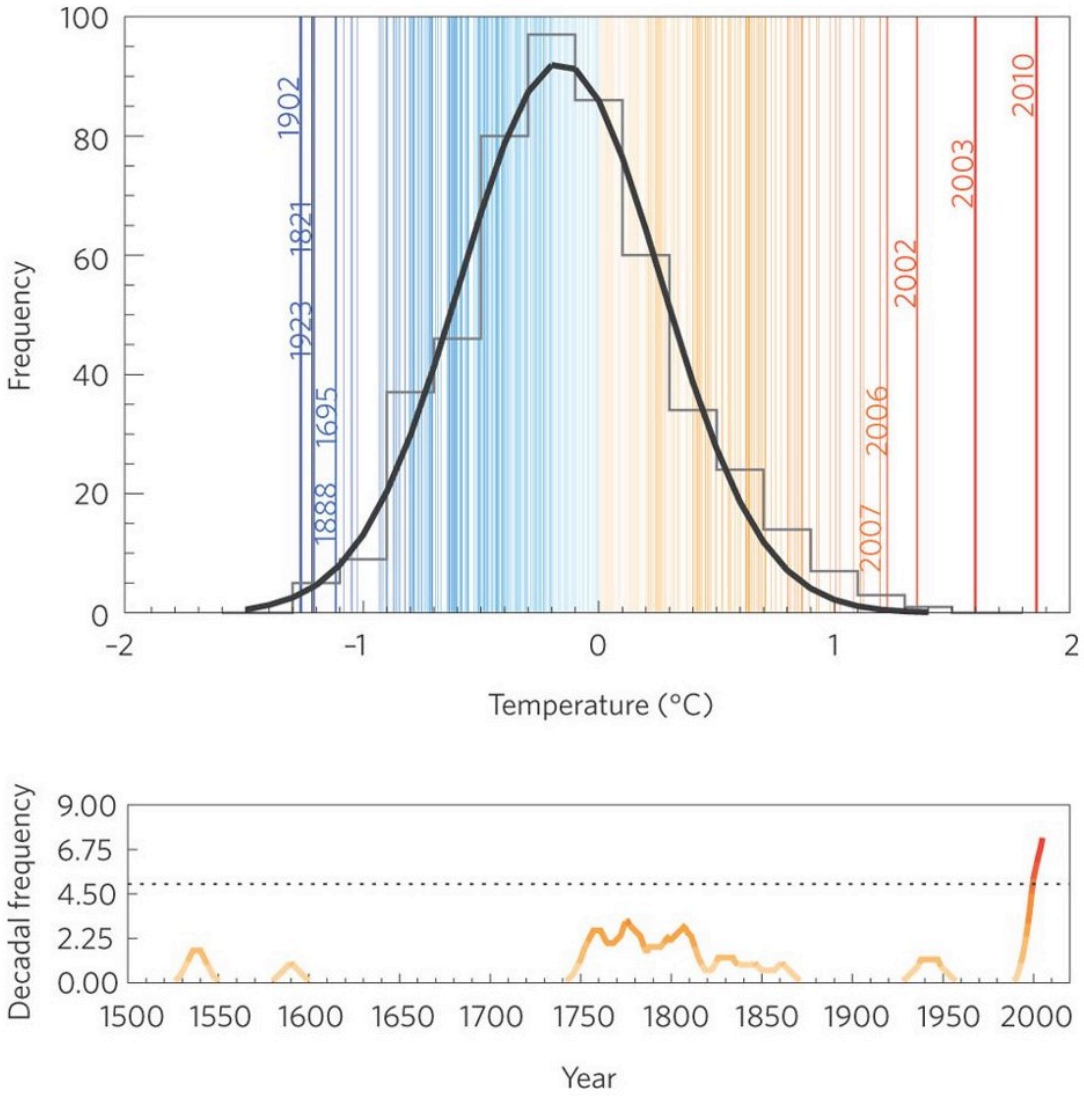

Figure 3.1: Distribution of European summer temperature anomalies between 1500 and 2010. The upper panel displays the distribution of European (35° N, 70° N; 25° W, 40°) summer temperatures anomalies during the period 1500–2010 (anomalies relative to a base climatology 1970–1999). The black line is a Gaussian fit to the histogram in grey. The vertical blue and red lines represent the temperature anomalies for each year between 1500 and 2010. The lower panel displays the "running decadal frequency" of summer temperatures above the 95th percentile, smoothed over a period of ten years. Extracted from Coumou & Rahmstorf (2012).

dataset I extracted $T_{max,d}$ (the maximum daily temperature on day d), $T_{min,d}$ (the minimum daily temperature on day d) and PPT_d (the sum of daily precipitation on day d).

3.2.2 Regionalization

The analysis was performed on the crop baskets as defined in Chapter 2 (Section 2.2.3). Although some research has shown that irrigation can significantly lower crops' sensitivity to temperature (Butler & Huybers 2013, 2015), I do not exclude irrigated areas from this analysis, due to lack of data. My aim is rather to characterize the main effective climate controls in the different baskets, implicitly taking into account agricultural practices (including irrigation) and thus providing an appropriate characterization of risks in the real world.

3.2.3 Agroclimatic variables

The cumulative sum of growing degree days (ΣGDD) correlates with the developmental phases of a crop (Ritchie & Nesmith 1991, Miller et al. 2001, Parthasarathi et al. 2013). This agroclimatic variable is used as a proxy for the favourable impact of temperatures on crop production and ultimately yield. I define GDD on day d as,

$$GDD_d = \frac{T^*_{min,d} + T^*_{max,d}}{2} - T_{low} \tag{3.1}$$

where,

$$T^*_{max,d} = \begin{cases} T_{max,d} & \text{if } T_{low} < T_{max,d} < T_{high} \\ T_{low} & \text{if } T_{max,d} \leq T_{low} \\ T_{high} & \text{if } T_{max,d} \geq T_{high} \end{cases} \tag{3.2}$$

$$T^*_{min,d} = \begin{cases} T_{min,d} & \text{if } T_{low} < T_{min,d} < T_{high} \\ T_{low} & \text{if } T_{min,d} \leq T_{low} \\ T_{high} & \text{if } T_{min,d} \geq T_{high} \end{cases} \tag{3.3}$$

where T_{high} and T_{low} are the minimum and maximum temperature thresholds beyond which crop

growth will be adversely impacted.

The deficit of growing degree days (dGDD) quantifies the accumulation of GDD below a set threshold during a given time window. In the present study I have used an annual time window. I have also experimented with defining separate phenological and cropping phases, but this added complexity did not add substantially to the analysis and is not reported here. In each grid cell, the threshold GDD_{90} is the 90th percentile of the historical distribution of ΣGDD during the period 1979–2012. dGDD is then defined as:

$$dGDD = GDD_{90} - \sum_{d=1}^{365} GDD_d \tag{3.4}$$

To quantify damage due to suboptimal and superoptimal temperatures, respectively, I use two variables: the sum of freezing degree days (ΣFDD) and the sum of killing degree days (ΣKDD). On day d, I define FDD and KDD as:

$$FDD_d = \begin{cases} T_{fdd} - T_{min,d} & \text{if } T_{min,d} < T_{fdd} \\ 0 & \text{if } T_{min,d} \geq T_{fdd} \end{cases} \tag{3.5}$$

$$KDD_d = \begin{cases} T_{max,d} - T_{kdd} & \text{if } T_{max,d} > T_{kdd} \\ 0 & \text{if } T_{max,d} \leq T_{kdd} \end{cases} \tag{3.6}$$

where T_{fdd} and T_{kdd} are the temperature thresholds for freezing degree days and killing degree days respectively. ΣFDD is then obtained by summing daily values (FDD_d) over the year, and similarly for ΣKDD. I set T_{low} and T_{high} to 9°C and 29°C according to values found in the literature, which range form 2°C to 10°C and from 29°C to 35°C, respectively (Hesketh et al. 1973, Porter & Gawith 1999, Egli et al. 2005, Schlenker & Roberts 2006, Setiyono et al. 2007, Cai et al. 2009, Abendroth et al. 2011, Butler & Huybers 2013, 2015, Gourdji et al. 2013, Asseng et al. 2015, Teixeira et al. 2013, Sánchez et al. 2014, Chavez et al. 2015, Tigchelaar et al. 2018). I applied a threshold of 8°C for T_{fdd} and 32°C for T_{kdd}, both in the mid-range of values in the literature, which range from 2°C to 9° for T_{fdd} and from 31°C to 36°C for T_{kdd}.

In reality, crops' threshold temperatures for damage depend on genotype. However, even for the same crop in the same region, there are debates in the literature about the most accurate values of

these thresholds, and there is no global information on the distribution of genotypes with different temperature responses. For this reason, and as discussed in Chapter 2 (Section 2.5), there is no evidential basis for varying these thresholds between crops or between regions. The values chosen for high-temperature thresholds are consistent with the observation that mild heat stress begins at around 30°C, progressing to enzyme inhibition and even irreversible damage to photosystems above about 42°C (Salvucci & Crafts-Brandner 2004). Low-temperature thresholds were chosen using similar logic.

High or low temperatures are not the only causes of crop damage. The duration and frequency of stress can also have an major impact on the final yield. For example, several days at 8°C during the emergence of maize can have more impact than a single night at < 0°C (Strigens et al. 2013). To analyse the impact of stress frequency and duration I have used the following measures: the length of heat waves (lHeatWaves), the number of heat waves (nHeatWaves), the length of cold waves (lColdWaves) and the number of cold waves (nColdWaves). Heat waves are defined by the number of consecutive days where $T_{max,d} \geq T_{kdd}$. Cold waves are defined by the number of consecutive days when $T_{min,d} \leq T_{fdd}$.

The precipitation deficit (dPPT) quantifies the deficit in total (accumulated) precipitation with respect to a threshold during a set time window. dPPT is defined analogously to dGDD:

$$dPPT = PPT_{90} - \sum_{d=1}^{365} PPT_d \tag{3.7}$$

To quantify the stress due to the lack or excess of precipitation, as well as the duration and frequency of such stresses, I have defined the following metrics: the length of dry and wet series (lDrySeries, lWetSeries) and the number of dry and wet series (nDrySries, nWetSeries). Wet and dry series are defined analogously to heatwaves and coldwaves. Dry series are consecutive days where $\mathrm{PPT_d} < 1$mm; wet series are consecutive days where $\mathrm{PPT_d} \geq 1$mm. The number of wet and dry series is computed over a fixed time window of one year.

3.2.4 Modelling of the responses to climate variables

The Gradient Boosting Machine

Responses to climate variables were modelled using Generalized Boosted Models, using an improvement of Friedman's gradient boosting machine (GBM) (Friedman 2001, 2002) and Freund and Schapire's adaboost algorithm (Schapire 2013, Natekin & Knoll 2013), implemented in the R package `gbm`.

Gradient boosting is a tree-based machine learning approach, conceptually similar to random forests. The method belongs to the broad class of non-parametric regression and classification models, appropriate for determining the most effective ensemble of predictors of a given response variable without requiring any prior assumptions about the shape of the functional relationships, or the distribution of errors. Explanatory (predictor) variables are classified as a function of their "link" (predictive importance) with respect to the response variable. The main differences with more traditional tree-based ensemble methods, such as random forests, lies in the strategy used to build the ensemble. The random forest approach relies on the averaging of independent trees over the ensemble. The GBM approach builds an ensemble of many successive "weak trees" so that each tree learns from previous trees. At each iteration, a newly spawned tree will learn from the errors of the whole previous ensemble and be sequentially added to that ensemble, progressively boosting the accuracy of the estimate of the response variable.

The downside of the extreme flexibility provided by GBMs is the challenge of identifying optimal values for the so-called "hyperparameters", of which the most important are (a) the number of trees to fit, (b) the depth of the trees, (c) the rate of learning and (d) sampling and subsampling. GBMs are computationally expensive and cannot easily be optimized by hand. Instead, a grid search method is used to find the optimum set of parameters. Parameter ranges and sampling intervals are defined initially; the model is then computed for every possible combination of values. The optimum parameter set is the one that yields the lowest root mean squared error of prediction (RMSE) in the response variable.

Variable importance

To identify the variables having the greatest influence on yield and assess their predictive power, I computed two importance measures: *relative influence* and *permutation importance*. Relative influence

measures the total averaged improvement provided by a variable across all the trees where the variable is present. The larger the gain (decrease in RMSE), the greater the relative influence of the variable. Permutation accuracy is computed as follows. For each tree, the Out of Bag (OOB) sample is run down the tree and the accuracy of the prediction is stored. A random permutation of the values of each variable is then performed and the prediction accuracy is re-computed iteratively. The resulting *decrease* in prediction accuracy is averaged over the trees for each variable in the model. The greater the decrease in accuracy (increase in RMSE), the more important the variable is considered to be (Friedman et al. 2001, Breiman 2001).

Partial dependence plots and conditional expectation

Partial dependence plots (PDPs) and individual conditional expectation (ICE) curves provide a framework for the interpretation of changes in the response variable as a function of the predictor variables. PDPs depict the average change in the response variable as a function of a given predictor varying over its marginal distribution, while other predictors are fixed at their mean values. Because PDPs plot an average, their main disadvantage is that they do not reveal interactions between explanatory variables, and therefore they can potentially hide heterogeneous relationships. ICE plots, by contrast, visualize the functional dependence of the response variable on the predictor variables for each observation separately. The advantage of the more complex ICE plots, as used here, is that they can display heterogeneous relationships, including alternative response "regimes" if they exist.

Functional forms of the responses

Using kernel regressions and Mahalanobis distances on ICE data, I excluded some of the instances, considered to be outliers, from the response function in order to model the functional response of yield as a function of each predictor variable. Linear functional forms were fitted using ordinary least-squares (OLS) regression implemented with the `lm` package in R. Non-linear functional forms were fitted using nonlinear least-squares regression implemented with the `nls` package in R. The adopted general form of the exponential decay function was:

$$f(x) = a * (b^x - 1) \tag{3.8}$$

where a and b are parameters controlling the curvature and decay of the function. I found a to be approximately equal to the mean value of the response variable (the yield) at the mean of the marginal distribution of the predictor variable. The adopted general form of the logistic function was:

$$f(x) = \frac{L}{1 + \exp^{-k*(x-x_0)}} \tag{3.9}$$

where x_0 is the midpoint of the sigmoid curve, L is the maximum value, and k is the logistic growth rate. The adopted general form of the inverted sigmoid function was:

$$f(x) = -a * \left(\frac{(\frac{x}{b})^c}{1 + (\frac{x}{b})^c} \right) \tag{3.10}$$

with a the maximum loss, b the mean of the marginal distribution of the predictor variable, and c the shape parameter. Optimum functions were estimated using Generalized Additive Models (GAMs) using the R function `gam`.

3.2.5 Distributions of agroclimatic variables

Distributions of agroclimatic variables were estimated using density histograms for the periods 1979–1999 and 1992–2012, using the R function `hist`. The bandwidth BW or bin size was estimated according to the formula:

$$BW = min \left(\frac{max(x) - min(x)}{2 * (1 + log(n))} \ , \ \frac{max(x) - min(x)}{\frac{2*IQR(x)}{n^{-1/3}}} \right) \tag{3.11}$$

where n is the number of observations for the climate variable, $max(x)$ and $min(x)$ the maximum and minimum values of x, and IQR the interquartile range. The first formula is one of the many "rules of thumb" for the optimization of bins in a histogram; the second is the Freedman-Diaconis rule. I used a mixture of rules, as the Freedman-Diaconis rule overestimated the bin size for gamma distributions with a short range, while the first formula underestimated the bin size for normal distributions with a large range.

Climate data show a global warming trend during the past 150 years (Jones et al. 1999); this warming has been accompanied by an increased incidence of heatwaves (Rahmstorf & Coumou 2011, Hunt-

ingford et al. 2013). Extensive discussion in the literature has concerned how methodological choices such as the normalization procedure, the choice of a baseline time period, and the length of the time period chosen to compute the distributions of anomalies influence estimates of the amount of climate change that has occurred, as well as the significance of any increase in climate variability. Huntingford et al. (2013) for example showed that normalizing temperature anomalies, and choosing the baseline for normalization as pre-1980, creates a biased impression of larger overall increases in both mean temperatures anomalies and their variability. To avoid some of these problems, I adopted a simple approach for my main analysis, contrasting two periods each of 20 years' duration (in order to allow a sufficient sample size within each period) with a small overlap.

3.2.6 Expected yield impact

I define the expected yield impact $E(y)$ of a given climate variable K with bounds K_{min} and K_{max}, for the climatology C_i with bounds $C_{i,min}$ and $C_{i,max}$ as:

$$E(y)_K = \int_{K_{min}}^{K_{max}} f(x)dx \times \int_{K_{min}}^{K_{max}} h(x)dx \tag{3.12}$$

where $f(x)$ is the functional form of the response and $h(x)$ is the density distribution of the climate variable K.

3.3 Results

3.3.1 Heterogeneity of crop responses to climate: an overview

Tables 3.1, 3.2 and 3.3 present the most important agroclimatic variables influencing the yield of each crop, in each basket. The first row (blue) indicates the variable making the largest contribution to the response. The colour intensity represents the percentage of its contribution in the GBM models. Rows 2 and 3 also display the greatest contribution, but now split as a function of the influence of the bioclimatic variable on the yield: variables inducing a loss are coloured red, and variables inducing a gain are coloured green. The percentage contribution is also coded in the colour intensity. Rows 4 to 13 display these contributions as function of the marginal distributions (for different percentiles). The contributions are weighted by the yield change, so that variables having a high contribution and a high

impact on yield are distinguished from variables having a proportionally lower contribution, or a lower impact on the yield. The results of Tables 3.1, 3.2 and 3.3 are extended by Figures 3.2a, 3.2b and 3.2c, which are heatmaps summarizing the contributions of each bioclimatic variable in each basket, weighted by the median yield change (in mt/ha) and grouped by temperature and precipitation. The colour coding is as in Tables 3.1, 3.2 and 3.3. Table 3.4 presents the results in an alternative way – how frequently, across baskets, the variable is the most important – in order to detect the dominant variable per crop across all baskets. Table 3.5 aggregates the results of Table 3.4 across crops and baskets.

The importance of bioclimatic variables and the nature of their impacts on crop yields are shown to be highly contrasted, both between baskets and between crops. One notable pattern is the importance of the adverse impact of ΣKDD on yield in the USA for both maize and soybean, consistent with the large negative correlation shown in Chapter 2 (Section 2.4). The impact of ΣKDD on these two crops, in the USA in particular, has been a focal point in the literature and is often cited in order to highlight the negative impact of a warming climate on crop yields (Muchow et al. 1990, Schlenker & Roberts 2006, 2009, Schlenker et al. 2013, Cai et al. 2009, Butler & Huybers 2013, 2015, Ummenhofer et al. 2015, Tigchelaar et al. 2018). But although the accumulation of extreme high temperatures induces yield losses in most baskets for all three crops, the contribution of ΣKDD and the resulting amplitude of yield variations induced are far less for wheat and soybean, and even for maize in other regions, than for maize in the USA.

Globally, deficits in growing degree days (dGDD) – which can be due to either suboptimal or super-optimal temperatures – seems to be as important as a predictor of yield losses as ΣKDD. In other words, the occurrence of temperatures outside the optimum range generally matters as much as (if not more than) the accumulation of extreme high temperatures. This is especially true for soybean and wheat.

The conditions favouring particularly high yields are more complex. Accumulated precipitation has a positive impact on yields up to the third quartile, after which increased precipitation (see for example soybean in Eastern China) can induce losses. The length of dry series is shown to have a positive effect on maize yields in Mexico, Brazil and Argentina; the same variable stands out when considered across baskets and crops. This counterintuitive result might be explained by the fact that dry spring and summer days provide more solar radiation; while irrigation in some regions, and past precipitation events (especially in soils with good water-holding capacity), may supply adequate moisture.

	USA	CHN	IDN	MEX	BRA	ARG	EU_C	EU_E & UKR	AFR_S	AFR_E	AFR_W
main variable	ΣKDD	ΣGDD	nHotDays	ΣGDD	dGDD	lDrySeries	dGDD	ΣGDD	ΣKDD	ΣKDD	nHotDays
main variable gain	ΣPPT	ΣGDD	nHotDays	lDrySeries	lDrySeries	lDrySeries	ΣPPT	ΣPPT	ΣKDD	nHotDays	ΣPPT
main variable loss	ΣKDD	ΣKDD	lHeatWaves	ΣGDD	dGDD	ΣKDD	dGDD	ΣGDD	dGDD	ΣKDD	nHotDays
variable (weighted)*											
p_{25}	ΣKDD	ΣGDD	lHeatWaves	lDrySeries	dGDD	lDrySeries	dGDD	ΣGDD	ΣKDD	ΣKDD	nHotDays
p_{50}	ΣKDD	ΣGDD	nHotDays	ΣGDD	lDrySeries	lDrySeries	dGDD	ΣGDD	ΣKDD	ΣKDD	ΣKDD
p_{75}	ΣKDD	ΣGDD	nHotDays	ΣGDD	lDrySeries	lDrySeries	dGDD	ΣGDD	ΣKDD	ΣKDD	ΣKDD
p_{90}	ΣKDD	ΣGDD	nHotDays	lDrySeries	lDrySeries	lDrySeries	dGDD	ΣGDD	ΣKDD	ΣKDD	ΣPPT
p_{95}	ΣKDD	ΣGDD	nHotDays	lDrySeries	lDrySeries	lDrySeries	dGDD	ΣGDD	ΣKDD	ΣKDD	ΣPPT
gain & loss (weighted)*											
p_{25}	-3.23	0.98	-1.85	1.37	-1.5	0.75	-0.72	-3.49	0.85	-1.27	-0.99
p_{50}	-4.11	1.82	1.87	-1.7	4.56	2.55	-1.45	-4.95	2.23	-1.26	-1.13
p_{75}	-4.3	2.68	4.4	-1.46	4.81	3.1	-2.46	-4.95	3.53	-1.27	-1.1
p_{90}	-3.73	3.1	4.4	1.36	4.81	3.1	-2.85	-4.58	4.4	-1.27	1.08
importance × yield p_{95}	-3.73	3.55	4.4	1.36	4.81	3.1	-2.85	-4.58	4.4	-1.27	1.08

* variable importance × expected yield at percentile

Table 3.1: Variable importance, based on the permutation importance, and associated yield losses in maize yield.

	USA	ARG	BRA_S	BRA_C	IND	CHN_NE	CHN_E
main variable	ΣKDD	dPPT	dGDD	dGDD	ΣKDD	ΣGDD	ΣPPT
main variable gain	ΣGDD	lDrySeries	lWetSeries	nDrySeries	ΣGDD	ΣGDD	ΣGDD
main variable loss	ΣKDD	dPPT	dGDD	dGDD	ΣKDD	dGDD	ΣPPT
variable (weighted)*							
p_{25}	ΣKDD	nWetSeries	dGDD	dGDD	ΣKDD	ΣGDD	ΣFDD
p_{50}	ΣKDD	lDrySeries	dGDD	dGDD	ΣKDD	lColdWaves	ΣFDD
p_{75}	ΣKDD	lDrySeries	dPPT	nDrySeries	ΣKDD	ΣGDD	ΣFDD
p_{90}	ΣKDD	dPPT	dPPT	nDrySeries	ΣKDD	ΣGDD	ΣPPT
p_{95}	ΣKDD	dPPT	dPPT	dGDD	ΣKDD	ΣGDD	ΣPPT
gain & loss (weighted)*							
p_{25}	-0.81	-0.55	-0.32	-0.18	-0.14	-0.23	-0.49
p_{50}	-1.22	0.63	-0.57	-0.6	-0.47	0.77	-1.45
p_{75}	-1.35	0.82	-0.96	1.54	-0.46	0.64	-1.16
p_{90}	-1.39	-0.63	-0.96	2	-0.33	0.71	-1.24
p_{95}	-1.39	-0.63	-0.96	1.89	-0.33	0.82	-1.25

* variable importance × expected yield at percentile

Table 3.2: Variable importance, based on the permutation importance, and associated yield losses in soybean yield.

	USA_N & CAN	**AUS_SE**	**USA_CS**	**ARG**	**EU_C**	**EU_E & RUS**	**TUR**	**EGY**	**IND & PAK**	**CHN**
main variable	ΣPPT	ΣPPT	ΣGDD	ΣGDD	ΣGDD	ΣGDD	ΣKDD	dGDD	ΣKDD	ΣPPT
main variable gain	ΣPPT	ΣPPT	ΣPPT	lDrySeries	ΣGDD	ΣPPT	ΣFDD	lHeatWaves	lWetSeries	lColdWaves
main variable loss	ΣKDD	lHeatWaves	ΣGDD	ΣGDD	dGDD	ΣGDD	ΣKDD	dGDD	ΣKDD	ΣPPT
variable (weighted)*										
p_{25}	lColdWaves	ΣPPT	ΣGDD	ΣGDD	ΣGDD	ΣPPT	ΣFDD	dGDD	lWetSeries	lColdWaves
p_{50}	ΣPPT	ΣPPT	ΣGDD	ΣGDD	dGDD	ΣGDD	ΣFDD	dGDD	ΣPPT	lColdWaves
p_{75}	ΣPPT	ΣPPT	ΣGDD	ΣGDD	dGDD	ΣGDD	ΣKDD	dGDD	ΣKDD	lColdWaves
p_{90}	ΣPPT	ΣPPT	ΣGDD	ΣGDD	ΣGDD	ΣGDD	ΣKDD	dGDD	ΣKDD	ΣPPT
p_{95}	ΣPPT	ΣPPT	ΣGDD	ΣGDD	ΣGDD	ΣGDD	ΣKDD	dGDD	ΣKDD	ΣPPT
gain & loss (weighted)*										
p_{25}	0.72	0.39	-0.19	-0.82	0.5	1.05	0.71	-1.06	0.62	0.73
p_{50}	0.65	0.54	-0.69	-1.01	-1.25	-1.72	0.43	-1.84	-0.89	1.35
p_{p75}	1.33	1.28	-1.3	-1.46	-2.04	-1.8	-0.58	-2.24	-0.56	1.63
p_{90}	1.53	1.3	-1.38	-1.86	-2.16	-1.76	-0.59	-2.34	-0.63	-1.66
p_{95}	1.53	1.3	-1.36	-1.86	-2.23	-1.76	-0.59	-2.34	-0.63	-1.65

* variable importance × expected yield at percentile

Table 3.3: Variable importance, based on the permutation importance, and associated yield losses in wheat.

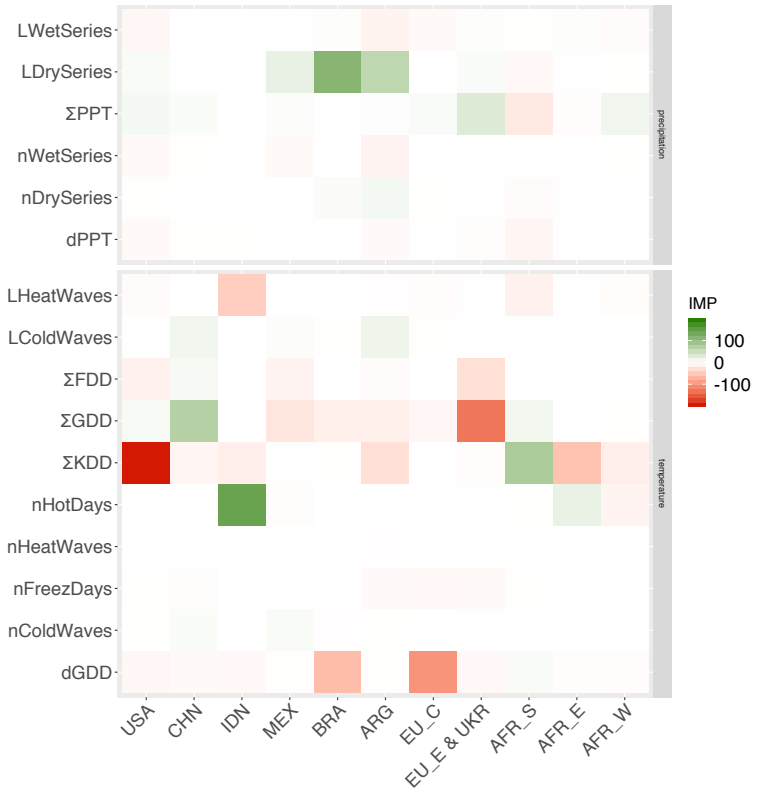

(a) Maize

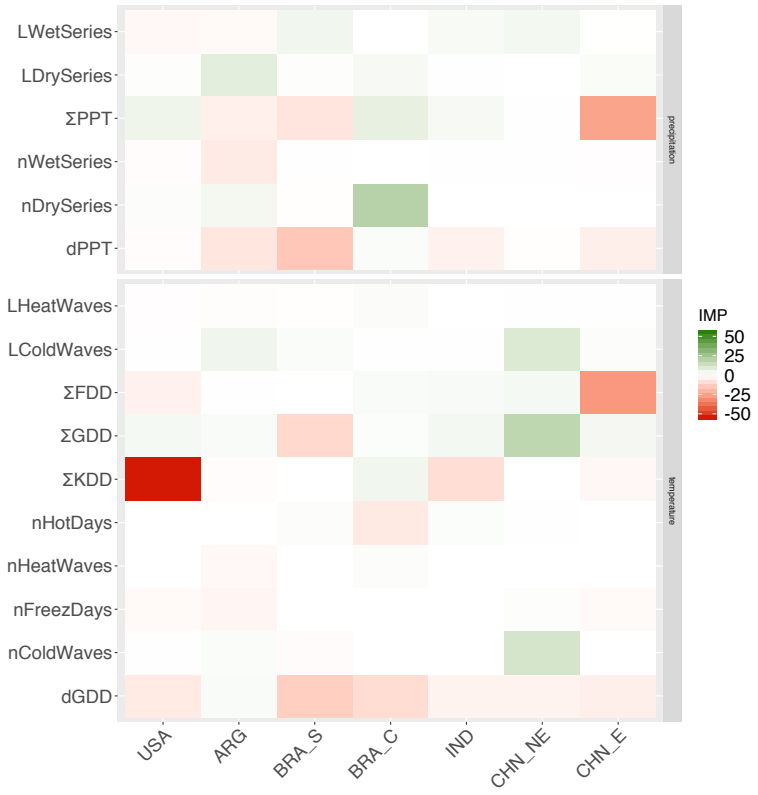

(b) Soybean

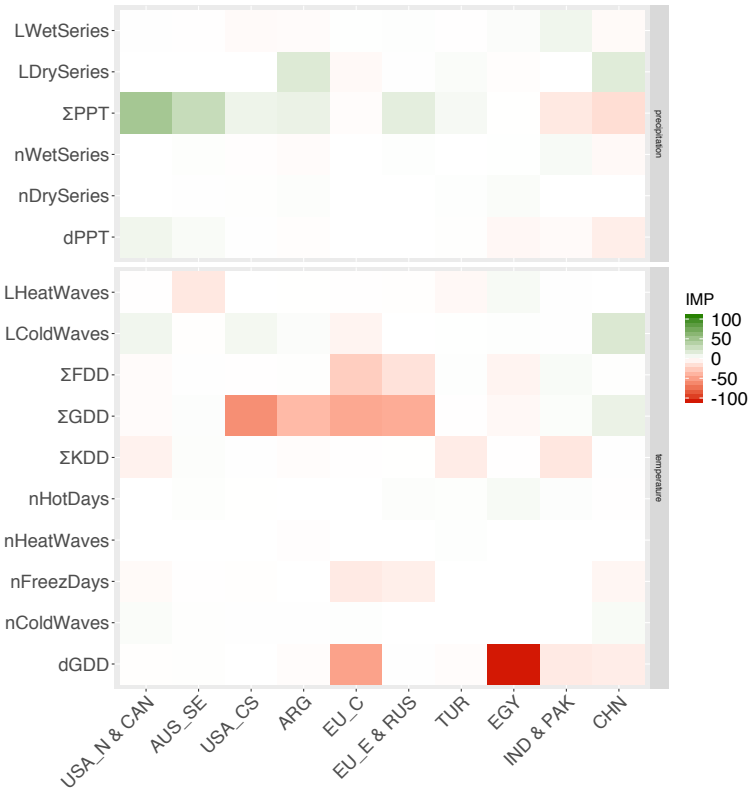

(c) Wheat

Figure 3.2: Heatmaps of variable importance, based on the permutation importance for (a) maize, (b) soybean and (c) wheat.

	imp	imp.loss	imp.gain	imp.x.yield*	imp.x.loss**	imp.x.gain***
Maize						
dGDD	0.18	0.27		0.09	0.18	
lDrySeries	0.09		0.27	0.18		0.27
lHeatWaves		0.09			0.09	
nHotDays	0.18	0.09	0.18	0.09		0.18
ΣGDD	0.27	0.18	0.09	0.27	0.18	0.09
ΣKDD	0.27	0.36	0.09	0.36	0.45	0.09
ΣPPT			0.36		0.09	0.36
Soybean						
dGDD	0.29	0.43		0.29	0.43	
dPPT	0.14	0.14				
lColdWaves				0.14		0.14
lDrySeries			0.14	0.14		0.14
lWetSeries			0.14			0.29
nDrySeries			0.14			
nWetSeries					0.14	
ΣFDD				0.14	0.14	
ΣGDD	0.14		0.57			0.14
ΣKDD	0.29	0.29		0.29	0.29	
ΣPPT	0.14	0.14				0.29
Wheat						
dGDD	0.1	0.20		0.20	0.30	
lColdWaves			0.10	0.10		0.10
lDrySeries			0.10			0.10
lHeatWaves		0.10	0.10		0.20	
lWetSeries			0.10			0.10
nHotDays						0.10
ΣFDD			0.10	0.10		0.10
ΣGDD	0.4	0.30	0.10	0.30	0.30	0.10
ΣKDD	0.2	0.30			0.10	
ΣPPT	0.3	0.10	0.40	0.30	0.10	0.40

* variable importance weighed by yield at p_{75}
** variable importance weighed by yield at p_{75} for variable variable associated with a yield loss
*** variable importance weighed by yield at p_{75} for variable variable associated with a yield gain

Table 3.4: Frequency of variable importance, based on the permutation importance, and associated yield losses for each crop across all baskets.

	imp	imp.loss	imp.gain	imp.x.yield*	imp.x.loss**	imp.x.gain***
Temperature						
dGDD	0.18	0.29		0.18	0.29	
ΣKDD	0.25	0.32	0.04	0.21	0.29	0.04
ΣGDD	0.29	0.18	0.21	0.21	0.18	0.11
lHeatWaves		0.07	0.04		0.11	
nHotDays	0.07	0.04	0.07	0.04		0.11
ΣFDD			0.04	0.07	0.04	0.04
lColdWaves			0.04	0.07		0.07
Precipitation						
ΣPPT	0.14	0.07	0.29	0.11	0.07	0.36
dPPT	0.04	0.04				
lDrySeries	0.04		0.18	0.11		0.18
nDrySeries			0.04			
lWetSeries			0.07			0.11
nWetSeries					0.04	

* variable importance weighed by yield at p_{75}
** variable importance weighed by yield at p_{75} for variable associated with a yield loss
*** variable importance weighed by yield at p_{75} for variable associated with a yield gain

Table 3.5: Frequency of variable importance, based on the permutation importance, and associated yield losses across all crops and baskets.

3.3.2 Distributions and changes of the main climate variables in each region

This section characterizes the statistical distributions of weather data and their changes between 1979–1999 and 1992–2012. I focus on the climate variables having the greatest importance for yield overall, namely ΣKDD, dGDD and ΣPPT.

Sum of Killing Degree Days

I identified three families of distributions of ΣKDD in the topmost baskets: gamma, normal, and mixed normal. In the topmost maize baskets, the distributions of ΣKDD all belong to the gamma family with a shape parameter $k = 1$ (exponential distribution). Soybean and wheat baskets show a greater heterogeneity, particularly in the shape parameter of the gamma distributions with k varying between 1, 2 (a negative skewed distribution with long tail), and $k \geq 3$ (a negatively skewed distribution, approaching a normal distribution).

Three baskets show distinctive ΣKDD distributions: Central Brazil soybean, India soybean, and India

and Pakistan wheat. India and Central Brazil have a higher mean ΣKDD per year compared to the other soybean baskets, with 870 and 500 KDD per year respectively during 1992–2012, contrasting with < 100 KDD elsewhere. Most importantly, in the topmost baskets and across crops, Brazil and India show the largest increases in mean ΣKDD between 1979–1999 and 1992–2012, by +86 and +37 KDD/year.

The baskets accounting for the largest share in the production of each crop generally have a low ΣKDD – except for India & Pakistan, and Central Brazil. The increase in mean ΣKDD in these regions from 1979–1999 to 1992–2012, and the fact that crop production is being redistributed and concentrated in the two areas (Chapter 2, Section 2.3.2), leads to a compounded increase in risk.

Between 1979—1999 and 1992—2012, there was an increase in mean ΣKDD in 21 out of the 28 baskets studied. The regions showing reductions in mean ΣKDD are USA and Argentina. The largest positive changes in mean ΣKDD are observed in Eastern Europe, Ukraine and Russia, up by 84% for the wheat baskets and 95% for the maize baskets. Aggregating across baskets for each crop, there has been an increase in mean ΣKDD for all three crops, with maize showing the lowest (+14 KDD) and soybean the largest (+20 KDD) increase. There were also increases in the standard deviation of ΣKDD, and these were greatest for those regions showing the largest increase in mean ΣKDD.

Sum of Growing Degree Days

Among the three variables investigated, dGDD shows the most significant changes from 1979–1999 to 1992–2012. All baskets saw a reduction in the mean dGDD during the two period compared. North American and Argentinean baskets are the only exception to these changes, showing non-significant changes in dGDD. All other baskets experienced a significant reduction of dGDD, roughly 35% from 1979–1999 to 1992–2012 (excluding USA and Argentina). Reductions in mean dGDD were accompanied by noteworthy changes in the shape of the distributions: generally symmetric, normal or platykurtic in 1979–1999, they become long-tailed and positively skewed in 1992–2012. Changes in dGDD were driven by changes in both superoptimal and suboptimal temperatures. While there has been an increase in mean ΣKDD across crops and baskets, the reduction in dGDD has mainly been driven by a reduction in the occurrence of suboptimal temperatures.

Table 3.5 shows that high dGDD has had a negative impact on crop yield as large as that of high ΣKDD. Observed changes in the statistical distributions of bioclimate variables highlight the fact

that a change in mean temperature implies not only increased high temperature extremes, but also a reduction in the occurrence of low temperatures that are suboptimal for growth. The data also show that increased precipitation and reduced dGDD have at least partially mitigated the negative effects of extreme high temperatures.

Sum of precipitations

The distributions observed for this variable (ΣPPT) are mainly normal distributions, or from the gamma family with a shape parameter $k \geq 2$. The only exception is Egypt wheat (where $k = 1$), characteristic of a very dry area. When considered across crops and baskets, there were no substantial changes in distribution shapes and family for ΣPPT except in one region (Argentina) which experienced a significant increase in precipitation between the two periods.

The mean ΣPPT in maize and soybean baskets (1150 mm/year) is nearly twice that in wheat baskets (610 mm/year). ΣPPT also shows large differences between baskets. The strongest drying trends (in both absolute amount and percentage) occurred in the wheat baskets of India & Pakistan (–42mm) and Egypt (-12%). Changes in other baskets were small (-4% to +4%). Mean precipitation increased in 21 out of the 28 baskets. Maize shows the largest increase (+22 mm) on average across baskets, contrasting with a slight increase (+4 mm) for soybean and wheat. Only the Central European basket experienced a decrease in precipitation. The USA and Southern Brazil are of particular interest here. In the USA, globally the largest producer of both maize and soybean, ΣKDD has the highest (negative) importance. But mean ΣKDD in the USA decreased from 1979–1999 to 1992–2012, while mean ΣPPT increased. Southern Brazil, the second or third largest producer of soybean, by contrast experienced an increase in ΣKDD and a decrease in ΣPPT; so in this region, the risks have increased, due to an unfavourable change in the sign of both variables.

3.3.3 Regional contrasts in crop responses to climate

Figure 3.3 shows the main functional responses of crop yields to the agroclimatic variables studied. The most prominent general result is the contrasting responses across regions to a given bioclimatic variable for any given crop. Non-linear relationships of yields to temperatures and precipitation are observed across baskets and across crops (Figure 3.3).

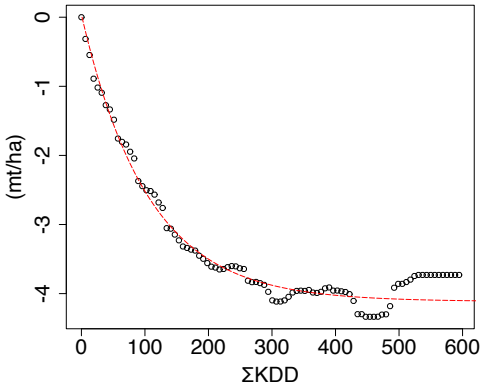

(a) Maize yield, USA

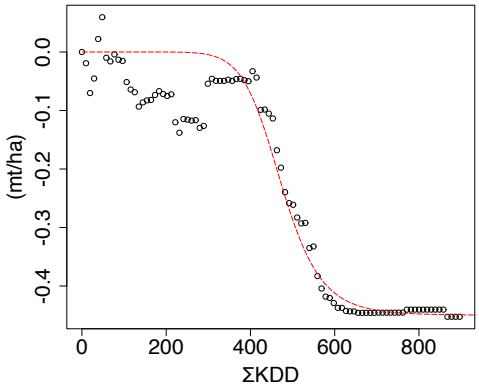

(b) Maize yield, Brazil

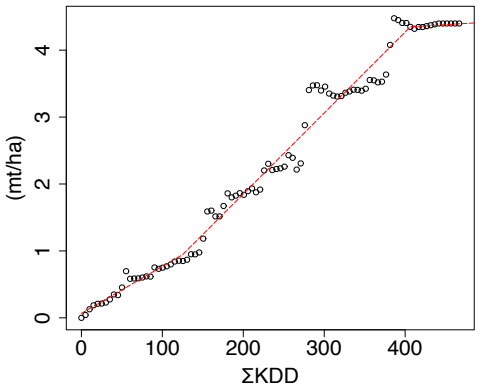

(c) Maize yield, South Africa

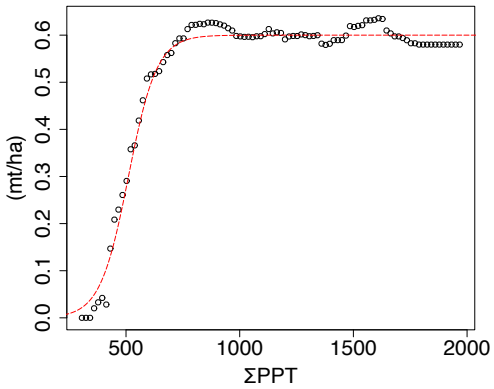

(d) Soybean yield, USA

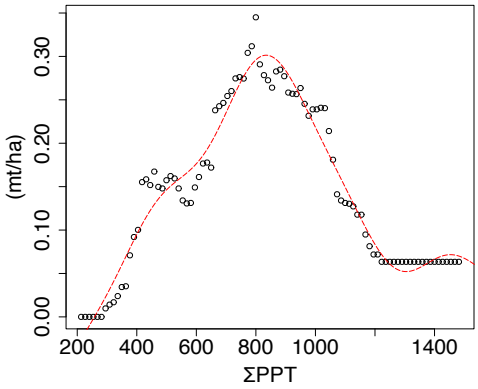

(e) Soybean yield, North East China

Figure 3.3: Examples of the modelled functional forms of the crop responses to the main climate variables for (from the top left to the bottom right), USA maize and ΣKDD, Brazil maize and ΣKDD, South Africa maize and ΣKDD, USA soybean and ΣPPT, North East China soybean and ΣPPT.

Sum of Killing Degree Days

Yield responses to variation in ΣKDD have varied between -4 and +4 mt/ha. Negative impacts with the form of an exponential decay curve are characteristic in the topmost baskets, i.e. USA and China (maize), USA (soybean), and EU and Russia (wheat). This result reinforces the point previously developed in Chapter 2, that the risks of climate-related crop failure are concentrated geographically. The nonlinearity of the observed functional responses provides additional information about the sensitivity to extreme temperatures. The topmost baskets show a high sensitivity to ΣKDD in the first part of its distribution (below the median) and a low sensitivity in the second part of the distribution. Taking USA maize as an example, the average sensitivity below the median is -2.34×10^{-2} mt/ha/KDD, but only -3.0×10^{-3} mt/ha/KDD above the median. The main producers are thus characterized by sensitivity to a slight increase in the occurrence of climate extremes, but this response reaches a plateau at higher levels of ΣKDD. Maize and soybean show a greater response to ΣKDD, as large as -4.0 mt/ha for maize and -1.5 mt/ha for soybean, in contrast with -0.5 to -0.8 mt/ha for wheat.

Sum of Growing Degree Days

Yield responses to dGDD show many similarities with the responses to ΣKDD. Overall, there is a negative effect of the accumulation of dGDD across baskets and crops. The topmost baskets show a predominance of nonlinear responses in Brazil and China (maize), USA and China (soybean), Central EU and India & Pakistan (wheat) while linear responses are shown in the USA, EU and Ukraine for maize and Southern Brazil for soybean. dGDD ranges with the highest sensitivity for crop yields differ among the regions.

Precipitation Sums

Yield responses to ΣPPT also vary among crops and regions. The main features of the observed responses to ΣPPT are (a) a generally positive effect; (b) the existence of optimum functions; and (c) low amplitudes, in the range from 0.5 to 2.0 mt/ha. The topmost baskets for maize and soybean however display positive and logistic yield responses. Wheat yields in the topmost baskets contrast with maize and soybean. Wheat yields are reduced in response to accumulated precipitation towards

the high end of the distributions, above the third quartile. In China, remarkably, wheat yields show an exponentially decaying yield response to accumulated precipitation.

3.3.4 Expected changes in yield and sensitivity

The previous sections identified the main variables influencing crop yields in the main baskets, and modelled the functional responses of yield to the most important variables. I also analysed changes in the statistical distributions of these variables between 1979–1999 and 1992–2012. Since I have computed both a functional response and a change in statistical distributions, I can now compute the expected impact of each climate variable and the resulting change in yield from one period to the other. I can also investigate the change in sensitivity and estimate the total production at risk, via weighting by acreage. For simplicity I take the average acreage in each basket.

Sum of Killing Degree Days

The largest expected loss in yield across climate variables and the main baskets results from ΣKDD and is achieved in the USA maize basket with an expected loss of 1.84 mt/ha during 1979–1999 and 1.73 mt/ha during 1992–2012. Expected losses due to ΣKDD range between 0.14 and 1.84 mt/ha (SI, Tables 3.6, 3.7 and 3.8). Maize shows the highest weighted average yield loss of the three crops across regions of productions (–0.7 mt/ha) due to ΣKDD. The expected impact of killing degree days in the other two crops is less than half that observed in maize: soybean and wheat respectively showing expected global yield losses of –0.22 and –0.06 mt/ha.

Of all the regions studied, the USA shows the greatest exposure to ΣKDD with an expected production loss of 36 million mt of maize, 2.5 million mt of wheat and 11.3 million metric tons of soybean per year during the period 1992–2012. The cumulative expected production loss across the three crops in China, the second region most at risk of ΣKDD, is estimated to be 15.4 million mt, i.e. only 30% of the loss expected in the USA. The USA is also the region with the highest sensitivity to KDD with a sensitivity of nearly –400,000 mt/KDD for maize (–0.02 mt/ha/KDD), –117,000 mt/KDD for soybean (–0.006 mt/ha/KDD), and –5,000 mt/KDD for wheat (–0.005 mt/ha/KDD). This contrasts with an average sensitivity in the other baskets of –20,000 mt/KDD, –2500 mt/KDD and –17,000 mt/KDD for maize, soybean and wheat respectively. The other baskets of interest with a high sensitivity to ΣKDD are maize in China (–0.015 mt/ha/KDD) and wheat in Central Europe (–0.01 mt/ha/KDD).

The global sensitivity of maize to KDD during 1992–2012 is estimated at –0.007 mt/ha/KDD, which is more than three times the sensitivity of wheat and soybean during the same period, and up 14% from 1979–1999. The global sensitivity of wheat remained stable at –0.002 mt/ha/KDD, while that of soybean was down 23% from –0.003 mt/ha/KDD in 1979–1999.

When comparing the periods 1979–1999 and 1992–2012, maize once again displays the largest changes in production at risk due to KDD. China shows the largest increase in loss with an extra 3 million mt of maize per year estimated to be lost due to KDD in 1992–2012, up 34% from 1979–1999, despite the 29% increase in acreage. Changes in expected losses in the USA are estimated to be around –911,000 mt/year.

The third and fourth largest losses due to ΣKDD are observed in the Eastern and Western Africa maize baskets, with an incremental change of production loss of –1.3 and –1.5 million mt per year respectively. Although not the major producers of maize, the incremental losses in these two regions roughly equate to the incremental losses of China. The total production lost in the two baskets during the period 1992–2012 was estimated to be of –9.6 million metric tons of maize, about 26% of what was lost in the USA, on a third of the area and representing only 1.5% of the average global production during 1992–2012.

A few baskets show a significant positive impact of ΣKDD on expected yield: Central EU, Eastern EU and Ukraine, South Africa for maize and Argentina, Southern Brazil, Central Brazil for soybean. The three maize baskets have similar profiles with ΣKDD distributions: gamma with $k = 1$, and a low mean compared to the rest of the baskets. A plausible interpretation of the positive impact of ΣKDD is that warmer years, associated with statistically more hot days, benefit the production of maize in these areas. This does not mean that more KDD benefit the crops as the yield responses are non-linear. Considering the Eastern EU and Ukraine response function and ΣKDD distribution for example, I observe a positive impact on yield up to the third quartile of the distribution of ΣKDD and a negative impact for the last quartile. The soybean baskets of Argentina and Southern Brazil have many similarities with the maize cases described above: a lower mean in the distribution of ΣKDD, a positive impact up to the third quartile and a negative impact thereafter.

A short summary of these results is that there has been an overall increase in losses due to ΣKDD between 1979–1999 and 1992–2012. In the latter period, expected losses due to ΣKDD reached 75 million mt per year. Losses in maize, soybean and wheat baskets accounted for respectively 75.5%,

16% and 8.5% of this. Compared to the average world production, these losses represent 7.5%, 6.7% and 1.1% respectively. Across crops, there has been an increase of the total amount of production exposed to killing degree days and a concentration of this loss within the topmost baskets. Africa is of particular interest because although not in the topmost baskets, Eastern and Western Africa show massive losses in production due to ΣKDD (SI, Table 3.6). These regions still have substantial scope for yield gap reduction (Mueller et al. 2012, West et al. 2014). However, this analysis questions at least the suitability of the maize varieties that are currently grown there, or perhaps even the appropriateness of growing maize there, as opposed to more heat-tolerant crops.

Sum of Growing Degree Days

Deficits in growing degree days universally have a negative impact on crop yields. Compared to ΣKDD and ΣPPT, the effect of dGDD across crops and baskets is much more homogeneous. The deficit was reduced from 1979–1999 to 1992–2012 in 93% of the baskets, driving an increase in crop yields.

Impacts of dGDD on expected crop yields range between -1.06 and +0.14 mt/ha for the period 1979–1999, compared to a range of -1.57 to 0.013 mt/ha for the period 1992–2012. The weighted effect on crop yields across baskets, and weighted changes between 1979–1999 and 1992–2012, rank as follows: (1) maize baskets at -0.41 mt/ha, up 25% from 1979–1999; (2) soybean baskets at -0.18 mt/ha up 35% from 1979–1999; and (3) wheat baskets at -0.17 mt/ha, up 32% from 1979–1999. Maize also shows the greatest sensitivity to dGDD with an average of –0.002 mt/ha/dGDD. The most sensitive baskets are also the topmost producers, ranked in order of sensitivity: Brazil, Cental EU, China and the USA.

Four out of the 28 baskets studied show a positive impact of dGDD. Three are wheat (USA and Canada, USA Centre South, South Eastern Australia). The positive impact is moderate and mainly achieved in the lower part of the distributions of dGDD, below the median. Physiologically, wheat requires some periods with relatively low temperatures (vernalization), and these three baskets have smaller median dGDD than the others. Argentina soybean also shows a moderate response. Soybean does not require periods with low temperatures, however, and I found a positive effect of ΣKDD and negative effect of low temperatures in the same basket, suggesting that what benefits the crop in the basket are higher temperatures and fewer FDD (not shown).

During 1992–2012, the estimated loss of production due to dGDD wordwide was greatly reduced: by 16%, 6% and 32% for maize, soybean and wheat respectively. These losses represent about 5%, 10%

and 2% of the global production of the three crops.

Sum of precipitation

The greatest expected gains in yield across baskets and crops were achieved in the USA maize basket with +1.42 mt/ha; about 3.5 times the average gain in other maize baskets at +0.35 mt/ha during the period 1992–2012. Soybeans and wheat expected yield gains due to cumulative precipitation at +0.2 mt/ha and +0.1 mt/ha respectively during the same period, down 18% and 6% from the previous period.

Between 1979–1999 and 1992–2012, I find a 10% expected increase in maize yield due to precipitation increase. Similarly to ΣKDD, the largest gains in production are achieved in the North American baskets and China for maize and soybean. In the case of wheat, the Eastern Europe and Russian baskets both show a high sensitivity to precipitation and high expected production gains due to precipitation. From 1992–2012 I find an expected average gain in production of +14.7 million mt/yr, which is 2.5% of the average world production of wheat.

The absolute sensitivity of crop yields to precipitation, however, is an order of magnitude lower than for ΣKDD. The highest sensitivity is observed in the Eastern Europe Ukraine and Russian maize and wheat baskets, with +0.002 mt/ha/mm. The topmost producers of maize and soybean show a decrease in the expected sensitivity of yield to precipitation. Results for wheat are more nuanced, with sensitivity increasing in some baskets (USA, India and Pakistan, Australia, Egypt) and decreasing in others.

The globally positive effect of precipitation on crop yields hides some regional contrasts. In South Africa, precipitation has a significant negative effect on maize yields (–2.2 mt/ha) while notably, in the same region, ΣKDD has a positive impact (+l mt/ha). Maize in South Africa is grown at above 1400 m altitude (Moeletsi 2017) and I can therefore hypothesize that increased precipitation in this region is associated with mechanical crop damage, and decreased solar radiation due to cloud cover; while hotter days (and KDD) have a positive impact due to increased solar radiation. Negative effects of precipitation and positive effects of ΣKDD are also observed for soybean in Argentina and Southern Brazil. But the differences in shapes of the yield responses functions to both ΣPPT and ΣKDD reveal highly damaging effects of both temperature and precipitation in these two baskets. A negative impact of precipitation is also found in the India Pakistan and China wheat baskets. As wheat is sensitive

to lodging (Berry & Spink 2012), it seems likely that this negative effect is linked to mechanical crop damage during intense precipitation events.

Overall, globally, precipitation has a positive effect on crop yields, despite some regional deviations described above. But the increase in mean precipitation between 1979–1999 and 1992–2012 only benefited maize yields, not those of soybean and wheat, which showed reduced yields. The principal reason is that the acreage of both soybean and wheat increased in regions where the effect of precipitation on yield is negative, while decreasing in regions where the effect is positive. There are a couple of regional exceptions to this pattern, however. In some areas an increase in yield outweighed the effect of a decrease in planted area, as exemplified by the Northern USA and Canada wheat basket. Globally, increasing precipitation and acreage redistribution between 1979–1999 and 1992–2012 resulted in a 25% increase in the production of maize (about 8% of world production), a 17% increase in soybean (about 6% of world production), and a 7% decrease in the production of wheat (about 2% of world production).

3.4 Discussion and conclusions

There is widespread agreement about the particular sensitivity of crops to heat-related stress (Killing Degree Days and heat waves) in the literature (Butler & Huybers 2015, Chavez et al. 2015, Tigchelaar et al. 2018), but this is evidently an oversimplification. My analysis has shown that there is no single model that would fit all countries and represent the diversity of responses shown in the data.

This chapter has expanded on the diversity of yield responses to heat stress noted in Chapter 2. The GBM approach was used to identify the main climate controls; to model a functional response type for each crop and basket; and to use the fitted models to assess the impact of climate change. The results indicate the importance of cumulative stresses, including the accumulated effects of suboptimal temperatures (the main contributor to variation in dGDD) and precipitation as well as killing degree days.

The analysis is simplified in the sense that I have not considered that some climate impacts may be specific to phenological stages, with anthesis, silking, and grain filling often mentioned as critical (Porter & Semenov 2005, Tao et al. 2006, Semenov 2007, Jones 2013). In exploratory work, however, I investigated the impact of stresses during specific crop growth-calendar windows by computing the

agroclimatic variables over planting, early growth, vegetative growth, flowering, drying, harvest stages, seasons, and other possible divisions; but I found no clear pattern, and obtained very little additional explanatory power relative to the increased number of parameters (SI, Tables 3.10 and 3.11).

The unusually high sensitivity of the USA baskets, and especially the US maize crop, to the sum of killing degree days is confirmed in this chapter. Across crops and baskets, the response of all three crops to superoptimal temperatures and precipitation variability is spatially heterogeneous. This finding implies that the risks posed by climate change to the agricultural system remain extremely uncertain. The change in dGDD between the time intervals considered, mainly caused by a reduction in the incidence of sub-optimal temperatures, shows an important positive impact. Effects of precipitation changes (increases in most regions) have been both positive and negative. In some regions, high cumulative precipitation results in losses that may be due to physical damage to the crop, as well as to a potential reduction of sunshine hours.

The combined effects of climate (as expressed by the three most influential agroclimatic variables) on the production and yield of all three crops show (a) reduced losses and increased gains of production over time in most baskets, and reduced losses and increased gains of yield in nearly all baskets. With growing-season temperatures rising, maize yields have been forecast to decline (Schlenker & Roberts 2006, 2009, Schlenker & Lobell 2010, Lobell, Bänziger, Magorokosho & Vivek 2011, Roberts & Schlenker 2011). The present study shows more nuanced results, with global crop yields having improved either though a gain in a few baskets, or a reduction of losses in others (SI, Table 3.9). The largest yield losses due to superoptimal temperatures are in the USA, which also shows the most uniform response. The main producing areas in Africa however show a particularly strong risk exposure to superoptimal temperatures.

These results pose questions of adaptation and varietal suitability. There was no apparent relationship between the mean temperature of a basket and the heat tolerance/sensitivity of the crops grown there; only a few baskets showed a decrease in the impact of ΣKDD on yield between the periods 1979–1999 and 1992–2012; and there was a high within- and between-basket variability in response either to superoptimal temperatures or to precipitation regimes. These findings suggest that the crop cultivars grown in some regions may not be optimal for those regions' climate, and also perhaps that there is scope for improved adaptation to a changing climate through a better selection of cultivars.

On average, the half-life of cultivars in production ranges from five to seven years. Butler & Huybers

(2015) argued that this turnover is sufficient to allow local adaptation to decadal changes in climate. This argument is debatable, however, as it does not account for the years of breeding and validation before a new variety becomes available on the market. A more realistic assessment of the actual development cycle is about a decade, implying that the rate of improvement by breeding could fall behind the rate of climate change. Hence, there could be a benefit in seeking genotypes among those already available (e.g. among hybdrids and landraces). Considering the gene pool already available and the range of latitudes at which crops are grown, there is a potential for a spatial redistribution of genotypes, which could contribute to stabilizing crop yields.

In conclusion, I have shown that crop responses to climate change are regionally contrasted, and that they include – alongside well-documented negative responses to heat stress – positive responses to warming (mainly due to reductions in the incidence of suboptimal temperatures for crop growth) and to lengthening dry periods (possibly due to increased solar radiation, provided soil moisture availability is adequate). Potential reductions in global production have largely been averted, due to the combined effects of increasing planted area and positive net impacts of climate on yields.

Whereas Chapter 2 (Section 2.4) focused on heat stress, the present chapter has delved more deeply into the sensitivity of major crops to climate-related stress by exploring a more complete set of agroclimatic variables. The next chapter will go further in analysing the interannual variability of agricultural production, by presenting a new approach to characterizing this variability in terms of shocks (i.e. large, unexpected changes in a time series) and an analysis of their causes.

3.5 Supplementary information

	E(yield loss/gain)[1]		E(sensitivity)		harvested area		E(production loss/gain)	
	1979-1999	1992-2012	1979-1999	1992-2012	1979-1999	1992-2012	absolute change	% change
ΣKDD								
USA	-1.84	-1.73	-0.018	-0.019	19,560,628	21,312,096	-911,017	2.54
MEX	0.03	0.03	0.000	0.000	5,138,001	5,188,300	15,835	11.97
BRA	-0.08	-0.10	0.000	0.000	7,617,475	8,451,089	-239,274	39.68
ARG	-0.45	-0.41	-0.009	-0.009	2,043,183	2,060,090	70,261	7.61
EU C	0.13	0.13	0.001	0.001	2,642,698	2,756,283	35,310	10.55
EU E & UKR	0.08	0.09	0.015	0.009	7,228,469	7,913,756	102,228	16.79
AFR S	0.82	1.00	0.011	0.011	4,306,923	3,397,592	-129,084	3.65
AFR E	-0.74	-0.81	-0.004	-0.004	3,928,967	5,237,600	-1,345,128	46.55
AFR W	-0.97	-0.99	-0.001	-0.001	3,909,487	5,409,381	-1,534,434	40.26
CHN	-0.66	-0.69	-0.016	-0.015	13,659,429	17,491,458	-3,074,898	34.10
IDN	-0.64	-0.58	-0.005	-0.005	2,016,945	2,265,376	-8,612	0.66
dGDD								
USA	-0.56	-0.55	-0.002	-0.002	19,560,628	21,312,096	-802,620	7.37
MEX	-0.18	-0.12	-0.001	-0.001	5,138,001	5,188,300	310,127	33.55
BRA	-1.47	-1.06	-0.004	-0.006	7,617,475	8,451,089	2,179,021	19.52
ARG	-0.11	-0.10	-0.001	-0.001	2,043,183	2,060,090	4,429	2.06
EU C	-1.04	-0.64	-0.005	-0.004	2,642,698	2,756,283	969,580	35.38
EU E & UKR	-0.41	-0.40	0.000	-0.001	7,228,469	7,913,756	-131,253	4.38
AFR S	-0.59	-0.54	-0.001	-0.002	4,306,923	3,397,592	723,857	28.35
AFR E	-0.12	0.00	-0.001	-0.001	3,928,967	5,237,600	453,653	97.43
AFR W	-0.21	-0.19	-0.001	-0.001	3,909,487	5,409,381	-242,314	30.09
CHN	-0.44	-0.20	-0.003	-0.003	13,659,429	17,491,458	2,531,328	41.84
IDN	-0.37	-0.23	-0.007	-0.006	2,016,945	2,265,376	231,745	30.64
ΣPPT								
USA	1.37	1.42	0.001	0.001	19,560,628	21,312,096	3,407,058	12.67
MEX	0.33	0.33	0.000	0.000	5,138,001	5,188,300	42,866	2.53
BRA	0.59	0.63	0.000	0.000	7,617,475	8,451,089	846,615	18.88
ARG	0.36	0.36	0.001	0.001	2,043,183	2,060,090	2,931	0.40
EU C	0.20	0.20	0.000	0.000	2,642,698	2,756,283	20,626	3.83
EU E & UKR	0.81	0.85	0.003	0.002	7,228,469	7,913,756	854,406	14.65
AFR S	-2.18	-2.20	-0.002	-0.002	4,306,923	3,397,592	1,933,658	20.55
AFR E	-0.32	-0.32	0.000	0.000	3,928,967	5,237,600	-432,702	34.85
AFR W	0.36	0.38	0.000	0.001	3,909,487	5,409,381	653,166	46.34
CHN	0.96	0.96	0.002	0.002	13,659,429	17,491,458	3,731,156	28.47
IDN	0.00	0.01	0.000	0.000	2,016,945	2,265,376	7,741	84.93

[1] E(yield loss/gain): expected change in yield;

Table 3.6: Expected changes in **maize** yield, yield sensitivity and production per agroclimatic variable (ΣKDD, dGDD and ΣPPT).

	E(yield loss/gain)[1]		E(sensitivity)		harvested area		E(production loss/gain)	
	1979-1999	**1992-2012**	**1979-1999**	**1992-2012**	**1979-1999**	**1992-2012**	**absolute change**	**% change**
ΣKDD								
USA	-0.58	-0.55	-0.005	-0.006	18,409,408	20,585,386	-590,857	5.54
ARG	0.14	0.16	0.000	0.000	3,742,260	9,026,343	879,984	169.28
BRA S	0.11	0.10	0.000	0.000	6,605,656	8,704,000	154,282	21.26
BRA C	0.07	0.09	0.001	0.001	1,707,539	4,414,211	279,035	218.26
IND	-0.42	-0.43	0.000	0.000	2,225,266	6,174,500	-1,711,898	183.52
CHN NE	0.00	-0.01	-0.004	-0.003	2,884,268	3,329,975	-7,128	51.73
CHN E	-0.46	-0.48	-0.004	-0.003	2,241,131	1,958,977	99,823	9.61
dGDD								
USA	-0.31	-0.30	-0.001	-0.001	18,409,408	20,585,386	-480,231	8.44
ARG	0.13	0.13	0.000	0.000	3,742,260	9,026,343	707,264	149.50
BRA S	-0.45	-0.30	-0.001	-0.001	6,605,656	8,704,000	312,815	10.60
BRA C	-0.41	-0.21	-0.001	-0.002	1,707,539	4,414,211	-215,876	30.70
IND	-0.12	-0.10	-0.001	-0.001	2,225,266	6,174,500	-323,110	116.73
CHN NE	-0.14	-0.04	-0.002	-0.001	2,884,268	3,329,975	281,547	68.82
CHN E	-0.26	-0.12	-0.002	-0.001	2,241,131	1,958,977	349,005	59.66
ΣPPT								
USA	0.56	0.58	0.000	0.000	18,409,408	20,585,386	1,528,904	14.70
ARG	-0.09	-0.11	0.000	0.000	3,742,260	9,026,343	-631,971	183.61
BRA S	-0.20	-0.17	0.000	0.000	6,605,656	8,704,000	-103,843	7.75
BRA C	0.29	0.30	0.001	0.001	1,707,539	4,414,211	825,586	165.66
IND	0.01	0.00	0.000	0.000	2,225,266	6,174,500	16,880	147.49
CHN NE	0.17	0.16	0.000	0.000	2,884,268	3,329,975	51,035	10.71
CHN E	0.05	0.06	0.000	-0.001	2,241,131	1,958,977	12,483	11.42

[1] E(yield loss/gain): expected change in yield;

Table 3.7: Expected changes in **soybean** yield, yield sensitivity and production per agroclimatic variable (ΣKDD, dGDD and ΣPPT).

	E(yield loss/gain)[1]		E(sensitivity)		harvested area		E(production loss/gain)	
	1979-1999	**1992-2012**	**1979-1999**	**1992-2012**	**1979-1999**	**1992-2012**	**absolute change**	**% change**
ΣKDD								
US N & CAN	-0.18	-0.17	-0.005	-0.005	17,937,006	15,516,152	636,285	19.85
USA CS	0.04	0.05	0.000	0.000	8,170,638	7,000,351	-16,596	4.53
ARG	0.00	0.01	-0.001	-0.001	4,222,053	3,806,090	49,144	1074.89
EU C	-0.05	-0.06	-0.010	-0.010	9,469,408	9,896,554	-123,454	28.14
EU E & RUS	0.00	-0.01	-0.002	-0.001	20,982,710	20,181,272	-151,822	165.27
TUR	0.00	-0.01	0.001	0.000	9,870,348	9,609,841	-88,891	1437.93
EGY	-0.40	-0.40	0.000	0.000	726,242	1,068,213	-143,395	49.87
IND & PAK	0.00	-0.04	-0.001	-0.001	22,954,555	25,723,708	-898,698	2560.88
CHN	-0.17	-0.16	0.000	0.000	14,420,952	14,044,976	176,252	7.11
AUS SE	0.10	0.10	0.001	0.001	3,241,803	3,798,864	72,325	23.31
dGDD								
US N & CAN	0.03	0.03	0.000	0.000	17,937,006	15,516,152	-58,079	12.85
USA CS	0.06	0.06	0.000	0.000	8,170,638	7,000,351	-28,836	5.97
ARG	-0.02	-0.03	-0.001	-0.001	4,222,053	3,806,090	-8,504	8.93
EU C	-0.81	-0.45	-0.004	-0.003	9,469,408	9,896,554	3,216,558	41.97
EU E & RUS	-0.01	-0.03	0.000	0.000	20,982,710	20,181,272	-302,632	126.64
TUR	-0.14	-0.11	0.000	0.000	9,870,348	9,609,841	334,833	23.74
EGY	-1.57	-0.83	-0.005	-0.007	726,242	1,068,213	250,131	21.98
IND & PAK	-0.48	-0.33	-0.002	-0.002	22,954,555	25,723,708	2,389,502	21.79
CHN	-0.53	-0.32	-0.003	-0.003	14,420,952	14,044,976	3,197,810	41.66
AUS SE	0.12	0.14	-0.001	-0.001	3,241,803	3,798,864	153,049	39.41
ΣPPT								
US N & CAN	0.39	0.46	0.002	0.002	17,937,006	15,516,152	95,348	1.36
USA CS	0.26	0.24	0.001	0.001	8,170,638	7,000,351	-399,674	19.09
ARG	0.51	0.52	0.001	0.001	4,222,053	3,806,090	-173,294	8.05
EU C	0.08	0.07	-0.001	-0.001	9,469,408	9,896,554	-20,236	2.68
EU E & RUS	0.71	0.73	0.002	0.002	20,982,710	20,181,272	-101,156	0.68
TUR	0.26	0.27	0.001	0.001	9,870,348	9,609,841	-9,782	0.38
EGY	0.00	0.01	-0.001	-0.002	726,242	1,068,213	5,845	176.26
IND & PAK	-0.51	-0.48	-0.001	-0.001	22,954,555	25,723,708	-678,223	5.84
CHN	-0.48	-0.49	-0.001	-0.001	14,420,952	14,044,976	123,385	1.77
AUS SE	0.52	0.51	0.001	0.001	3,241,803	3,798,864	245,086	14.54

[1] E(yield loss/gain): expected change in yield;

Table 3.8: Expected changes in **wheat** yield, yield sensitivity and production per agroclimatic variable (ΣKDD, dGDD and ΣPPT).

	E(production loss/gain)			E(yield loss/gain)			E(sensitivity)		
	1979-1999	**1992-2012**	**% change**	**1979-1999**	**1992-2012**	**% change**	**1979-1999**	**1992-2012**	**% change**
Maize									
USA	-19,926,863	-18,233,442	8.50	-1.02	-0.86	16.02	-0.0191	-0.0198	3.47
MEX	899,648	1,268,477	41.00	0.18	0.24	39.63	-0.0007	-0.0002	76.34
BRA	-7,279,736	-4,493,374	38.28	-0.96	-0.53	44.36	-0.0036	-0.0055	54.29
ARG	-398,074	-320,453	19.50	-0.19	-0.16	20.16	-0.0090	-0.0098	9.53
EU C	-1,866,522	-841,006	54.94	-0.71	-0.31	56.80	-0.0028	-0.0024	14.03
EU E & UKR	3,443,423	4,268,804	23.97	0.48	0.54	13.23	0.0175	0.0110	37.28
AFR S	-8,430,654	-5,902,223	29.99	-1.96	-1.74	11.25	0.0087	0.0068	22.43
AFR E	-4,596,655	-5,920,832	28.81	-1.17	-1.13	3.38	-0.0053	-0.0047	10.47
AFR W	-3,207,204	-4,330,786	35.03	-0.82	-0.80	2.41	-0.0008	-0.0007	8.99
CHN	-1,961,681	1,225,904	162.49	-0.14	0.07	148.80	-0.0172	-0.0159	7.42
IDN	-2,046,082	-1,815,207	11.28	-1.01	-0.80	21.01	-0.0121	-0.0118	2.65
Soybean									
USA	-5,965,202	-5,507,387	7.67	-0.32	-0.27	17.43	-0.0061	-0.0064	5.29
ARG	648,745	1,604,022	147.25	0.17	0.18	2.51	0.0001	-0.0001	140.05
BRA S	-3,565,020	-3,201,766	10.19	-0.54	-0.37	31.84	-0.0016	-0.0016	0.37
BRA C	-77,054	811,692	1153.41	-0.05	0.18	507.49	0.0007	-0.0012	264.39
IND	-1,198,187	-3,216,316	168.43	-0.54	-0.52	3.26	-0.0014	-0.0014	6.58
CHN NE	53,843	379,297	604.45	0.02	0.11	510.17	-0.0058	-0.0035	38.98
CHN E	-1,514,629	-1,053,318	30.46	-0.68	-0.54	20.44	-0.0063	-0.0053	15.69
Wheat									
US N & CAN	4,252,731	4,926,286	15.84	0.24	0.32	33.91	-0.0026	-0.0026	0.75
USA CS	2,943,385	2,498,278	15.12	0.36	0.36	0.93	0.0008	0.0010	19.89
ARG	2,051,889	1,919,235	6.46	0.49	0.50	3.76	-0.0008	-0.0009	9.85
EU C	-7,348,248	-4,275,379	41.82	-0.78	-0.43	44.33	-0.0147	-0.0139	5.68
EU E & RUS	14,477,106	13,921,496	3.84	0.69	0.69	0.02	0.0006	0.0008	38.87
TUR	1,163,424	1,399,584	20.30	0.12	0.15	23.56	0.0009	0.0007	19.62
EGY	-1,422,218	-1,309,637	7.92	-1.96	-1.23	37.40	-0.0069	-0.0091	32.25
IND & PAK	-22,614,660	-21,802,079	3.59	-0.99	-0.85	13.97	-0.0034	-0.0040	15.05
CHN	-17,141,877	-13,644,429	20.40	-1.19	-0.97	18.27	-0.0037	-0.0033	10.08
AUS SE	2,384,615	2,855,076	19.73	0.74	0.75	2.17	0.0013	0.0012	4.09

Table 3.9: Expected changes in production, yield and yield sensitivity in maize, soybean and wheat as a *cumulative* effect of the three most important agroclimatic variables (ΣKDD, dGDD and ΣPPT).

Table 3.10: **Maize** crop calendar (extract, crop calendar based on cropping season phases). Data sources: USDA International Production Assessment Division (IPAD), FAO Famine Early Warning Systems Network (FEWS NET), FAO Global Information and Early Warning System (GIEWS).

Crop rotation	Phase	Start	End	Critical	Overlap
USA					
1	planting_start	March	March	0	0
1	planting_peak	April	May	0	0
1	growing	June	July	1	0
1	harvest_start	August	August	1	0
1	harvest_peak	September	October	0	0
1	harvest_end	November	November	0	0
Mexico					
1	planting_start	January	January	0	0
1	planting_peak	February	February	1	0
1	growing	March	May	1	0
1	harvest_start	May	May	1	0
1	harvest_peak	June	June	0	0
1	harvest_end	July	July	0	0
2	planting_start	April	April	0	0
2	planting_peak	May	June	1	0
2	growing	July	September	1	0
2	harvest_start	October	October	1	0
2	harvest_peak	November	November	0	0
2	harvest_end	December	December	0	0
Brazil					
1	planting_start	September	September	0	1
1	planting_peak	October	November	0	1
1	growing	December	February	1	2
1	harvest_start	March	March	0	0
1	harvest_peak	March	April	0	0

Table 3.10: Crop calendar **maize** *(continued)*

Crop rotation	Phase	Start	End	Critical	Overlap
1	harvest_end	April	April	0	0
2	planting_start	January	January	0	0
2	planting_peak	January	February	0	0
2	growing	March	May	1	0
2	harvest_start	June	June	0	0
2	harvest_peak	July	August	0	0
2	harvest_end	September	October	0	0
Argentina					
1	planting_start	September	September	0	1
1	planting_peak	October	October	0	1
1	growing	November	December	1	1
1	harvest_start	January	January	0	0
1	harvest_peak	February	April	0	0
1	harvest_end	May	June	0	0
Central EU					
1	planting_start	March	March	0	0
1	planting_peak	April	May	0	0
1	growing	June	August	1	0
1	harvest_start	September	September	0	0
1	harvest_peak	September	October	0	0
1	harvest_end	September	October	0	0
Eastern EU & Ukraine					
1	planting_start	March	March	0	0
1	planting_peak	April	May	0	0
1	growing	June	August	1	0
1	harvest_start	September	September	0	0
1	harvest_peak	September	October	0	0
1	harvest_end	September	October	0	0

Table 3.10: Crop calendar **maize** *(continued)*

Crop rotation	Phase	Start	End	Critical	Overlap
South Africa					
1	planting_start	January	January	0	0
1	planting_peak	February	February	1	0
1	growing	March	May	1	0
1	harvest_start	June	June	1	0
1	harvest_peak	July	July	0	0
1	harvest_end	July	July	0	0
East Africa					
1	planting_start	March	March	0	0
1	planting_peak	April	April	0	0
1	growing	May	July	1	0
1	harvest_start	August	August	1	0
1	harvest_peak	September	September	0	0
1	harvest_end	October	October	0	0
West Africa					
1	planting_start	March	March	0	0
1	planting_peak	April	April	0	0
1	growing	May	August	1	0
1	harvest_start	September	September	1	0
1	harvest_peak	October	October	0	0
1	harvest_end	November	November	0	0
China					
1	planting_start	February	February	0	0
1	planting_peak	March	April	1	0
1	growing	May	July	1	0
1	harvest_start	July	July	1	0
1	harvest_peak	August	August	0	0
1	harvest_end	September	September	0	0

Table 3.10: Crop calendar **maize** *(continued)*

Crop rotation	Phase	Start	End	Critical	Overlap
Indonesia					
1	planting_start	April	April	0	0
1	planting_peak	May	May	0	0
1	growing	June	July	1	0
1	harvest_start	August	August	0	0
1	harvest_peak	September	September	0	0
1	harvest_end	September	September	1	0

		Permutation importance		Relative influence	
	Vars	**Most important**	**Second most important**	**Most important**	**Second most important**
USA	hty[1]	ΣKDD	ΣPPT	ΣKDD	dGDD
USA	htycp[2]	ΣKDD	dGDD	ΣKDD	dGDD
MEX	hty	ΣGDD	lDrySeries	ΣFDD	lDrySeries
MEX	htycp	ΣGDD	dPPT (planting start)	dPPT (planting start)	lDrySeries
BRA	hty	dGDD	lDrySeries	dGDD	lDrySeries
BRA	htycp	lDrySeries	dGDD (harvest end)	dGDD (harvest end)	dGDD
ARG	hty	lDrySeries	ΣKDD	ΣKDD	lWetSeries
ARG	htycp	ΣKDD (growing)	dGDD (planting start)	ΣKDD (growing)	dGDD (planting start)
C EU	hty	dGDD	ΣFDD	dGDD	ΣPPT
C EU	htycp	dGDD (planting peak)	dGDD (growing)	dGDD (planting peak)	dGDD (growing)
E EU & UKR	hty	ΣGDD	ΣFDD	ΣPPT	ΣGDD
E EU & UKR	htycp	ΣGDD	ΣFDD	ΣPPT	ΣFDD
S AFR	hty	ΣKDD	ΣGDD	ΣGDD	ΣFDD
S AFR	htycp	ΣKDD	dPPT (harvest peak)	dPPT (harvest peak)	ΣFDD
E AFR	hty	ΣKDD	nHotDays	ΣKDD	dGDD
E AFR	htycp	ΣKDD	lWetSeries	lWetSeries	dPPT (harvest start)
W AFR	hty	ΣPPT	ΣKDD	dGDD	ΣPPT
W AFR	htycp	dGDD (harvest peak)	ΣPPT	dGDD (harvest peak)	dGDD (harvest start)
CHN	hty	ΣGDD	ΣFDD	dGDD	ΣFDD
CHN	htycp	ΣGDD	ΣFDD	ΣFDD	dGDD
IDN	hty	lHeatWaves	nHotDays	nHotDays	lHeatWaves
IDN	htycp	dGDD (planting peak)	dGDD	dGDD (planting peak)	dGDD (harvest start)

[1] hty: Agroclimatic variables (h: hydric, t: temperature, y: yield) computed for a time window of one year;

[2] htycp: Agroclimatic variables (cp: crop phase) computed for a time window of one year and per cropping/development phase;

Table 3.11: **Maize** permutation importance and relative influence of agroclimatic variables per set of agroclimatic variables. Comparison hty (annual) and htycp (crop calendar by cropping phases).

Chapter 4

Quantifying shocks in agricultural time series

Abstract

The past sixty years have seen a dramatic increase in global agricultural production, driven both by the increasing demand for food as the population grows, and by the globalization of commodity markets for major crops. In many regions agriculture has become increasingly tied to market prices and profit, which could lead to a decoupling of decisions as to what is grown (and where) from the global food system's function of feeding the world. Decision-making in agriculture is also strongly influenced by national policies (such as subsidies) and regulations (such as trade agreements). This complexity may have led to increasing risk to the world food supply, because the various conflicting interests involved (a) are not aligned with a goal of ensuring global food security, and (b) operate on different time scales: national policies, for example, are slow to respond to "shocks" in agricultural production, whose effects are nonetheless observed rapidly in commodity markets. Major agricultural shocks make global news; yet understanding of their nature and causes is limited, and left mainly to expert opinion. This chapter focuses on the statistical identification of shocks (large and rapid variations of agricultural production – also called "volatility" in financial time series) in historical agricultural data. I introduce a new approach to shock detection and classification. I make use of the different properties of an ensemble of historical time-series models to estimate a likelihood that each year's data in a time series represents a shock. Noting that shocks are more easily identified

a posteriori (i.e. with the benefit of hindsight) than *a priori* (i.e. relative to a one-point-ahead forecast), I also present a second ensemble of models that treats the identification of shocks as a forecasting problem. To my knowledge, neither of these approaches – quantifying shocks via ensemble modelling, and identifying shocks relative to a point-ahead forecast – has any parallel in the current literature. I show the existence of substantial variation in the incidence of shocks across regions, and differences in what events are identified as shocks by different models. However, I show that all kinds of models – including so-called "naive" models – have the ability to capture different types of shocks. I find no significant positive trend in the number of "most important" shocks (i.e. those detected by nearly all models) over the period studied (1961 to 2012). These shocks were generally caused either by a sudden change in yield, or (about as often) by a sudden change in harvested area, in one or more major producing regions. This result suggests that the greatest disruption to production is not necessarily caused by climate events, but can equally be due to policy shifts. Finally, when all shocks (major and minor) are considered together, the data do show a significant increase in the instability of agricultural production; however, this trend also is not driven solely by instability in yield.

4.1 Introduction

"It's difficult to make predictions, especially about the future" (Anon.)

Many time series show variations contingent on both endogenous and exogenous factors. Disentangling their influences is a challenge. Natural systems are multivariate and complex. They are subject to stochastic processes such as extreme weather events, floods, diseases and financial crashes. Moreover, there is no necessary relationship between the frequency of occurrence of a process and its life span. For example, a short-lived flood in SE Asia happening in an industrialized area could provoke long-lasting water-table pollution. The tsunami at Fukushima, Japan represents an extreme example of a short- term event with long-lasting consequences.

In agriculture, endogenous variations may relate to a change in agricultural practices, or in planted area. Exogenous variations may relate to policy changes, or to macroeconomic shifts. Stochastic processes, superimposed on endogenous and exogenous variations, include the consequences of weather variability and climate change. Although farmers have scope to adapt to climate change on a decadal time scale, they cannot adapt to subseasonal variations (once a crop is planted, it is subject to the vagaries of the weather), and also very limited scope for adaptation to interannual variations.

Thus, agricultural production (and with it, commodity prices) may be subject to shocks for various reasons related to exogenous, endogenous and/or stochastic influences. Time series can be affected by both permanent and temporary shocks (Atkinson et al. 1997, Lee & Brorsen 2017). Technological and policy changes can permanently alter the structure of a time series in terms of mean, variance and stationarity. Clements & Hendry (2006) showed that such permanent and infrequent shocks are pre-eminent causes of the failure of forecasts based on historical time series.

Serial correlation is a feature of all agricultural time series. Any given agricultural region is more suitable for particular crops (in terms of competitive advantage) than others. Supply chain infrastructures, once built, are there to stay. Agriculture is a cultural phenomenon; farmers in any one region are accustomed to planting specific crops. Models for such time series, and statistics for detecting structural changes, must take this necessary serial correlation into account (Lloyd 1993, Lin et al. 2015, Lee & Brorsen 2017).

The detection and characterization of shocks is an outlier detection problem (Balke & Fomby 1994, Atkinson et al. 1997). Given a time series and a fitted model, the aim is to detect what movements, and of what amplitude, are not accounted for by the fitted model. There is some inevitable subjectivity here because the model structure depends on choices made by the modeller, and to some extent also on what is traditional and accepted within a particular field. Many methods exist to detect outliers. In a regression model, an outlier can be detected by measuring the influence of its removal on the residual sum of squares in the model. This approach is called deletion diagnostics (Atkinson 1985). Cook's distance is a metric often used to quantify the influence of a given observation in a regression model (Cook 1977, Cook & Weisberg 1982).

Shocks can be of several kinds, including “additive shocks” that are simply spikes (lasting just one timestep); transient shocks that take several timesteps to decay; and level shifts, which are permanent. However, all shocks are defined by their context (Chandola et al. 2009) and can be characterized *a posteriori* by examination of surrounding data. Shock detection is inevitably more accurate when we have knowledge of what happened before *and after* the event. But in real time we have no knowledge of the future. As a result, what is seen a shock today could very well be seen as part of a trend tomorrow. This is an important practical point. Because it is always easier to characterize a phenomenon retrospectively than to predict its future evolution, it is very often possible to find putative explanations for a current phenomenon – for example, to associate current changes in commodity prices with a covariate (such as oil price); but such associations may not stand the test of time.

Here I present a new approach to shock detection in time series of agricultural production, yields and harvested area. I compare two ensembles of models. The first ensemble, which I call "historical", is composed of a number of existing, widely used models that are computed and fitted on the full time series from 1961 to 2012. Each model in the ensemble has different properties. For example, some models capture more of the underlying trend observed over a longer period of time; others capture more of the deviations from the trend; some deal with lags explicitly. The second ensemble, which I call "predictive", represents a novel approach that treats the detection of shocks as a forecasting problem. Given a time series, a fitted model, and a set of projections, a shock according to this new approach is defined simply as a value that we were not expecting from the model's projections (i.e. the forecast falls outside the confidence intervals of the projection).

The predictive approach is based on the following premises. The shocks are unknown *a priori*; structural changes are also unknown; and each data point is associated with a frequentist likelihood (called f throughout this chapter) of being a shock. I rely on the pragmatic assumption that a forecast from an ensemble of models is more accurate and informative than a single model. The influence of specific model choices is thereby reduced.

An analogy can be drawn with the Delphi process. The "experts" are the models; the consensus is the average of the models; I am the facilitator. The objective is not to find the "best" forecast model. Instead the objective is to identify shocks, and then examine (for example) how they correlate with change in harvested area or yield – and if the latter, then to see whether the change can be associated with climate statistics, as calculated in previous chapters.

I first examine the results from the historical ensemble. I compare models according to the number of shocks detected for different values of f; analyse the difference in numbers of shocks between baskets (I retain the definition of baskets used in previous chapters), crops (maize, soybean and wheat), and the three agricultural variables studied (harvested area, yield per unit area, and total production); and investigate the trend in the number of shocks over time, per crop and agricultural variable, and globally for the three crops considered together. The historical ensemble is considered as a benchmark, since it is run on the full time series. Next, I follow the same schema for the predictive ensemble, and compare the results with those obtained from the historical ensemble.

Current understanding of the causes of shocks in crop production is surprisingly limited. Yet, because of their huge importance for global food supplies, it would be valuable to understand them better. Here,

as in previous chapters, I focus on maize, soybean and wheat. This is primarily because these three are the most important globally traded crops, in terms of both tonnage and value. In addition, these crops have multiple uses, including biofuel and animal fodder as well as food for human consumption. Shocks in their production therefore have the potential to disrupt multiple supply chains, and to have widespread social and economic consequences.

4.2 Material and methods

Time series can be decomposed into their generating components: trend (a non-seasonal, long-term pattern), seasonality (a regular and predictable pattern of fluctuation that repeats itself annually and does not drift over time), cycles (patterns that repeat over time periods longer than one year), and stochastic variations. Cycles may not be exactly periodic; for example, there is cyclical fluctuation in stock markets, and in recurring climatic phenomena such as the El Niño-Southern Oscillation. In this chapter however I conflate seasonal and cyclical phenomena, for the purpose of simplification – because my focus is on shock detection, rather than on the identification of repeating patterns. Seasonal and cyclical phenomena are nonetheless taken into account by the models.

Each model consists of a set of equations that describe the realizations (observed values) in the time series. Some comprise "state components" that describe how unobserved components (or states: level, trend and seasonality) change over time. Such models are called "state space models". Autoregressive integrated moving average (ARIMA) models are of this type. The selection of models for each ensemble is not arbitrary. Each of the models that I have applied, from the most naive to the most complex, is commonly used in time series analysis in order to detrend, smooth or forecast (Atkinson et al. 1997, Calderini & Slafer 1998, Lloyd 1993, Chandola et al. 2009, Aljoumani et al. 2012, Iizumi et al. 2013, 2014, Ben-Ari & Makowski 2014, Licker et al. 2013, Ben-Ari et al. 2016, Cernay et al. 2015, Lee & Brorsen 2017, Maleki et al. 2018). The ensembles were built to encompass the diversity of models, with the intention of bringing together their strengths as well as their limitations. The models are all extensively described in the time-series analysis literature. I will therefore not detail all the mathematics behind them, but rather present their most important properties. The dataset analysed has already been presented in Chapter 2, section 2.2.1.

4.2.1 The ensembles

All models included in the *historical* ensemble are computed over the full time series from 1961 to 2012. Outlier detection is based on the complete set of residuals from each model. For each fit, I compute the mean and standard deviation of the residuals. I define an outlier as being a point that is more than two standard deviations away from the mean of the residuals, applying the empirical 68-95-99.7 rule (these are the approximate percentages of data that fall with one, two and three standard deviations of the mean of a normal distribution). In addition, a normality test is performed on the residuals using the Shapiro-Wilks test for normality and implemented via the function `shapiro.test` in the R package `stats`. When the distribution of the residuals does not follow a normal distribution, I use Chebyshev's inequality (Bienaymé 1853, Tchebichef 1867) to compute the bounds of the random variable. Outliers are then identified by residuals falling outside the bounds defined by Chebyshev's inequality for $k = 2$ (i.e. two standard deviations from the mean).

In the *predictive* ensemble, models are recursively fitted on subsets of the time series. With t, the time index of a given data point, between 5 and 51 (1965–2011), the model is fitted on the $t \geq 5$ data points in the time series and a point-ahead-forecast is made for time $(t + 1)$. I define a point to be an outlier when, in a point-ahead-forecast, it falls outside the 95% confidence intervals of the projection of the model. For one neural network model (described below) these confidence intervals are computed by simulation. Otherwise the confidence intervals of the projections are computed using the method `forecast` in the R package `forecast`. This method automatically selects the appropriate model to compute the 95% projection intervals, such that for a h-step forecast, where $\hat{\sigma_h}$ is an estimate of the standard deviation of the h-step forecast distribution, then a 95% prediction interval is given by

$$y_{t+h|t} \pm 1.96 \times \hat{\sigma_h} \tag{4.1}$$

Below I present each model, and the motivation behind the selection of each model.

4.2.2 Simple Moving Average (SMA)

Some forecasting methods are extremely simple and are sometimes called “naive”, but they can be surprisingly effective. Simplicity is in fact one of their core advantages. Moving averages are widely used in fields such as trading, in which they are a fundamental technical indicator that captures trends.

Variations above or below the moving average are the base that define trading signals, and on which trading strategies are based. In SMA, forecast future values are simply given by the average of data within a time window of chosen width.

SMA can be centred (the average is taken in the middle of the window), left (the average is taken from the following time periods within the window), or right (the average is taken from past time periods within the window). All observations within the window have equal weight when computing the average. The narrower the window, the smaller the lag in the fitted values, and the more variation that is captured. Choosing too small a window means that noise may overwhelm the signal; broader windows imply a longer lag, but also capture more of any trend that is present. Two important limitations of SMA are (a) that the amplitude of fitted values can never reach the full peak-to-trough variation of the underlying series, due to averaging; and (b) extreme historical values can skew the analysis.

The SMA was selected for its dual property of being a smoother, and its extremely simple approach to forecasting. I selected four window sizes (3, 5, 7, 9) for both right (equation 4.2) and centred (equation 4.3) moving average options. Moving averages were computed using the following formulas:

$$\begin{aligned} \overline{y}_{\text{SMA}} &= \frac{y_t + y_{t-1} + \cdots + y_{t-(n-1)}}{n} \\ &= \frac{1}{n} \sum_{i=0}^{n-1} y_{n-i} \end{aligned} \tag{4.2}$$

$$\begin{aligned} \overline{y}_{\text{SMA}} &= \frac{y_{t-(n/2)} + \cdots + y_{t+(n/2)}}{n} \\ &= \frac{1}{2k+1} \sum_{i=-k}^{k} y_{t+i} \end{aligned} \tag{4.3}$$

where $\overline{y}$ is the fitted value at time t, and n is the size of the window. SMA models, presented in tables 4.1 and 4.5, are named according to their type and window, e.g. `ma_c3` is a centred moving average with a window width of 3.

4.2.3 Exponential Moving Average (EMA)

The exponential moving average lies behind many forecasting methods (Brown 1959, Winters 1960, Holt 2004). Fitted values and forecasts generated by EMA are temporally weighted averages of past data points. The weights decay exponentially with distance in time. The EMA puts therefore most weight on the most recent observations, and as a result, is sensitive to local extreme values. This sensitivity is not a major issue in the present analysis, however, as (a) this is only one model of an ensemble; (b) the EMA is computed for the whole time series and not used as a forecasting method, hence it is not attempting to make a point-ahead forecast based on a current extreme value; (c) I use a variant of the EMA that factors in and smooths the trend.

The EMA was computed by using the function `es` from the R package `smooth`, using a simple exponential smoothing. The degree of smoothing (denoted) was chosen for each series so as to minimize the residual sum of squares. In Table 4.1, the model is named ETS.

4.2.4 Polynomial models

Polynomial models are a standard tool in regression analysis. The inclusion of terms with degree > 1 allows non-linear relationships to be fitted using what is still, mathematically, a linear model. However, high-degree polynomials can almost fit all data points: the higher the degree chosen, the better the fit, but the greater the risk of overfitting.

A spline is a piecewise polynomial function, with each piece being locally fitted. Splines are extremely flexible functions used in a wide range of applications including detrending, modelling arbitrary functions that have no known functional forms, and computer graphics rendering (Hyndman et al. 2005). A cubic spline is a spline built from piecewise third-degree polynomials. Each piece is computed from a range of continous values of the output variable (time, in the present case). The length of the ranges determines the number of the knots and the level of smoothing of the final cubic spline. Because cubic splines are piecewise fits, there the choice of nodes has an impact on the final fitted model. The more knots are used, the closer the fit to the data. Theoretically, a cubic spline can be found to approximate any continuous function, although in practice, there is no simple choice of node that will give an approximation to a LOESS fit, which I will now introduce.

LOESS stands for locally estimated scatterplot smoothing. LOESS models were introduced by Sav-

itzky and Golay (Savitzky & Golay 1964). LOESS is a generalization of both moving average and polynomial regressions (Garimella 2017). It shares with cubic splines the ability to represent complicated functions without the need to know anything about the functional form or the data generation process. It differs in that it is fitted point-by-point instead of between nodes, using a nearest-neighbour procedure. LOESS can therefore capture more local variability, and more of the local data structure, than cubic splines.

In Table 4.1, models are named according to their class, degree and bandwdith. `poly_3` is a third-degree polynomial, and `loe_03` is a LOESS model with a smoothing bandwith (the proportion of the nearest neighbours included in the model) of 0.30. Polynomial and LOESS models were computed using the functions `lm` and `loess` respectively in the R package `stats`. The cubic spline model, denoted `spline` in Table 4.1, was computed using the package `splinef` from the package `forecast` in R, which implements the procedure described by Hyndman et al. (2005). For the splines, the number of knots was determined by optimization using a maximum likelihood method, described in the same article.

4.2.5 ARIMA models

Autoregressive Integrated Moving Average (ARIMA) models are one of the most widely used model categories in time-series analysis and forecasting (Valipour et al. 2013). They are a generalization of Autoregressive Moving Average (ARMA) models, which address issues of time-lag effects and serial correlations in time series (Piwowar & LeDrew 2002, El-Gohary & McNames 2007). While smoothing models are built on the characterization of the trend (with some also taking into account seasonality), ARIMA models have complementary features, focusing on identifying temporal autocorrelations. Autoregressive models, as their name suggests, perform regressions of a variable on to itself – thus they are a kind of multiple regression model in which lagged values of the variable of interest are included among the predictors of its current value. Such models shine by their ability to handle a large range of time-series patterns.

Fitting an ARIMA model requires the specification of three parameters: the number of autoregressive terms (p), the number of seasonal differences needed to stationarize the series (d) and the number of lagged forecast errors in the prediction equation (q). Models were fitted using the `arima` function in the R package `forecast`. I followed the same procedure for each time series. This procedure,

described by Hyndman et al. (2007) and Box et al. (2013), combines unit root tests (tests for whether a time series is non-stationary), minimization of the Akaike Information Criteria (AIC, an estimator of the comparative quality of different statistical models to make predictions on the same dataset) to determine the orders of the model, the values of p and q and the best model (p, q, d) and finally maximum likelihood estimation of the model's parameters. When the series presented non-stationarity, a Box-Cox transformation (Box & Cox 1964) (function `boxcox` in the R package `MASS`) was used to stabilize the variance.

Finally, a State Space ARIMA (SSARIMA) was used in the predictive ensemble. The detailed differences between ARIMA and SSARIMA are beyond the scope of this thesis, but a full comparison is made by Svetunkov & Boylan (2020). In short, the use of SSARIMA is motivated for time series that contain few data points, a situation that applies when making point-ahead forecasts for the predictive approach during the early part of the time series.

4.2.6 Neural network models

Artificial Neural Networks (ANNs) are intended to loosely mimic the decision-making models of the human brain. The very first ANN model was presented by Frank Rosenblatt, an American psychologist, in 1957. The simplest possible neural network is mathematically equivalent to a linear regression model, where the output or forecast is a linear combination of the inputs. More complex networks include several "hidden layers" juxtaposed between the inputs and outputs. The weights (the coefficients in a linear model) are computed by the network through minimization of a cost function by iterative methods.

Among all the models used in this chapter, ANN is both the most complex and the most versatile. The motivation behind the inclusion of an ANN in the predictive ensemble is that ANNs have shown the ability to represent complex non-linear relationships between the response variable and its predictors (Raghu et al. 2017), and can approximate any function (Zhang & Qi 2005, Hanin & Sellke 2017, Hanin 2019). Unlike most of the models presented in this chapter, ANNs are not based on a specific equation that describes the data generation process. Computing the prediction intervals is therefore not straightforward – it requires the use of simulations where point-ahead projections are made by bootstrapping the residuals, either from a defined normal distribution, or from a sampling of the errors in the historical data. Confidence intervals can thus be obtained by generating a large number (here

1000) of alternative predictions. A point was considered to be a shock if the one-step-ahead realization of the time series fell outside the range of the 2.5th and 97.5th percentiles of the range of forecast values generated by simulation.

ANNs have been used in many fields including environmental time series analysis (Rostami Fasih et al. 2015, Khodadadi et al. 2016). Neural Network Autoregressive (NNAR) models are a type of ANN that uses the lagged values of the time series as input. NNAR models are a natural choice among ANNs for the present application, being suited to the analysis of univariate time series (Zhang et al. 1998, Zhang & Qi 2005) and conceptually related to ARIMA models. NNAR models however differ from ARIMA models in that they do not impose conditions of stationarity on the parameters (Thoplan 2014).

NNAR modelling was implemented with the `nnetar` function in the R library `forecast` using a three-layer feed-forward trained network for one-step-ahead forecasting. Parameters were optimized by minimization of the model's root-mean-squared error (RMSE).

4.2.7 Naive and Random Walk Forecasts (RWF)

Some time series present no particular structure, with no trend or seasonality, and their properties do not depend on the time at which a realization occurs. In other words, each data point is independent of the previous ones; the variable of interest takes independent and random steps up or down. This is called a "random walk" process. There are many real-world examples of random walk time series. An example is the daily exchange rate from USD to EUR, which shows almost completely random day-to-day changes, with zero autocorrelation.

In a random walk without drift, past knowledge of the time series provides no information at all about the direction of the change in future time steps. A random walk with drift is similar except that the mean value of the step forward is not zero. Random walk with drift can be an appropriate model for some time series that contain a long term trend. Because most agricultural time series studied in this thesis do show long-term trends, I implemented a random walk with drift model, using the function `rwf` in the R package `forecast`.

4.2.8 Automatic outliers detection: Anomalize and Time Series Outliers

Anomalize is a procedure, developed by Twitter, to automatically detect anomalies in time series. The procedure is based on a Seasonal Hybrid Extreme Studentized Deviate (S-H-ESD) algorithm, which builds on the Generalized ESD test for anomaly detection (Rosner 1983, Vieira et al. 2018). S-H-ESD models can be used to detect both local and global anomalies in univariate time series. They work through piecewise time series decomposition. The piecewise component is meant to deal with the extraction of the trend, which – according to Vallis et al. (2014) – is a non-trivial problem in the presence of shocks. This last point, along with the use of ESD (which addresses smaller samples and extremes distributions), is the main motivation for including this methodology in the ensemble. The model was implemented using the function `AnomalyDetectionTs` from the R package `AnomalyDetection`. The maximum number of anomalies that S-H-ESD could detect was set to 20% by trial and error on a random subset of half of the time series. Adopting this threshold, all identified anomalies matched observed sudden changes in the series. There was no increase in the number of anomalies detected past this threshold.

The last model used in the ensemble is an automatic procedure for the detection of time-series outliers implemented with the function `tso`, part of the R package `tsoutliers`. This function implements a procedure described in Chen & Liu (1993). The procedure was designed to detect non-systematic changes in time series that are not captured by standard methods. The procedure is based on the joint estimate of outliers via a combination of ARIMA and structural time series modelling, as detailed in López-de Lacalle (2016).

4.2.9 Tukey's Honestly Significant Test (HSD)

Tukey's HSD test is a single-step multiple comparison procedure used to find significant differences among all possible pairs of means (Steel 1997). It is a generalization of the Student's t-test with a correction for the family-wise error rate (FWER), which is the probability of making a Type I error when testing multiple hypotheses. Tukey's HSD is considered a conservative procedure that is suitable when the samples are of unequal sizes (one motivation to use this methodology here). The assumptions are that the groups associated with each mean in the test are normally distributed. As we are working with real-world data, the normal distribution of the groups was sometimes violated, which is a possible criticism. In most cases, however, this assumption held. Tukey's HSD statistics

were calculated with a significance level $\alpha = .05$ and performed with the function `HSD.test` in the R package `agricolae`. Tukey's HSD between groups are represented by letters, so for example if three groups are shown with the letters a, ab and b, there is a significant difference between groups 1 and 3, but not between 1 and 2 or between 2 and 3.

4.3 Results: the historical ensemble

4.3.1 Comparison of models

Table 4.1 summarizes the total number of shocks (whether positive, i.e. anomalously high values, or negative, i.e. anomalously low values) detected for each model used in the ensemble, after running them on the full time series. Since it is not possible to obtain a reliable forecast based on a small set of data, and because of the required windows for the moving averages being used, I excluded the first years of data from the analysis. The row entry "At Least 1" contains the results from the ensemble of models; it is the count, across all models, of the number of shocks that have been detected by at least one model.

The total number of shocks is aggregated per model, across all times series: (a) all three crops (maize, soybean, wheat), (b) all three agricultural variables (production, yield, harvested area), and (c) all baskets (252 univariate time series). Recall that f is the frequency with which a given point in a time series has been found to be a shock. As an example, `ma_c3` for $f > 0.5$: using a centred moving average with a window of 3 (three data points), 117 data points were categorized as being shocks, under the condition that each of these data points has been categorized as a shock by at least half of the models in the ensemble. For each model I present the results of Tukey's HSD test with a significance level = 0.05.

	$f > \mathbf{0}$		$f > \mathbf{.5}$		$f > \mathbf{.75}$		$f > \mathbf{.9}$	
Model	**N**	**Tukey**	**N**	**Tukey**	**N**	**Tukey**	**N**	**Tukey**
ma_c3	235	bcd	117	cde	61	a	27	a
ma_c5	230	bcd	146	abc	71	a	29	a
ma_c7	207	cd	142	abcd	68	a	29	a
ma_c9	191	cd	134	abcde	61	a	28	a
ma_r3	241	bcd	121	bcde	66	a	29	a
ma_r5	209	cd	124	bcde	70	a	29	a
ma_r7	191	cd	106	de	67	a	29	a
ma_r9	187	d	101	e	62	a	28	a
loe_02	243	bcd	135	abcde	70	a	29	a
loe_03	243	bcd	155	abc	72	a	29	a
loe_04	237	bcd	160	ab	72	a	29	a
loe_05	234	bcd	159	ab	72	a	29	a
poly_3	225	bcd	134	abcde	63	a	29	a
poly_5	228	bcd	145	abcd	70	a	29	a
splines	176	d	45	f	29	b	15	b
ETS	235	bcd	128	bcde	70	a	29	a
ARIMA	224	bcd	118	cde	69	a	29	a
S-H-ESD	288	b	117	cde	55	a	28	a
TSoutliers	264	bc	98	e	55	a	28	a
At Least 1	846	a	171	a	72	a	29	a

Table 4.1: Total number of detected shocks (N) per model of the *historical* ensemble and Tukey's HSD groups (Tukey), as a function of the frequentist likelihood f.

	$f > \mathbf{0}$	$f > \mathbf{.5}$	$f > \mathbf{.75}$	$f > \mathbf{.9}$
min	176	45	29	15
max	846	171	72	29
mean (SD)	256.70 ± 141.26 (***)	127.80 ± 28.00 (***)	64.75 ± 10.00 (***)	28.00 ± 3.11 (***)
median (IQR)	232.00 (208.50, 241.50)	131.00 (117.00, 145.25)	68.50 (61.75, 70.25)	29.00 (28.00, 29.00)

***: p-value < 0.001 (Tukey's HSD test for equality of means);

SD: Standard Deviation;

IQR: Interquartile Range;

Table 4.2: Summary statistics of the number of shocks detected by the *historical* ensemble of models as a function of the frequentist likelihood f.

When considering all detected shocks ($f > 0$), I observed a large variability (Tables 4.1 and 4.2) between models, which fell into four significantly different groups. The ensemble represented by "At Least 1" sits apart from all other models with a larger number of shocks detected (about four times more shocks). At the other end of the range, with the smallest number of detected shocks, I found two models (the cubic spline, and right-moving average with a window of 9 years) to be non-significantly different. These two models are structurally similar in that they provide a much higher level of smoothing than a moving average with a small window (in fact, `splines` and `ma_r9` present a similar amount of smoothing on visual inspection of the plots), and capture more trend relative to local variations.

Variations in the numbers of shocks detected are also found within classes of models. This is true for the moving average models in particular; here variability is a function of the size of the moving window, and of its alignment (to the center or the right). I found no significant differences within the polynomial types of models (poly and cubic splines). The results illustrate that even the simplest and so-called "naive" models such as moving averages are able to pick up different levels of shocks. There was no significant difference between a centered moving average with a window of 3 and the ARIMA models.

A key general result of this comparison is the convergence of all models as f increases – in other words, as we consider shocks that are detected by more and more models. With increasing f, (a) the number of shocks detected decreases for all models; (b) variation among models becomes non-significant (for $f > 0.75$, except for the splines model, all models were assigned to the same group by Tukey's HSD test); and (c) the number of shocks detected by the ensemble converges toward the number detected by each individual model.

This result indicates that the most frequently detected shocks (hereafter called "major" shocks), which are also those showing the largest amplitude of change from time (t) to time ($t + 1$), are robustly identified irrespective of the nature and complexity of the models used to detect them. In other words, the models agree on the most important shocks despite their conceptual and mathematical diversity. However, the use of an ensemble of models allows shocks to be ranked from least important ($f < 0.5$) to most important ($f > 0.75$) according to the proportion of models in which they are detected.

4.3.2 Characterization of shocks

Although the raw material for this analysis consists of univariate time series, characterizing shocks in these series is a multi-dimensional problem involving three crops, three agricultural variables and 28 baskets. I use several visualizations and Tables to show the resulting space-time patterns.

Figure 4.1 depicts the historical occurrence of shocks in four selected maize baskets (from top left to bottom right: USA, Central EU, Eastern EU & Ukraine and China), as found by the historical ensemble of models. For each basket, I plot production, yield and harvested area, for easy visual matching. Each data point is coloured along a blue to red gradient. Blue is for the points that are less frequently detected by the ensemble of models but are detected at least once; red is for the points that are detected by all or nearly all models. Each times series is accompanied by a barplot of the frequency of detection for each of its data points.

The differences between baskets are summarized in Figures 4.3, 4.4 and 4.5, with summary statistics in Table 4.3. These outputs summarize the group differences for each crop, for different values of f. Similarly, differences between crops, and between variables, are summarized in Table 4.4.

4.3.3 Shocks in a temporal perspective

The literature often associates the notion of agricultural shocks, especially in the context of climate change, to drastic drops in yield or production linked to climate events such as droughts (Easterling et al. 2000, Rahmstorf & Coumou 2011, Coumou & Rahmstorf 2012, Berry et al. 2014, Butler & Huybers 2015, Chavez et al. 2015, Ummenhofer et al. 2015, Lesk et al. 2016, Ben-Ari et al. 2016, Tigchelaar et al. 2018, Porter et al. 2019). Anomalies in real time series however are much more diverse than this. They can be positive or negative. An example of a positive anomaly would be an increase in production due to a combination of a large increase in cultivated area and yield improvement. Robust detection of positive anomalies is just as important as the detection of negative anomalies, since they reflect more structural changes (increased planted area, crop improvement, yield gap reduction) than negative ones. Favourable weather will bring the crop close to its maximum potential (which has a plateau), while bad weather can bring the yield close to zero. In other words, since the response of crops to weather is non-linear (Chapter 3, Section 3.3.3), the difference between favourable and extremely favourable weather is less important than the difference between unfavourable and extremely unfavourable weather (Lobell, Bänziger, Magorokosho & Vivek 2011, Jones 2013).

A clear relationship can be observed (see Figure 4.1) between the amplitude of a shock (i.e. a substantial deviation at time $(t+1)$ either from the underlying trend, or from the value of the quantity at time t), and its likelihood of being identified as a shock. This relationship can be confirmed statistically, as the regression of f against Δy (the change of y from time t to time $(t+1)$) shows a significant ($p < 0.001$) and positive ($f = .15 \times \Delta y$) relationship between the amplitude of the shock and its likelihood. The likelihoods show a positively skewed and long-tailed distribution (Figure 4.2) with a peak in the range $0 < f < .2$.

Now consider the USA basket for maize (Figure 4.1a, upper left). Generally the largest shocks in production coincided with shocks in yield. However, an exception must be made for 1983, when a negative shock in yield was accompanied by a two-fold reduction in planted area – which, in turn, can be linked to the act of 1983 that limited maize acreage in the USA. The largest shocks in this basket were negative shocks. But this is far from being a universal pattern, and this case highlights how shocks can be a direct consequence of policy.

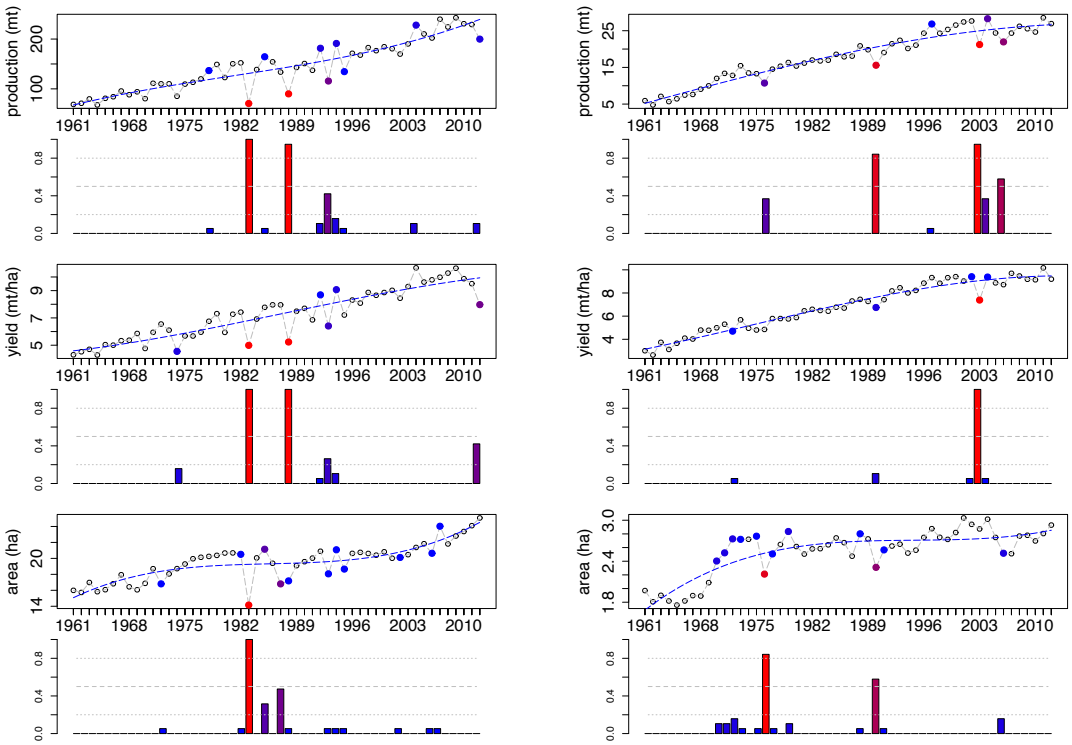

(a) Maize USA

(b) Maize Central EU

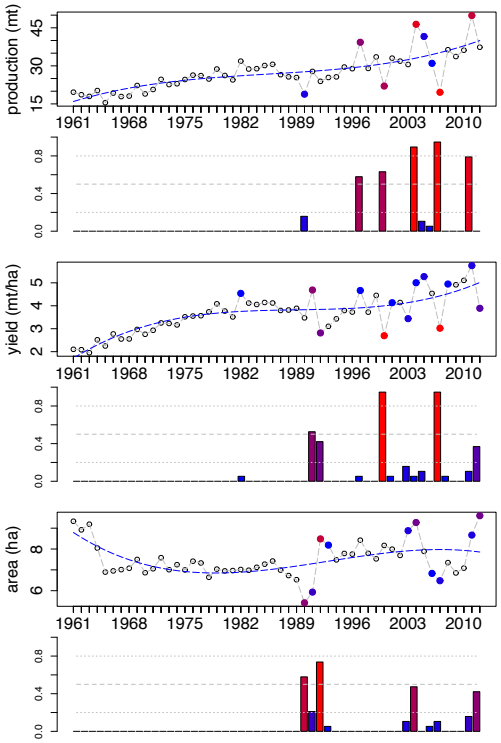

(c) Maize Eastern EU & Ukraine

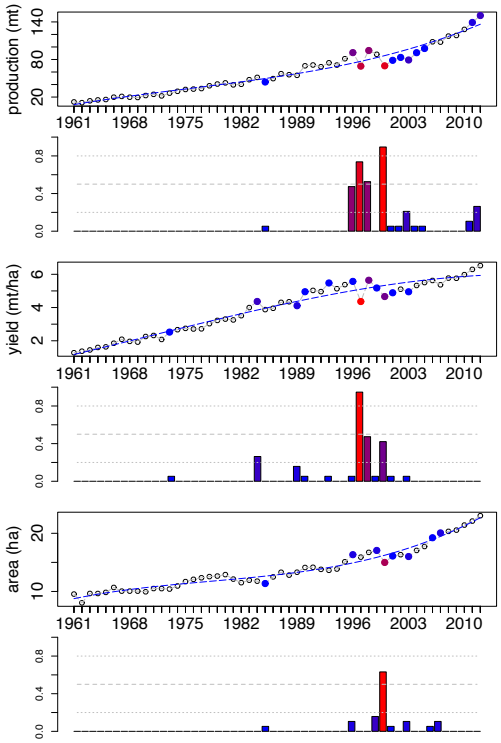

(d) Maize China

Figure 4.1: Maize production (mt), yield (mt/ha), area (ha), and frequentist likelihood of shocks (histograms) for the *historical* ensemble, in the USA, Central EU, Eastern EU & Ukraine and China (from top left to bottom right).

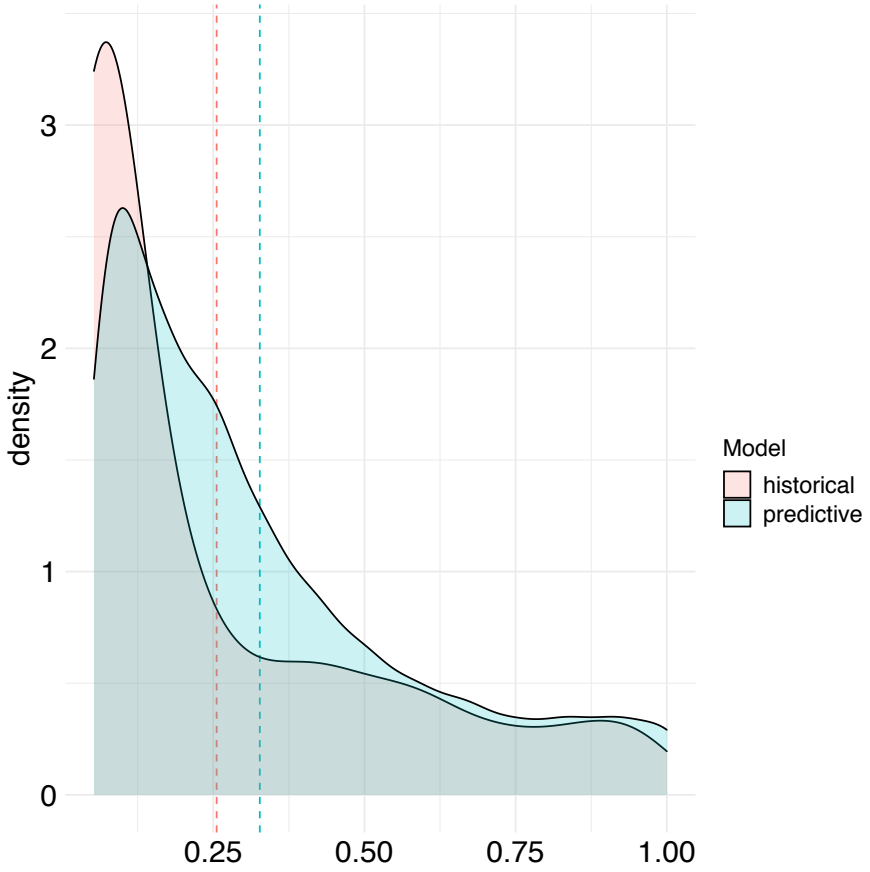

Figure 4.2: Density distributions and means (dashed vertical lines) of the frequentist likelihood f for the *historical* (red) and *predictive* (blue) ensembles.

4.3.4 Comparison among crops, variables and baskets

Overall, there appear to be no direct link between shocks in production, yield and area. Shocks are caused about as often by changes in harvested area as by changes in yield. In a few cases, production shocks are not caused by either yield or area shocks, but rather by a synergy between them (Table 4.3, Figures 4.3, 4.4 and 4.5).

For $f > 0$ (i.e. considering all shocks), soybean shows the greatest variability among baskets for all variables (yield, area and production). Soybean is also characterized by more baskets showing more area shocks than yield shocks. Soybean also shows significantly more shocks in harvested area than maize, but no significant difference with wheat. This result does not hold, however, for higher values of f. The ranking of baskets by the total number of production shocks detected (and the average number of shocks detected by all models in the ensemble) is not maintained for higher values of f, but rather stabilizes for $f > 0.5$.

For higher values of f (i.e. major shocks), comparing crops:

- **Maize** shows the greatest variability among baskets in the number of shocks detected. The shocks identified for maize are primarily in yield and production, rather than area. The baskets with significantly elevated number of production shocks are Eastern EU & Ukraine (Tukey's HSD group a), followed by USA and Central Europe (Tukey's group b). These baskets are among the top five maize producers, so these findings indicate a large global risk for maize production.
- **Soybean** shows no clear dominance of either yield or area as the driver of production shocks. The Indian basket (the fifth-ranked producer on average) is distinguished by a larger number of production shocks than other baskets.
- For **wheat**, production shocks tend to be caused more by yield than by harvested area, although this tendency is not clearcut. The basket most at risk for production shocks is Central Europe.

For higher values of f (major shocks), most production shocks are caused by sudden large changes either in yield or in area. Major shocks in production caused by the combination of yield and area shocks (see Table 4.3) do occur, but they are relatively rare. This property of the data emphasizes (a) that production shocks are usually due to a sudden change in one variable only, and (b) that production shocks are not predominantly caused by yield shocks, nor by area shocks, but rather that

both are important contributors. Exceptions are some important maize baskets, including the USA, where major shocks are disproportionately yield-driven.

	$f > 0$							$f > .5$							$f > .75$						
	production	**T**[1]	**yield**	**T**	**area**[2]	**T**	**y & ha**[3]	**p (only)**[4]	**production**	**T**	**yield**	**T**	**area**	**T**	**y & ha**	**p (only)**	**production**	**T**	**yield**	**T**	**area**	**T**	**y & ha**	**p (only)**
Maize																								
USA	10	ab	7	bc	12	ab	4	2	2	bcd	2	bcd	1	bcd	1	0	2	b	2	a	1	a	1	0
MEX	8	abc	12	abc	7	ab	2	0	2	de	2	cde	2	a	0	0	1	c	2	a	1	a	0	0
BRA	17	ab	13	a	9	ab	4	4	4	b	5	a	2	abcd	1	0	1	c	2	a	0	b	0	0
ARG	7	bc	8	cd	8	ab	3	0	2	de	2	de	0	e	0	0	1	c	1	b	0	b	0	0
C EU	6	ab	5	d	12	ab	2	1	3	bc	1	ef	2	ab	0	0	2	b	1	b	1	a	0	0
E EU & UKR	8	a	13	ab	10	a	7	0	5	a	3	bc	2	ab	0	0	3	a	2	a	0	b	0	0
S AFR	6	bc	8	bc	6	ab	1	0	2	cd	2	de	1	bcd	0	0	1	c	1	b	1	a	0	0
E AFR	11	ab	11	ab	8	ab	3	4	3	bcd	4	b	2	ab	1	0	0	d	1	b	1	a	1	0
W AFR	11	bc	12	abc	15	ab	6	1	1	ef	3	bcd	1	cd	0	0	0	d	1	b	0	b	0	0
CHN	12	ab	12	bc	8	b	5	5	3	bcd	1	ef	1	d	0	0	1	c	1	b	0	b	0	0
IDN	7	c	11	cd	5	ab	0	2	1	f	1	f	2	abc	0	0	0	d	0	d	0	b	0	0
Soybean																								
USA	9	a	8	ab	6	a	0	0	2	b	2	bc	2	ab	0	0	1	b	1	b	2	a	0	0
ARG	17	a	7	bc	18	a	3	4	2	b	2	c	2	bc	0	0	1	b	1	b	0	c	0	0
S BRA	11	a	11	ab	10	a	1	3	4	a	2	c	1	c	0	0	0	c	1	b	0	c	0	0
C BRA	21	a	5	c	12	a	1	9	3	ab	1	d	3	ab	0	0	1	b	0	c	0	c	0	0
IND	12	a	15	ab	18	a	6	1	3	ab	1	d	3	ab	0	0	2	a	1	b	1	b	0	0
NE CHN	15	a	13	a	15	a	5	0	1	c	3	a	3	a	0	0	0	c	3	a	2	a	0	0
E CHN	6	a	12	ab	9	a	4	1	2	b	3	b	2	ab	0	0	1	b	1	b	1	b	0	0
Wheat																								
N USA & CAN	6	b	5	b	8	ab	2	0	2	bc	2	ab	1	bc	0	0	1	b	1	a	1	a	0	0
CS USA	8	ab	11	ab	10	b	3	0	1	d	1	c	0	d	0	0	1	b	0		0	b	0	0
ARG	5	b	9	ab	9	ab	2	0	1	d	2	ab	2	ab	0	0	1	b	1	a	1	a	0	0
C EU	6	ab	6	ab	6	ab	2	1	3	a	2	ab	2	ab	0	0	2	a	1	a	0	b	0	0
E EU & RUS	4	b	7	ab	4	ab	1	0	2	bc	2	b	2	a	1	0	1	b	1	a	1	a	0	0
TUR	10	a	10	ab	13	a	3	0	3	ab	2	ab	2	ab	0	0	1	b	1	a	1	a	0	0
EGY	12	a	14	ab	11	a	4	1	2	cd	2	ab	2	abc	0	0	1	b	1	a	0	b	0	0
IND & PAK	9	ab	10	b	15	a	4	0	1	d	1	c	1	c	0	0	1	b	0	b	0	b	0	0
CHN	16	a	10	a	12	a	3	4	1	d	2	b	2	abc	0	0	0	c	0	b	0	b	0	0
SE AUS	11	a	8	a	16	a	4	2	3	ab	3	a	2	ab	1	0	1	b	1	a	0	b	0	0

[1] T: Tukey's HSD group;

[2] area: harvested area;

[3] y & ha: yield and harvested area shocks only (without a shock in production);

[4] p (only): production shocks only (shock in production with no shock in yield or harvested area);

Table 4.3: Total number of shocks per basket and agricultural variable and Tukey's HSD groups (T), as a function of the frequentist likelihood f (*historical* ensemble).

Figure 4.3: **Maize** number of shocks in production (prod.), yield and area (ha) per basket as a function of the frequentist likelihood f (*historical* ensemble).

Figure 4.4: **Soybean** number of shocks in production (prod.), yield and area (ha) per basket as a function of the frequentist likelihood f (*historical* ensemble).

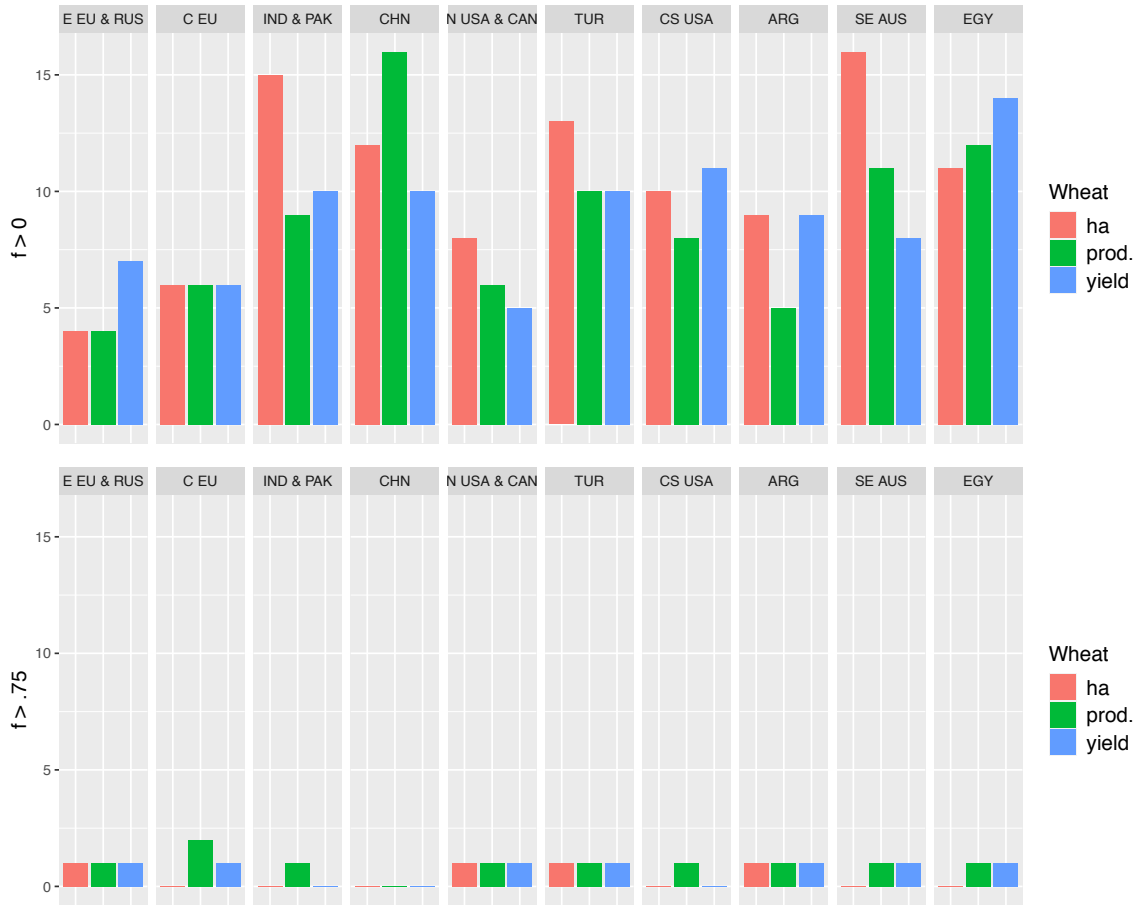

Figure 4.5: **Wheat** number of shocks in production (prod.), yield and area (ha) per basket as a function of the frequentist likelihood f (*historical* ensemble).

4.3.5 Global perspective

In this section I consider shocks detected at the global scale (see Table 4.4). In line with the results discussed above, I find a convergence of the mean of number of shocks in production, harvested area and yield for larger values of f. For smaller values of f, soybean presents a higher mean and standard deviation compared to maize and wheat. Nonetheless, overall (for all values of f), there are no significant differences in the mean number of shocks detected (according to Tukey's HSD test) between crops, or between variables. There is also no clear dominance of yield-driven shocks over area-driven shocks.

Considering the length of the time series studied (47 years, after the first five have been removed), the number of major shocks ($f > 0.75$) is low, ranging from 1.11 ($\pm$ 0.33) to 1.5 ($\pm$ 0.76) shocks in production – less than one per decade. This result contrasts with a prevalent narrative in the literature on agricultural production under climate change. Despite a statistically proven increase in risk due to an increase in climate variability (Huntington 2006, Hansen et al. 2012, Huntingford et al. 2013, Tigchelaar et al. 2018), the average number of major shocks in production of the most important crops remains low. This finding motivates the next question: has the incidence of shocks increased over time? This question is addressed in the following section.

	$f >$ **0**			$f >$ **.5**			$f >$ **.75**			$f >$ **.9**		
	mean	**STD**[1]	**IQR**[2]	**mean**	**STD**	**IQR**	**mean**	**STD**	**IQR**	**mean**	**STD**	**IQR**
Maize												
harvestedarea	9.09	2.95	3.50	1.60	0.52	1.00	1.00	0.00	0	1.00	0.00	0.0
production	9.36	3.29	4.00	2.55	1.21	1.00	1.50	0.76	1	1.33	0.58	0.5
yield	10.18	2.71	4.00	2.36	1.29	1.50	1.40	0.52	1	1.29	0.49	0.5
Soybean												
harvestedarea	12.57	4.61	7.00	2.29	0.76	1.00	1.50	0.58	1	1.00	0.00	0.0
production	13.00	5.07	6.00	2.43	0.98	1.00	1.20	0.45	0	0.00	0.00	0.0
yield	10.14	3.58	5.00	2.00	0.82	1.00	1.33	0.82	0	1.00	0.00	0.0
Wheat												
harvestedarea	10.40	3.81	4.50	1.78	0.44	0.00	1.00	0.00	0	1.00	0.00	0.0
production	8.70	3.68	4.75	1.90	0.88	1.75	1.11	0.33	0	1.00	0.00	0.0
yield	9.00	2.62	2.75	1.90	0.57	0.00	1.00	0.00	0	1.00	0.00	0.0

[1] STD: Standard Deviation;
[2] IQR: Interquartile Range;

Table 4.4: Summary statistics, per crop and agricultural variable, of the number of shocks detected by the *historical* ensemble of models as a function of the frequentist likelihood f.

4.3.6 Trends over time

The existence (or otherwise) of a temporal trend in the incidence of shocks was examined with a simple linear model (number-of-shocks versus time). The simplicity of this choice could be debated, but given the relative rarity of shocks, it is likely *a priori* that no more complex model could be justified. Tests were nonetheless also carried out using a more flexible Generalized Additive Model (GAM), but no additional insight was obtained and the results are therefore not reported here.

Results of these linear regressions are shown in Figure 4.6 for (from top to bottom) maize, soybean and wheat, for (from left to right) $f > 0$ and $f > 0.75$, aggregated for all baskets. Summary statistics for each linear model, adjusted R^2, regression coefficients and p-values are presented in SI (Section 4.6, Table 4.9). Considering all types of shocks detected by the ensemble ($f > 0$), there is a significant increasing trend in the number of shocks over time for all crops, and all agricultural variables. The largest R^2 values are shown for maize production (0.63) and yield (0.66), and soybean production (0.67) and harvested area (0.57), all with positive and significant ($p < 0.01$) trends over time. The strongest positive trend in the number of shocks is for maize yield, consistent with the observation that maize production shocks tend to be more often yield-driven (see Chapter 2, Section 2.3.3). For soybean, the increase in harvested-area shocks is in agreement with the large variations and particularly the increase in planted area described in Chapter 2, especially in the second half of the period.

For all three crops and all agricultural variables, I find significant ($p < 0.05$) positive trends in both the number of positive and negative shocks, but only for values of $0 < f < .3$ (SI, Section 4.6, Tables 4.9, 4.10, 4.11 and 4.12), a result that suggests an increase in variability rather than an increase in major shocks. When comparing the slopes, I find no difference between the slopes in negative vs positive shocks except for soybean yield, which shows a steeper increase in negative than positive shocks. The trends in positive and negative shocks complement results previously described in Chapter 2 (Sections 2.3.2 and 2.3.3), where I showed that maize showed the largest interannual variability in production, rooted in a dominance of yield variability over harvested area. Accordingly, maize yield shows a greater temporal slope in the incidence of shocks in yield (both positive and negative) than shocks in harvested area (Figures 4.6a, 4.6b, and SI, Section 4.6, Figures 4.11 and 4.13).

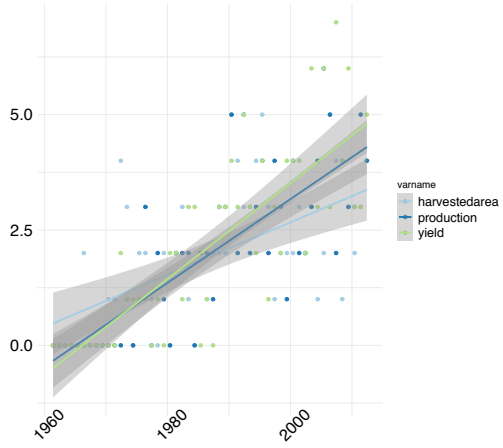

(a) Maize, $f > 0$

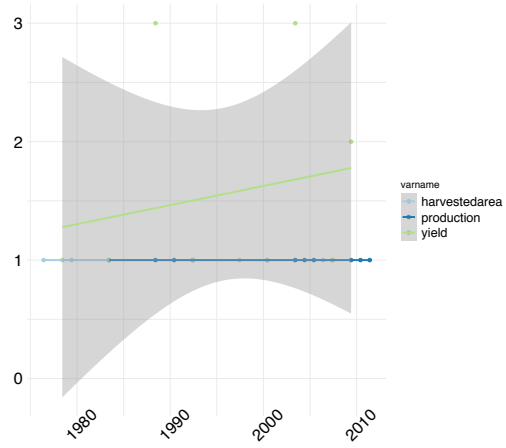

(b) Maize, $f > .75$

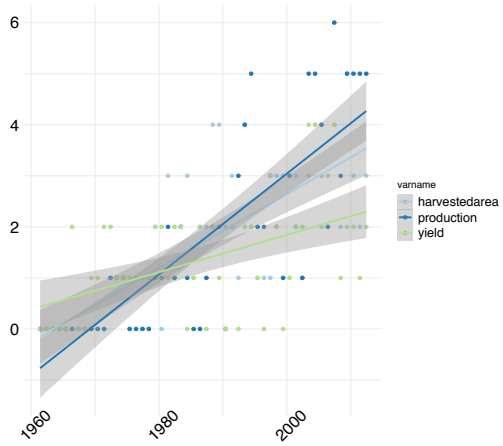

(c) Soybean, $f > 0$

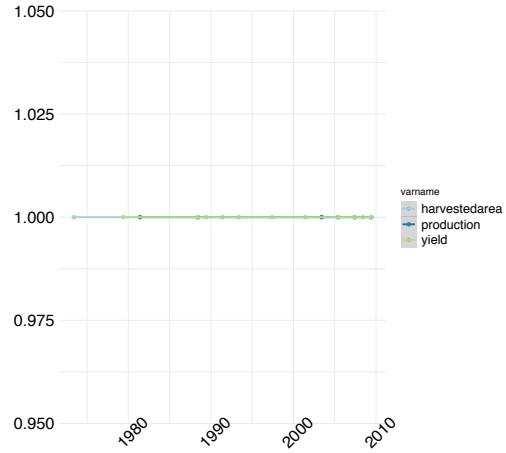

(d) Soybean, $f > .75$

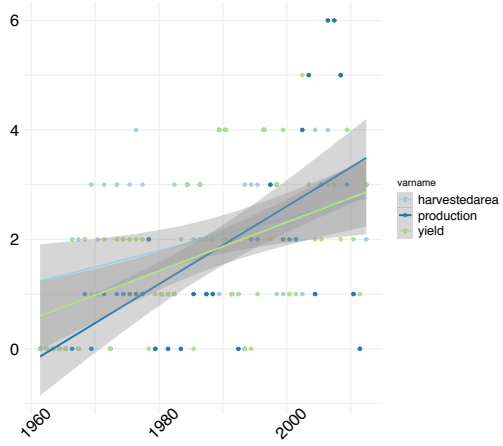

(e) Wheat, $f > 0$

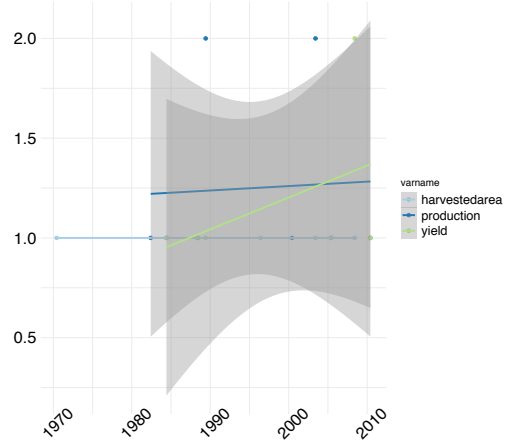

(f) Wheat, $f > .75$

Figure 4.6: Trends in shocks, *historical* ensemble; linear models of the evolution of the number of shocks over time, per crop and per agricultural variable, for different values of the frequentist likelihood f.

Aggregating all crops together and looking at production, yield and harvested area globally, I again find significant and positive trends in both positive and negative shocks (SI, Section 4.6, Tables 4.13, 4.14 and 4.15). There are no major differences between positive or negative shocks for each agricultural variable, although slopes in negative shocks tend to be slightly higher than positive shocks for production and yield. The temporal slopes for negative shocks are steeper for production and yield than for harvested area. These findings corroborate results in previous Chapter 2 concerning the asymmetry in the distributions of residuals toward negative values (Section 2.3.2, Figure 2.3), as well as the fact that harvested area is of great importance (Section 2.3.3). Interannual variability (considering all types and magnitudes of shocks) in yield has increased over time, at a slightly faster rate than harvested area.

As we consider shocks detected by a greater number of models, the proportion of variance explained by linear trends drops and the upward trend converges toward zero, becoming non-significant ($p > 0.05$) for all crops and all agricultural variables at values of $f > 0.3$. No firm inference can be made from this analysis, because of the small sample size (i.e. there have been too few major shocks to achieve statistical significance in the temporal trend). It may be relevant, however, that the positive trend in number of shocks consistently decreases as f increases.

The linear regression conducted per crop, over all agricultural variables, yields results no different from those obtained from separate regressions per crop and per agricultural variable (Figure 4.10 and Table 4.12). The only noticeable difference is that the upward trend is maintained as significant for f values up to 0.5.

Maize and soybean show stronger positive trends in the occurrence of shocks compared to wheat; wheat is influenced by low shock counts at the end of the series. These results are in line with the previous analysis (per crop and per agricultural variable), and there is a significantly positive trend in variability (for all shocks), but no major differences among crops.

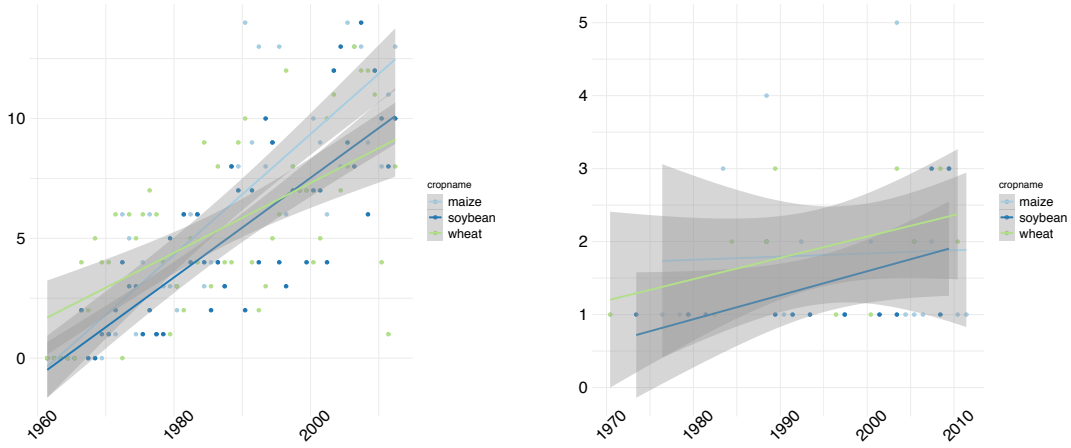

(a) $f > 0$ (b) $f > .75$

Figure 4.7: Trends in shocks, *historical* ensemble; linear models of the evolution of the number of shocks over time, per crop, for different values of the frequentist likelihood f.

4.4 Results: the predictive ensemble

The ensemble of models used in the predictive approach contains many of the same models used in the historical approach. After investigation, however, I removed the polynomial regressions (LOESS and cubic splines models), and the ETS model, from the predictive ensemble because they proved ill-adapted to this new approach – classifying nearly all points as shocks. On the other hand the predictive ensemble includes three models that were not included in the historical ensemble, namely State Space ARIMA, a random walk with drift (RWF), and a neural network specifically suited to forecasting univariate time series. Two other state space models were tested – ADAM (a dynamic adaptive model based on ETS and ARIMA processes) and GUM (Generalized Univariate Model), a model based on a generalization of exponential smoothing – but these proved to make excessive data demands, i.e. they required as much as half of the time series length simply to fit parameter values. In all analyses the first five years were removed from the series as there were too few data points to train any of the models in the ensemble, or to compute their confidence intervals.

The results from the predictive ensemble (Tables 4.5 and 4.6) are similar in many respects to the results obtained with the historical ensemble. The models showed considerable variation from one another; and the number of shocks detected converged towards a common value as f increased. The main difference between the two ensembles lies in the total number of shocks detected, which was two to five times greater for all values of f. This large increase in the number of detected shocks can be interpreted as reflecting the predictive models' poor ability to forecast future values. This interpretation is corroborated by the random walk with drift model, which detected far fewer shocks than the other models. In other words: many events that appeared immediately as shocks (and were identified as such by the predictive approach, which precludes knowledge of the future) turn out not to be so, with the benefit of hindsight, which is allowed in the historical approach.

	$f > \mathbf{0}$		$f > \mathbf{.5}$		$f > \mathbf{.75}$		$f > \mathbf{.9}$	
Model	**N**	**Tukey**	**N**	**Tukey**	**N**	**Tukey**	**N**	**Tukey**
sma_3	522	f	418	bcd	235	a	161	a
sma_5	532	f	406	cd	243	a	160	ab
sma_7	536	f	382	d	225	a	160	ab
sma_9	530	f	346	de	210	a	153	ab
ma_c3	1141	d	458	abc	240	a	161	a
ma_c5	1480	bc	485	ab	243	a	162	a
ma_c7	1533	b	482	abc	244	a	162	a
ma_c9	1603	b	488	abc	241	a	162	a
ARIMA	845	e	478	abc	241	a	161	a
SSARIMA	767	e	446	bcd	224	a	154	ab
RWF	344	f	227	e	131	b	106	b
NNAR	1272	cd	411	bcd	214	a	159	ab
At Least 1	2787	a	542	a	245	a	162	a

Table 4.5: Total number of detected shocks (N) per model of the *predictive* ensemble and Tukey's HSD groups (Tukey), as a function of the frequentist likelihood f.

	$f > \mathbf{0}$	$f > \mathbf{.5}$	$f > \mathbf{.75}$	$f > \mathbf{.9}$
min	344	227	131	106
max	2787	542	245	162
mean (SD)	1,068.62 ± 676.79 (***)	428.38 ± 79.89 (***)	225.85 ± 30.85 (***)	155.62 ± 15.2 (***)
median (IQR)	845.00 (532.00, 1,480.00)	446.00 (406.00, 482.00)	240.00 (224.00, 243.00)	161.00 (159.00, 162.00)

***: p-value < 0.001 (Tukey's HSD test for equality of means);
SD: Standard Deviation;
IQR: Interquartile Range;

Table 4.6: Summary statistics of the number of shocks detected by the *predictive* ensemble of models as a function of the frequentist likelihood f.

There are some more specific differences between the two ensembles, summarized below.

The likelihoods (Figure 4.8) of the identified shocks seem visually to better emphasize the weight of yield versus harvested area on consequent production shocks. As an example, for the USA and Eastern EU & Ukraine maize baskets, the predictive ensemble shows a higher density of production and yield shocks (both less important shocks and major shocks) than harvested area shocks. In addition, in contrast with the historical ensemble, the likelihoods are more evenly spread across the full range of f. Their distribution (Figure 4.2) is still positively skewed but the values are more uniformly distributed for $0.1 < f < 0.5$, and the peak is shifted to the right, to the range 0.2–0.4 (as compared to 0.0–0.2 for the historical ensemble). There is also an enhanced frequency of shocks with high (0.8–1.0) f values. The historical and predictive approaches generally identify the same major shocks. Nonetheless, a close look at the time series (e.g. the Eastern EU & Ukraine maize basket) shows that high-amplitude shocks are better captured by the predictive ensemble.

Table 4.7 summarizes the number of shocks per basket, as detected by the predictive ensemble. Again, the predictive ensemble shows many similarities to the historical ensemble, with large variability between baskets for each crop, for the whole range of f. Again, production shocks are most commonly traceable either to yield or harvested area shocks. However, for intermediate values of f, the predictive ensemble identifies more shocks related to the combination of yield and harvested area shocks than the historical ensemble does.

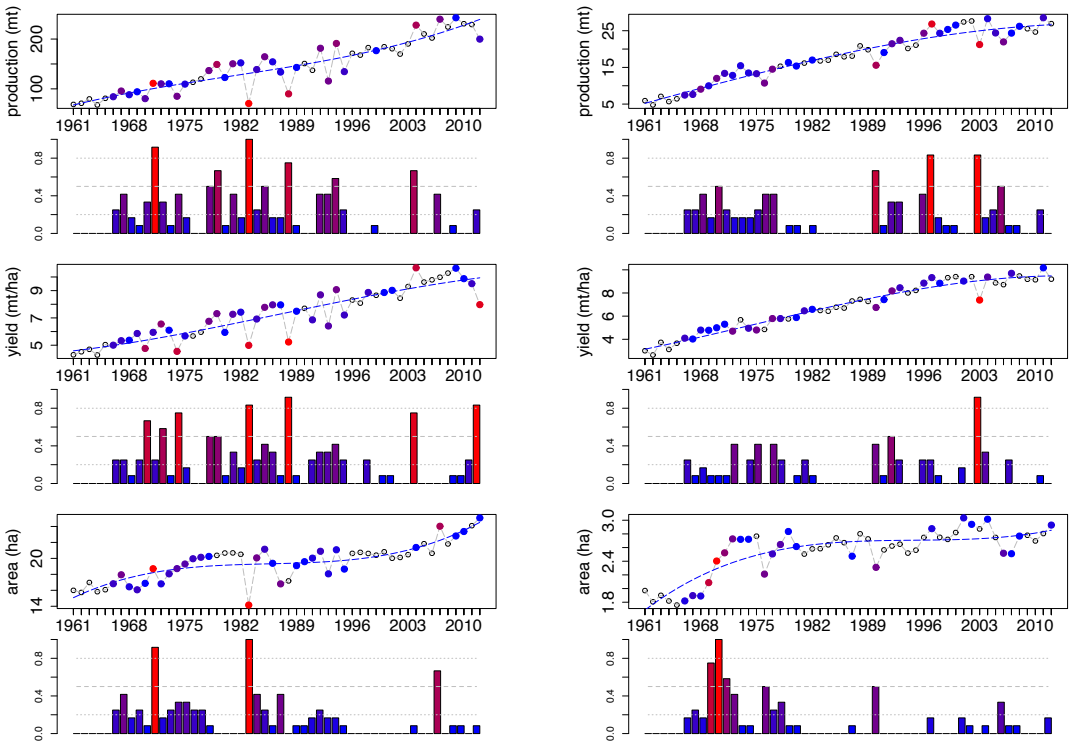

(a) Maize USA

(b) Maize Central EU

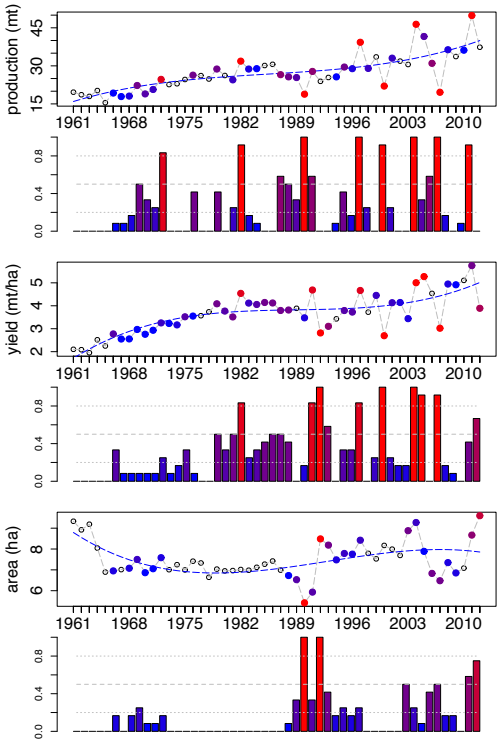

(c) Maize Eastern EU & Ukraine

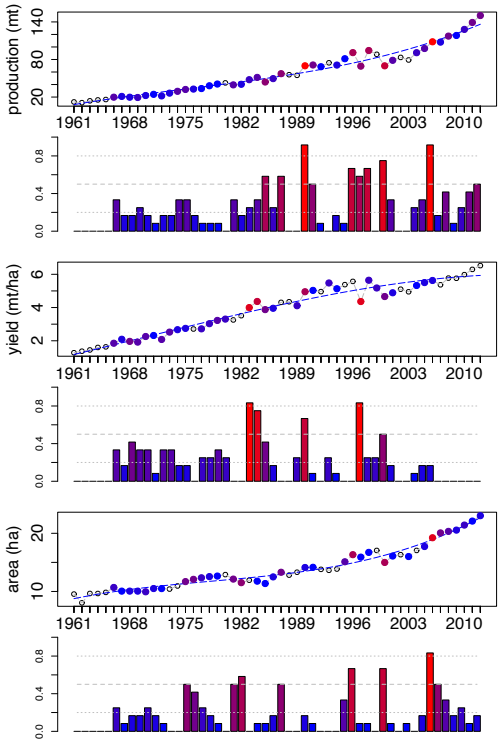

(d) Maize China

Figure 4.8: Maize production (mt), yield (mt/ha), area (ha), and frequentist likelihood of shocks (histograms) for the *predictive* ensemble, in the USA, Central EU, Eastern EU & Ukraine and China (from top left to bottom right).

	$f > 0$								$f > .5$							$f > .75$							
	production	**T**[1]	**yield**	**T**	**area**[2]	**T**	**y & ha**[3]	**p (only)**[4]	**production**	**T**	**yield**	**T**	**area**	**T**	**y & ha**	**p (only)**	**production**	**T**	**yield**	**T**	**area**	**T**	**y & ha**	**p (only)**
Maize																								
USA	31	a	35	ab	30	a	26	1	8	def	9	bcd	3	cd	1	0	3	de	5	b	2	de	1	0
MEX	35	a	27	ab	26	a	18	5	7	def	9	bcd	4	cd	0	0	4	d	4	bc	1	f	0	0
BRA	37	a	35	ab	42	a	32	0	16	a	14	a	8	b	3	0	10	a	8	a	2	de	1	0
ARG	33	a	41	ab	31	a	29	1	10	bcde	12	ab	7	bc	3	0	6	c	5	b	1	f	0	0
C EU	31	a	26	b	24	a	16	3	5	f	2	e	5	bcd	0	0	2	e	1	d	2	e	0	0
E EU $ UKR	32	a	40	a	25	a	22	2	13	ab	14	a	6	bc	3	0	8	ab	8	a	3	c	1	0
S AFR	35	a	32	ab	37	a	26	1	7	ef	8	bcd	12	a	2	0	4	d	5	b	4	b	0	0
E AFR	35	a	38	ab	32	a	24	1	13	bc	14	a	7	bc	2	0	7	c	9	a	3	cd	1	0
W AFR	30	a	32	ab	34	a	27	2	11	bcd	7	cd	10	a	1	0	7	bc	4	bc	6	a	0	0
CHN	40	a	31	ab	35	a	22	1	10	cde	5	de	8	bc	1	0	3	de	3	c	1	f	0	0
IDN	44	a	38	ab	31	a	24	2	14	abc	11	abc	3	d	1	0	4	d	5	b	0	g	0	0
Soybean																								
USA	29	ab	36	a	25	b	19	0	9	cd	10	a	5	c	2	0	3	d	7	a	2	b	0	0
ARG	40	ab	32	a	38	a	28	3	19	ab	7	ab	15	a	4	0	4	cd	5	ab	5	a	1	0
S BRA	34	ab	40	a	28	ab	26	0	14	abc	7	bc	6	bc	1	0	9	a	2	c	2	b	0	0
C BRA	44	a	37	a	37	a	29	2	19	ab	3	c	15	a	1	0	8	ab	2	c	4	a	0	0
IND	45	a	24	a	41	a	21	2	20	a	6	bc	14	a	3	0	6	bc	3	c	6	a	0	0
NE CHN	33	ab	33	a	39	ab	27	0	10	bcd	9	ab	10	ab	3	0	5	cd	5	b	4	a	0	0
E CHN	30	b	29	a	26	b	16	1	5	d	12	a	5	c	3	0	4	cd	5	b	2	b	0	0
Wheat																								
N USA & CAN	33	a	31	a	28	a	20	3	6	bc	4	cd	3	cd	0	0	2	ef	1	e	1	e	0	0
CS USA	35	a	32	a	23	a	18	4	6	bc	8	b	6	bc	2	0	3	cd	5	b	2	de	0	0
ARG	31	a	34	a	28	a	21	1	6	bc	6	bc	6	bc	1	0	4	bc	3	c	3	bc	1	0
C EU	32	a	37	a	33	a	29	0	5	c	2	d	6	bc	1	0	1	f	1	e	2	cde	0	0
E EU & RUS	37	a	33	a	39	a	27	0	8	bc	7	bc	9	a	4	0	3	cd	1	e	6	a	0	0
TUR	28	a	34	a	23	a	17	3	6	bc	6	bc	6	ab	1	0	4	bc	3	cd	5	a	0	0
EGY	31	a	28	a	33	a	22	1	8	ab	7	b	6	bc	0	0	5	b	4	b	4	b	0	0
IND & PAK	38	a	33	a	31	a	22	2	7	bc	2	d	2	d	1	0	2	ef	1	e	1	e	1	0
CHN	26	a	25	a	41	a	22	0	8	b	6	bc	6	bc	0	0	3	de	2	d	3	bcd	0	0
SE AUS	38	a	35	a	32	a	22	0	10	a	12	a	6	bc	1	0	7	a	6	a	2	de	0	0

[1] T: Tukey's HSD group;

[2] area: harvested area;

[3] y & ha: yield and harvested area shocks only (without a shock in production);

[4] p (only): production shocks only (shock in production with no shock in yield or harvested area);

Table 4.7: Total number of shocks per basket and agricultural variable and Tukey's HSD groups (T), as a function of the frequentist likelihood f (*predictive* ensemble).

The large variability among baskets makes it hard to discern a clear geographic pattern. A few baskets however stand out by having a significantly lower or higher number of shocks than the average, and some contrasts are indicated that were less clear in the historical analysis:

- For **maize**, the Central Europe and South African baskets show a significantly lower production shock count compared to the other baskets. The Brazilian and Indonesian baskets stand out by showing a much higher number of production shocks than other baskets.
- For **soybean**, the Argentinean and South and Central Brazil baskets show many more "mid-level" ($0.3 < f < 0.75$) shocks as well as major production shocks. In contrast, the North American baskets (USA and Canada) shows a low shock count for $f > 0.5$ and the lowest count of major shocks. The North East China basket shows exceptional stability, with few mid-level or major shocks.
- For **wheat**, the Northern American, Central European and India-Pakistan baskets show low counts of both mid level and major shocks, contrasting with the South East Australian basket showing the highest variability and major shock counts. This is in line with the reported sensitivity of the SE Australia wheat basket to production shocks.

Table 4.8 summarizes the shocks detected at the global level (all baskets) for each crop and agricultural variable. The historical approach showed no significant differences (according to Tukey's HSD) between agricultural variables per crop for different values of f at the global level. The results from the predictive approach are little different, except for maize harvested area at $f > .75$, which showed significantly fewer shocks than yield and production. The predictive approach thus confirms the indication in the historical analysis that major maize production shocks have been primarily driven by yield rather than harvested area.

Results from trend analysis based on the predictive ensemble show the greatest contrast with the historical ensemble. For both the agricultural variable (per crop) and global-scale crop comparisons, there is a significant (negative) trend in shocks for $f > 0.1$ only. However, weakly negative trends were typical (Figures 4.9 and 4.10, and SI, Section 4.6, Tables 4.16 and 4.17).

	$f > 0$			$f > .5$			$f > .75$			$f > .9$		
	mean	**STD**[1]	**IQR**[2]	**mean**	**STD**	**IQR**	**mean**	**STD**	**IQR**	**mean**	**STD**	**IQR**
Maize												
harvestedarea	31.55	5.39	6.50	4.55	2.46	2.00	2.00	1.41	1.0	1.78	1.09	1.00
production	34.82	4.24	4.50	8.09	3.02	3.00	3.91	2.21	2.0	3.22	1.64	2.00
yield	34.09	4.99	6.50	7.91	3.36	4.00	4.18	2.36	3.5	2.78	1.86	3.00
Soybean												
harvestedarea	33.43	6.80	11.50	8.00	4.08	6.00	2.71	1.38	2.5	2.33	1.37	2.25
production	36.43	6.55	10.50	11.43	4.16	6.00	4.00	1.63	2.0	2.43	0.53	1.00
yield	33.00	5.35	6.00	6.29	1.98	2.00	3.57	1.27	2.0	2.57	1.40	1.50
Wheat												
harvestedarea	31.10	5.95	5.00	4.40	1.78	1.00	1.89	1.27	1.0	1.60	0.89	1.00
production	32.90	4.12	5.50	5.30	1.77	1.75	2.60	1.71	1.0	2.11	1.54	1.00
yield	32.20	3.49	2.75	3.90	2.69	3.50	2.33	1.73	2.0	2.00	1.41	1.25

[1] STD: Standard Deviation;

[2] IQR: Interquartile Range;

Table 4.8: Summary statistics, per crop and agricultural variable, of the number of shocks detected by the *predictive* ensemble of models as a function of the frequentist likelihood f.

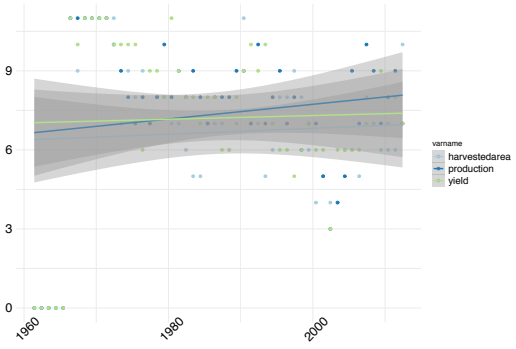

(a) Maize, $f > 0$

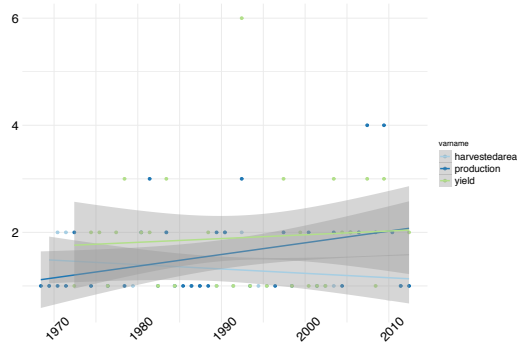

(b) Maize, $f > .75$

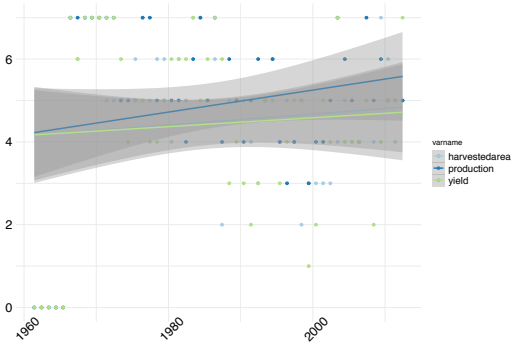

(c) Soybean, $f > 0$

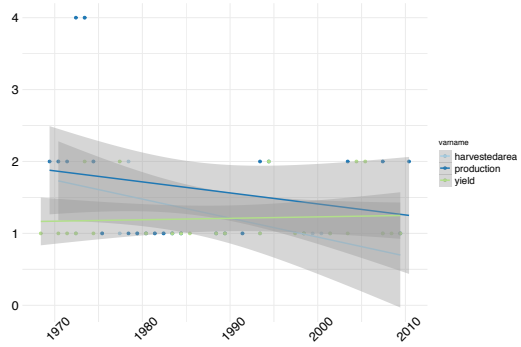

(d) Soybean, $f > .75$

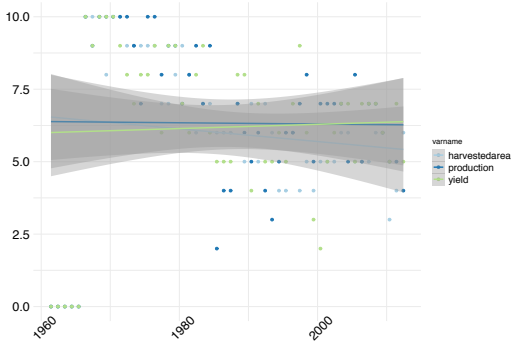

(e) Wheat, $f > 0$

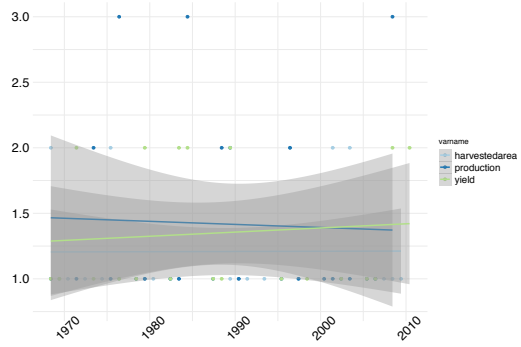

(f) Wheat, $f > .75$

Figure 4.9: Trends in shocks, *predictive* ensemble; linear models of the evolution of the number of shocks over time, per crop and per agricultural variable, for different values of the frequentist likelihood f.

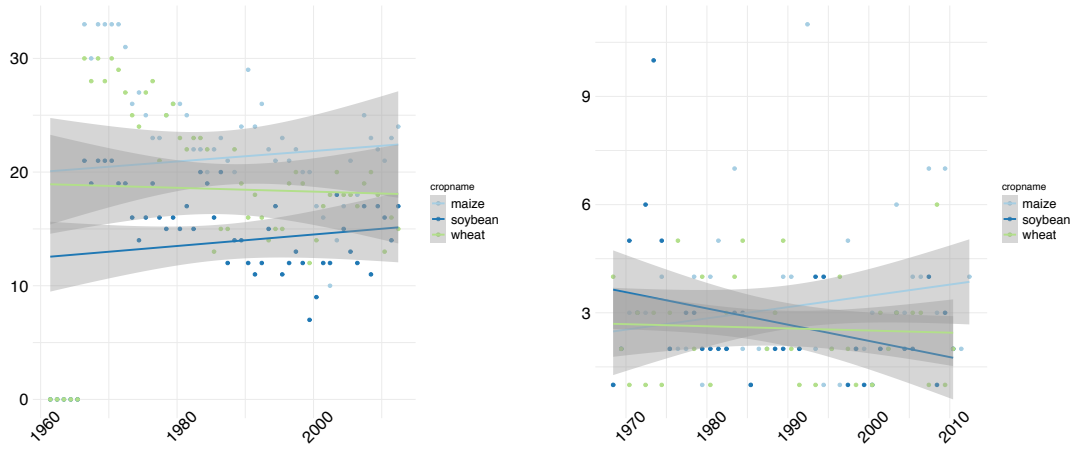

(a) $f > 0$ (b) $f > .75$

Figure 4.10: Trends in shocks, *predictive* ensemble; linear models of the evolution of the number of shocks over time, per crop, for different values of the frequentist likelihood f.

4.5 Discussion and Conclusions

Empirical agricultural datasets, as illustrated in this chapter, are rarely "well-behaved" and commonly include data points that seem dissonant with the rest of the time series. Such aberrant observations, depending on the objective of the study (defining the best model, removing seasonality, detrending, forecasting), as well as the field of study (statistics, economics, data quality), can be labelled by many different terms, including disturbances, anomalies, outliers, and shocks – the generic term I have used here. Outlier detection is a common process in statistical modelling; its purpose is to identify data points that could create a bias in the model (Guttman & Tiao 1978, Lloyd 1993). The decision as to whether to include or remove outliers is key, as all models depend on minimizing a loss function defined on the residuals, which are disproportionately influenced by outliers (Chuang & Lee 2011, Wang & Zhong 2014). Outliers nontheless constitute important information that may be invaluable, cannot be ignored, and need to be studied. This is part of the motivation of this chapter, which differs from other "robust" methods in that I associate "aberrant" data with a likelihood, estimated via the application of multiple models.

Space and time are essential elements of agricultural data. Here, I have addressed the time component in two ways: via a historical approach, in which models are fitted using data from both before and after putative shocks; and a predictive approach, in which models are denied access to data from

the future. The predictive approach, of course, more closely resembles the situation faced by decision makers in real time. The space component has been addressed through the definition of baskets, which are major and geographically separated production areas, determined separately for each crop.

Results obtained for all shocks ($f > 0$) are not consistent, varying from model to model and between the historical and predictive ensembles. However, irrespective of the model's complexity, all models have been shown to capture all types of shocks. So-called "naive" models do not substantively differ from more complex models; they all capture about as many shocks as one another, and show convergence towards higher values of f. In other words, models with very different structure all identify a common set of major shocks. The predictive ensemble, however, captured some finer details at mid-level values of f; and showed clearer patterns of differences among baskets.

The full set of identified shocks ($f > 0$) proved to be various and inconsistent, varying from region to region, and from crop to crop. Nonetheless, a unifying result in this chapter is that the most important production shocks (detected by nearly all models) were caused either by a sudden change in yield, or a sudden change in harvested area. However, not every sudden change in yield or planted area caused a production shock (consider e.g. the Southern Brazil basket for soybean). Maize was shown to be more yield-driven than the other crops, and to show on average more shocks and major shocks in production than soybean or wheat. It remains true that on average, for the time period considered (1961–2012), the number of major production shocks was small. No positive trend in the number of shocks over time was found for major shocks. A significant and positive trend in all three crops, and in all crops together, was detected only when considering all shocks regardless of their importance. This finding corroborates findings in the literature (Ben-Ari & Makowski 2014, 2016, Tigchelaar et al. 2018) of an increase in the number of anomalies (or variability) over time, but adds the important nuance that there has been no increase in major shocks.

This conclusion does not take into consideration the increased pressure of demand due to rising population, and increasing interdependencies due to global trade. It is possible, for these reasons, that production shocks could have had more "snowballing" effects in recent years than they used to in the past. This possibility is not addressed in this study. Another issue not considered is the possible relationship between observed variability and levels of stocks.

This analysis has underlined that production shocks are not linked only to climate variability, but also to policy shifts. It does not uphold the simple narrative of increasing volatility due to a changing

climate. However, emerging markets show signs of increased volatility in recent years.

The approach to characterizing shocks presented in this chapter has no equivalent in the literature. A number of methodological improvements and extensions could be envisaged, including applications of multivariate and cluster analyses, breakpoint modelling, and a leave-one-model-out approach to quantify the sensitivity of results to the choice of models. Nonetheless, the ensemble and likelihood approaches have yielded insights that cannot be found elsewhere; while the comparison of a historical with a novel, predictive definition of shocks has highlighted the subtle differences between analysis informed by hindsight, and the interpretation of current events in real time.

4.6 Supplementary Information

	f	R^2	R^2-adj	intercept	intercept.pval	time	time.pval
Maize							
production	0.00	0.63	0.62	-0.43	0.16	0.09	0.00
	0.10	0.36	0.34	0.26	0.64	0.06	0.00
	0.20	0.04	0.01	1.22	0.03	0.01	0.29
	0.50	0.03	-0.02	0.93	0.21	0.01	0.46
	0.75	0.53	0.49	1.00	0.00	0.00	0.05
yield	0.00	0.66	0.65	-0.60	0.07	0.10	0.00
	0.10	0.35	0.33	0.03	0.96	0.07	0.00
	0.20	0.13	0.09	0.65	0.48	0.04	0.09
	0.50	0.11	0.04	0.94	0.19	0.02	0.23
	0.75	0.04	-0.10	0.99	0.41	0.02	0.61
harvested area	0.00	0.34	0.32	0.42	0.23	0.06	0.00
	0.10	0.05	0.02	1.41	0.00	0.02	0.21
	0.20	0.01	-0.04	1.57	0.01	-0.01	0.71
	0.50	0.00	-0.09	1.18	0.02	0.00	0.90
	0.75	0.44	0.25	1.00	0.00	0.00	0.35
Soybean							
production	0.00	0.67	0.67	-0.87	0.01	0.10	0.00
	0.10	0.37	0.34	-1.17	0.29	0.10	0.00
	0.20	0.40	0.37	-1.19	0.26	0.09	0.00
	0.50	0.19	0.09	0.06	0.96	0.04	0.20
	0.75	0.52	0.39	1.00	0.00	0.00	0.08
yield	0.00	0.26	0.25	0.40	0.14	0.04	0.00
	0.10	0.13	0.09	0.79	0.04	0.02	0.06
	0.20	0.12	0.06	0.67	0.20	0.02	0.15
	0.50	0.05	-0.06	0.87	0.18	0.01	0.51
	0.75	0.55	0.48	1.00	0.00	0.00	0.07
harvested area	0.00	0.57	0.56	-0.22	0.41	0.07	0.00
	0.10	0.31	0.29	0.29	0.44	0.04	0.00
	0.20	0.14	0.09	0.66	0.15	0.02	0.09
	0.50	0.08	0.00	0.81	0.03	0.01	0.32
	0.75	0.65	0.56	1.00	0.00	0.00	0.04
Wheat							
production	0.00	0.41	0.40	-0.21	0.56	0.07	0.00
	0.10	0.26	0.23	0.14	0.84	0.06	0.00
	0.20	0.14	0.11	0.29	0.74	0.04	0.07
	0.50	0.18	0.10	0.60	0.33	0.02	0.15
	0.75	0.00	-0.16	1.17	0.12	0.00	0.90
yield	0.00	0.26	0.25	0.55	0.09	0.04	0.00
	0.10	0.05	0.02	1.17	0.01	0.02	0.20
	0.20	0.04	0.00	1.02	0.03	0.01	0.30
	0.50	0.05	-0.03	1.11	0.04	0.01	0.45
	0.75	0.20	0.01	0.57	0.40	0.02	0.37
harvested area	0.00	0.12	0.10	1.21	0.00	0.03	0.01
	0.10	0.06	0.03	1.43	0.00	0.01	0.17
	0.20	0.10	0.06	1.13	0.00	0.01	0.12
	0.50	0.38	0.33	0.62	0.03	0.02	0.02
	0.75	0.00	0.00	1.00	0.00	0.00	0.00

Table 4.9: Summary statistics for the linear models of the trends in number of shocks over time (Figure 4.6) for different values of the frequentist likelihood f (*historical* ensemble).

f	R^2	R^2-adj	intercept	intercept.pval	time	time.pval
Maize						
0.00	0.56	0.55	-0.51	0.31	0.13	0.00
0.10	0.49	0.48	-0.72	0.36	0.12	0.00
0.20	0.24	0.21	0.09	0.91	0.06	0.01
0.30	0.28	0.25	0.48	0.31	0.04	0.01
0.40	0.07	0.02	0.97	0.03	0.01	0.23
0.50	0.01	-0.04	1.14	0.01	0.00	0.64
0.75	0.00	-0.24	1.31	0.29	0.00	0.90
Soybean						
0.00	0.37	0.35	-0.11	0.85	0.10	0.00
0.10	0.28	0.26	0.22	0.76	0.07	0.00
0.20	0.22	0.18	0.48	0.58	0.05	0.03
0.30	0.08	0.02	0.82	0.50	0.03	0.28
0.40	0.17	0.11	0.51	0.57	0.04	0.13
0.50	0.12	0.04	0.90	0.21	0.02	0.26
0.75	0.00	0.00	1.00	0.00	0.00	0.00
Wheat						
0.00	0.19	0.18	0.93	0.13	0.07	0.00
0.10	0.03	0.00	1.75	0.03	0.02	0.32
0.20	0.03	-0.01	1.34	0.07	0.02	0.36
0.30	0.04	-0.01	1.18	0.11	0.02	0.37
0.40	0.20	0.14	0.39	0.60	0.04	0.07
0.50	0.19	0.11	0.54	0.59	0.04	0.16
0.75	0.01	-0.24	1.50	0.17	0.00	0.86

Table 4.10: Summary statistics for the linear models of the trends in number of *positive* shocks per crop over time, for different values of the frequentist likelihood f (*historical* ensemble).

f	R^2	R^2-adj	intercept	intercept.pval	time	time.pval
Maize						
0.00	0.36	0.35	-0.09	0.89	0.12	0.00
0.10	0.12	0.09	1.22	0.31	0.07	0.05
0.20	0.09	0.06	1.18	0.25	0.05	0.11
0.30	0.08	0.05	1.24	0.26	0.04	0.15
0.40	0.09	0.05	0.98	0.37	0.04	0.15
0.50	0.25	0.20	0.39	0.72	0.07	0.04
0.75	0.02	-0.06	1.37	0.08	0.01	0.62
Soybean						
0.00	0.55	0.54	-0.59	0.18	0.11	0.00
0.10	0.36	0.34	-0.54	0.52	0.09	0.00
0.20	0.36	0.33	-0.61	0.52	0.08	0.00
0.30	0.27	0.23	-0.59	0.63	0.08	0.03
0.40	0.18	0.12	0.00	1.00	0.05	0.10
0.50	0.13	0.06	0.32	0.78	0.04	0.20
0.75	0.33	0.20	0.18	0.85	0.04	0.18
Wheat						
0.00	0.24	0.23	0.62	0.29	0.08	0.00
0.10	0.19	0.17	0.85	0.23	0.06	0.01
0.20	0.25	0.22	0.51	0.50	0.06	0.01
0.30	0.18	0.14	0.74	0.35	0.05	0.04
0.40	0.19	0.15	0.91	0.16	0.04	0.05
0.50	0.16	0.09	1.02	0.26	0.04	0.15
0.75	0.23	0.03	1.35	0.17	0.02	0.34

Table 4.11: Summary statistics for the linear models of the trends in number of *negative* shocks per crop over time, for different values of the frequentist likelihood f (*historical* ensemble).

f	R^2	R^2-adj	intercept	intercept.pval	time	time.pval
Maize						
0.00	0.73	0.72	-0.61	0.36	0.25	0.00
0.10	0.47	0.45	-0.63	0.55	0.18	0.00
0.20	0.28	0.26	0.30	0.75	0.10	0.00
0.30	0.18	0.16	0.64	0.51	0.07	0.01
0.40	0.14	0.11	0.91	0.30	0.06	0.03
0.50	0.10	0.06	1.17	0.19	0.04	0.11
0.75	0.00	-0.06	1.67	0.12	0.00	0.87
0.90	0.00	-0.14	1.54	0.32	0.01	0.87
Soybean						
0.00	0.69	0.69	-0.69	0.25	0.21	0.00
0.10	0.49	0.48	-1.41	0.17	0.17	0.00
0.20	0.43	0.41	-1.09	0.29	0.13	0.00
0.30	0.23	0.20	-0.49	0.72	0.09	0.02
0.40	0.16	0.13	0.32	0.77	0.06	0.05
0.50	0.14	0.10	0.32	0.76	0.05	0.08
0.75	0.25	0.19	0.29	0.63	0.03	0.07
0.90	0.00	0.00	1.00	0.00	0.00	0.00
Wheat						
0.00	0.38	0.37	1.55	0.06	0.15	0.00
0.10	0.23	0.21	1.39	0.11	0.09	0.00
0.20	0.26	0.24	0.56	0.52	0.09	0.00
0.30	0.20	0.18	0.80	0.28	0.06	0.01
0.40	0.24	0.22	0.48	0.45	0.06	0.00
0.50	0.20	0.16	0.54	0.53	0.06	0.03
0.75	0.20	0.11	0.91	0.23	0.03	0.17
0.90	0.17	-0.03	0.99	0.17	0.02	0.41

Table 4.12: Summary statistics for the linear models of the trends in number of *positive* and *negative* shocks per crop over time, for different values of the frequentist likelihood f (*historical* ensemble).

f	R^2	R^2-adj	intercept	intercept.pval	time	time.pval
Production						
0.00	0.63	0.62	-0.78	0.07	0.13	0.00
0.10	0.46	0.44	-1.15	0.20	0.12	0.00
0.20	0.37	0.34	-0.35	0.69	0.08	0.00
0.30	0.37	0.33	-0.63	0.48	0.07	0.00
0.40	0.15	0.10	0.11	0.93	0.05	0.11
0.50	0.11	0.04	0.52	0.66	0.04	0.23
0.75	0.04	-0.09	0.90	0.04	0.01	0.60
Yield						
0.00	0.41	0.40	0.31	0.48	0.08	0.00
0.10	0.30	0.27	0.20	0.75	0.06	0.00
0.20	0.13	0.09	0.54	0.42	0.03	0.07
0.30	0.18	0.13	0.55	0.29	0.03	0.06
0.40	0.11	0.06	0.80	0.02	0.01	0.17
0.50	0.05	-0.02	0.90	0.01	0.01	0.41
0.75	0.16	-0.01	0.55	0.43	0.02	0.38
Harvested Area						
0.00	0.42	0.41	0.78	0.08	0.09	0.00
0.10	0.24	0.22	1.05	0.01	0.04	0.00
0.20	0.09	0.06	1.01	0.01	0.02	0.09
0.30	0.06	0.02	1.09	0.00	0.01	0.24
0.40	0.10	0.06	0.87	0.01	0.02	0.12
0.50	0.22	0.16	0.80	0.05	0.02	0.08
0.75	0.36	0.15	1.00	0.00	0.00	0.02

Table 4.13: Summary statistics for the linear models of the trends in number of *positive* shocks per agricultural variable over time, as detected by the *historical* ensemble of models, as a function of the frequentist likelihood f.

f	R^2	R^2-adj	intercept	intercept.pval	time	time.pval
Production						
0.00	0.61	0.60	-0.73	0.12	0.13	0.00
0.10	0.35	0.33	-0.66	0.48	0.10	0.00
0.20	0.23	0.20	-0.38	0.74	0.08	0.01
0.30	0.14	0.10	0.32	0.78	0.06	0.07
0.40	0.18	0.13	0.20	0.84	0.05	0.06
0.50	0.20	0.15	0.34	0.71	0.05	0.07
0.75	0.01	-0.10	1.83	0.13	-0.01	0.80
Yield						
0.00	0.44	0.43	0.05	0.93	0.10	0.00
0.10	0.22	0.20	0.41	0.54	0.07	0.00
0.20	0.14	0.11	0.70	0.28	0.04	0.03
0.30	0.09	0.05	1.09	0.12	0.03	0.13
0.40	0.04	0.00	1.32	0.09	0.02	0.32
0.50	0.04	-0.01	1.17	0.23	0.02	0.36
0.75	0.00	-0.08	1.54	0.08	0.00	0.96
Harvested Area						
0.00	0.40	0.39	0.62	0.11	0.07	0.00
0.10	0.16	0.14	0.82	0.09	0.04	0.01
0.20	0.07	0.03	1.12	0.03	0.02	0.17
0.30	0.06	0.02	1.15	0.04	0.02	0.24
0.40	0.08	0.05	0.94	0.02	0.02	0.15
0.50	0.09	0.04	0.84	0.07	0.02	0.22

Table 4.14: Summary statistics for the linear models of the trends in number of *negative* shocks per agricultural variable over time, as detected by the *historical* ensemble of models, as a function of the frequentist likelihood f.

f	R^2	R^2-adj	intercept	intercept.pval	time	time.pval
Production						
0.00	0.85	0.84	-1.50	0.00	0.26	0.00
0.10	0.60	0.59	-2.57	0.03	0.23	0.00
0.20	0.40	0.38	-1.76	0.20	0.17	0.00
0.30	0.39	0.36	-1.21	0.32	0.13	0.00
0.40	0.30	0.27	-1.00	0.39	0.10	0.00
0.50	0.22	0.18	-0.40	0.75	0.08	0.02
0.75	0.13	0.07	0.63	0.44	0.03	0.16
Yield						
0.00	0.69	0.68	0.35	0.52	0.18	0.00
0.10	0.45	0.44	-0.14	0.87	0.14	0.00
0.20	0.25	0.23	0.25	0.79	0.09	0.00
0.30	0.17	0.14	0.62	0.50	0.06	0.02
0.40	0.08	0.04	1.15	0.21	0.04	0.13
0.50	0.16	0.12	0.60	0.52	0.05	0.05
0.75	0.08	0.01	0.90	0.39	0.03	0.30
Harvested Area						
0.00	0.59	0.59	1.40	0.02	0.16	0.00
0.10	0.38	0.37	1.36	0.02	0.09	0.00
0.20	0.13	0.11	1.57	0.01	0.04	0.03
0.30	0.11	0.08	1.58	0.01	0.03	0.06
0.40	0.12	0.09	1.40	0.00	0.03	0.05
0.50	0.23	0.20	0.87	0.02	0.03	0.01
0.75	0.05	-0.03	0.94	0.00	0.00	0.46

Table 4.15: Summary statistics for the linear models of the trends in number of *positive* and *negative* shocks per agricultural variable over time, for different values of the frequentist likelihood f (*historical* ensemble).

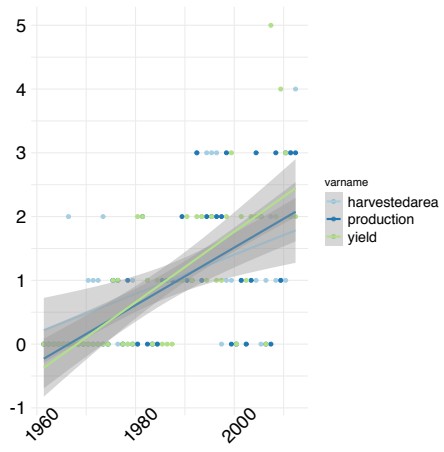

(a) Maize, $f > 0$

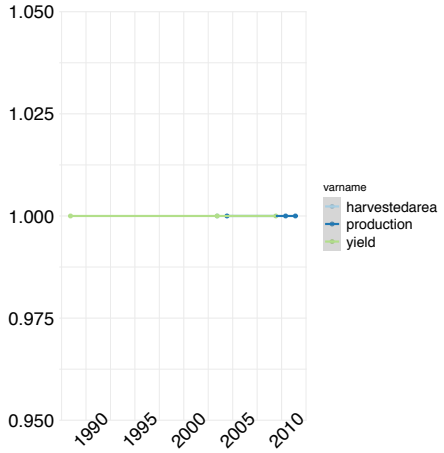

(b) Maize, $f > .75$

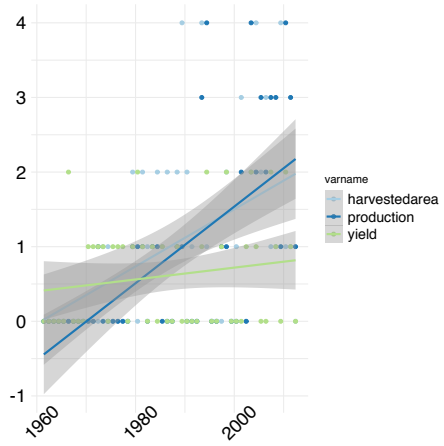

(c) Soybean, $f > 0$

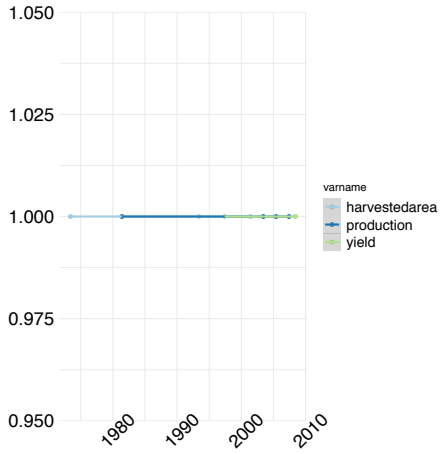

(d) Soybean, $f > .75$

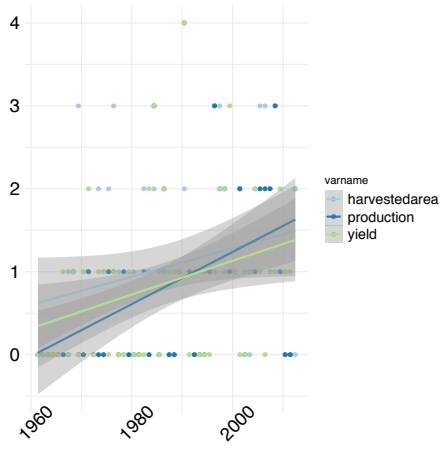

(e) Wheat, $f > 0$

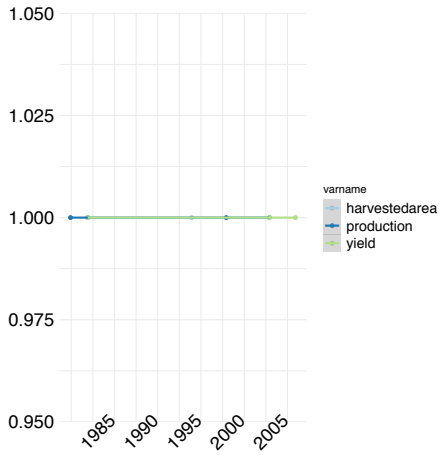

(f) Wheat, $f > .75$

Figure 4.11: Trends in *positive* shocks, *historical* ensemble; linear models of the evolution of the number of shocks over time, per crop and per agricultural variable, for different values of the frequentist likelihood f.

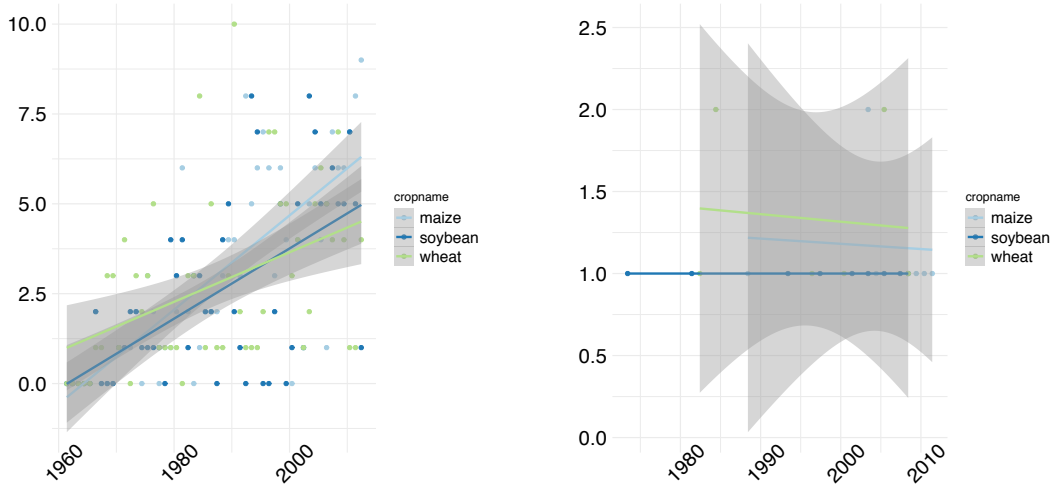

(a) $f > 0$ (b) $f > .75$

Figure 4.12: Trends in *positive* shocks, *historical* ensemble; linear models of the evolution of the number of shocks over time, per crop, for different values of the frequentist likelihood f.

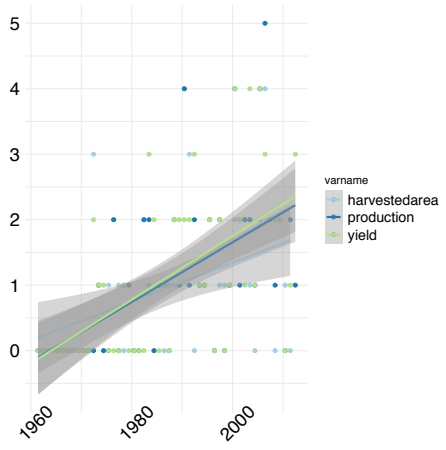

(a) Maize, $f > 0$

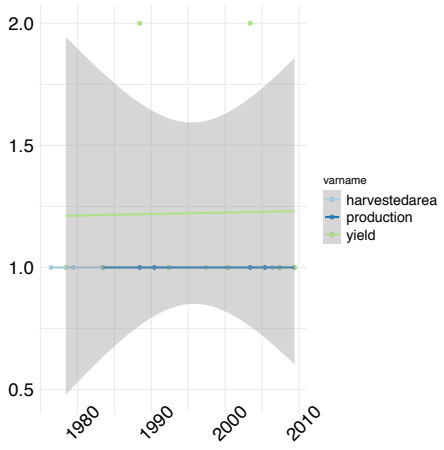

(b) Maize, $f > .75$

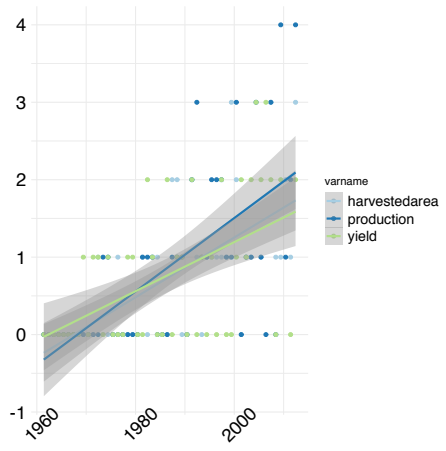

(c) Soybean, $f > 0$

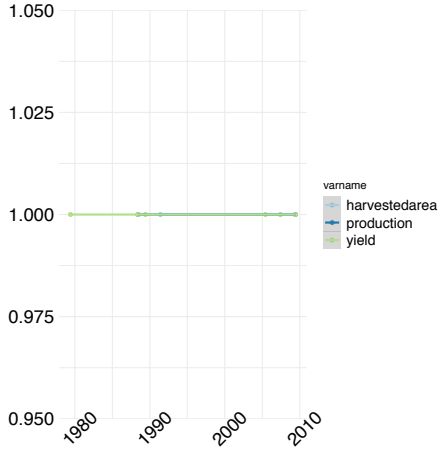

(d) Soybean, $f > .75$

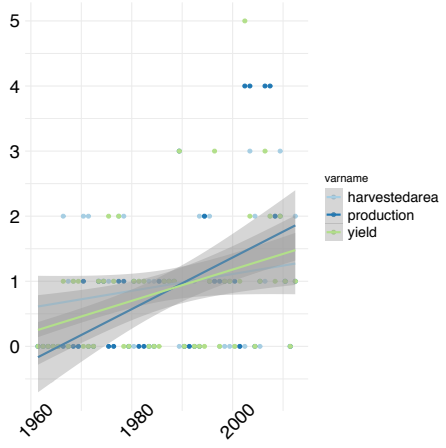

(e) Wheat, $f > 0$

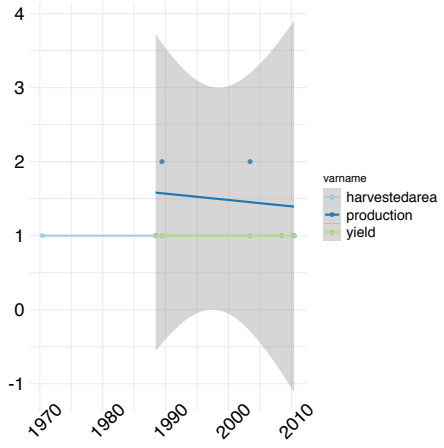

(f) Wheat, $f > .75$

Figure 4.13: Trends in *negative* shocks, *historical* ensemble; linear models of the evolution of the number of shocks over time, per crop and per agricultural variable, for different values of the frequentist likelihood f.

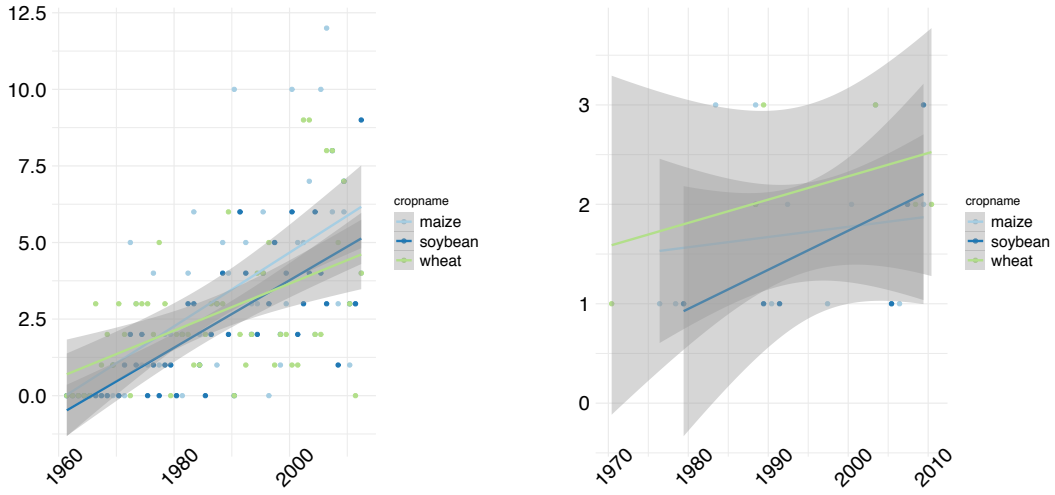

(a) $f > 0$ (b) $f > .75$

Figure 4.14: Trends in *negative* shocks, *historical* ensemble; linear models of the evolution of the number of shocks over time, per crop, for different values of the frequentist likelihood f.

	f	R^2	R^2-adj	intercept	intercept.pval	time	time.pval
Maize							
production	0.00	0.020	0.001	6.627	0.000	0.028	0.316
	0.10	0.259	0.243	8.594	0.000	-0.067	0.000
	0.20	0.011	-0.011	5.691	0.000	-0.013	0.487
	0.50	0.112	0.092	1.678	0.000	0.030	0.024
	0.75	0.126	0.100	0.942	0.007	0.022	0.034
yield	0.00	0.001	-0.019	7.025	0.000	0.007	0.803
	0.10	0.259	0.242	8.222	0.000	-0.063	0.000
	0.20	0.115	0.095	6.404	0.000	-0.043	0.020
	0.50	0.000	-0.026	2.581	0.000	-0.001	0.968
	0.75	0.006	-0.030	1.676	0.008	0.007	0.685
harvested area	0.00	0.003	-0.017	6.378	0.000	0.011	0.685
	0.10	0.275	0.259	7.719	0.000	-0.077	0.000
	0.20	0.170	0.152	5.310	0.000	-0.046	0.004
	0.50	0.002	-0.023	1.688	0.000	0.003	0.759
	0.75	0.052	-0.004	1.559	0.000	-0.008	0.348
Soybean							
production	0.00	0.000	-0.020	6.385	0.000	-0.002	0.936
	0.10	0.372	0.358	7.446	0.000	-0.079	0.000
	0.20	0.123	0.103	5.181	0.000	-0.043	0.017
	0.50	0.041	0.011	1.615	0.000	0.014	0.246
	0.75	0.002	-0.044	1.485	0.001	-0.002	0.853
yield	0.00	0.002	-0.018	5.998	0.000	0.007	0.774
	0.10	0.336	0.321	7.312	0.000	-0.077	0.000
	0.20	0.086	0.066	4.679	0.000	-0.029	0.045
	0.50	0.008	-0.021	1.535	0.000	0.005	0.604
	0.75	0.008	-0.047	1.263	0.000	0.003	0.712
harvested area	0.00	0.015	-0.005	6.561	0.000	-0.022	0.385
	0.10	0.476	0.465	7.706	0.000	-0.103	0.000
	0.20	0.208	0.190	5.098	0.000	-0.058	0.001
	0.50	0.165	0.138	2.466	0.000	-0.027	0.019
	0.75	0.000	-0.045	1.204	0.000	0.000	0.980
Wheat							
production	0.00	0.042	0.023	4.199	0.000	0.027	0.146
	0.10	0.006	-0.017	4.551	0.000	-0.007	0.607
	0.20	0.020	-0.003	4.224	0.000	-0.016	0.358
	0.50	0.074	0.047	3.475	0.000	-0.028	0.108
	0.75	0.050	0.006	2.016	0.000	-0.015	0.295
yield	0.00	0.006	-0.014	4.158	0.000	0.011	0.586
	0.10	0.245	0.228	5.092	0.000	-0.055	0.000
	0.20	0.031	0.009	3.037	0.000	-0.017	0.247
	0.50	0.005	-0.027	1.765	0.000	-0.005	0.692
	0.75	0.004	-0.041	1.150	0.000	0.002	0.759
harvested area	0.00	0.010	-0.009	4.149	0.000	0.013	0.474
	0.10	0.176	0.158	5.055	0.000	-0.046	0.003
	0.20	0.159	0.139	4.428	0.000	-0.039	0.007
	0.50	0.143	0.114	3.047	0.000	-0.029	0.033
	0.75	0.191	0.144	1.995	0.000	-0.026	0.061

Table 4.16: Summary statistics for the linear models of the trends in number of shocks over time (Figure 4.9) for different values of the frequentist likelihood f (*predictive* ensemble).

f	R^2	R^2-adj	intercept	intercept.pval	time	time.pval
Maize						
0.00	0.01	-0.01	20.03	0.00	0.05	0.56
0.10	0.40	0.38	24.54	0.00	-0.21	0.00
0.20	0.13	0.11	17.41	0.00	-0.10	0.01
0.30	0.03	0.01	12.02	0.00	-0.05	0.25
0.40	0.00	-0.02	8.51	0.00	0.00	0.94
0.50	0.01	-0.01	5.62	0.00	0.02	0.52
0.75	0.04	0.02	2.23	0.01	0.03	0.19
0.90	0.00	-0.03	1.88	0.00	0.00	0.84
Soybean						
0.00	0.00	-0.02	18.94	0.00	-0.02	0.82
0.10	0.56	0.55	22.59	0.00	-0.26	0.00
0.20	0.29	0.27	14.93	0.00	-0.13	0.00
0.30	0.06	0.04	9.10	0.00	-0.05	0.09
0.40	0.01	-0.01	6.02	0.00	-0.02	0.43
0.50	0.01	-0.01	4.68	0.00	-0.02	0.50
0.75	0.00	-0.03	2.74	0.00	-0.01	0.75
0.90	0.00	-0.05	1.95	0.00	0.00	0.86
Wheat						
0.00	0.02	0.00	12.51	0.00	0.05	0.33
0.10	0.20	0.18	14.71	0.00	-0.11	0.00
0.20	0.09	0.07	11.32	0.00	-0.08	0.04
0.30	0.04	0.02	8.67	0.00	-0.05	0.19
0.40	0.05	0.02	7.34	0.00	-0.05	0.16
0.50	0.04	0.01	6.55	0.00	-0.05	0.23
0.75	0.11	0.09	4.00	0.00	-0.04	0.05
0.90	0.09	0.05	3.14	0.00	-0.04	0.14

Table 4.17: Summary statistics for the linear models of the trends in number of *positive* and *negative* shocks per crop over time, for different values of the frequentist likelihood f (*predictive* ensemble).

Chapter 5

Discussion and conclusions

In this thesis I have adopted a novel, empirical approach to the analysis of crop production and yield, the impacts of climate on yield, and their potential implications for global food security.

I use the term global food security in reference to global crop production by the main producing areas (baskets) in relation to global demand, and I focus on the three crops that represent the greatest volume of traded production – wheat, soybean and maize. For practical reasons, my analysis does not consider nutritional quality or affordability, which are also important dimensions of food security, but rather focuses on the most basic aspect, i.e. food supply.

My analysis decomposes food production into its two constituents: planted area, and crop yield per unit area. The analysis has been made possible by (a) the existence of a comprehensive global data set of planted areas and crop yields, which has enabled me to consider smaller and more climatically coherent regions than the national or state level adopted by many published studies; and (b) the advent of powerful machine learning techniques that can help to identify likely causal relationships.

Underlying my approach is the idea that in-depth study of observations over recent decades can provide insights into the operation of the global food system in the real world. Results presented in the thesis support this idea. They indicate that some statements in the recent literature regarding climate-change impacts are simplistic, and in many cases biased towards specific regions, notably the USA. The global reality, perhaps unsurprisingly, proves to be considerably more complex and nuanced.

Main conclusions, and some broader inferences

1. There are many complementary ways to improve global food security. These include: potential gains in resilience through diversification of the regions where particular crops are grown; risk reduction through change of diets; reductions of food waste at all points in the supply chain; redistribution of varieties; genetic improvements; and a focus on achieving a stable yield rather than maximizing yield. I suggest that such developments could, collectively, produce gains in food security far outweighing both any plausible population increase, and the potential negative effects of a warmer climate on yields.

2. The yield gap is a useful metric to indicate where improvements could be made. However, variations in production (which are what matters, from the food-supply perspective) in general are not well correlated with variations in yield. This decoupling is due to socio-economic factors, including explicit policies, that can (and frequently do) produce large temporal variations in planted areas of any given crop. It follows that food security is not just a matter of maximizing yields. It is also a matter of providing conditions conducive to farmers growing a variety of crops, across a wider range of countries and environments.

3. High levels of production of a crop in limited regions can amplify price "shocks", which are associated with serial correlation in commodity markets. Research aimed solely at maximizing production in a given region could have perverse, negative consequences. Global food security would be better served by more distributed measures aimed at stabilizing global markets. Finally, there is a need for further research on the quantitative characterization of shocks in production and how they are related to prices.

Implications of the research

Research presented in this thesis supports some statements found in the recent literature, but by no means all. Here I summarize some main points of agreement and disagreement in order to situate this work in the broader context of climate-impacts research.

I have emphasized that the risks to global food supplies are amplified by the extreme concentration (that is, the allocation of a large acreage, relative to the world's total planted area) of crop production in particular baskets. The major producing regions exert a huge leverage on global crop production. It follows that (a) the traded volume of production risks not meeting the global demand, and (b) that

people in low- and middle-income countries, with smaller production, live with an unnecessarily high risk of food shortages. In Chapter 2, I showed that the risk, as measured by the variability in the residuals of production, is mostly concentrated in a few baskets – and that these are also the regions that have the highest mean production and yield. This finding is consistent with Ben-Ari & Makowski (2014) and Ben-Ari & Makowski (2016), who also demonstrated the concentration of production, and found a significant and positive relationship across regions between the mean yield and its variability.

The situation is extreme for maize, where yield variability is mostly contained in the USA basket – which also contains the largest losses. Maize is the crop species that shows the largest inter-basket differences at the global scale, and the largest interannual variability in production. The concentration of maize planting in regions showing a large interannual variability of yield increases the risk of negative shocks to global maize production. This risk could be reduced: Ben-Ari & Makowski (2016), for example, found that maize's allocation is far from being optimal.

For soybean, the global risk is again mostly contained in the USA, but Argentina and Southern Brazil are also significant. Soybean and maize are generally planted in similar bioclimatic regions (Ben-Ari & Makowski 2016); however, their responses to climate variability in regions outside the USA are different, opening up the possibility that the concentration of risk could be alleviated by a redistribution of their acreage.

Only wheat shows a more homogeneous spread of variability between regions. Unlike maize and soybean, the wheat baskets showing the highest interannual variability in yield are not the regions with the highest planted area of wheat. Another crucial difference from maize and soybean is that negative effects of high temperatures, expressed by the ΣKDD metric, are much less pronounced for wheat. However, as with maize and soybean, wheat production could still benefit (in the sense of buffering the interannual variability of global total production) from a redistribution of production areas, including increased acreage in India and China (Chapter 2, Section 2.4, Figure 2.10). Chapters 2 and 3 support and amplify the findings by Ben-Ari & Makowski (2014) and Ben-Ari & Makowski (2016), that there is a potential to increase average production – without increasing either interannual variability or average yield – by optimization of crop allocation in the world's most productive regions, and redistributing acreage towards regions with a lower sensitivity to super-optimal temperatures.

Yield contrasts between regions can be explained to a significant extent by differences in cropping systems: topography, soil heterogeneity and erosion (Si & Farrell 2004, Amundson et al. 2015), in-

tensification practices, inputs, irrigation, and mechanization of farming (Neumann et al. 2010). Yet, when projecting the impacts of climate changes, much of the literature (especially the most highly cited segments) focuses on temperature effects rather than any other climatic and atmospheric influences (solar radiation, precipitation, CO_2, evapotranspiration) (Lobell & Field 2007, Lobell, Schlenker & Costa-Roberts 2011, Lobell, Bänziger, Magorokosho & Vivek 2011, Iizumi et al. 2013, Schlenker et al. 2013, Butler & Huybers 2013, 2015, Tigchelaar et al. 2018); and cropping systems are largely ignored. It certainly is important to consider temperature effects: an increase in the incidence of super-optimal temperatures is projected, and high temperatures negatively impact plant development through a variety of mechanisms including reduced grain filling, increased water use and reduced fertility (Lobell & Burke 2009, Jones 2013, Sánchez et al. 2014, Tigchelaar et al. 2018). It has been hypothesized that the negative impacts of projected warming on yield will outweigh the negative effect of precipitation changes (Lobell & Burke 2008, Tigchelaar et al. 2018). It has also been proposed that contrasts in yield and its interannual variability due to cropping systems will dwindle as yield gaps are reduced (Grassini et al. 2013).

In this thesis I, too, have adopted a strong focus on temperature. However, my analysis has considered a wider range of controls on crop yield. I have shown moreover that the negative effect of high temperature on crop yields is by no means universal, with different responses shown by different crops and in different regions. In some cases, the impact of high temperatures is positive. Semenov (2007) previously argued that a warmer climate might benefit crops whose phenological stages are mainly determined by the temperature sums.

It follows that the appropriate strategy for plant breeding is not simply to try to increase heat tolerance. Guilpart et al. (2020) supplies further support to the arguments that (a) a climate change-driven increase in temperatures can have a positive outcome, depending on the crop and where it is growing, and (b) there would be a benefit from diversification of the regions of production. Guilpart et al. (2020) also showed that scenarios of moderate to intense climate change have the potential to “improve Europe's soybean self-sufficiency” while having beneficial side-effects, including a reduction of the economic driving forces for deforestation and biodiversity in South America, and reducing fertilizer use in Europe through the incorporation of a leguminous plant in crop rotations.

My results indicate that some high-profile projections of (negative) climate-change impacts on crop yields are flawed, because they fail to consider the global picture. Effects of high temperatures and drought on crop yields differ, sometimes in sign, among crops and regions. Heat deficits during

the growing season can (for some crops and regions) be at least as detrimental as extreme high temperatures. Crop yields in the real world are therefore likely to show gains as well as losses due to climate change.

Further to the temperature impact, results from Chapter 3 show that longer dry periods have a positive effect on maize yields in Mexico, Brazil and Argentina. The same variable also stands out when considered across baskets and crops. This (surprising) finding calls into question the common view that regular precipitation provides the most favourable climate for crop growth. It contrasts with the simplistic narrative that climate change means crop failure. It may be that the alternation of wet days and longer dry periods is favourable to crop yield, at least up to a certain optimum.

Crop responses to heat stress and the results from chapters 2 and 3 suggest that there is a concentration of risk in the most productive baskets. This situation potentially translates into an increase in the exposure and sensitivity of the global food supply chain to production shocks, including those caused by climatic events. Nonetheless, for the period considered (1961–2012) – a period that includes effect of a warming climate (Hansen et al. 2012, Huntingford et al. 2013, Lobell & Burke 2008, 2009, Lobell, Schlenker & Costa-Roberts 2011, Butler & Huybers 2013) – I found no significant increase in the incidence of major production shocks. This result applies for all three crops studied and in the two approaches proposed to identify shocks (Chapter 4). There was however a positive trend in production variability, as signified by less important shocks.

These findings are in line with Tigchelaar et al. (2018), who found no significant positive trend in maize production shocks. These authors nonetheless asserted that future global warming (based on scenarios and simulations of climate change) will lead to an increase in the "probability of synchronized maize production shocks". I will consider this conclusion further, as my analysis suggests that it is not well-founded.

Biases in the current literature?

A key limitation of Tigchelaar et al. (2018) is that the future projection is based entirely on the maize temperature-yield relationship as observed in the USA. I have shown in this thesis that except for maize and soybean in the USA, the response to temperature is not a simple decline, and that the effect of warming can even be positive (e.g. South Africa, Chapter 3, Figure 3.3c). I have also shown that the functional forms of the response to ΣKDD for maize vary by region (Figure 3.3). Thus, for

example, maize in the USA has an exponentially declining response to increasing ΣKDD, while maize in Brazil has a sigmoid response. Such differences suggest that (a) the real-world response of yield in the cultivated area may differ from responses measured under laboratory conditions or plot trials, and (b) that yield responses can include plateaus – in other words, over some range of temperatures, damage does not necessarily increase as stress increases.

I suggest that Tigchelaar et al. (2018) exemplifies a bias in the current literature towards an excessive focus on temperature effects on maize in the USA, resulting in extrapolations to the rest of the world that are not defensible in a global perspective. Tigchelaar et al. (2018) also make a general recommendation of breeding for heat tolerance. This is a simplistic conclusion. It neglects the likelihood of trade-offs (breeding for a specific trait is usually at the expense of yield). More fundamentally, it assumes that the desired response to climate change is to develop crop varieties that allow the planted area to remain in the same place.

Predicting future crop failures based on present interannual variability (Lobell, Schlenker & Costa-Roberts 2011, Tigchelaar et al. 2018) is problematic more generally, for the following reasons.

- It implies that farmers will not adapt to changes in climate – for example, by growing different crops that are better adapted to the changed climate. Moore & Lobell (2014) have shown that long-term responses of crop yield to climate are broader than responses based on interannual variability, supporting my argument against relying on short-term signals (to which farmers cannot adapt) to predict longer-term impacts.

- It disregards the fact that statistical relationships solely based on temperature and precipitation might not hold under future conditions. These include higher CO_2 (allowing water saving in all rainfed crops, including C_4 crops such as maize, and increasing the productivity of C_3 crops) and different precipitation regimes, such as projected increases in the length of dry periods, which may sometimes be beneficial (Chapter 3).

- It does not factor in regionally specific crop responses, and ignores the heterogeneity of climatic responses shown by the data from different regions (Chapter 3).

- It encourages a focus on yield, and explaining production as a function of yield. Findings in this thesis highlight the fact that variations in planted area can be equally important in explaining variations and shocks in crop production (Chapters 2 and 4).

The importance of planted area

The decomposition of agricultural production by leverages (Chapter 2) and shocks (Chapter 4) has provided clear evidence that interannual variability in production is not only driven by yield. For many baskets, interannual variability is driven by a positive covariance of yield and planted acreage (harvested area being a fairly constant fraction of the planted acreage), especially for maize and wheat. In other baskets, such as Indonesia and Mexico, gains and losses are primarily driven by area rather than yield. For the largest shocks, yield-driven shocks and area-driven shocks are independent events. Therefore, any analysis of systemic risk should include consideration of the drivers of planting decisions, with equal weight to the drivers of crop yields.

Harvested area is determined not only by climatic suitability, but also by socio-economic factors. Production of a given crop naturally tends to be concentrated in the regions that are suited for them to be grown and where they have a competitive advantage (in terms of economics, as well as yield). Policy can also drive planting. Agriculture is heavily subsidized, and interwined with policies, in many countries. For example, the USA has declared agriculture a matter of national security. With changes in climate, bioclimatic regions will shift, and other regions can become productive even as some existing regions become less productive for a given crop. These shifts may be encouraged, or discouraged, by political decisions.

Over the past 60 years agricultural production has increased to meet rapidly rising global demand, with exponential expansion in many areas of the world (Chapter 2). Production dynamics (Chapter 2, Figure 2.2) show a universal positive trend in production for all crops and almost no signs of levelling off during the period studied. The associated figures for trends in yield and acreage show that yield has been increasing in all baskets (Chapter 2, Figures 2.12 and 2.13). Meanwhile, planted area is levelling off or even declining in many baskets (6 out of 11 for maize, 2 out of 7 for soybean, and 9 out of 10 for wheat). The implications of this phenomenon could be considered in one of two ways. It could be that the potential for agricultural expansion lies in the largest producers, which are those where the acreage is still increasing and that have the highest yield. Alternatively, however, there may be a large potential for diversification in countries where the acreage is no longer increasing. This possibility merits serious examination, because it could possibly allow the global food system to adapt to climate change in a way that both decreases volatility in global food supplies, and avoids placing excessive reliance on plant breeding for heat tolerance – which may be a misplaced strategy, as I have

argued above.

In summary, agricultural production might be maximized by a precise matching of production areas with regions of highest suitability for each crop (Beddow et al. 2010, Ben-Ari & Makowski 2014, 2016) – but this is not the optimal strategy in terms of food security, because the resulting concentration of production increases systemic risk. The results presented in this thesis highlight the potential benefits of promoting yield and acreage stability over maximizing output. The decomposition of year-by-year production changes into leverages, as well as the analysis on shocks, highlighted the importance of yield, but also showed the importance of the positive covariation of yield and cultivated area. This result points to a potential to stabilize yield through a better planning of crop rotations to maintain the total planted area in the baskets. In principle, incentives could be applied to decorrelate rotations from global or regional market prices. But this is a hypothetical scenario, which presumes that scientific analysis could translate into real-world economics and politics.

As shown in the trend analysis (Chapter 2, Section 2.3.1), there has been an explosion of agriculture through the world; crops have become a traded commodity; infrastructures, developed around specific crops, limit flexibility; and other factors including national self-sufficiency, land tenure systems, planning regulations, and measures to protect or increase biodiversity all come into play. There is no internationally agreed agricultural policy, beyond trade agreements or market regulations that are not primarily aimed at promoting food security. Agricultural insurance is currently the least developed field of all insurances; the protection gap is the highest of any insured sector; and country-specific regulations make it virtually impossible to work toward an international solution. Yet my analysis leads inexorably to the conclusion that international coordination could promote a more effective approach to climate-change impacts than relying on plant-breeding strategies that focus on adaptation *in situ* to rising temperatures.

Limitations, and potential for future research

The decomposition of agricultural production time series into yield and area components is a novel feature of this thesis. I have shown that part of the interannual variability in production is rooted in the covariation of yield and harvested area, while major shocks are usually attributable to either one or the other. This is a new finding, although some authors have touched on it (e.g. Lesk et al. (2016)). This research could be extended e.g. by combining the leverage methods with yield variance decomposition

into three sub-components, as proposed by (Ben-Ari & Makowski 2014), to account for the spatial spread of global production in the leverages; and by running the methodology developed for shocks on the leverage components themselves, which could bring further granularity to the understanding of shocks.

The use of machine learning to capture complex relationships is not new, but to my knowledge there has been no previous attempt to use machine learning specifically to investigate the importance of agroclimatic variables on yield. My analysis of potential causes focused on climatic influences on yield, rather than on economic and policy influences on planted area. Such influences could be quantified by means of national or subnational metrics such as the level of subsidies, the size of landholdings, and the proportion of agriculture in gross domestic product. This could be a potentially fruitful area for quantitative social-science research on the global food system and might help to illuminate, for example, why basket-scale responses of production to climate variability can be different from theoretically expected responses.

The Chapter 4 presents a novel methodology. To the best of my knowledge, this is the first application of ensemble modelling and frequentist likelihood characterization of interannual variability and shocks in agricultural production. An obvious limitation is the method's dependence on the subjective choice of models, and its reliance on the “widsom of crowds” assumption that an ensemble of disparate models together performs better than any single model. However, this chapter showed a number of apparently robust characteristics of the time series analysed, and highlighted the important difference between attribution with and without hindsight. The methodology could certainly be refined, and extended to considering time series together using multivariate techniques.

Bibliography

Abdi, H. & Williams, L. J. (2010), 'Principal component analysis', *Wiley interdisciplinary reviews: computational statistics* **2**(4), 433–459.

Abendroth, L. J., Elmore, R. W., Boyer, M. J. & Marlay, S. K. (2011), 'Corn growth and development', *Ames, Iowa, Iowa State University, University Extension* .

Abrahamsen, P. & Hansen, S. (2000), 'Daisy: an open soil-crop-atmosphere system model', *Environmental modelling & software* **15**(3), 313–330.

Ainsworth, E. A. (2008), 'Rice production in a changing climate: a meta-analysis of responses to elevated carbon dioxide and elevated ozone concentration', *Global Change Biology* **14**(7), 1642–1650.

Ainsworth, E. A. & Long, S. P. (2005), 'What have we learned from 15 years of free-air co2 enrichment (face)? a meta-analytic review of the responses of photosynthesis, canopy properties and plant production to rising co2', *New phytologist* **165**(2), 351–372.

Ainsworth, E. A. & Long, S. P. (2021), '30 years of free-air carbon dioxide enrichment (face): What have we learned about future crop productivity and its potential for adaptation?', *Global change biology* **27**(1), 27–49.

Ainsworth, E. A. & Rogers, A. (2007), 'The response of photosynthesis and stomatal conductance to rising [co2]: mechanisms and environmental interactions', *Plant, cell & environment* **30**(3), 258–270.

Aljoumani, B., Sànchez-Espigares, J. A., Canameras, N., Josa, R. & Monserrat, J. (2012), 'Time series outlier and intervention analysis: Irrigation management influences on soil water content in silty loam soil', *Agricultural water management* **111**, 105–114.

Allen, M. R. & Ingram, W. J. (2002), 'Constraints on future changes in climate and the hydrologic cycle', *Nature* **419**(6903), 228.

Amundson, R., Berhe, A. A., Hopmans, J. W., Olson, C., Sztein, A. E. & Sparks, D. L. (2015), 'Soil and human security in the 21st century', *Science* **348**(6235).

Asseng, S., Ewert, F., Martre, P., Rötter, R. P., Lobell, D. B., Cammarano, D., Kimball, B. A., Ottman, M. J., Wall, G., White, J. W. et al. (2015), 'Rising temperatures reduce global wheat production', *Nature climate change* **5**(2), 143–147.

Atkinson, A. C. (1985), *Plots, transformations and regression; an introduction to graphical methods of diagnostic regression analysis*, Oxford University Press, Oxford.

Atkinson, A. C., Koopman, S.-J. & Shephard, N. (1997), 'Detecting shocks: Outliers and breaks in time series', *Journal of Econometrics* **80**(2), 387–422.

Balke, N. S. & Fomby, T. B. (1994), 'Large shocks, small shocks, and economic fluctuations: outliers in macroeconomic time series', *Journal of Applied Econometrics* **9**(2), 181–200.

Barriopedro, D., Fischer, E. M., Luterbacher, J., Trigo, R. M. & García-Herrera, R. (2011), 'The hot summer of 2010: redrawing the temperature record map of europe', *Science* **332**(6026), 220–224.

Bauer, S. E., Tsigaridis, K. & Miller, R. (2016), 'Significant atmospheric aerosol pollution caused by world food cultivation', *Geophysical Research Letters* **43**(10), 5394–5400.

Bechini, L., Bocchi, S., Maggiore, T. & Confalonieri, R. (2006), 'Parameterization of a crop growth and development simulation model at sub-model components level. an example for winter wheat (triticum aestivum l.)', *Environmental Modelling & Software* **21**(7), 1042–1054.

Beddow, J. M., Pardey, P. G., Koo, J. & Wood, S. (2010), 'The changing landscape of global agriculture', *The shifting patterns of agricultural production and productivity worldwide* pp. 7–38.

Bellmann, C. (2019), 'Subsidies and sustainable agriculture: Mapping the policy landscape'.

Ben-Ari, T., Adrian, J., Klein, T., Calanca, P., Van der Velde, M. & Makowski, D. (2016), 'Identifying indicators for extreme wheat and maize yield losses', *Agricultural and Forest Meteorology* **220**, 130–140.

Ben-Ari, T. & Makowski, D. (2014), 'Decomposing global crop yield variability', *Environmental Research Letters* **9**(11), 114011.

Ben-Ari, T. & Makowski, D. (2016), 'Analysis of the trade-off between high crop yield and low yield instability at the global scale', *Environmental Research Letters* **11**(10), 104005.

Berg, P., Moseley, C. & Haerter, J. O. (2013), 'Strong increase in convective precipitation in response to higher temperatures', *Nature Geoscience* **6**(3), 181–185.

Berry, P. M. & Spink, J. (2012), 'Predicting yield losses caused by lodging in wheat', *Field Crops Research* **137**, 19–26.

Berry, P. & Spink, J. (2006), 'A physiological analysis of oilseed rape yields: past and future', *The Journal of Agricultural Science* **144**(5), 381–392.

Berry, S. T., Roberts, M. J. & Schlenker, W. (2014), Corn production shocks in 2012 and beyond: Implications for harvest volatility, *in* 'The Economics of Food Price Volatility', University of Chicago Press, pp. 59–81.

Beyene, K. & Bekele, S. A. (2016), 'Assessing univariate and multivariate homogeneity of variance: A guide for practitioners', *J Math Theory Model* **6**, 13–17.

Bhuvandas, N., Timbadiya, P., Patel, P. & Porey, P. (2014), 'Review of downscaling methods in climate change and their role in hydrological studies', *Int J Environ Chem Ecol Geol Geophys Eng* **8**(10), 648–653.

Bienaymé, I.-J. (1853), *Considérations à l'appui de la découverte de Laplace sur la loi de probabilité dans la méthode des moindres carrés*, Imprimerie de Mallet-Bachelier.

Boko, M., Niang, I., Nyong, A., Vogel, C., Githeko, A., Medany, M., Osman-Elasha, B., Tabo, R. & Yanda, P. (2007), 'Impacts, adaptation and vulnerability. contribution of working group ii to the fourth assessment report of the intergovernmental panel on climate change', *Africa. Climate Change* pp. 433–467.

Boucher, O. & Best, M. (2010), 'The watch forcing data 1958-2001: A meteorological forcing dataset for land surface-and hydrological-models', *WATCH technical report* .

Bouman, B., Van Keulen, H., Van Laar, H. & Rabbinge, R. (1996), 'The 'school of de wit'crop growth simulation models: a pedigree and historical overview', *Agricultural systems* **52**(2-3), 171–198.

Box, G. E. & Cox, D. R. (1964), 'An analysis of transformations', *Journal of the Royal Statistical Society: Series B (Methodological)* **26**(2), 211–243.

Box, G. E., Jenkins, G. M., Reinsel, G. C. & Ljung, G. M. (2013), *Time series analysis: forecasting and control*, John Wiley & Sons.

Breiman, L. (2001), 'Random forests', *Machine learning* **45**(1), 5–32.

Brooks, A. & Farquhar, G. (1985), 'Effect of temperature on the co 2/o 2 specificity of ribulose-1, 5-bisphosphate carboxylase/oxygenase and the rate of respiration in the light', *Planta* **165**(3), 397–406.

Brown, L. (2012), *World on the edge: how to prevent environmental and economic collapse*, Routledge.

Brown, R. G. (1959), *Statistical forecasting for inventory control*, McGraw/Hill.

Busuioc, A., Chen, D. & Hellström, C. (2001), 'Performance of statistical downscaling models in gcm validation and regional climate change estimates: application for swedish precipitation', *International Journal of Climatology: A Journal of the Royal Meteorological Society* **21**(5), 557–578.

Busuioc, A. & von Storch, H. (2003), 'Conditional stochastic model for generating daily precipitation time series', *Climate Research* **24**(2), 181–195.

Busuioc, A., Von Storch, H. & Schnur, R. (1999), 'Verification of gcm-generated regional seasonal precipitation for current climate and of statistical downscaling estimates under changing climate conditions', *Journal of Climate* **12**(1), 258–272.

Butler, E. E. & Huybers, P. (2013), 'Adaptation of us maize to temperature variations', *Nature Climate Change* **3**(1), 68.

Butler, E. E. & Huybers, P. (2015), 'Variations in the sensitivity of us maize yield to extreme temperatures by region and growth phase', *Environmental Research Letters* **10**(3), 034009.

Cai, X., Wang, D. & Laurent, R. (2009), 'Impact of climate change on crop yield: a case study of rainfed corn in central illinois', *Journal of Applied Meteorology and Climatology* **48**(9), 1868–1881.

Calderini, D. F. & Slafer, G. A. (1998), 'Changes in yield and yield stability in wheat during the 20th century', *Field Crops Research* **57**(3), 335–347.

Cassidy, E. S., West, P. C., Gerber, J. S. & Foley, J. A. (2013), 'Redefining agricultural yields: from tonnes to people nourished per hectare', *Environmental Research Letters* **8**(3), 034015.

Cassman, K. G., Dobermann, A., Walters, D. T. & Yang, H. (2003), 'Meeting cereal demand while protecting natural resources and improving environmental quality', *Annual Review of Environment and Resources* **28**(1), 315–358.

Cavazos, T. (1999), 'Large-scale circulation anomalies conducive to extreme precipitation events and derivation of daily rainfall in northeastern mexico and southeastern texas', *Journal of Climate* **12**(5), 1506–1523.

Cernay, C., Ben-Ari, T., Pelzer, E., Meynard, J.-M. & Makowski, D. (2015), 'Estimating variability in grain legume yields across europe and the americas', *Scientific reports* **5**(1), 1–11.

Challinor, A., Wheeler, T., Craufurd, P., Slingo, J. & Grimes, D. (2004), 'Design and optimisation of a large-area process-based model for annual crops', *Agricultural and forest meteorology* **124**(1-2), 99–120.

Challinor, A., Wheeler, T., Garforth, C., Craufurd, P. & Kassam, A. (2007), 'Assessing the vulnerability of food crop systems in africa to climate change', *Climatic change* **83**(3), 381–399.

Chandola, V., Banerjee, A. & Kumar, V. (2009), 'Anomaly detection: A survey', *ACM computing surveys (CSUR)* **41**(3), 1–58.

Chang, K.-H. (2011), 'Modeling carbon dynamics in agriculture and forest ecosystems using the process-based models daycent and cn-class', *PhD thesis, Department of Land Resource Science, University of Guelph* .

Chavez, E., Conway, G., Ghil, M. & Sadler, M. (2015), 'An end-to-end assessment of extreme weather impacts on food security', *Nature Climate Change* **5**(11), 997.

Chen, C. & Liu, L.-M. (1993), 'Joint estimation of model parameters and outlier effects in time series', *Journal of the American Statistical Association* **88**(421), 284–297.

Chuang, C.-C. & Lee, Z.-J. (2011), 'Hybrid robust support vector machines for regression with outliers', *Applied Soft Computing* **11**(1), 64–72.

Clements, M. P. & Hendry, D. F. (2006), 'Forecasting with breaks', *Handbook of economic forecasting* **1**, 605–657.

Cook, R. D. (1977), 'Detection of influential observation in linear regression', *Technometrics* **19**(1), 15–18.

Cook, R. D. & Weisberg, S. (1982), *Residuals and influence in regression*, New York: Chapman and Hall.

Cooper, P. (2004), 'Coping with climatic variability and adapting to climate change: rural water management in dry-land areas', *International Development Research Centre, London* .

Coumou, D. & Rahmstorf, S. (2012), 'A decade of weather extremes', *Nature climate change* **2**(7), 491.

Crawford, R. M. (2003), 'Seasonal differences in plant responses to flooding and anoxia', *Canadian Journal of Botany* **81**(12), 1224–1246.

Dai, A. (2013), 'Increasing drought under global warming in observations and models', *Nature Climate Change* **3**(1), 52.

Dai, A., Trenberth, K. E. & Qian, T. (2004), 'A global dataset of palmer drought severity index for 1870–2002: Relationship with soil moisture and effects of surface warming', *Journal of Hydrometeorology* **5**(6), 1117–1130.

D'Aleo, J. & Watts, A. (2010), 'Surface temperature records: Policy driven deception', *Science and Public Policy Institute* **23**.

Davies, W. P. (2003), 'An historical perspective from the Green Revolution to the gene revolution.', *Nutrition reviews* **61**(6 Pt 2), S124–34.
URL: *http://www.ncbi.nlm.nih.gov/pubmed/12908744*

De Graaff, M.-A., Van Groenigen, K.-J., Six, J., Hungate, B. & van Kessel, C. (2006), 'Interactions between plant growth and soil nutrient cycling under elevated co2: a meta-analysis', *Global Change Biology* **12**(11), 2077–2091.

Dimaranan, B. V. & McDougall, R. A. (2006), 'The gtap 6 data base', *Center for Global Trade Analysis, Department of Agricultural Economics, Purdue University* **6**.

Donohue, R. J., McVicar, T. R. & Roderick, M. L. (2010), 'Assessing the ability of potential evaporation formulations to capture the dynamics in evaporative demand within a changing climate', *Journal of Hydrology* **386**(1-4), 186–197.

Dowgert, M. F. & Fresno, C. (2010), The impact of irrigated agriculture on a stable food supply, *in* 'Proceedings of the 22nd Annual Central Plains Irrigation Conference, Kearney, NE', pp. 24–25.

Duque, J. C., Anselin, L. & Rey, S. J. (2012), 'The max-p-regions problem', *Journal of Regional Science* **52**(3), 397–419.

Durman, C., Gregory, J. M., Hassell, D. C., Jones, R. & Murphy, J. (2001), 'A comparison of extreme european daily precipitation simulated by a global and a regional climate model for present and future climates', *Quarterly Journal of the Royal Meteorological Society* **127**(573), 1005–1015.

Easterling, D. R., Evans, J., Groisman, P. Y., Karl, T. R., Kunkel, K. E. & Ambenje, P. (2000), 'Observed variability and trends in extreme climate events: a brief review', *Bulletin of the American Meteorological Society* **81**(3), 417–426.

Egli, D., TeKrony, D., Heitholt, J. & Rupe, J. (2005), 'Air temperature during seed filling and soybean seed germination and vigor', *Crop Science* **45**(4), 1329–1335.

El-Gohary, M. & McNames, J. (2007), 'Establishing causality with whitened cross-correlation analysis', *IEEE transactions on biomedical engineering* **54**(12), 2214–2222.

FAOSTAT, F. (2016), 'Statistical databases (2016) food and agriculture organization of the united nations, statistics division'.

Fischer, G., Shah, M., van Velthuizen, H. & Nachtergaele, F. O. (2001), 'Global agro-ecological assessment for agriculture in the 21st century'.

Foley, J. A., DeFries, R., Asner, G. P., Barford, C., Bonan, G., Carpenter, S. R., Chapin, F. S., Coe, M. T., Daily, G. C., Gibbs, H. K. et al. (2005), 'Global consequences of land use', *science* **309**(5734), 570–574.

Foley, J. A., Ramankutty, N., Brauman, K. A., Cassidy, E. S., Gerber, J. S., Johnston, M., Mueller, N. D., O'Connell, C., Ray, D. K., West, P. C. et al. (2011), 'Solutions for a cultivated planet', *Nature* **478**(7369), 337.

Frei, C., Schöll, R., Fukutome, S., Schmidli, J. & Vidale, P. L. (2006), 'Future change of precipitation extremes in europe: Intercomparison of scenarios from regional climate models', *Journal of Geophysical Research: Atmospheres* **111**(D6).

Friedman, J. H. (2001), 'Greedy function approximation: A gradient boosting machine.', *Ann. Statist.* **29**(5), 1189–1232.

Friedman, J. H. (2002), 'Stochastic gradient boosting', *Computational Statistics and Data Analysis* **38**(4), 367–378.

Friedman, J., Hastie, T. & Tibshirani, R. (2001), *The elements of statistical learning*, Vol. 1, Springer series in statistics New York.

Garimella, R. V. (2017), A simple introduction to moving least squares and local regression estimation, Technical report, Los Alamos National Lab.(LANL), Los Alamos, NM (United States).

Giorgi, F. & Mearns, L. O. (1999), 'Introduction to special section: Regional climate modeling revisited', *Journal of Geophysical Research: Atmospheres* **104**(D6), 6335–6352.

Godfray, H. C. J., Beddington, J. R., Crute, I. R., Haddad, L., Lawrence, D., Muir, J. F., Pretty, J., Robinson, S., Thomas, S. M. & Toulmin, C. (2010), 'Food security: the challenge of feeding 9 billion people', *science* **327**(5967), 812–818.

Goudriaan, J. & Van Laar, H. (1994), *Modelling potential crop growth processes: textbook with exercises*, Vol. 2, Springer Science & Business Media.

Gourdji, S. M., Sibley, A. M. & Lobell, D. B. (2013), 'Global crop exposure to critical high temperatures in the reproductive period: historical trends and future projections', *Environmental Research Letters* **8**(2), 024041.

Grassini, P., Eskridge, K. M. & Cassman, K. G. (2013), 'Distinguishing between yield advances and yield plateaus in historical crop production trends', *Nature communications* **4**(1), 1–11.

Guereña, A., Ruiz-Ramos, M., Díaz-Ambrona, C. H., Conde, J. R. & Mínguez, M. I. (2001), 'Assessment of climate change and agriculture in spain using climate models', *Agronomy Journal* **93**(1), 237–249.

Guilpart, N., Iizumi, T. & Makowski, D. (2020), 'Data-driven yield projections suggest large opportunities to improve europe's soybean self-sufficiency under climate change', *bioRxiv* .

Gustavsson, J., Cederberg, C., Sonesson, U., Van Otterdijk, R. & Meybeck, A. (2011), *Global food losses and food waste*, FAO Rome.

Guttman, I. & Tiao, G. C. (1978), 'Effect of correlation on the estimation of a mean in the presence of spurious observations', *Canadian Journal of Statistics* **6**(2), 229–247.

Hanin, B. (2019), 'Universal function approximation by deep neural nets with bounded width and relu activations', *Mathematics* **7**(10), 992.

Hanin, B. & Sellke, M. (2017), 'Approximating continuous functions by relu nets of minimal width', *arXiv preprint arXiv:1710.11278* .

Hansen, J., Sato, M. & Ruedy, R. (2012), 'Perception of climate change', *Proceedings of the National Academy of Sciences* **109**(37), E2415–E2423.

Harding, R., Best, M., Blyth, E., Hagemann, S., Kabat, P., Tallaksen, L. M., Warnaars, T., Wiberg, D., Weedon, G. P., Lanen, H. v. et al. (2011), 'Watch: Current knowledge of the terrestrial global water cycle', *Journal of Hydrometeorology* **12**(6), 1149–1156.

Hennessy, K., Gregory, J. M. & Mitchell, J. (1997), 'Changes in daily precipitation under enhanced greenhouse conditions', *Climate Dynamics* **13**(9), 667–680.

Hesketh, J., Myhre, D. & Willey, C. (1973), 'Temperature control of time intervals between vegetative and reproductive events in soybeans 1', *Crop Science* **13**(2), 250–254.

Hobbins, M. T., Dai, A., Roderick, M. L. & Farquhar, G. D. (2008), 'Revisiting the parameterization of potential evaporation as a driver of long-term water balance trends', *Geophysical Research Letters* **35**(12).

Hoegh-Guldberg, O., Jacob, D., Taylor, M., Bindi, M., Brown, S., Camilloni, I., Diedhiou, A., Djalante, R., Ebi, K., Engelbrecht, F. et al. (2018), 'Impacts of 1.5 °c global warming on natural and human systems'.

Holmgren, P. (2006), 'Global land use area change matrix. input to the fourth global enviromental outlook (geo-4)'.

Holt, C. C. (2004), 'Forecasting seasonals and trends by exponentially weighted moving averages', *International journal of forecasting* **20**(1), 5–10.

Huntingford, C., Jones, P. D., Livina, V. N., Lenton, T. M. & Cox, P. M. (2013), 'No increase in global temperature variability despite changing regional patterns', *Nature* **500**(7462), 327.

Huntington, T. G. (2006), 'Evidence for intensification of the global water cycle: review and synthesis', *Journal of Hydrology* **319**(1-4), 83–95.

Hussain, H. A., Hussain, S., Khaliq, A., Ashraf, U., Anjum, S. A., Men, S. & Wang, L. (2018), 'Chilling and drought stresses in crop plants: implications, cross talk, and potential management opportunities', *Frontiers in plant science* **9**, 393.

Hyndman, R. J., Khandakar, Y. et al. (2007), *Automatic time series for forecasting: the forecast package for R*, Vol. 27, Journal of Statistical Software.

Hyndman, R. J., King, M. L., Pitrun, I. & Billah, B. (2005), 'Local linear forecasts using cubic smoothing splines', *Australian & New Zealand Journal of Statistics* **47**(1), 87–99.

Iizumi, T., Luo, J.-J., Challinor, A. J., Sakurai, G., Yokozawa, M., Sakuma, H., Brown, M. E. & Yamagata, T. (2014), 'Impacts of el niño southern oscillation on the global yields of major crops', *Nature communications* **5**(1), 1–7.

Iizumi, T., Sakuma, H., Yokozawa, M., Luo, J.-J., Challinor, A. J., Brown, M. E., Sakurai, G. & Yamagata, T. (2013), 'Prediction of seasonal climate-induced variations in global food production', *Nature climate change* **3**(10), 904–908.

IPCC (2018), *IPCC, 2018: Summary for Policymakers*, Press.

IPCC, I. P. (2007), *Fourth Assessment Report: Climate Change 2007: Working Group I Report: The Physical Science Basis*, Geneva: IPCC.
URL: *http://www.ipcc.ch/ipccreports/ar4-wg1.htm*

Jamieson, P., Semenov, M., Brooking, I. & Francis, G. (1998), 'Sirius: a mechanistic model of wheat response to environmental variation', *European Journal of Agronomy* **8**(3-4), 161–179.

Jenkins, G. & Lowe, J. (2003), *Handling uncertainties in the UKCIP02 scenarios of climate change*, Met Office.

Jolliffe, I. T. (2002), 'Principal components in regression analysis', *Principal component analysis* pp. 167–198.

Jones, H. G. (2013), 'Plants and microclimate: A quantitative approach to environmental plant physiology', *Cambridge University Press* .

Jones, J., Tsuji, G., Hoogenboom, G., Hunt, L., Thornton, P., Wilkens, P., Imamura, D., Bowen, W. & Singh, U. (1998), Decision support system for agrotechnology transfer: Dssat v3, *in* 'Understanding options for agricultural production', Springer, pp. 157–177.

Jones, P. D., New, M., Parker, D. E., Martin, S. & Rigor, I. G. (1999), 'Surface air temperature and its changes over the past 150 years', *Reviews of Geophysics* **37**(2), 173–199.

Jones, P. G. & Thornton, P. K. (2003), 'The potential impacts of climate change on maize production in africa and latin america in 2055', *Global environmental change* **13**(1), 51–59.

Jones, P. G. & Thornton, P. K. (2009), 'Croppers to livestock keepers: livelihood transitions to 2050 in africa due to climate change', *Environmental Science & Policy* **12**(4), 427–437.

Katz, R. W. (2002), 'Techniques for estimating uncertainty in climate change scenarios and impact studies', *Climate Research* **20**(2), 167–185.

Khodadadi, M., Mesdaghinia, A., Nasseri, S., Ghaneian, M. T., Ehrampoush, M. H. & Hadi, M. (2016), 'Prediction of the waste stabilization pond performance using linear multiple regression and multi-layer perceptron neural network: a case study of birjand, iran', *Environmental Health Engineering and Management Journal* **3**(2), 81–89.

Koester, U. (2008), 'Poverty & the wto. impacts of the doha development agenda'.

Kummu, M., Gerten, D., Heinke, J., Konzmann, M. & Varis, O. (2014), 'Climate-driven interannual variability of water scarcity in food production potential: a global analysis', *Hydrology and Earth System Sciences* **18**(2), 447–461.

Kunkel, K. E., Andsager, K. & Easterling, D. R. (1999), 'Long-term trends in extreme precipitation events over the conterminous united states and canada', *Journal of climate* **12**(8), 2515–2527.

Kupika, O. L., Gandiwa, E., Kativu, S. & Nhamo, G. (2018), 'Impacts of climate change and climate variability on wildlife resources in southern africa: Experience from selected protected areas in zimbabwe', *Selected Studies in Biodiversity* p. 1.

Kurukulasuriya, P., Mendelsohn, R., Hassan, R., Benhin, J., Deressa, T., Diop, M., Eid, H. M., Fosu, K. Y., Gbetibouo, G., Jain, S. et al. (2006), 'Will african agriculture survive climate change?', *The World Bank Economic Review* **20**(3), 367–388.

Laflamme, E. M., Linder, E. & Pan, Y. (2016), 'Statistical downscaling of regional climate model output to achieve projections of precipitation extremes', *Weather and Climate Extremes* **12**, 15–23.

Leakey, A. D., Ainsworth, E. A., Bernacchi, C. J., Rogers, A., Long, S. P. & Ort, D. R. (2009), 'Elevated co2 effects on plant carbon, nitrogen, and water relations: six important lessons from face', *Journal of experimental botany* **60**(10), 2859–2876.

Lee, Y. & Brorsen, B. W. (2017), 'Permanent breaks and temporary shocks in a time series', *Computational Economics* **49**(2), 255–270.

Lesk, C., Rowhani, P. & Ramankutty, N. (2016), 'Influence of extreme weather disasters on global crop production', *Nature* **529**(7584), 84–87.

Levin, J. (2006), 'General equilibrium', *San Francisco* .

Li, G., Harrison, S. P., Bartlein, P. J., Izumi, K. & Prentice, I. C. (2013), 'Precipitation scaling with temperature in warm and cold climates: an analysis of cmip5 simulations', *Geophysical Research Letters* **40**(15), 4018–4024.

Licker, R., Kucharik, C. J., Doré, T., Lindeman, M. J. & Makowski, D. (2013), 'Climatic impacts on winter wheat yields in picardy, france and rostov, russia: 1973–2010', *Agricultural and Forest Meteorology* **176**, 25–37.

Lin, Y., Xin, X., Zhang, H. & Wang, X. (2015), 'The implications of serial correlation and time-lag effects for the impact study of climate change on vegetation dynamics–a case study with hulunber meadow steppe, inner mongolia', *International Journal of Remote Sensing* **36**(19-20), 5031–5044.

Lloyd, T. A. (1993), 'Outliers in agriculture: An intervention analysis of agricultural land values', *Journal of Agricultural Economics* **44**(3), 443–455.

Lobell, D. B., Bänziger, M., Magorokosho, C. & Vivek, B. (2011), 'Nonlinear heat effects on african maize as evidenced by historical yield trials', *Nature climate change* **1**(1), 42–45.

Lobell, D. B. & Burke, M. (2009), *Climate change and food security: adapting agriculture to a warmer world*, Vol. 37, Springer Science & Business Media.

Lobell, D. B. & Burke, M. B. (2008), 'Why are agricultural impacts of climate change so uncertain? the importance of temperature relative to precipitation', *Environmental Research Letters* **3**(3), 034007.

Lobell, D. B., Burke, M. B., Tebaldi, C., Mastrandrea, M. D., Falcon, W. P. & Naylor, R. L. (2008), 'Prioritizing climate change adaptation needs for food security in 2030', *Science* **319**(5863), 607–610.

Lobell, D. B. & Field, C. B. (2007), 'Global scale climate–crop yield relationships and the impacts of recent warming', *Environmental research letters* **2**(1), 014002.

Lobell, D. B., Roberts, M. J., Schlenker, W., Braun, N., Little, B. B., Rejesus, R. M. & Hammer, G. L. (2014), 'Greater sensitivity to drought accompanies maize yield increase in the us midwest', *Science* **344**(6183), 516–519.

Lobell, D. B., Schlenker, W. & Costa-Roberts, J. (2011), 'Climate trends and global crop production since 1980', *Science* **333**(6042), 616–620.

Long, S. P., Ainsworth, E. A., Leakey, A. D., Nösberger, J. & Ort, D. R. (2006), 'Food for thought: lower-than-expected crop yield stimulation with rising co2 concentrations', *science* **312**(5782), 1918–1921.

López-de Lacalle, J. (2016), 'tsoutliers r package for detection of outliers in time series', *CRAN, R Package* .

MacDonald, G. K., Brauman, K. A., Sun, S., Carlson, K. M., Cassidy, E. S., Gerber, J. S. & West, P. C. (2015), 'Rethinking agricultural trade relationships in an era of globalization', *BioScience* **65**(3), 275–289.

Maleki, A., Nasseri, S., Aminabad, M. S. & Hadi, M. (2018), 'Comparison of arima and nnar models for forecasting water treatment plant's influent characteristics', *KSCE Journal of Civil Engineering* **22**(9), 3233–3245.

Maraun, D., Wetterhall, F., Ireson, A., Chandler, R., Kendon, E., Widmann, M., Brienen, S., Rust, H., Sauter, T., Themeßl, M. et al. (2010), 'Precipitation downscaling under climate change: Recent developments to bridge the gap between dynamical models and the end user', *Reviews of Geophysics* **48**(3).

McCown, R. L., Hammer, G. L., Hargreaves, J. N. G., Holzworth, D. P. & Freebairn, D. M. (1996), 'Apsim: a novel software system for model development, model testing and simulation in agricultural systems research', *Agricultural systems* **50**(3), 255–271.

Miller, P., Lanier, W. & Brandt, S. (2001), 'Using growing degree days to predict plant stages', *Ag/Extension Communications Coordinator, Communications Services, Montana State University-Bozeman, Bozeman, MO* **59717**(406), 994–2721.

Milly, P. C., Betancourt, J., Falkenmark, M., Hirsch, R. M., Kundzewicz, Z. W., Lettenmaier, D. P. & Stouffer, R. J. (2008), 'Stationarity is dead: Whither water management?', *Science* **319**(5863), 573–574.

Moeletsi, M. E. (2017), 'Mapping of maize growing period over the free state province of south africa: Heat units approach', *Advances in Meteorology* **2017**.

Monfreda, C., Ramankutty, N. & Foley, J. A. (2008), 'Farming the planet: 2. geographic distribution of crop areas, yields, physiological types, and net primary production in the year 2000', *Global biogeochemical cycles* **22**(1).

Monfreda, C., Ramankutty, N., Hertel, T. W. et al. (2009), 'Global agricultural land use data for climate change analysis', *Economic analysis of land use in global climate change policy* **14**, 33.

Moore, F. C. & Lobell, D. B. (2014), 'Adaptation potential of european agriculture in response to climate change', *Nature Climate Change* **4**(7), 610–614.

Muchow, R. C., Sinclair, T. R. & Bennett, J. M. (1990), 'Temperature and solar radiation effects on potential maize yield across locations', *Agronomy journal* **82**(2), 338–343.

Mueller, N. D., Gerber, J. S., Johnston, M., Ray, D. K., Ramankutty, N. & Foley, J. A. (2012), 'Closing yield gaps through nutrient and water management', *Nature* **490**(7419), 254.

Mueller, N. D., West, P. C., Gerber, J. S., MacDonald, G. K., Polasky, S. & Foley, J. A. (2014), 'A tradeoff frontier for global nitrogen use and cereal production', *Environmental Research Letters* **9**(5), 054002.

Natekin, A. & Knoll, A. (2013), 'Gradient boosting machines, a tutorial', *Frontiers in neurorobotics* **7**, 21.

Nelson, G. C. & Shively, G. E. (2014), 'Modeling climate change and agriculture: an introduction to the special issue', *Agricultural Economics* **45**(1), 1–2.

Neumann, K., Verburg, P. H., Stehfest, E. & Müller, C. (2010), 'The yield gap of global grain production: A spatial analysis', *Agricultural systems* **103**(5), 316–326.

Osborne, T. M. & Wheeler, T. R. (2013), 'Evidence for a climate signal in trends of global crop yield variability over the past 50 years', *Environmental Research Letters* **8**(2), 024001.

Paillard, S., Dorin, B., Le Cotty, T., Ronzon, T., Treyer, S. et al. (2011), 'Food security by 2050: Insights from the agrimonde project', *European Foresight Platform Brief* (196).

Parry, M., Parry, M. L., Canziani, O., Palutikof, J., Van der Linden, P. & Hanson, C. (2007), *Climate change 2007-impacts, adaptation and vulnerability: Working group II contribution to the fourth assessment report of the IPCC*, Vol. 4, Cambridge University Press.

Parthasarathi, T., Velu, G. & Jeyakumar, P. (2013), 'Impact of crop heat units on growth and developmental physiology of future crop production: A review', *Journal of Crop Science and Technology* **2**(1), 2319–3395.

Peltonen-Sainio, P., Jauhiainen, L. & Laurila, I. P. (2009), 'Cereal yield trends in northern european conditions: Changes in yield potential and its realisation', *Field Crops Research* **110**(1), 85–90.

Peng, S., Huang, J., Sheehy, J. E., Laza, R. C., Visperas, R. M., Zhong, X., Centeno, G. S., Khush, G. S. & Cassman, K. G. (2004), 'Rice yields decline with higher night temperature from global warming', *Proceedings of the National Academy of Sciences* **101**(27), 9971–9975.

Peres-Neto, P. R., Jackson, D. A. & Somers, K. M. (2005), 'How many principal components? stopping rules for determining the number of non-trivial axes revisited', *Computational Statistics & Data Analysis* **49**(4), 974–997.

Phalan, B., Green, R. & Balmford, A. (2014), 'Closing yield gaps: perils and possibilities for biodiversity conservation', *Philosophical Transactions of the Royal Society B: Biological Sciences* **369**(1639), 20120285.

Piwowar, J. M. & LeDrew, E. F. (2002), 'Arma time series modelling of remote sensing imagery: A new approach for climate change studies', *International Journal of Remote Sensing* **23**(24), 5225–5248.

Ponnamperuma, F. (1984), 'Effects of flooding on soils. in 'flooding and plant growth'.(ed. tt kozlowski) pp. 9–45'.

Ponnamperuma, F. N. (1972), The chemistry of submerged soils, *in* 'Advances in agronomy', Vol. 24, Elsevier, pp. 29–96.

Porter, J. R., Challinor, A. J., Henriksen, C. B., Howden, S. M., Martre, P. & Smith, P. (2019), 'Invited review: Intergovernmental panel on climate change, agriculture, and food-a case of shifting cultivation and history', *Global change biology* **25**(8), 2518–2529.

Porter, J. R. & Gawith, M. (1999), 'Temperatures and the growth and development of wheat: a review', *European journal of agronomy* **10**(1), 23–36.

Porter, J. R. & Semenov, M. A. (2005), 'Crop responses to climatic variation', *Philosophical Transactions of the Royal Society B: Biological Sciences* **360**(1463), 2021–2035.

Portmann, F. T., Siebert, S. & Döll, P. (2010), 'Mirca2000—global monthly irrigated and rainfed crop areas around the year 2000: A new high-resolution data set for agricultural and hydrological modeling', *Global biogeochemical cycles* **24**(1).

Pradhan, P., Fischer, G., van Velthuizen, H., Reusser, D. E. & Kropp, J. P. (2015), 'Closing yield gaps: how sustainable can we be?', *PloS one* **10**(6), e0129487.

Prentice, I., Liang, X., Medlyn, B. & Wang, Y.-P. (2015), 'Reliable, robust and realistic: the three r's of next-generation land-surface modelling', *Atmospheric Chemistry and Physics* **15**, 5987–6005. **URL:** *http://dx.doi.org/10.5194/acp-15-5987-2015*

Raghu, M., Poole, B., Kleinberg, J., Ganguli, S. & Sohl-Dickstein, J. (2017), On the expressive power of deep neural networks, *in* 'international conference on machine learning', PMLR, pp. 2847–2854.

Rahmstorf, S. & Coumou, D. (2011), 'Increase of extreme events in a warming world', *Proceedings of the National Academy of Sciences* **108**(44), 17905–17909.

Rauscher, S. A., Coppola, E., Piani, C. & Giorgi, F. (2010), 'Resolution effects on regional climate model simulations of seasonal precipitation over europe', *Climate Dynamics* **35**(4), 685–711.

Ray, D. K., Gerber, J. S., MacDonald, G. K. & West, P. C. (2015), 'Climate variation explains a third of global crop yield variability', *Nature communications* **6**, 5989.

Ray, D. K., Mueller, N. D., West, P. C. & Foley, J. A. (2013), 'Yield trends are insufficient to double global crop production by 2050', *PloS one* **8**(6), e66428.

Ray, D. K., Ramankutty, N., Mueller, N. D., West, P. C. & Foley, J. A. (2012), 'Recent patterns of crop yield growth and stagnation', *Nature communications* **3**(1), 1–7.

Ritchie, J. T. & Nesmith, D. S. (1991), 'Temperature and crop development', *Modeling plant and soil systems* **31**, 5–29.

Roberts, M. J. & Schlenker, W. (2011), The evolution of heat tolerance of corn: Implications for climate change, *in* 'The economics of climate change: adaptations past and present', University of Chicago Press, pp. 225–251.

Rosenzweig, C., Elliott, J., Deryng, D., Ruane, A. C., Müller, C., Arneth, A., Boote, K. J., Folberth, C., Glotter, M., Khabarov, N. et al. (2014), 'Assessing agricultural risks of climate change in the 21st century in a global gridded crop model intercomparison', *Proceedings of the National Academy of Sciences* **111**(9), 3268–3273.

Rosenzweig, C., Iglesias, A. et al. (1994), 'Implications of climate change for international agriculture: Crop modeling study'.

Rosenzweig, C., Jones, J., Hatfield, J., Ruane, A., Boote, K., Thorburn, P., Antle, J., Nelson, G., Porter, C., Janssen, S., Asseng, S., Basso, B., Ewert, F., Wallach, D., Baigorria, G. & Winter, J. (2013), 'The Agricultural Model Intercomparison and Improvement Project (AgMIP): Protocols and pilot studies', *Agricultural and Forest Meteorology* **170**, 166–182.
URL: *http://linkinghub.elsevier.com/retrieve/pii/S0168192312002857*

Rosenzweig, C. & Parry, M. L. (1994), 'Potential impact of climate change on world food supply', *Nature* **367**(6459), 133.

Rosenzweig, C., Tubiello, F. N., Goldberg, R., Mills, E. & Bloomfield, J. (2002), 'Increased crop damage in the us from excess precipitation under climate change', *Global Environmental Change* **12**(3), 197–202.

Rosner, B. (1983), 'Percentage points for a generalized esd many-outlier procedure', *Technometrics* **25**(2), 165–172.

Rostami Fasih, Z., Mesdaghinia, A., Nadafi, K., Nabizadeh Nodehi, R., Mahvi, A. H. & Hadi, M. (2015), 'Forecasting the air quality index based on meteorological variables and autocorrelation terms using artificial neural network', *Razi Journal of Medical Sciences* **22**(137), 31–43.

Salvucci, M. E. & Crafts-Brandner, S. J. (2004), 'Inhibition of photosynthesis by heat stress: the activation state of rubisco as a limiting factor in photosynthesis', *Physiologia plantarum* **120**(2), 179–186.

Samadi, S., Ehteramian, K. & Sarraf, B. S. (2011), 'Sdsm ability in simulate predictors for climate detecting over khorasan province', *Procedia-Social and Behavioral Sciences* **19**, 741–749.

Sánchez, B., Rasmussen, A. & Porter, J. R. (2014), 'Temperatures and the growth and development of maize and rice: a review', *Global change biology* **20**(2), 408–417.

Sanford, T., Frumhoff, P. C., Luers, A. & Gulledge, J. (2014), 'The climate policy narrative for a dangerously warming world', *Nature Climate Change* **4**(3), 164.

Savitzky, A. & Golay, M. J. (1964), 'Smoothing and differentiation of data by simplified least squares procedures.', *Analytical chemistry* **36**(8), 1627–1639.

Schapire, R. E. (2013), Explaining adaboost, *in* 'Empirical inference', Springer, pp. 37–52.

Schellnhuber, H. J., Hare, W., Serdeczny, O., Adams, S., Coumou, D., Frieler, K., Martin, M., Otto, I. M., Perrette, M., Robinson, A., Rocha, M., Schaeffer, M., Schewe, J., Wang, X. & Warszawski, L. (2012), Turn Down the Heat: Why a 4 °C Warmer World Must Be Avoided, Technical report, Washington, DC.
URL: *https://openknowledge.worldbank.org/handle/10986/11860*

Schlenker, W. & Lobell, D. B. (2010), 'Robust negative impacts of climate change on african agriculture', *Environmental Research Letters* **5**(1), 014010.

Schlenker, W. & Roberts, M. J. (2006), 'Nonlinear effects of weather on corn yields', *Review of agricultural economics* **28**(3), 391–398.

Schlenker, W. & Roberts, M. J. (2009), 'Nonlinear temperature effects indicate severe damages to us crop yields under climate change', *Proceedings of the National Academy of sciences* **106**(37), 15594–15598.

Schlenker, W., Roberts, M. J. & Lobell, D. B. (2013), 'Us maize adaptability', *Nature Climate Change* **3**(8), 690.

Schneider, U., Becker, A., Finger, P., Meyer-Christoffer, A., Ziese, M. & Rudolf, B. (2014), 'Gpcc's new land surface precipitation climatology based on quality-controlled in situ data and its role in quantifying the global water cycle', *Theoretical and Applied Climatology* **115**(1), 15–40.

Seager, R., Naik, N. & Vecchi, G. A. (2010), 'Thermodynamic and dynamic mechanisms for large-scale changes in the hydrological cycle in response to global warming', *Journal of Climate* **23**(17), 4651–4668.

Semenov, M. A. (2007), 'Development of high-resolution ukcip02-based climate change scenarios in the uk', *Agricultural and Forest Meteorology* **144**(1-2), 127–138.

Setiyono, T., Weiss, A., Specht, J., Bastidas, A., Cassman, K. G. & Dobermann, A. (2007), 'Understanding and modeling the effect of temperature and daylength on soybean phenology under high-yield conditions', *Field crops research* **100**(2-3), 257–271.

Sheffield, J., Goteti, G. & Wood, E. F. (2006), 'Development of a 50-year high-resolution global dataset of meteorological forcings for land surface modeling', *Journal of climate* **19**(13), 3088–3111.

Sheffield, J., Wood, E. F. & Roderick, M. L. (2012), 'Little change in global drought over the past 60 years', *Nature* **491**(7424), 435.

Si, B. C. & Farrell, R. E. (2004), 'Scale-dependent relationship between wheat yield and topographic indices: A wavelet approach', *Soil Science Society of America Journal* **68**(2), 577–587.

Sinclair, T. R. & Seligman, N. (2000), 'Criteria for publishing papers on crop modeling', *Field Crops Research* **68**(3), 165–172.

Smith, P., Bustamante, M., Ahammad, H., Clark, H., Dong, H., Elsiddig, E. A., Haberl, H., Harper, R., House, J., Jafari, M. et al. (2014), Agriculture, forestry and other land use (afolu), *in* 'Climate change 2014: mitigation of climate change. Contribution of Working Group III to the Fifth Assessment Report of the Intergovernmental Panel on Climate Change', Cambridge University Press.

Steel, R. (1997), 'Analysis of variance ii: multiway classifications', *Principles and procedures of statistics: A biometrical approach* pp. 204–252.

Stocker, T. F., Qin, D., Plattner, G.-K., Tignor, M., Allen, S. K., Boschung, J., Nauels, A., Xia, Y., Bex, V., Midgley, P. M. et al. (2013), 'Climate change 2013: The physical science basis'.

Strigens, A., Freitag, N. M., Gilbert, X., Grieder, C., Riedelsheimer, C., Schrag, T. A., Messmer, R. & Melchinger, A. E. (2013), 'Association mapping for chilling tolerance in elite flint and dent maize inbred lines evaluated in growth chamber and field experiments', *Plant, cell & environment* **36**(10), 1871–1887.

Sun, F., Roderick, M. L. & Farquhar, G. D. (2012), 'Changes in the variability of global land precipitation', *Geophysical Research Letters* **39**(19).

Svetunkov, I. & Boylan, J. E. (2020), 'State-space arima for supply-chain forecasting', *International Journal of Production Research* **58**(3), 818–827.

Tao, F., Yokozawa, M., Xu, Y., Hayashi, Y. & Zhang, Z. (2006), 'Climate changes and trends in phenology and yields of field crops in china, 1981–2000', *Agricultural and forest meteorology* **138**(1-4), 82–92.

Tchebichef, P. (1867), *Des valeurs moyennes*.

Teixeira, E. I., Fischer, G., Van Velthuizen, H., Walter, C. & Ewert, F. (2013), 'Global hot-spots of heat stress on agricultural crops due to climate change', *Agricultural and Forest Meteorology* **170**, 206–215.

Thoplan, R. (2014), 'Simple v/s sophisticated methods of forecasting for mauritius monthly tourist arrival data', *International Journal of Statistics and Applications* **4**(5), 217–223.

Tigchelaar, M., Battisti, D. S., Naylor, R. L. & Ray, D. K. (2018), 'Future warming increases probability of globally synchronized maize production shocks', *Proceedings of the National Academy of Sciences* **115**(26), 6644–6649.

Tilman, D. (1999), 'Global environmental impacts of agricultural expansion: the need for sustainable and efficient practices', *Proceedings of the National Academy of Sciences* **96**(11), 5995–6000.

Tilman, D., Balzer, C., Hill, J. & Befort, B. L. (2011), 'Global food demand and the sustainable intensification of agriculture', *Proceedings of the National Academy of Sciences* **108**(50), 20260–20264.
URL: *http://dx.doi.org/10.1073/pnas.1116437108*

Tilman, D., Cassman, K. G., Matson, P. a., Naylor, R. & Polasky, S. (2002), 'Agricultural sustainability and intensive production practices.', *Nature* **418**(6898), 671–7.
URL: *http://www.ncbi.nlm.nih.gov/pubmed/12167873*

Tilman, D., Reich, P. B., Knops, J., Wedin, D., Mielke, T. & Lehman, C. (2001), 'Diversity and productivity in a long-term grassland experiment', *Science* **294**(5543), 843–845.

Trenberth, K. E. (1999), Conceptual framework for changes of extremes of the hydrological cycle with climate change, *in* 'Weather and Climate Extremes', Springer, pp. 327–339.

Trenberth, K. E. (2011), 'Changes in precipitation with climate change', *Climate Research* **47**(1-2), 123–138.

Trenberth, K. E., Dai, A., Rasmussen, R. M. & Parsons, D. B. (2003), 'The changing character of precipitation', *Bulletin of the American Meteorological Society* **84**(9), 1205–1218.

Trenberth, K. E., Dai, A., Van Der Schrier, G., Jones, P. D., Barichivich, J., Briffa, K. R. & Sheffield, J. (2014), 'Global warming and changes in drought', *Nature Climate Change* **4**(1), 17.

Tsay, R. S. (2014), *An introduction to analysis of financial data with R*, John Wiley & Sons.

Tscharntke, T., Clough, Y., Wanger, T. C., Jackson, L., Motzke, I., Perfecto, I., Vandermeer, J. & Whitbread, A. (2012), 'Global food security, biodiversity conservation and the future of agricultural intensification', *Biological conservation* **151**(1), 53–59.

Tubiello, F. N., Salvatore, M., Rossi, S., Ferrara, A., Fitton, N. & Smith, P. (2013), 'The faostat database of greenhouse gas emissions from agriculture', *Environmental Research Letters* **8**(1), 015009.

Uehara, G. & Tsuji, G. (1993), The ibsnat project, *in* 'Systems approaches for agricultural development', Springer, pp. 505–513.

Ummenhofer, C. C., Xu, H., Twine, T. E., Girvetz, E. H., McCarthy, H. R., Chhetri, N. & Nicholas, K. A. (2015), 'How climate change affects extremes in maize and wheat yield in two cropping regions', *Journal of Climate* **28**(12), 4653–4687.

Valipour, M., Banihabib, M. E. & Behbahani, S. M. R. (2013), 'Comparison of the arma, arima, and the autoregressive artificial neural network models in forecasting the monthly inflow of dez dam reservoir', *Journal of hydrology* **476**, 433–441.

Vallis, O., Hochenbaum, J. & Kejariwal, A. (2014), A novel technique for long-term anomaly detection in the cloud, *in* '6th {USENIX} workshop on hot topics in cloud computing (HotCloud 14)'.

Van der Schrier, G., Jones, P. & Briffa, K. (2011), 'The sensitivity of the pdsi to the thornthwaite and penman-monteith parameterizations for potential evapotranspiration', *Journal of Geophysical Research: Atmospheres* **116**(D3).

Van Groenigen, K. J., Van Kessel, C. & Hungate, B. A. (2013), 'Increased greenhouse-gas intensity of rice production under future atmospheric conditions', *Nature Climate Change* **3**(3), 288.

Vergara, B., Tanaka, A., Lilis, R. & Puranabhavung, S. (1966), 'Relationship between growth duration and grain yield of rice plants', *Soil Science and Plant Nutrition* **12**(1), 31–39.

Vieira, R. G., Leone Filho, M. A. & Semolini, R. (2018), An enhanced seasonal-hybrid esd technique for robust anomaly detection on time series, *in* 'Anais do XXXVI Simpósio Brasileiro de Redes de Computadores e Sistemas Distribuídos', SBC.

Von Storch, H. & Navarra, A. (2013), *Analysis of climate variability: Applications of statistical techniques proceedings of an autumn school organized by the Commission of the European Community on Elba from October 30 to November 6, 1993*, Springer Science & Business Media.

Wang, K. & Zhong, P. (2014), 'Robust non-convex least squares loss function for regression with outliers', *Knowledge-Based Systems* **71**, 290–302.

Webb, M. J., Lambert, F. H. & Gregory, J. M. (2013), 'Origins of differences in climate sensitivity, forcing and feedback in climate models', *Climate Dynamics* **40**(3-4), 677–707.

Weedon, G. P., Balsamo, G., Bellouin, N., Gomes, S., Best, M. J. & Viterbo, P. (2014), 'The wfdei meteorological forcing data set: Watch forcing data methodology applied to era-interim reanalysis data', *Water Resources Research* **50**(9), 7505–7514.

West, P. C., Gerber, J. S., Engstrom, P. M., Mueller, N. D., Brauman, K. A., Carlson, K. M., Cassidy, E. S., Johnston, M., MacDonald, G. K., Ray, D. K. et al. (2014), 'Leverage points for improving global food security and the environment', *Science* **345**(6194), 325–328.

Wilby, R. L., Charles, S., Zorita, E., Timbal, B., Whetton, P. & Mearns, L. (2004), 'Guidelines for use of climate scenarios developed from statistical downscaling methods', *Supporting material of the Intergovernmental Panel on Climate Change, available from the DDC of IPCC TGCIA* **27**.

Wilby, R. L., Dawson, C. W. & Barrow, E. M. (2002), 'Sdsm—a decision support tool for the assessment of regional climate change impacts', *Environmental Modelling & Software* **17**(2), 145–157.

Wilks, D. S. (1992), 'Adapting stochastic weather generation algorithms for climate change studies', *Climatic change* **22**(1), 67–84.

Winters, P. R. (1960), 'Forecasting sales by exponentially weighted moving averages', *Management science* **6**(3), 324–342.

Yang, H. & Huntingford, C. (2018), 'Brief communication. drought likelihood for east africa', *Natural Hazards and Earth System Sciences* **18**(2), 491–497.

Young, A. (1999), 'Is there really spare land? a critique of estimates of available cultivable land in developing countries', *Environment, Development and Sustainability* **1**(1), 3–18.

Zhang, G. P. & Qi, M. (2005), 'Neural network forecasting for seasonal and trend time series', *European journal of operational research* **160**(2), 501–514.

Zhang, G., Patuwo, B. E. & Hu, M. Y. (1998), 'Forecasting with artificial neural networks:: The state of the art', *International journal of forecasting* **14**(1), 35–62.

Zhang, W., Cao, G., Li, X., Zhang, H., Wang, C., Liu, Q., Chen, X., Cui, Z., Shen, J., Jiang, R. et al. (2016), 'Closing yield gaps in china by empowering smallholder farmers', *Nature* **537**(7622), 671–674.

Ziska, L. H. (2008), 'Rising atmospheric carbon dioxide and plant biology: the overlooked paradigm', *DNA and Cell Biology* **27**(4), 165–172.